

## **General Disclaimer**

### **One or more of the Following Statements may affect this Document**

- This document has been reproduced from the best copy furnished by the organizational source. It is being released in the interest of making available as much information as possible.
- This document may contain data, which exceeds the sheet parameters. It was furnished in this condition by the organizational source and is the best copy available.
- This document may contain tone-on-tone or color graphs, charts and/or pictures, which have been reproduced in black and white.
- This document is paginated as submitted by the original source.
- Portions of this document are not fully legible due to the historical nature of some of the material. However, it is the best reproduction available from the original submission.

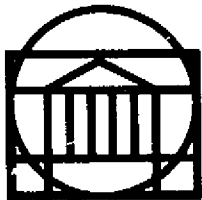
(NASA-CR-157781) DYNAMIC ANALYSIS OF  
FLEXIBLE ROTOR-BEARING SYSTEMS USING A MODAL  
APPROACH Final Report, 1 Sep. 1976 - 31  
Aug. 1977 (Virginia Univ.) 371 p HC A16/MF  
A01

N79-10446

Unclas  
33876

CSCS 20K G3/39

RESEARCH LABORATORIES FOR THE ENGINEERING SCIENCES



# SCHOOL OF ENGINEERING AND APPLIED SCIENCE

UNIVERSITY OF VIRGINIA

Charlottesville, Virginia 22901

DYNAMIC ANALYSIS OF FLEXIBLE ROTOR-BEARING  
SYSTEMS USING A MODAL APPROACH

Final Report under NASA Contract NSG-3104  
Period 9/1/76 - 8/31/77

Submitted to:

NASA Lewis Research Center  
21000 Brookpark Road  
Cleveland, OH 44135

Submitted by:

K. C. Choy  
Research Associate

E. J. Gunter  
Professor and Principal Investigator

L. E. Barrett  
Research Assistant Professor

Department of Mechanical and Aerospace Engineering  
School of Engineering and Applied Science  
University of Virginia  
Charlottesville, VA 22901

Report No. UVA/528144/MAE78/106

October 1978



## **RESEARCH LABORATORIES FOR THE ENGINEERING SCIENCES**

Members of the faculty who teach at the undergraduate and graduate levels and a number of professional engineers and scientists whose primary activity is research generate and conduct the investigations that make up the school's research program. The School of Engineering and Applied Science of the University of Virginia believes that research goes hand in hand with teaching. Early in the development of its graduate training program, the School recognized that men and women engaged in research should be as free as possible of the administrative duties involved in sponsored research. In 1959, therefore, the Research Laboratories for the Engineering Sciences (RLES) was established and assigned the administrative responsibility for such research within the School.

The director of RLES—himself a faculty member and researcher—maintains familiarity with the support requirements of the research under way. He is aided by an Academic Advisory Committee made up of a faculty representative from each academic department of the School. This Committee serves to inform RLES of the needs and perspectives of the research program.

In addition to administrative support, RLES is charged with providing certain technical assistance. Because it is not practical for each department to become self-sufficient in all phases of the supporting technology essential to present-day research, RLES makes services available through the following support groups: Machine Shop, Instrumentation, Facilities Services, Publications (including photographic facilities), and Computer Terminal Maintenance.

DYNAMIC ANALYSIS OF FLEXIBLE ROTOR-BEARING  
SYSTEMS USING A MODAL APPROACH

Final Report

NASA Contract NSG-3104

Period 9/1/76 - 8/31/77

Submitted By

K. C. Choy  
Research Associate

E. J. Gunter  
Professor and Principal Investigator

L. E. Barrett  
Research Assistant Professor

Department of Mechanical and Aerospace Engineering  
School of Engineering and Applied Science

University of Virginia  
Charlottesville, Virginia

Report No. UVA/528144/MAE78/106

October, 1978



## ABSTRACT

The generalized dynamic equations of motion have been obtained by the direct stiffness method for multimass flexible rotor-bearing systems including the effects of unbalance, shaft bow, disk skew, rotor acceleration, gyroscopic moments, and nonlinear bearing forces. The direct solution of the equations of motion is illustrated on a simple 3-mass system. However, for complex rotor-bearing systems, the direct solution of the equations becomes very difficult due to the large number of equations necessary to describe the dynamics of the system. The transformation of the equations of motion into modal coordinates can greatly simplify the computation for the solution. The use of undamped and damped system mode shapes in the transformation are discussed.

A set of undamped critical speed modes is used to transform the equations of motion into a set of coupled modal equations of motion. A rapid procedure for computing stability, steady state unbalance response, and transient response of the rotor-bearing system is presented. Examples of the application of this modal approach are presented and results are compared to those of other methods and to experimental data. The dynamics of the system is further investigated with frequency spectrum analysis of the transient response through the use of numerical fast Fourier Transformation.

PRECEDING PAGE BLANK NOT FILMED

## ACKNOWLEDGEMENTS

This work was supported by NASA Lewis Research Center,  
Contract No. NSG-3104. The authors would like to express their  
appreciation to NASA and to Dr. David P. Flemming, Contract Monitor.

TABLE OF CONTENTS

	<u>Page</u>
ABSTRACT . . . . .	iv
ACKNOWLEDGEMENTS . . . . .	v
LIST OF FIGURES . . . . .	ix
LIST OF TABLES . . . . .	xiii
NOMENCLATURE . . . . .	xiv
CHAPTER I. INTRODUCTION AND BACKGROUND	
1.1 Introduction . . . . .	1
1.2 Background . . . . .	3
1.3 Statement of the Problem . . . . .	9
CHAPTER II. FORMULATION OF EQUATIONS OF MOTION	
2.1 General Equations of Motion . . . . .	10
2.2 Illustration of Equations of Motion for a 3-Mass Rotor . . . . .	24
2.3 Direct Method of Solution . . . . .	31
CHAPTER III. METHODS OF MODAL ANALYSIS	
3.1 Uncoupled Modal Analysis . . . . .	37
3.1.1 Orthogonality of Normal Modes . .	39
3.1.2 Uncoupled Modal Equations of Motion . . . . .	42
3.1.3 Damped Natural Frequencies and Forced Response of Uncoupled System . . . . .	45
3.2 Modal Analysis Using Damped Modes . . .	48
3.2.1 Reduction to Standard Form . . .	48
3.2.2 Orthogonality of Eigenvectors . .	50
3.2.3 Forced Response Using Damped Modes . . . . .	54

TABLE OF CONTENTS (Continued)

	<u>Page</u>
3.3 Coupled Undamped Modal Analysis . . . . .	62
3.3.1 Orthogonality of Planar Modes . . . . .	63
3.3.2 Planar Modal Analysis . . . . .	66
CHAPTER IV. STABILITY ANALYSIS USING MODAL APPROACH	
4.1 Modal Equations for Stability Analysis . . . . .	69
4.2 Solution Procedure for Modal Stability Analysis . . . . .	74
4.3 Applications and Comparisons of Different Modal Methods . . . . .	79
CHAPTER V. FORCED RESPONSE ANALYSIS USING MODAL ANALYSIS	
5.1 Solutions of Modal Equations of Motion . . . . .	100
5.2 Applications and Comparisons of Steady State Solutions . . . . .	113
5.3 Verification of Transient Response Solutions . . . . .	122
CHAPTER VI. NON-LINEAR MODAL TRANSIENT ANALYSIS	
6.1 Application of Numerical Integration Procedures . . . . .	136
6.2 Effects of Nonlinear Bearing Supports . . . . .	147
6.3 Frequency Analysis of Transient Response Using Discrete Fast Fourier Transformation . . . . .	157
6.4 Correlation of Experimental Data with Modal Analysis . . . . .	169
CHAPTER VII. APPLICATION OF MODAL ANALYSIS ON SPACE SHUTTLE OXYGEN PUMP	
7.1 Undamped Modes of Oxygen Pump . . . . .	177

TABLE OF CONTENTS (Continued)

	<u>Page</u>
7.2 Stability Analysis of Oxygen Pump . . .	188
7.3 Transient Analysis of Oxygen Pump . . .	192
CHAPTER VIII. CONCLUSIONS	
8.1 Summary & Conclusions . . . . .	200
8.2 Suggestions for Future Research . . . .	204
BIBLIOGRAPHY . . . . .	206
APPENDIX A - DISC ROTATIONAL EQUATIONS OF MOTION -	
LANGRANGIAN APPROACH . . . . .	213
APPENDIX B - BASIC EQUATIONS OF MOTION FOR A BOW SHAFT . .	220
APPENDIX C - INTEGRATION PROCEDURES . . . . .	223
APPENDIX D - INPUT INSTRUCTIONS AND LISTING OF COMPUTER	
PROGRAM MODAL 1 . . . . .	225
APPENDIX E - INPUT INSTRUCTIONS AND LISTING OF COMPUTER	
PROGRAM MODAL 2 . . . . .	296

LIST OF FIGURES

<u>Figure</u>		<u>Page</u>
2.1	Forces and Moments Acting at Rotor Mass Station In X-Z Plane . . . . .	12
2.2	Displacements and Rotations of Shaft Element In X-Z Plane . . . . .	14
2.3	Right-Hand Convention used in Rotor Model . . . . .	17
2.4	Three Mass Bowed Rotor System With Skewed Disc . . . .	25
4.1	Critical Speeds of Uniform Lund Rotor For $k_b = 60,000 \text{ lb/in}$ . . . . .	80
4.2	First Three Undamped Compressor Planar Mode Shapes .	90
4.3	4th and 5th Undamped Compressor Planar Mode Shapes .	91
4.4	First Damped Forward Mode Shape of the Compressor .	92
4.5	First Damped Backward Mode Shape of the Compressor .	93
4.6	Second Damped Forward Mode Shape of the Compressor .	95
4.7	Second Damped Backward Mode Shape of the Compressor .	96
5.1	Orientation of Elliptical Orbit Motion . . . . .	109
5.2	Phase Angles in Elliptical Orbit Motion . . . . .	111
5.3	Unbalance Response Plot of the Compressor Bearing Station With First Mode Excitation . . . . .	114
5.4	Unbalance Response Plot of the Mid-Span of Compressor Rotor With First Mode Excitation . . . . .	115
5.5	Comparison of Experimental and Theoretical Results of a Three-Mass Rotor . . . . .	120
5.6	Schematic of Jeffcott Rotor . . . . .	123
5.7	Test Case with Single Mass Rotor with Rigid Supports	124
5.8	Test Case with Single Mass Rotor With Rigid Supports	125
5.9	Transient Analysis of Single Mass Rotor Using Modal Method - Speed = 707 Rad/Sec . . . . .	128

LIST OF FIGURES (Continued)

<u>Figure</u>	<u>Page</u>
5.10 Transient Analysis of Single Mass Rotor Using Modal Method - Speed = 707 Rad/Sec . . . . .	129
5.11 Forced Response of Single Mass Rotor From Analog Program . . . . .	131
5.12 Transient Response of Single Mass Rotor - Modal Method at 3,200 Rad/Sec . . . . .	132
5.13 Transient Response of Single Mass Rotor - Modal Method at 3,200 Rad/Sec . . . . .	133
5.14 Transient Response of Single Mass Rotor by Analog Computer . . . . .	134
6.1(a) Transient Orbit at Left Bearing of 8-Stage Compressor By Newmark Beta Integration Procedure . .	142
(b) Transient Orbit at Left Bearing of 8-Stage Compressor By Modified Euler Integration Procedure .	142
6.2(a) Transient Motion at Left Bearing of 8-Stage Compressor (Newmark Beta Procedure). . . . .	143
(b) Transient Motion at Left Bearing of 8-Stage Compressor (Modified Euler Procedure). . . . .	143
6.3(a) Transient Response Orbit at Unbalance Location of 8-Stage Compressor By Newmark Beta Procedure . . . .	144
(b) Transient Response Orbit at Unbalance Location of 8-Stage Compressor By Modified Euler Procedure . . .	144
6.4(a) Transient Motion at Unbalance Location of 8-Stage Compressor (Newmark Beta Procedure). . . . .	145
(b) Transient Motion at Unbalance Location of 8-Stage Compressor (Modified Euler Procedure). . . . .	145
6.5 Short Journal Bearing With 180 Cavitation Fluid Film . . . . .	150
6.6 Transient Motion of a Balanced Horizontal Rotor From Bearing Force Equations . . . . .	153
6.7 Journal Orbit of a Balanced Horizontal Rotor . . . .	154

LIST OF FIGURES (Continued)

<u>Figure</u>		<u>Page</u>
6.8	Transient Motion of Unbalanced Rotor From Bearing Force Equations . . . . .	155
6.9	Journal Orbit of an Unbalanced Vertical Rotor . . . .	156
6.10	Transient Motion of a Single Mass Rotor at 10,000 RPM . . . . .	161
6.11	Transient Motion of a Single Mass Rotor at 15,000 RPM . . . . .	162
6.12	Transient Motion of a Single Mass Rotor at 20,000 RPM . . . . .	163
6.13	Transient Motion of a Single Mass Rotor at 25,000 RPM . . . . .	164
6.14	Transient Motion of a Single Mass Rotor at 30,000 RPM . . . . .	165
6.15	Transient Motion of a Single Mass Rotor at 35,000 RPM . . . . .	166
6.16	Frequency Campbell Diagram of a Single Mass Rotor With Effects of Internal Friction . . . . .	167
6.17	Experimental Campbell Diagram of the 3-Mass Rotor . .	170
6.18	Transient and Synchronous Response of the 3-Mass Rotor . . . . .	171
6.19	Transient Motion of Center Mass at 2550 RPM . . . .	173
6.20	Transient Motion of the Center Mass at 6350 RPM . .	174
6.21	Transient Motion of the Center Mass at 7000 RPM . .	175
6.22	Transient Motion of Rotor Center After 160 Cycles of Motion . . . . .	176
6.23	Cambell Diagram of Three- Mass Rotor using Fourier Transformation . . . . .	177
7.1	Rotating Assembly of Space Shuttle Main Engine Oxygen Pump . . . . .	180



LIST OF FIGURES (Continued)

<u>Figure</u>		<u>Page</u>
7.2	Computer Simulation of the Oxygen Pump Rotating Assembly . . . . .	182
7.3	Undamped Mode Shapes of Oxygen Pump . . . . .	183
7.4	Damped Mode Shape of the Oxygen Pump at First Critical Speed . . . . .	190
7.5	Transient Motion at the First Seal Location . . . . .	195
7.6	Transient Motion at the Pump Bearing . . . . .	195
7.7	Transient Motion at the Turbine Bearing . . . . .	196
7.8	Transient Motion at the Second Seal Location . . . . .	196
7.9	Transient Motion at the Turbine End . . . . .	197
7.10	Forced Response of SSME-HPOTP at the Turbine End . . . . .	208

LIST OF TABLES

<u>Table No.</u>		<u>Page</u>
4.1	Comparison of Damped and Undamped Critical Speeds and Amplification Factors . . . . .	81
4.2	Geometric Properties of Lund [11] Compressor . .	87
4.3	Bearing Characteristics Used for Simulation of the 8-Stage Compressor . . . . .	88
4.4	Comparison of the Complex Eigenvalues Calculated by the Model and Transfer Matrix Method . . . .	98
5.1	Comparison of Compressor Unbalance Response by Modal and Transfer Matrix Methods . . . . .	116
5.2	Rotor Geometry and Bearing Characteristics of the Three-Mass Rotor . . . . .	119
5.3	Comparison of Transient Response Results of Jeffcott Rotor . . . . .	127
6.1	Bearing & Internal Damping Coefficients for a Single Mass Rotor Model . . . . .	160
7.1	Rotor Geometry of the Space Shuttle Oxygen Pump	181
7.2	Oxygen Pump Orthonormal Mode of the First Critical Speed . . . . .	184
7.3	Oxygen Pump Orthonormal Mode of the Second Critical Speed . . . . .	185
7.4	Oxygen Pump Orthonormal Mode of the Third Critical Speed . . . . .	186
7.5	Seal Coefficient used in SSME-HPOTP Analysis . .	189
7.6	Steady State Unbalance Response (in mils) of Oxygen Pump with 6 gm. in. Unbalance at Turbine	193

## NOMENCLATURE

<u>Symbol</u>	<u>Description</u>
$A_i$	Modal amplification factor for the <u><i>i</i></u> th mode
$A_{ui}$	Amplification factor at the <u><i>i</i></u> th resonance speed
$[A]$	Orthonormal mode matrix = $\begin{bmatrix} A_e \\ A_\beta \end{bmatrix}$
$[A_e]$	Translation orthonormal mode matrix
$[A_\beta]$	Rotational orthonormal mode matrix
$B_i$	Modal Constants for damped modes
$C_{ij}$	Modal damping coefficients
$C_{xx}, C_{xy}, C_{yx}, C_{yy}$	Bearing damping coefficients
$[C]$	Damping matrix
$[C_b]$	Bearing damping matrix
$[C_x], [C_y]$	Modal damping matrix
$[CM_x], [CM_y]$	modal gyroscopic matrix
$[D_x], [D_y]$	Modal cross-coupling damping matrix
$(EI)_i$	Material property of <u><i>i</i></u> th element
$E_i$	Modal unbalance eccentricity of <u><i>i</i></u> th mode
$[E_x], [E_y]$	Modal cross-coupling stiffness matrix
$[EA_x], [EA_y]$	Modal acceleration matrix
$F_D(x, y, \dot{x}, \dot{y})$	Nonlinear bearing forces
$F(t)$	External applied forcing function
$f_i$	Modal forcing function of <u><i>i</i></u> th mode
$f_r$	Radial nonlinear bearing force
$f_t$	Tangential nonlinear bearing force
$[I]$	Unity matrix

<u>Symbol</u>	<u>Description</u>
$I_{ti}$	Transverse moment of inertia at <u>ith</u> station
$I_{pi}$	Polar moment of inertia at <u>ith</u> station
$[K]$	Total system stiffness matrix
$[K_A]$	Acceleration stiffness matrix
$[K_B]$	Bearing stiffness matrix
$[K_S], [K_W]$	Shaft stiffness matrix
$[K_x], [K_y]$	Modal stiffness matrix
$L_i$	Length of the <u>ith</u> shaft element
$M_i$	Modal mass of <u>ith</u> mode
$m_i$	Mass at <u>ith</u> mass station
$M_i^L, M_i^R$	Moment acting at <u>ith</u> shaft element
$P_i$	Damping exponent or real part of complex eigenvalue of <u>ith</u> mode
$Q$	Aerodynamic cross-coupling coefficient
$q_i(\tau)$	Modal constant of <u>ith</u> undamped mode
$[R_x], [R_y]$	Modal coordinates for shaft bow displacement
$U_i$	Modal unbalance of <u>ith</u> mode
$\{U\}$	Displacement vector of system
$V_i^L, V_i^R$	Shear force acting at <u>ith</u> shaft element
$V_{n+1}$	Velocity at $n+1$ time step
$\dot{V}_{n+1}$	Acceleration at $n+1$ time step
$W$	Weight acting at the journal
$W_i$	Modal weight of <u>ith</u> mode
$x_i, y_i$	Total displacement at <u>ith</u> mass station
$x_{ei}, y_{ei}$	Elastic displacement at <u>ith</u> mass station

<u>Symbol</u>	<u>Description</u>
$x_{di}, y_{di}$	Shaft mechanical bow at <u>i</u> th mass station
$\{XF\}, \{YF\}$	Modal external force vector
$\beta$	Phase angle of maximum disc skew to shaft timing mark
$\beta_x, \beta_y$	Phase angle of timing mark from x-probe and y-probe
$\{\alpha_i\}$	Normalized undamped mode of <u>i</u> th critical speed
$\epsilon$	Eccentricity ratio of journal
$\xi_i$	Damping ratio of the <u>i</u> th mode
$[\Lambda]$	Diagonal matrix of $\omega_i^2$
$\lambda_i$	Complex eigenvalue of the <u>i</u> th damped mode
$\lambda_i^*$	Complex conjugate of $\lambda_i$
$\tau_j$	Permanent disc skew in the <u>i</u> th mass station
$\tau_x$	$\tau \cos \beta$
$\tau_y$	$\tau \sin \beta$
$\mu$	Viscosity of fluid lubricant
$\sigma$	Modified sommerfeld number
$\{\phi_i\} = \begin{Bmatrix} \phi_i \\ \phi_i \end{Bmatrix}$	Orthonormal modes of the <u>i</u> th undamped critical speed
$\{\psi_i\} = \begin{Bmatrix} \lambda \phi_{di} \\ \phi_{di} \end{Bmatrix}$	Normalized damped mode of the <u>i</u> th critical speed
$\omega_i$	The <u>i</u> th undamped critical speed of the system
$\omega_{di}$	The <u>i</u> th damped critical speed of the system

## I. INTRODUCTION AND BACKGROUND

### 1.1 Introduction

Long before the design and manufacturing of large complex turbo-machinery when the wheel was invented, man has been plagued with both technical and theoretical problems of bearing lubrication and shaft dynamics. With the design and operation of large turbine rotors that power jetliners and vast streams of process machinery that operates the industrial community, these problems concerning the dynamics of rotor-bearing systems have become more pronounced. Engineers are faced with the problem of designing a rotor capable of operating through various adverse conditions of temperature, speed, and load. As an example, turbo-rotors designed for fuel pump units of space applications must have satisfactory performance under extreme temperature and gravitation loadings at very high speed. In many of these applications, the designed unit must operate through several basic critical speeds (or natural vibration frequencies) of the system. Under these circumstances, it is extremely difficult to insure that the unit will operate with a stable and low-amplitude of vibration performance.

The instability and high amplitude vibration problems may come from the erroneous design of the machinery, the misassembly of the system, and the operation under adverse conditions.

The major causes can be stated as follows:

1. large mass unbalance in the rotor
2. high rotor amplification factor

3. large bearing hydrodynamic cross-coupling effects
4. large turbine (impeller) aerodynamic cross-coupling forces
5. shaft thermal and mechanical bow and disk skew effects
6. misalignment of shaft and bearing elements
7. effects of internal friction
8. large shaft assymetry in the system
9. support motion from housing vibration or seismic effects
10. large overhang in the system (gyroscopic effects)
11. operation near the critical speed of the system
12. impeller or turbine blade loss
13. rubbing of bearing or seal
14. fast start up or shut down

A vast amount of information has been developed concerning the above problems separately. The interests and means of solving the combined problem has been evolving since the early 60's. The next section will discuss the earliest work briefly but will concentrate more on the present state of art in the field of dynamics of rotor-bearing systems.

## 1.2 Background

Advances in the design and operation of rotating machinery in modern engineering are closely linked with solutions of several problems in the field of rotor dynamics. These problems have been investigated separately by various researchers. The earliest recorded article on this subject was introduced by Rankine [1] in 1869. He examined the neutral or "indifferent" equilibrium conditions of a shaft operating through its first critical speed. Without taking into consideration support damping and Coriolis force, he concluded that the rotor system would be unstable if operated beyond its first critical speed. His conclusion has led engineers in the next several decades to believe that rotor systems were not capable of operating beyond the first critical speed. In 1894, Dunkerley [8] reported his study on rotor dynamic behavior near its critical speed regions. He showed that by neglecting unbalance and damping, the rotor whirling frequencies can be replaced by the lateral vibration frequencies of a simply supported rotor system. As a result of his investigations, rotor manufacturers tried to design rotors with rigid shaft such that their critical speeds were raised beyond the operating speed range. In 1919, Jeffcott [2] made an intensive investigation in the dynamics of simple rotor models in two dimensional form with the inclusion of damping effects. He further explained the meaning of critical speed and introduced the new terminology of "whirl instability."

In the 1920's, turbine and compressor manufacturers began to see a trend of the reverse concept. They tried to design rotors with lighter weight such that the first critical speed of the system is



much lower than the operating speed range. Later, Newkirk [3] made an intensive investigation on stability of rotor-bearing systems and concluded that the rotor dynamic behavior could not be attributed to a critical speed resonance and the reduction of unbalance had no effect upon rotor whirl amplitudes. During the same time, a group of investigators concentrated on the study of hydrodynamic behaviors of fluid film bearings. Using the Sommerfeld treatment, they found that the hydrodynamic profile predicts a negative fluid film pressure of the same order as the positive pressure. This negative pressure causes the fluid film to cavitate and results in radial bearing force in the system. In 1952, Poritsky [57] reported that the cavitation of the fluid film can excite the "half-whirl" instability of the system.

In 1944, Myklestad and in 1945, Prohl [4] had extended the Holzer method of calculating torsional frequencies into the matrix transfer method of calculating lateral critical speeds of rotor-bearing systems. It became one of the most powerful tools in solving rotor dynamical problems in the last two decades. More recent investigations have made a slight extension of this work by Myklestad - Prohl to include various effects such as shear deformation and gyroscopic moments. In 1954, Yamamoto [5] presented his study on the rotor forward and backward whirl due to gyroscopic effects. His report gave the researchers deeper insight in the dynamic behavior of simple rotor systems.

With the development of large digital computers, the simulation of complex rotor-bearing systems is made possible. The matrix

transfer method of Myklestad and Prohl has been fully extended into the analysis of critical speeds [6, 7], stability [10, 11], and forced response [17] of complex turborotors. Other methods such as the finite difference and finite element [14, 22, 37] approach were also used in the study of rotor dynamics. The rotor system is simulated by the combination of a large number of small elastic shaft elements. Rotor weights and inertia moment effects are lumped at the mass stations, which are the interconnecting node points of the shaft elements. If a large number of node points (or shaft elements) are used, this discrete element approach usually can give a very close approximation of the real system. With the advances of high-speed computers, transient response motion of rotor-bearing systems were investigated through real time numerical integration of rotor acceleration. Gunter [9] presented analog computer-produced transient orbits of simple rotor models with both linear bearing characteristics and nonlinear fluid film bearing forces. Orbits showing combined effects of synchronous unbalance response and half-frequency whirl instability were presented. The nonlinear case formed finite limit cycles, whereas the linear systems were unbounded. Shen [34] presented a formulation for flexible rotor analysis using the influence coefficient approach. Kirk [33] further discussed the transient motion of multi-mass rotor systems with effects of nonlinear bearing support. He concluded that linear stability analysis of the system can be verified using transient response results. However, he did not point out the use of transient response motion to predict nonlinear stability of the system. Breed

and Castelli [35] also discussed the use of time transient approach in solving shaft dynamic problems with various types of bearings. Their results are compared to theoretical verifications with excellent agreement. Hitching [37] outlined transient approach using finite element approach. He also discussed the effects of random excitation functions and the application of Taylor series and curve fitting to the transient solution.

In the case of simple rotor systems, investigators had found that the transient behavior of the rotor may readily be obtained from direct numerical integration of the equations of motion. However, this may not be the case for a more complex rotor system with a large number of mass stations. The integration of large numbers of equations of motion is extremely time consuming and may lead to serious numerical problems. A more efficient way to compute transient response of rotor-bearing systems is the modal [39-55] (building block) approach which had long been applied by the structural engineers. Foss [39] in 1958 has outlined the transient response calculations using the damped modes of the system. The system of equations of motion is uncoupled through modal transformation, and the transient response of the system can be calculated directly as a linear function of the damped mode shapes. Lund [51] generalized this concept of using damped modes in transient analysis of large, complex turborotors. He demonstrated the procedure by its application on an industrial 8-stage compressor and obtained transient results with close accuracy. Black [29] further expanded this concept of modal resolution in the balancing of

synchronous vibration in flexible multimass rotors with nonconservative cross-coupling.

Since damped modes of rotor systems are more difficult and time consuming to obtain than the undamped modes, the similar trend of modal analysis using the undamped modes were also suggested. Caughey [54] presented a detailed discussion on the orthogonality conditions of modes (or eigenvectors) in damped linear dynamic systems. Bishop [27] used the undamped modes to uncouple the dynamical equations of motion in his modal balancing procedure. He adopted the "proportional damping" assumption, which is a common practice for structural engineers to further simplify modal equations of motion. However, this assumption is accurate only when small damping is present in the system and will not be accurate for systems with hydrodynamic bearings or seals. Lund [31] further expanded this concept of modal balancing using the free shaft modes. Klosterman [53] investigated the experimental extraction of free undamped modes from a shaker table and the use of the free modes in a building block approach to system analysis. He illustrated his method on the balancing of multi-plane rotor bearing system as well as transient dynamic analysis. Childs [40 - 44] performed a complete investigation in using undamped modes calculated from the averaged vertical and horizontal support stiffness of the system. He outlined the modal treatment by rigid body dynamics derived from rotating coordinates. This formulation takes into account bearing constraints which may be nonlinear, such as fluid film bearings [60] or elastic rolling element bearings with dead band. He demonstrated the use of this modal

analysis by a complete dynamic analysis of the space shuttle main engine fuel pump. His solutions were verified by experimental results from test facilities.

Morton [32] reported that better accuracy can be achieved by using both "free-free" and "pin-pin" modes during modal treatment of the equations of motion. He pointed out that the modal equations are coupled when both sets of modes are used, but the computational effort for solution will not be much greater than solving the uncoupled equations. He verified this procedure by comparing his solutions to the exact solution and came up with excellent agreement.

The formulations for the transient solution of flexible rotor-bearing systems are excellent approaches to a very difficult problem. However, a simple but complete scheme of simulating the dynamics of rotor-bearing systems has not been developed. The following analysis presents a derivation of the equations of motion for rotor-bearing systems including the effects of gyroscopic, unbalance, disk skew, shaft bow, nonlinear bearings, moment-resisting bearings, and rotor acceleration. The application of modal analysis to uncouple the equations of motion simplifies stability, steady state unbalance response, and transient response analysis of the system. Nonlinear stability of the system can be predicted by frequency spectrums calculated from Fourier transformation of the transient solution.

### 1.3 Statement of the Problem

The purpose of this analysis is to present the formulation of a simple and fast method for the complete simulation of rotor-bearing systems. This analysis will provide designers with complete design information such as critical speed and modes, amplification factors, stability, steady state and transient forced response, and frequency spectrum of the system without involving a large scale of computational costs.

## II. FORMULATION OF EQUATIONS OF MOTION

In the design of high speed rotating machinery, it is often necessary that the machinery must operate through several rotor bending critical speeds to obtain the speed required in present applications and optimal operations. In order to simulate real rotor motion or to predict rotor dynamic behavior accurately, this class of machinery must be analyzed under the general field of study known as flexible rotor dynamics. This assumes that neither the rotor itself will act as a rigid body nor the bearings in the system will be infinitely stiff, but their stiffness may vary with operating speeds and applied external loadings. The general assumption of "small deflection" is used in this study such that the shaft is linearly elastic with applied loads. This assumption is valid for most rotor systems as the deformation of the rotor is always quite small in comparison to the shaft span, but it may not be accurate for bearing force calculations when the rotor motion is relatively large. When large rotor response occurs at the bearings, nonlinear bearing forces have to be incorporated in the system for accurate forced transient response analysis.

In general, a typical rotor system may consist of multiple bearings, and the rotor shaft may have disks or impellers located inboard or outboard to the main bearings. Special characteristics may include unbalances in the disks and impellers, skew of the disk to the rotor shaft, and mechanical bow of the shaft, which may be considered as part of the external forces acting on the rotor.

## 2.1 General Equations of Motion

In deriving the general equations of motion for a multimass bearing system, the rotor is divided into discrete mass stations such that the dynamics of the rotor system can be represented by forces and displacements at the mass stations. The rotor section between two consecutive mass stations is assumed to be massless while the weight of the rotor element is lumped at the two mass stations at each side of the element. Bending moments are assumed to vary linearly along the element using the "small deflection" assumption.

The general equations of motion for a multimass rotor system can be obtained by summing all the forces and moments acting at the  $i^{\text{th}}$  station of the shaft. The forces and moments acting at the  $i^{\text{th}}$  station may generally be composed of shaft elastic reactions, unbalance forces, inertia moments, shaft mechanical bow reactions, bearing or seal forces, or other external hydraulic forces acting on the system. A schematic of the forces and moments acting at the  $i^{\text{th}}$  station in the x-y plane is shown in Figure 2.1. The forces and moments acting at this station are represented by

$V_{i-1x}^R$  = shear force acting the right end of shaft element  $i-1$  (left side of station  $i$ ) in the x-direction

$V_{ix}^L$  = shear force acting at the left end of shaft element  $i$  (right side of station  $i$ ) in the x-direction

$m_i \ddot{x}_i$  = inertia force of the concentrated mass at station  $i$



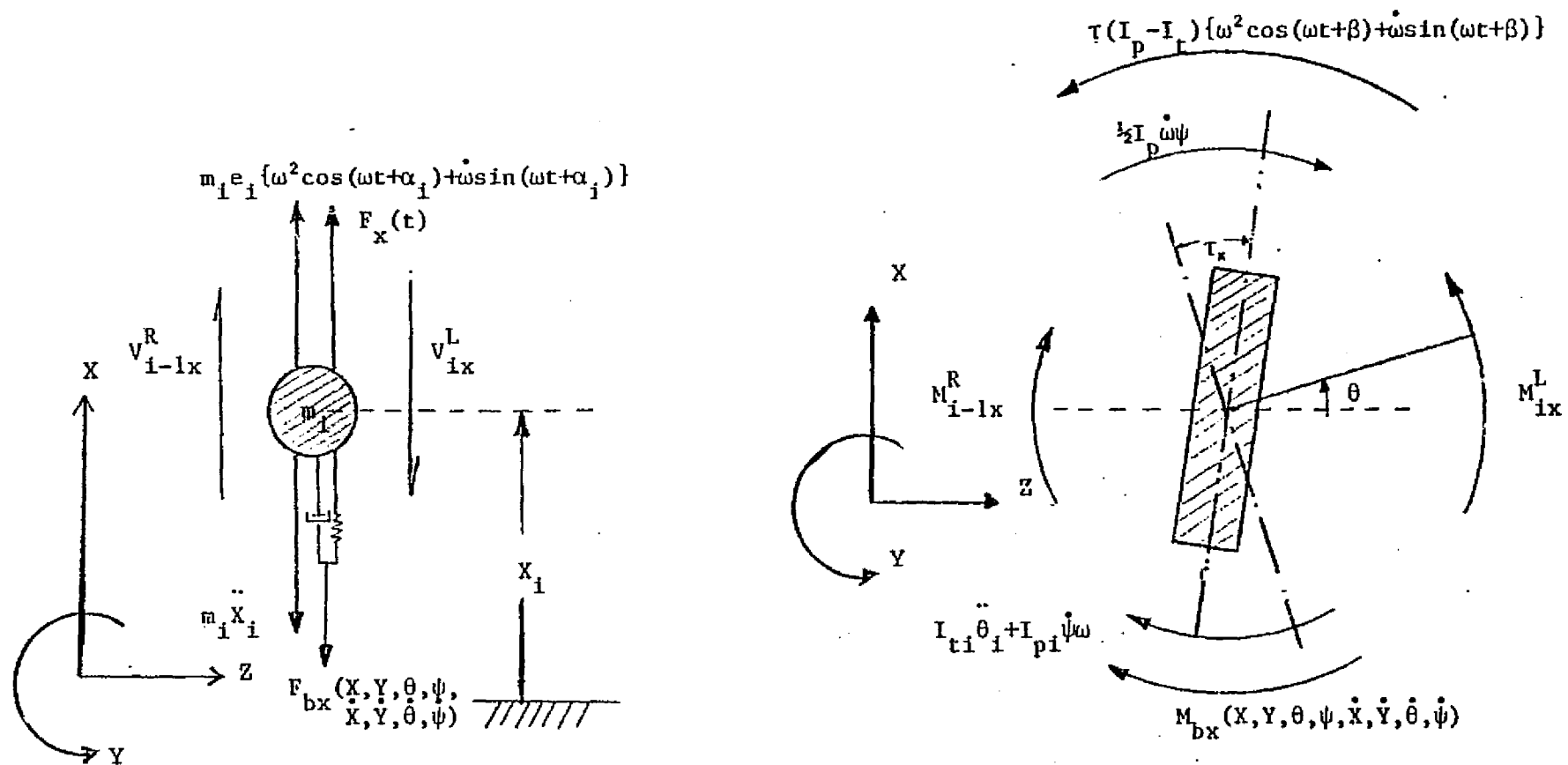


Figure 2.1 FORCES AND MOMENTS ACTING AT ROTOR MASS STATION IN X-Z PLANE

$F_{bx}(x, y, \dot{x}, \dot{y})$  = bearing forces acting at station  $i$  in x-direction

$m_i e_i [\omega^2 \cos(\omega t + \alpha_i) + \dot{\omega} \sin(\omega t + \alpha_i)]$  = x-direction unbalance  
force at stations  $i$  [33]

$F_x(t)$  = external force in x-direction at  $i^{\text{th}}$  station

$M_{i-1}^R$  = moment acting at right end of  $(i-1)^{\text{th}}$  shaft member (left side of  $i^{\text{th}}$  station)

$M_{ix}^L$  = moment acting at left end of  $i^{\text{th}}$  shaft member (right side of  $i^{\text{th}}$  station)

$I_{ti} \ddot{\theta}_i$  = moment due to angular acceleration at  $i^{\text{th}}$  station in x-z planes

$I_{pi} \dot{\omega}$  = gyroscopic moment at  $i^{\text{th}}$  station in x-z plane

$I_{pi} \dot{\omega} \psi$  = moment at  $i^{\text{th}}$  station in x-z plane due to rotor acceleration

$(I_p - I_{ti})_i [\omega^2 \cos(\omega t + \beta_i) + \dot{\omega} \sin(\omega t + \beta_i)]$  [33] = moment at  $i^{\text{th}}$   
station in the x-z plane due to disc skew

$M_{bx}(x, y, \theta, \psi, \dot{x}, \dot{y}, \dot{\theta}, \dot{\psi})$  = moment due to fluid film bearing forces

Figure 2.2 represents the translational and rotational displacements of the  $i^{\text{th}}$  shaft element (located between mass stations  $i$  and  $i+1$ ) and their displacements are represented by

$x_i$  = total displacement in x-direction at  $i^{\text{th}}$  station

$x_{ei}$  = elastic displacement in x-direction at  $i^{\text{th}}$  station

$x_{di}$  = residual (mechanical) bow in x-direction at  $i^{\text{th}}$  station

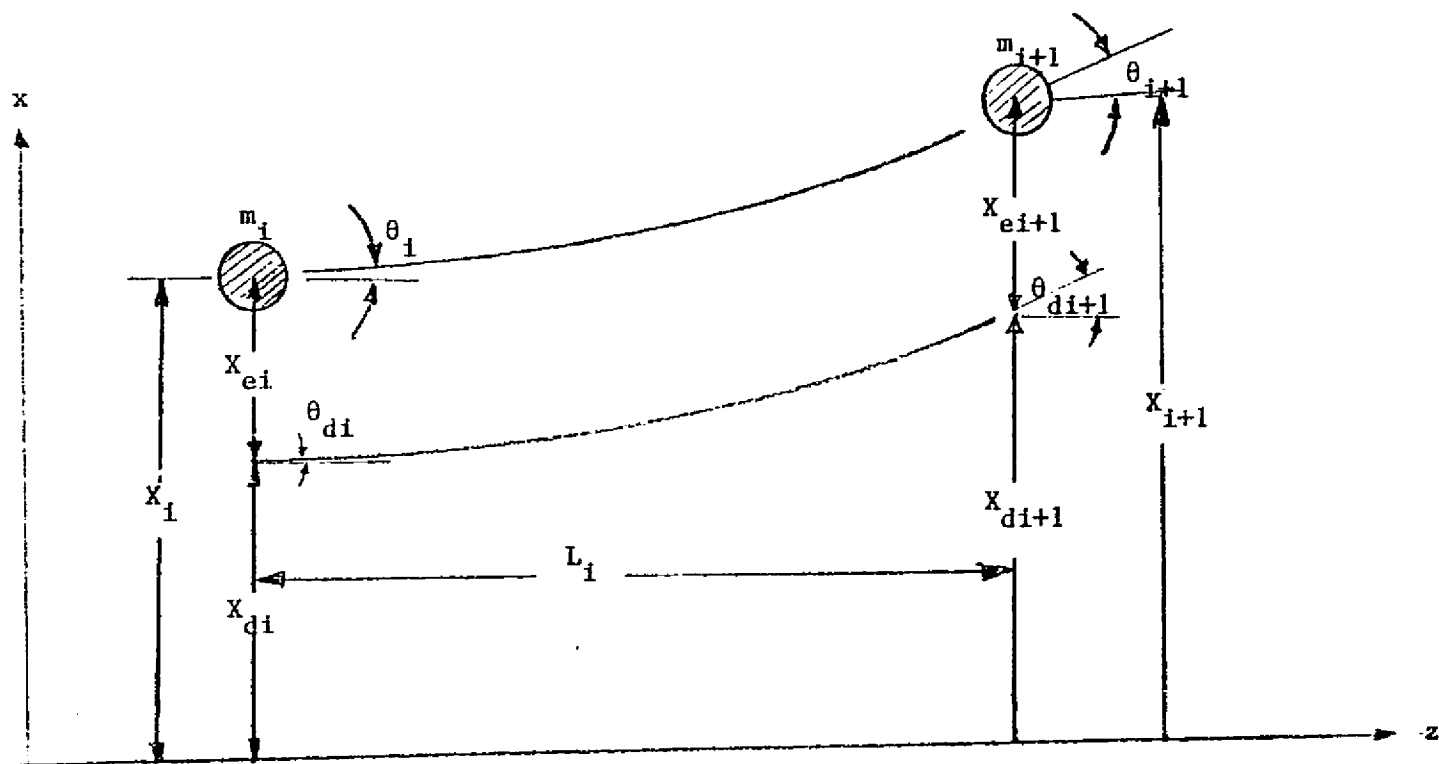


Figure 2.2 DISPLACEMENTS AND ROTATIONS OF SHAFT ELEMENT IN  $X$ - $Z$  PLANE

- $\theta_i$  = total rotation at  $i^{\text{th}}$  station (x-z plane)  
 $\psi_i$  = total rotation at  $i^{\text{th}}$  station (y-z plane)  
 $\theta_{ei}$  = elastic rotation of shaft at  $i^{\text{th}}$  station  
 $\theta_{di}$  = rotation at  $i^{\text{th}}$  station due to residual bow  
 $\tau$  = permanent disk skew at  $i^{\text{th}}$  station  
 $\tau_x = \tau \cos \beta$   
 $\tau_y = \tau \sin \beta$

The basic equations of motion can now be obtained by summing the external and inertia forces and moments in figure 2.1. Thus:

1. Summation of forces in x-direction

$$M_i \ddot{x}_i + V_{ix}^L - V_{i-1x}^R + F_{bx}(x, y, \theta, \psi, \dot{x}, \dot{y}, \dot{\theta}, \dot{\psi}) = F_{xi}(t) \quad (2.1)$$

2. Summation of forces in y-direction

$$M_i \ddot{y}_i + V_{iy}^L - V_{i-1y}^R + F_{by}(x, y, \theta, \psi, \dot{x}, \dot{y}, \dot{\theta}, \dot{\psi}) = F_{yi}(t) \quad (2.2)$$

3. Summation of moments at the  $i^{\text{th}}$  station

$$I_{ti} \ddot{\theta}_i + I_{pi} \dot{\omega} + M_{i-1x}^R - M_{ix}^L + I_{pi} \dot{\omega} \psi + M_{bx}(x, y, \theta, \psi, \dot{x}, \dot{y}, \dot{\theta}, \dot{\psi}) = M_{xi}(t) \quad (2.3)$$

$$\begin{aligned}
 I_{ti} \ddot{\psi}_i - I_{pi} \ddot{\theta} \omega + M_{i-1y}^R - M_{iy}^L - \frac{1}{2} I_{pi} \dot{\omega} \theta + M_{by} (x, y, \theta, \psi, \dot{x}, \dot{y}, \dot{\theta}, \dot{\psi}) \\
 = M_{yi}(t)
 \end{aligned}
 \quad (2.4)$$

The total system equations of motion may now be obtained by substituting the relationships for the unbalance and external forces, bearing forces, and elastic shaft moment-shear deflection relationships into equations (2.1) through (2.4) for the  $i^{\text{th}}$  mass station and summing the  $i^{\text{th}}$  station equations. The generalized shaft stiffness matrix  $[K_x]$  is a function of the assumed boundary conditions which are normally taken to be free-free ( $V_0^R = M_0^R = V_N^L = M_N^L = 0$ ).

If the external forces and moments are due to the unbalance of the rotor and the skew of the disk, then

$$\begin{Bmatrix} F_{xi}(t) \\ F_{yi}(t) \end{Bmatrix} = M_i e_i \left\{ \omega^2 \begin{Bmatrix} \cos(\omega t + \alpha_i) \\ \sin(\omega t + \alpha_i) \end{Bmatrix} + \dot{\omega} \begin{Bmatrix} \sin(\omega t + \alpha_i) \\ -\cos(\omega t + \alpha_i) \end{Bmatrix} \right\}
 \quad (2.5)$$

$$\begin{Bmatrix} M_{xi}(t) \\ M_{yi}(t) \end{Bmatrix} = \tau_i (I_p - I_t)_i \left\{ \omega^2 \begin{Bmatrix} \cos(\omega t + \beta_i) \\ \sin(\omega t + \beta_i) \end{Bmatrix} + \dot{\omega} \begin{Bmatrix} \sin(\omega t + \beta_i) \\ -\cos(\omega t + \beta_i) \end{Bmatrix} \right\}
 \quad (2.6)$$

where  $\alpha_i$  and  $\beta_i$  are the angles of the unbalance and disk skew with respect to the shaft and reference mark. The shear and moment relations are given as follows (see Appendix B)

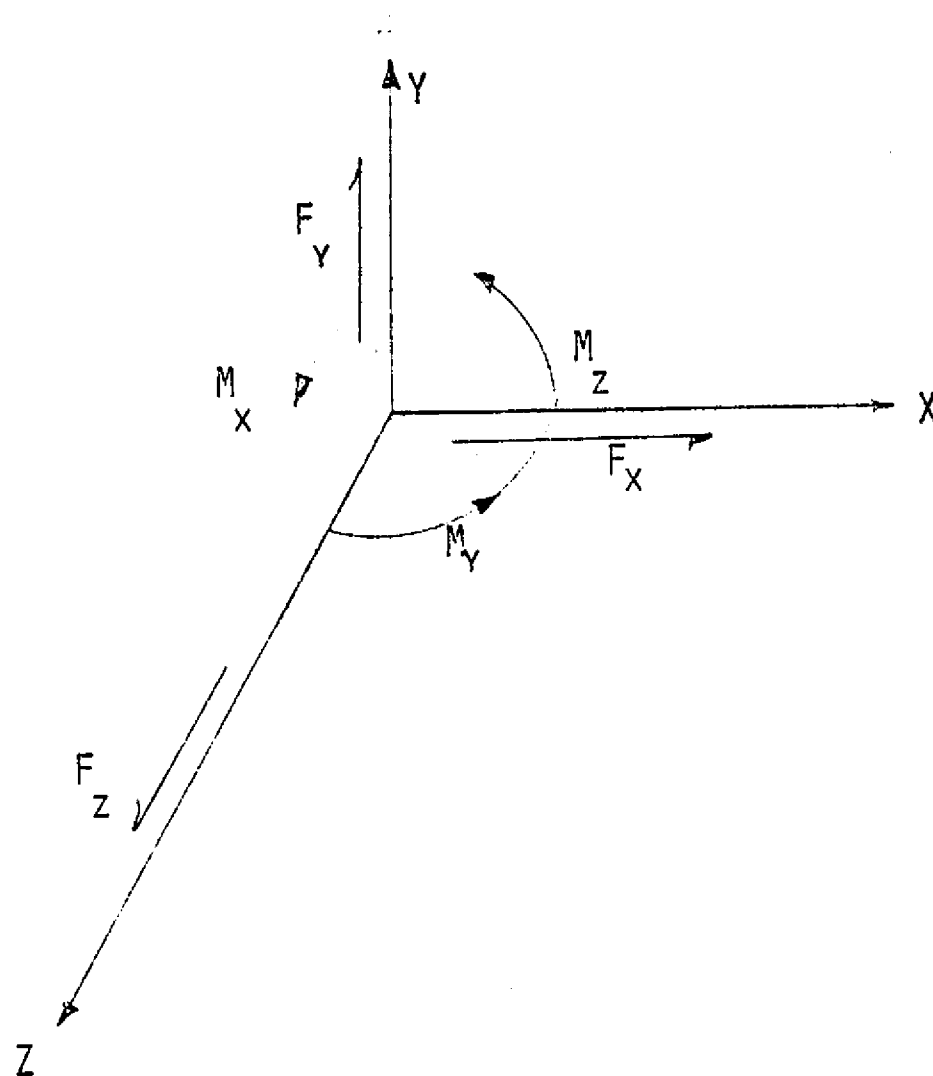


Figure 2.3 RIGHT-HAND CONVENTION USED IN ROTOR MODEL

$$v_{ix}^L = v_{ix}^R = \left(\frac{6EI}{L^3}\right)_i \left[ 2X_{ei} + \theta_{ei} L_i - 2X_{ei+1} + \theta_{ei+1} L_i \right] \quad (2.7)$$

$$M_{ix}^L = \left(\frac{2EI}{L^2}\right)_i \left[ -3X_{ei} - 2\theta_{ei} L_i + 3X_{ei+1} - \theta_{ei+1} L_i \right] \quad (2.8)$$

$$M_{ix}^R = L_i v_{ix}^L + M_{ix}^L \quad (2.9)$$

In terms of total deflections and residual deflections, equation (2.7) and (2.8) can be written as

$$v_{ix}^L = v_{ix}^R = \left(\frac{6EI}{L^3}\right)_i \left[ 2X_i + \theta_i L_i - 2X_{i+1} + \theta_{i+1} L_i \right] - \left(\frac{6EI}{L^3}\right)_i \left[ 2X_{di} + \theta_{di} L_i - 2X_{di+1} + \theta_{di+1} L_i \right] \quad (2.10)$$

$$M_{ix}^L = \left(\frac{2EI}{L^2}\right)_i \left[ -3X_i - 2\theta_i L_i + 3X_{i+1} - \theta_{i+1} L_i \right] - \left(\frac{2EI}{L^2}\right)_i \left[ -3X_{di} - 2\theta_{di} L_i + 3X_{di+1} - \theta_{di+1} L_i \right] \quad (2.11)$$

$$M_{ix}^R = \left(\frac{2EI}{L^2}\right)_i \left[ 3X_i + \theta_i L_i - 3X_{i+1} + 2\theta_{i+1} L_i \right] - \left(\frac{2EI}{L^2}\right)_i \left[ 3X_{di} + \theta_{di} L_i - 3X_{di+1} + 2\theta_{di+1} L_i \right] \quad (2.12)$$

The moment and shear relationships given by equations (2.9) through (2.12) for the massless uniform shaft element may be expressed in terms of the stiffness matrix for the  $i^{\text{th}}$  section as follows:

$$\begin{bmatrix} V_{ix}^L \\ M_{ix}^L \\ V_{ix}^R \\ M_{ix}^R \end{bmatrix} = \left( \frac{EI}{L^3} \right)_i \begin{bmatrix} 12 & 6L & -12 & 6L \\ -6L & -4L^2 & 6L & -2L^2 \\ 12 & 6L & -12 & 6L \\ 6L & 2L^2 & -6L & 4L^2 \end{bmatrix} \begin{bmatrix} X_i - X_{di} \\ \theta_i - \theta_{di} \\ X_{i+1} - X_{di+1} \\ \theta_{i+1} - \theta_{di+1} \end{bmatrix} \quad (2.13)$$

In finite element theory, a right-hand coordinate system is used such as shown in figure 2.3. With this coordinate system, the shears and moment are given by

$$\begin{bmatrix} F_{ix} \\ \bar{M}_{iy} \\ F_{i+1x} \\ \bar{M}_{i+1y} \end{bmatrix} = \left( \frac{EI}{L^3} \right)_i \begin{bmatrix} 12 & 6L & -12 & 6L \\ 6L & 4L^2 & -6L & 2L^2 \\ -12 & -6L & 12 & -6L \\ 6L & 2L^2 & -6L & -4L^2 \end{bmatrix} \begin{bmatrix} X_i - X_{di} \\ \theta_i - \theta_{di} \\ X_{i+1} - X_{di+1} \\ \theta_{i+1} - \theta_{di+1} \end{bmatrix} \quad (2.14)$$

and, similarly, for the y-z plane as



$$\begin{bmatrix} F_{iy} \\ -M_{ix} \\ F_{i+1y} \\ -M_{i+1x} \end{bmatrix} = \left( \frac{EI}{L^3} \right)_i \begin{bmatrix} 12 & -6L & -12 & -6L \\ -6L & 4L^2 & 6L & 2L^2 \\ -12 & 6L & 12 & 6L \\ -6L & 2L^2 & 6L & 4L^2 \end{bmatrix} \begin{bmatrix} Y_i - Y_{di} \\ \psi_i - \psi_{di} \\ Y_{i+1} - Y_{di+1} \\ \psi_{i+1} - \psi_{di+1} \end{bmatrix} \quad (2.15)$$

The stiffness matrices in equation (2.14) and (2.15) represent the generalized element stiffness matrix for a beam, which are derived from first principles [67, 68]. The bearing forces can be expanded, and if a linear bearing is assumed, then in matrix form the bearing forces and moments are given by

$$\begin{Bmatrix} F_{bx} \\ M_{bx} \\ F_{by} \\ M_{by} \end{Bmatrix}_i = \begin{bmatrix} K_{xx} & K_{x\theta} & K_{xy} & K_{x\psi} \\ K_{\theta x} & K_{\theta\theta} & K_{\theta y} & K_{\theta\psi} \\ K_{yx} & K_{y\theta} & K_{yy} & K_{y\psi} \\ K_{\psi x} & K_{\psi\theta} & K_{\psi y} & K_{\psi\psi} \end{bmatrix}_i \begin{Bmatrix} x \\ \theta \\ y \\ \psi \end{Bmatrix}_i + \begin{bmatrix} C_{xx} & C_{x\theta} & C_{xy} & C_{x\psi} \\ C_{\theta x} & C_{\theta\theta} & C_{\theta y} & C_{\theta\psi} \\ C_{yx} & C_{y\theta} & C_{yy} & C_{y\psi} \\ C_{\psi x} & C_{\psi\theta} & C_{\psi y} & C_{\psi\psi} \end{bmatrix}_i \begin{Bmatrix} \dot{x} \\ \dot{\theta} \\ \dot{y} \\ \dot{\psi} \end{Bmatrix}_i \quad (2.16)$$

Substituting the above relationships into equations (2.1), (2.2), (2.3) and (2.4), the system equations of motion can now be written in matrix form as follows:

$$[M] \{\ddot{U}\} + [C] \{\dot{U}\} + [K] \{U\} = \{F(t)\} + [K_g] \{U_d\} \quad (2.17)$$

where

$$U = \begin{Bmatrix} (x) \\ (\theta) \\ (y) \\ (\psi) \end{Bmatrix}, \quad U_d = \begin{Bmatrix} (x_d) \\ (\theta_d) \\ (y_d) \\ (\psi_d) \end{Bmatrix}$$

and

$$[\bar{M}] = \begin{bmatrix} [M] & 0 & 0 & 0 \\ 0 & [I_t] & 0 & 0 \\ 0 & 0 & [M] & 0 \\ 0 & 0 & 0 & [I_t] \end{bmatrix}$$

The damping matrix can be decomposed into the gyroscopic and bearing damping submatrices for future convenience as follows

$$[C] = \begin{bmatrix} 0 & 0 & 0 & 0 \\ 0 & 0 & 0 & [\omega I_p] \\ 0 & 0 & 0 & 0 \\ 0 & [-\omega I_p] & 0 & 0 \end{bmatrix}_G + \begin{bmatrix} [c_{xx}] & [c_{x\theta}] & [c_{xy}] & [c_{x\psi}] \\ [c_{\theta x}] & [c_{\theta\theta}] & [c_{\theta y}] & [c_{\theta\psi}] \\ [c_{yx}] & [c_{y\theta}] & [c_{yy}] & [c_{y\psi}] \\ [c_{\psi x}] & [c_{\psi\theta}] & [c_{\psi y}] & [c_{\psi\psi}] \end{bmatrix}_B \quad (2.18)$$

The general stiffness matrix may also be decomposed into three submatrices representing the symmetric shaft stiffness matrix, the linear bearing stiffness matrix, and the skew symmetric acceleration matrix as follows

$$\begin{aligned}
 [K] = & \begin{bmatrix} [k_{xx}] & [k_{x\theta}] & 0 & 0 \\ [k_{\theta x}] & [k_{\theta\theta}] & 0 & 0 \\ 0 & 0 & [k_{xx}] & [k_{x\theta}] \\ 0 & 0 & [k_{\theta x}] & [k_{\theta\theta}] \end{bmatrix}_S + \begin{bmatrix} [K_{xx}] & [K_{x\theta}] & [K_{xy}] & [K_{x\psi}] \\ [K_{\theta x}] & [K_{\theta\theta}] & [K_{\theta y}] & [K_{\theta\psi}] \\ [K_{yx}] & [K_{y\theta}] & [K_{yy}] & [K_{y\psi}] \\ [K_{\psi x}] & [K_{\psi\theta}] & [K_{\psi y}] & [K_{\psi\psi}] \end{bmatrix}_B \\
 & + \begin{bmatrix} 0 & 0 & 0 & 0 \\ 0 & 0 & 0 & \left[ \frac{\dot{\omega}}{2} I_P \right] \\ 0 & 0 & 0 & 0 \\ 0 & \left[ -\frac{\dot{\omega}}{2} I_P \right] & 0 & 0 \end{bmatrix}_A
 \end{aligned} \quad (2.19)$$

For free-free boundary conditions, the shaft stiffness submatrices are given by (see Appendix B)

$$[k_{xx}] = 2 \begin{bmatrix} E_1 & -E_1 & 0 & \dots & 0 & 0 \\ -E_1 & E_1 + E_2 & -E_2 & \dots & 0 & 0 \\ \dots & \dots & \dots & -E_{n-2} & E_{n-2} + E_{n-1} & -E_{n-1} \\ 0 & 0 & 0 & 0 & -E_{n-1} & E_{n-1} \end{bmatrix}$$

$$\begin{bmatrix} k_{x\theta} \end{bmatrix} = \begin{bmatrix} k_{\theta x} \end{bmatrix}^T =$$

$$\begin{bmatrix} E_1 L_1 & E_1 L_1 & 0 & \dots & 0 & 0 \\ -E_1 L_1 & -E_1 L_1 + E_2 L_2 & E_2 L_2 & \dots & 0 & 0 \\ \dots & \dots & \dots & -E_{n-2} L_{n-2} & -E_{n-2} L_{n-2} + E_{n-1} L_{n-1} & E_{n-1} L_{n-1} \\ 0 & 0 & \dots & 0 & -E_{n-1} L_{n-1} & -E_{n-1} L_{n-1} \end{bmatrix}$$

$$\begin{bmatrix} k_{\theta\theta} \end{bmatrix} = \frac{1}{3} \begin{bmatrix} 2E_1 L_1^2 & E_1 L_1^2 & 0 & 0 & 0 & 0 \\ E_1 L_1^2 & 2E_1 L_1^2 + 2E_2 L_2^2 & E_2 L_2^2 & 0 & 0 & 0 \\ \dots & \dots & \dots & E_{n-2} L_{n-2}^2 & 2E_{n-2} L_{n-2}^2 + 2E_{n-1} L_{n-1}^2 & E_{n-1} L_{n-1}^2 \\ 0 & 0 & \dots & 0 & E_{n-1} L_{n-1}^2 & 2E_{n-1} L_{n-1}^2 \end{bmatrix}$$

$$\text{where } E_i = \left( \frac{6EI}{L^3} \right)_i$$

## 2.2 Illustration of Equations of Motion for a 3-Mass Rotor

In order to illustrate the development of the generalized equations for an arbitrary N-mass rotor system with the appropriate boundary conditions, a derivation is applied to a 3-mass rotor as shown in figure 2.4. This model consists of a skewed disc in the center of a flexible shaft supported by two linear bearings. The shaft has a mechanical bow of  $x_{d2}$  at the disc location while  $x_{d1}$  and  $x_{d3}$  at the bearings are assumed to be zero.

Summing the forces in the x-direction for the left bearing station (station 1), equation (2.1) can be written as

$$m_1 \ddot{X}_1 + C_{xx}^1 \dot{X}_1 + C_{xy}^1 \dot{Y}_1 + K_{xx}^1 X_1 + K_{xy}^1 Y_1 + V_1^L - V_0^R = F_{x1}(t) \quad (2.20)$$

Equation 2.20 can be further expanded assuming  $V_0^R = 0$

$$\begin{aligned} m_1 \ddot{X}_1 + C_{xx}^1 \dot{X}_1 + C_{xy}^1 \dot{Y}_1 + K_{xx}^1 X_1 + K_{xy}^1 Y_1 + \left( \frac{12EI}{L_1^3} (X_1 - x_{d1}) \right. \\ \left. + \frac{6EI}{L_1^2} (\theta_1 - \theta_{d1}) - \frac{12EI}{L_1^3} (X_2 - x_{d2}) + \frac{6EI}{L_1^2} (\theta_2 - \theta_{d2}) \right) = 0 \end{aligned} \quad (2.21)$$

For station 2, the summation of forces at x-direction gives

$$m_2 \ddot{X}_2 + V_{2x}^L - V_{1x}^R = F_{x2}(t) \quad (2.22)$$

\*Superscripts in bearing coefficients indicate station numbers.

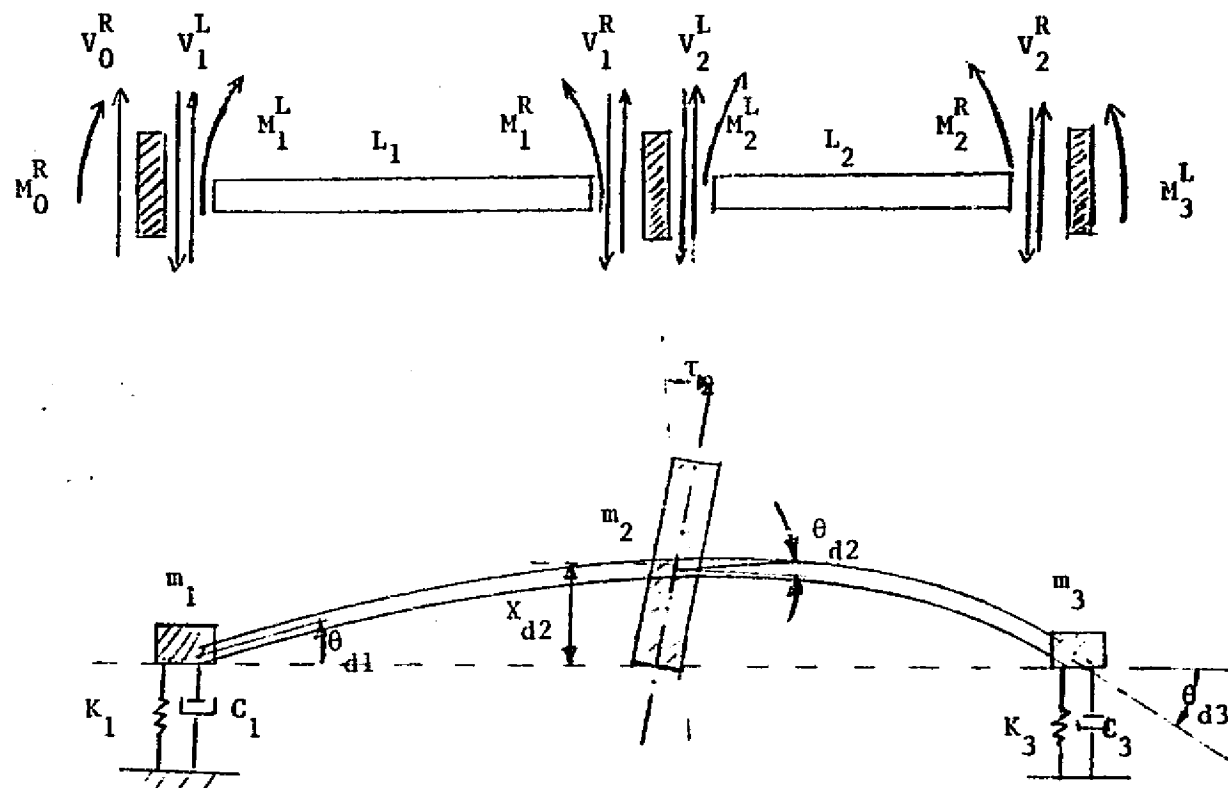


Figure 2.4 THREE MASS BOWED ROTOR SYSTEM WITH SKEWED DISC

and by substituting the shear-displacement relationships, equation (2.22) becomes

$$\begin{aligned}
 m_2 \ddot{x}_2 + \left[ \frac{12EI}{L_2^3} (x_2 - x_{d2}) + \frac{6EI}{L_2^2} (\theta_2 - \theta_{d2}) - \frac{12EI}{L_2^3} (x_3 - x_{d3}) \right. \\
 \left. + \frac{6EI}{L_2^2} (\theta_3 - \theta_{d3}) \right] - \left[ \frac{12EI}{L_1^3} (x_1 - x_{d1}) + \frac{6EI}{L_1^2} (\theta_1 - \theta_{d1}) - \frac{12EI}{L_1^3} (x_2 - x_{d2}) \right. \\
 \left. + \frac{6EI}{L_1^2} (\theta_2 - \theta_{d2}) \right] = m_2 e_2 \left[ \omega^2 \cos (\omega t + \alpha_2) + \dot{\omega} \sin (\omega t + \alpha_2) \right] \quad (2.23)
 \end{aligned}$$

Similarly, the summation of forces at station 3 gives

$$m_3 \ddot{x}_3 + V_{3x}^L - V_{2x}^R = F_{x3}$$

where  $V_{3x}^L = 0$

$$\begin{aligned}
 m_3 \ddot{x}_3 + c_{xx}^3 \dot{x}_3 + c_{xy}^3 \dot{y}_3 + k_{xx}^3 x_3 + k_{xy}^3 y_3 - \left[ \frac{12EI}{L_2^3} x_2 - x_{d2} \right. \\
 \left. + \frac{6EI}{L_2^2} (\theta_2 - \theta_{d2}) - \frac{12EI}{L_2^3} (x_3 - x_{d3}) + \frac{6EI}{L_2^2} (\theta_3 - \theta_{d3}) \right] = 0 \quad (2.24)
 \end{aligned}$$

The moment equations are obtained by summing the moments at each individual station. At station 1 assuming no gyroscopic or bearing moments

$$M_0^R = M_1^L = 0 \quad (2.25)$$

or

$$\left[ \frac{6EI}{L_1^2} (x_1 - x_{d1}) + \frac{4EI}{L_1} (\theta_1 - \theta_{d1}) - \frac{6EI}{L_1^2} (x_2 - x_{d2}) + \frac{2EI}{L_1} (\theta_2 - \theta_{d2}) \right] = 0 \quad (2.26)$$

at station 2, the moment equation is

$$M_1^R - M_2^L + M_2^G = M_2(t) \quad (2.27)$$

or Equation (2.24) can be expanded with the following form

$$\begin{aligned} & \left[ \frac{6EI}{L_1^2} (x_1 - x_{d1}) + \frac{2EI}{L_1} (\theta_1 - \theta_{d1}) - \frac{6EI}{L_1^2} (x_2 - x_{d2}) + \frac{4EI}{L_1} (\theta_2 - \theta_{d2}) \right] \\ & - \left[ -\frac{6EI}{L_2^2} (x_2 - x_{d2}) - \frac{4EI}{L_2} (\theta_2 - \theta_{d2}) + \frac{6EI}{L_2^2} (x_3 - x_{d3}) - \frac{2EI}{L_2} (\theta_3 - \theta_{d3}) \right] \\ & + I_{t2} \ddot{\theta}_2 + \omega I_{p2} \dot{\psi}_2 + 1/2 \dot{\omega} I_{p2} \psi_2 = \tau (I_{p2} - I_{t2}) \left( \omega^2 \cos(\omega t + \beta_2) + \dot{\omega} \sin(\omega t + \beta_2) \right) \end{aligned} \quad (2.28)$$



The moment relationship at station 3 is similar to station 1 and can be written as

$$M_3^L = M_2^R = 0 = E_2 L_2 \left( x_{e2} + L_2 \frac{\theta_2}{3} - x_{e3} + \frac{2}{3} L_2 \theta_3 \right) \quad (2.29)$$

Combining the three force equations and the three moment equations, the equations of motion for the x-z plane can be written in matrix form as follows

$$\begin{bmatrix} m_1 & 0 & 0 & 0 & 0 & 0 \\ 0 & m_2 & 0 & 0 & 0 & 0 \\ 0 & 0 & m_3 & 0 & 0 & 0 \\ \hline 0 & 0 & 0 & 0 & 0 & 0 \\ 0 & 0 & 0 & 0 & I_{t2} & 0 \\ 0 & 0 & 0 & 0 & 0 & 0 \end{bmatrix} \begin{bmatrix} \ddot{x}_1 \\ \ddot{x}_2 \\ \ddot{x}_3 \\ \hline \ddot{\theta}_1 \\ \ddot{\theta}_2 \\ \ddot{\theta}_3 \end{bmatrix} + \begin{bmatrix} C_{xx}^1 & 0 & 0 & 0 & 0 & 0 \\ 0 & 0 & 0 & 0 & 0 & 0 \\ 0 & 0 & C_{xx}^1 & 0 & 0 & 0 \\ \hline 0 & 0 & 0 & 0 & 0 & 0 \\ 0 & 0 & 0 & 0 & 0 & 0 \\ 0 & 0 & 0 & 0 & 0 & 0 \end{bmatrix} \begin{bmatrix} \dot{x}_1 \\ \dot{x}_2 \\ \dot{x}_3 \\ \hline \dot{\theta}_1 \\ \dot{\theta}_2 \\ \dot{\theta}_3 \end{bmatrix}$$

$$\begin{bmatrix} 2E_1 & -2E_1 & 0 & E_1 L_1 & E_1 L_1 & 0 \\ -2E_1 & 2E_1 + 2E_2 & -2E_2 & -E_1 L_1 & -E_1 L_1 + E_2 L_2 & E_2 L_2 \\ 0 & -2E_2 & 2E_2 & 0 & -E_2 L_2 & -E_2 L_2 \\ \hline E_1 L_1 & -E_1 L_1 & 0 & \frac{2}{3} E_1 L_1^2 & \frac{1}{3} E_1 L_1^2 & 0 \\ E_1 L_1 & -E_1 L_1 + E_2 L_2 & -E_2 L_2 & \frac{1}{3} E_1 L_1^2 & \frac{2}{3} E_1 L_1^2 + \frac{2}{3} E_2 L_2^2 & \frac{1}{3} E_2 L_2^2 \\ 0 & E_2 L_2 & -E_2 L_2 & 0 & \frac{1}{3} E_2 L_2^2 & \frac{2}{3} E_2 L_2^2 \end{bmatrix} \begin{bmatrix} x_1 - x_{d1} \\ x_2 - x_{d2} \\ x_3 - x_{d3} \\ \hline \theta_1 - \theta_{d1} \\ \theta_2 - \theta_{d2} \\ \theta_3 - \theta_{d3} \end{bmatrix} +$$

$$\begin{bmatrix} K_{xx}^1 & 0 & 0 & 0 & 0 & 0 \\ 0 & 0 & 0 & 0 & 0 & 0 \\ 0 & 0 & K_{xx}^3 & 0 & 0 & 0 \\ \hline 0 & 0 & 0 & 0 & 0 & 0 \\ 0 & 0 & 0 & 0 & 0 & 0 \\ 0 & 0 & 0 & 0 & 0 & 0 \end{bmatrix} \begin{bmatrix} x_1 \\ x_2 \\ x_3 \\ \psi_1 \\ \psi_2 \\ \psi_3 \end{bmatrix} + \begin{bmatrix} C_{xy}^1 & 0 & 0 & 0 & 0 & 0 \\ 0 & 0 & 0 & 0 & 0 & 0 \\ 0 & 0 & C_{xy}^3 & 0 & 0 & 0 \\ \hline 0 & 0 & 0 & 0 & 0 & 0 \\ 0 & 0 & 0 & 0 & \omega I_{p2} & 0 \\ 0 & 0 & 0 & 0 & 0 & 0 \end{bmatrix} \begin{bmatrix} \dot{y}_1 \\ \dot{y}_2 \\ \dot{y}_3 \\ \dot{\psi}_1 \\ \dot{\psi}_2 \\ \dot{\psi}_3 \end{bmatrix} +$$

$$\begin{bmatrix} K_{xy}^1 & 0 & 0 & 0 & 0 & 0 \\ 0 & 0 & 0 & 0 & 0 & 0 \\ 0 & 0 & K_{xy}^3 & 0 & 0 & 0 \\ \hline 0 & 0 & 0 & 0 & 0 & 0 \\ 0 & 0 & 0 & 0 & \omega I_p & 0 \\ 0 & 0 & 0 & 0 & 0 & 0 \end{bmatrix} \begin{bmatrix} y_1 \\ y_2 \\ y_3 \\ \psi_1 \\ \psi_2 \\ \psi_3 \end{bmatrix} = \begin{bmatrix} 0 \\ m_2 e_2 [\omega^2 \cos(\omega t + \alpha_2) + \dot{\omega} \sin(\omega t + \alpha_2)] \\ 0 \\ \hline 0 \\ \tau(I_p - I_t) [\omega^2 \cos(\omega t + \beta_2) + \dot{\omega} \sin(\omega t + \beta_2)] \\ 0 \end{bmatrix}$$

(2.30)

where  $K_x$  is a 6 x 6 stiffness matrix of the shaft element.

Similarly, a set of matrix equations can be written for the y-z plane as follows

$$\begin{bmatrix} H_1 & 0 & 0 & 0 & 0 & 0 \\ 0 & H_2 & 0 & 0 & 0 & 0 \\ 0 & 0 & H_3 & 0 & 0 & 0 \\ \hline 0 & 0 & 0 & 0 & 0 & 0 \\ 0 & 0 & 0 & 0 & I_{t2} & 0 \\ 0 & 0 & 0 & 0 & 0 & 0 \end{bmatrix} \begin{bmatrix} \dot{y}_1 \\ \dot{y}_2 \\ \dot{y}_3 \\ \dot{\psi}_1 \\ \dot{\psi}_2 \\ \dot{\psi}_3 \end{bmatrix} + \begin{bmatrix} C_{xy}^1 & 0 & 0 & 0 & 0 & 0 \\ 0 & 0 & 0 & 0 & 0 & 0 \\ 0 & 0 & C_{xy}^3 & 0 & 0 & 0 \\ \hline 0 & 0 & 0 & 0 & 0 & 0 \\ 0 & 0 & 0 & 0 & 0 & 0 \\ 0 & 0 & 0 & 0 & 0 & 0 \end{bmatrix} \begin{bmatrix} \dot{y}_1 \\ \dot{y}_2 \\ \dot{y}_3 \\ \dot{\psi}_1 \\ \dot{\psi}_2 \\ \dot{\psi}_3 \end{bmatrix} +$$

$$\begin{bmatrix}
 2E_1 & -2E_1 & 0 & E_1 L_{11} & E_1 L_{11} & 0 \\
 -2E_1 & 2E_1 + 2E_2 & -2E_2 & -E_1 L_{11} & -E_1 L_{11} + E_2 L_{22} & E_2 L_{22} \\
 0 & -2E_2 & 2E_2 & 0 & -E_2 L_{22} & -E_2 L_{22} \\
 \hline
 E_1 L_{11} & -E_1 L_{11} & 0 & 2E_1 L_{11}^2 & \frac{1}{3}E_1 L_{11}^2 & 0 \\
 E_1 L_{11} & -E_1 L_{11} + E_2 L_{22} & -E_2 L_{22} & \frac{1}{3}E_1 L_{11}^2 & \frac{2}{3}E_1 L_{11}^2 + \frac{2}{3}E_2 L_{22}^2 & \frac{1}{3}E_2 L_{22}^2 \\
 0 & E_2 L_{22} & -E_2 L_{22} & 0 & \frac{1}{3}E_2 L_{22}^2 & \frac{2}{3}E_2 L_{22}^2
 \end{bmatrix}
 \begin{bmatrix}
 y_1 - y_{d1} \\
 y_2 - y_{d2} \\
 y_3 - y_{d3} \\
 \psi_1 - \psi_{d1} \\
 \psi_2 - \psi_{d2} \\
 \psi_3 - \psi_{d3}
 \end{bmatrix} +$$

$$\begin{bmatrix}
 K_{yy}^1 & 0 & 0 & 0 & 0 & 0 \\
 0 & 0 & 0 & 0 & 0 & 0 \\
 0 & 0 & K_{yy}^3 & 0 & 0 & 0 \\
 \hline
 0 & 0 & 0 & 0 & 0 & 0 \\
 0 & 0 & 0 & 0 & 0 & 0 \\
 0 & 0 & 0 & 0 & 0 & 0
 \end{bmatrix}
 \begin{bmatrix}
 y_1 \\
 y_2 \\
 y_3 \\
 \psi_1 \\
 \psi_2 \\
 \psi_3
 \end{bmatrix} +
 \begin{bmatrix}
 C_{yx}^1 & 0 & 0 & 0 & 0 & 0 \\
 0 & 0 & 0 & 0 & 0 & 0 \\
 0 & 0 & C_{yx}^3 & 0 & 0 & 0 \\
 \hline
 0 & 0 & 0 & 0 & 0 & 0 \\
 0 & 0 & 0 & 0 & -\omega I_{p2} & 0 \\
 0 & 0 & 0 & 0 & 0 & 0
 \end{bmatrix}
 \begin{bmatrix}
 \dot{x}_1 \\
 \dot{x}_2 \\
 \dot{x}_3 \\
 \dot{\theta}_1 \\
 \dot{\theta}_2 \\
 \dot{\theta}_3
 \end{bmatrix} +$$

$$\begin{bmatrix}
 K_{yx}^1 & 0 & 0 & 0 & 0 & 0 \\
 0 & 0 & 0 & 0 & 0 & 0 \\
 0 & 0 & K_{yx}^3 & 0 & 0 & 0 \\
 \hline
 0 & 0 & 0 & 0 & 0 & 0 \\
 0 & 0 & 0 & 0 & -\frac{1}{2}\omega I_p & 0 \\
 0 & 0 & 0 & 0 & 0 & 0
 \end{bmatrix}
 \begin{bmatrix}
 x_1 \\
 x_2 \\
 x_3 \\
 \theta_1 \\
 \theta_2 \\
 \theta_3
 \end{bmatrix} =
 \begin{bmatrix}
 0 \\
 m_2 e_2 [\omega^2 \sin(\omega t + \alpha_2) - \dot{\omega} \cos(\omega t + \alpha_2)] \\
 0 \\
 \hline
 0 \\
 \tau(I_p - I_e) [\omega^2 \sin(\omega t + \beta_2) - \dot{\omega} \cos(\omega t + \beta_2)] \\
 0
 \end{bmatrix}$$

### 2.3 Direct Method of Solution

In order to illustrate the use of direct method of solution, the three-mass rotor model discussed is used as an example. To simplify numerical computations, the 12th order system as illustrated by equations (2.30) and (2.31) can be reduced to a 6th order system by Guyan reduction. For example, if there are no transverse moments or products of inertia in the system (no rotor gyroscopic or disc skew effects), equation (2.30) can be written as

$$\begin{aligned}
 & \begin{bmatrix} [M] & 0 \\ 0 & 0 \end{bmatrix} \begin{bmatrix} \ddot{(x)} \\ \ddot{(\theta)} \end{bmatrix} + \begin{bmatrix} [C_{xx}] & 0 \\ 0 & 0 \end{bmatrix} \begin{bmatrix} \dot{(x)} \\ \dot{(\theta)} \end{bmatrix} + \begin{bmatrix} [k_{xx}] & [k_{x\theta}] \\ [k_{\theta x}] & [k_{\theta\theta}] \end{bmatrix} \begin{bmatrix} (x - x_d) \\ (\theta - \theta_d) \end{bmatrix} \\
 & + \begin{bmatrix} [K_{xx}] & 0 \\ 0 & 0 \end{bmatrix} \begin{bmatrix} (x) \\ (\theta) \end{bmatrix} + \begin{bmatrix} [C_{xy}] & 0 \\ 0 & 0 \end{bmatrix} \begin{bmatrix} \dot{(y)} \\ \dot{(\psi)} \end{bmatrix} + \\
 & \begin{bmatrix} [k_{xy}] & 0 \\ 0 & 0 \end{bmatrix} \begin{bmatrix} (y) \\ (\psi) \end{bmatrix} = \begin{bmatrix} (F_x) \\ (0) \end{bmatrix} \quad (2.32)
 \end{aligned}$$

and the moment equation can be extracted by

$$[k_{\theta x}] (x - x_d) + [k_{\theta\theta}] (\theta - \theta_d) = 0 \quad (2.33)$$

Assuming  $L_1 = L_2$ ,  $E_1 = E_2$  and using Guyan reduction

$$[M] \ddot{x} + [C_{xx}] \dot{x} + \left[ [k_{xx}] - [k_{x\theta}] [k_{\theta\theta}]^{-1} [k_{\theta x}] \right] (x - x_d) + [C_{xy}] \dot{y}$$

$$[K_{xy}] (y) = (F_x) \quad (2.34)$$

or written in full matrix form as

$$\begin{aligned} & \begin{bmatrix} m_1 & 0 & 0 \\ 0 & m_2 & 0 \\ 0 & 0 & m_3 \end{bmatrix} \begin{Bmatrix} \ddot{x}_1 \\ \ddot{x}_2 \\ \ddot{x}_3 \end{Bmatrix} + \begin{bmatrix} C_{xx}^1 & 0 & 0 \\ 0 & 0 & 0 \\ 0 & 0 & C_{xx}^3 \end{bmatrix} \begin{Bmatrix} \dot{x}_1 \\ \dot{x}_2 \\ \dot{x}_3 \end{Bmatrix} \\ & + \frac{3EI}{L^3} \begin{bmatrix} k_2 & -1 & k_2 \\ -1 & 2 & -1 \\ k_2 & -1 & k_2 \end{bmatrix} \begin{Bmatrix} x_1 - x_{d1} \\ x_2 - x_{d2} \\ x_3 - x_{d3} \end{Bmatrix} + \begin{bmatrix} K_{xx}^1 & 0 & 0 \\ 0 & 0 & 0 \\ 0 & 0 & K_{xx}^3 \end{bmatrix} \begin{Bmatrix} x_1 \\ x_2 \\ x_3 \end{Bmatrix} \\ & + \begin{bmatrix} C_{xy}^1 & 0 & 0 \\ 0 & 0 & 0 \\ 0 & 0 & C_{xy}^3 \end{bmatrix} \begin{Bmatrix} \dot{y}_1 \\ \dot{y}_2 \\ \dot{y}_3 \end{Bmatrix} + \begin{bmatrix} K_{xy}^1 & 0 & 0 \\ 0 & 0 & 0 \\ 0 & 0 & K_{xy}^3 \end{bmatrix} \begin{Bmatrix} y_1 \\ y_2 \\ y_3 \end{Bmatrix} \\ & - \begin{Bmatrix} 0 \\ m_2 e_2 [\omega^2 \cos(\omega t - \alpha_2) + \omega \sin(\omega t - \alpha_2)] \\ 0 \end{Bmatrix} \end{aligned} \quad (2.35)$$

In the set of equations of motion of equation (2.30) and (2.31), there is a disc effect only at the center station. Therefore, the equations of motion corresponding to  $\theta_1$ ,  $\theta_3$  and  $\psi_1$ ,  $\psi_3$  may be eliminated by expressing these quantities in terms of the other station displacement and rotation coordinates.

Using the boundary conditions, equations (2.26) and (2.29) where  $M_{1X}^L = M_{2X}^R = 0$  yields the following relationships

$$\theta_{e1} = \frac{3}{2} \left( \frac{x_{e2} - x_{e1}}{L_1} \right) - \frac{\theta_{e2}}{2} \quad (2.36)$$

$$\theta_{e3} = \frac{3}{2} \left( \frac{x_{e3} - x_{e2}}{L_2} \right) - \frac{\theta_{e2}}{2} \quad (2.37)$$

There is a corresponding set of relationships for the  $\psi_{e1}$  and  $\psi_{e3}$  coordinates.

By the substitution of these relationships into equation (2.30) and (2.31), the 12th order system is reduced to an 8th order system with equations in the x-z plane as follows

$$\begin{bmatrix} m_1 & 0 & 0 & | & 0 \\ 0 & m_2 & 0 & | & 0 \\ 0 & 0 & m_3 & | & 0 \\ \hline 0 & 0 & 0 & | & I_{t2} \end{bmatrix} \begin{Bmatrix} \ddot{x}_1 \\ \ddot{x}_2 \\ \ddot{x}_3 \\ \ddot{\theta}_2 \end{Bmatrix} + \begin{bmatrix} C_{xx}^1 & 0 & 0 & | & 0 \\ 0 & 0 & 0 & | & 0 \\ 0 & 0 & C_{xx}^3 & | & 0 \\ \hline 0 & 0 & 0 & | & 0 \end{bmatrix} \begin{Bmatrix} \dot{x}_1 \\ \dot{x}_2 \\ \dot{x}_3 \\ \dot{\theta}_2 \end{Bmatrix}$$

$$+ \frac{1}{2} \left[ \begin{array}{ccc|c} E_1 & -E_1 & 0 & E_1 L_1 \\ -E_1 & E_1 + E_2 & -E_2 & -E_1 L_1 + E_2 L_2 \\ 0 & -E_2 & E_2 & -E_2 L_2 \\ \hline E_1 L_1 & -E_1 L_1 + E_2 L_2 & -E_2 L_2 & E_1 L_1^2 + E_2 L_2^2 \end{array} \right] \begin{Bmatrix} x_1 \\ x_2 \\ x_3 \\ \theta_2 \end{Bmatrix}$$

$$+ \left[ \begin{array}{ccc|c} K_{xx}^1 & 0 & 0 & 0 \\ 0 & 0 & 0 & 0 \\ 0 & 0 & K_{xx}^3 & 0 \\ \hline 0 & 0 & 0 & 0 \end{array} \right] \begin{Bmatrix} x_1 \\ x_2 \\ x_3 \\ \theta_2 \end{Bmatrix} + \left[ \begin{array}{ccc|c} C_{xy}^1 & 0 & 0 & 0 \\ 0 & 0 & 0 & 0 \\ 0 & 0 & C_{xy}^3 & 0 \\ \hline 0 & 0 & 0 & 0 \end{array} \right] \begin{Bmatrix} \dot{y}_1 \\ \dot{y}_2 \\ \dot{y}_3 \\ \dot{\psi}_2 \end{Bmatrix}$$

$$+ \left[ \begin{array}{ccc|c} K_{xy}^1 & 0 & 0 & 0 \\ 0 & 0 & 0 & 0 \\ 0 & 0 & K_{xy}^3 & 0 \\ \hline 0 & 0 & 0 & 0 \end{array} \right] \begin{Bmatrix} y_1 \\ y_2 \\ y_3 \\ \psi_2 \end{Bmatrix}$$

$$= \left\{ \begin{array}{c} 0 \\ m_2 e_2 [\omega^2 \cos(\omega t + \alpha_2) + \dot{\omega} \sin(\omega t + \alpha_2)] \\ 0 \\ \hline \tau(I_p - I_{t_2}) [\omega^2 \cos(\omega t + \beta_2) + \dot{\omega} \sin(\omega t + \beta_2)] \end{array} \right\}$$

Since the above equations of motion are uncoupled in the rotor mass matrix, the transient response of the system can be calculated by direct integration of the rotor acceleration, which is given as follows

$$\begin{Bmatrix} \ddot{X}_1 \\ \ddot{X}_2 \\ \ddot{X}_3 \end{Bmatrix} = \begin{Bmatrix} 0 \\ e_2 [\omega^2 \cos (\omega t + \alpha_2) + \dot{\omega} \sin (\omega t + \alpha_2)] \\ 0 \end{Bmatrix}$$

$$- \begin{bmatrix} \frac{C_{xx}^1}{M_1} & 0 & 0 \\ 0 & 0 & 0 \\ 0 & 0 & \frac{C_{xx}^3}{M_3} \end{bmatrix} \begin{Bmatrix} \dot{X}_1 \\ \dot{X}_2 \\ \dot{X}_3 \end{Bmatrix} - \frac{1}{2} \begin{bmatrix} \frac{E_1}{M_1} & -\frac{E_1}{M_1} & 0 \\ -\frac{E_1}{M_2} & \frac{E_1+E_2}{M_2} & -\frac{E_2}{M_2} \\ 0 & -\frac{E_2}{M_3} & \frac{E_2}{M_3} \end{bmatrix} \begin{Bmatrix} X_1 \\ X_2 \\ X_3 \end{Bmatrix}$$

$$= \begin{bmatrix} \frac{K_{xx}^1}{M_1} & 0 & 0 \\ 0 & 0 & 0 \\ 0 & 0 & \frac{K_{xx}^3}{M_3} \end{bmatrix} \begin{Bmatrix} X_1 \\ X_2 \\ X_3 \end{Bmatrix} - \begin{bmatrix} \frac{C_{xy}^1}{M_1} & 0 & 0 \\ 0 & 0 & 0 \\ 0 & 0 & \frac{C_{xy}^3}{M_3} \end{bmatrix} \begin{Bmatrix} Y_1 \\ Y_2 \\ Y_3 \end{Bmatrix}$$



$$- \begin{bmatrix} \frac{K_{xy}^1}{M_1} & 0 & 0 \\ 0 & 0 & 0 \\ 0 & 0 & \frac{K_{xy}^3}{M_3} \end{bmatrix} \begin{Bmatrix} Y_1 \\ Y_2 \\ Y_3 \end{Bmatrix} \quad (2.39)$$

Transient response analysis using direct integration of equations of motion has been extensively investigated by Kirk [33], Shen [34], and others [35 - 38]. This direct approach has been shown to be very effective in analyzing simple rotor systems. In the case of large complex rotor bearing systems, the use of this direct method is very inefficient and time consuming due to the large number of equations to be solved. The use of modal transformation [39 - 55] in reducing the number of equations of the system has been found to be very satisfactory. The use of modal transformation in rotor-bearing systems dynamic analysis will be discussed in the following chapters.

The above application of the general equations of motion to a 3-mass rotor model provides a deeper understanding of the effects of unbalance, disk skew, shaft bow, rotor acceleration, and gyroscopic moment, which cannot be easily visualized in the modal equations of motion after the transformation.

### III. METHODS OF MODAL ANALYSIS

In the case of simple rotor systems, the dynamic behavior of the rotor may readily be obtained from solving the rotor equations of motion directly [33, 34, 35]. However, this may not be the case for a more complex system or rotor system with a large number of mass stations (e.g. over 50 mass stations), particularly in the analysis of rotor transient response of the system. The integration of large numbers of equations of motion are very time consuming [33, 34, 35] and may lead to serious numerical problems. A more efficient way to compute transient response of the rotor system suggests to be the modal approach. Using modal analysis [39-55], the number of equations of motion can be greatly reduced (depending on the number of modes necessary to accurately approximate the system) to lower the computational costs and to avoid certain numerical problems encountered in the integration of the direct equations of motion. As an additional bonus, unbalance response and stability of the rotor system can be obtained with a small additional effort. The use of the modal approach in dynamic analysis has been extensively investigated and can be divided into three major categories as in the following sections.

### 3.1 Uncoupled Modal Analysis

The linear equations of motion for an N-degrees of freedom system in matrix form can be written as

$$[M] \{\ddot{X}\} + [C] \{\dot{X}\} + [K] \{X\} = \{f(t)\} \quad (3.1)$$

For a circular shaft with symmetric supports if the generalized displacement  $\{X\}$  is measured from a fixed point in space, it can be shown that the mass matrix  $[M]$  and stiffness matrix  $[K]$  are symmetric matrices [50]. These are the basic assumptions used in the derivation of the orthogonality conditions of the undamped mode shapes. With these orthogonality conditions, the mass matrix  $[M]$  and the stiffness matrix  $[K]$  in the matrix equations of motion (3.1) can be uncoupled such that the modal response of the system can be solved by direction integration of the modal accelerations.

The general equations of motion for a multimass rotor including disc gyroscopic effects and generalized bearing properties of stiffness and damping produce a set of equations in which the total stiffness and damping matrices  $[K]$  and  $[C]$  matrices are symmetric.

### 3.1.1 Orthogonality of Normal Modes

In the calculation of normal modes of a system, free vibration of an undamped system is assumed. Equation (3.1) can be written in undamped free vibration form as

$$[M] \ddot{\{X\}} + [K] \{X\} = \{0\} \quad (3.2)$$

Assuming harmonic motion for the system such that

$$\{X\} = A e^{i\omega t}$$

and

$$\ddot{\{X\}} = -\omega^2 \{X\}$$

Then, equation (3.2) can be reduced to a standard eigenvalue form as the following

$$([M]^{-1} [K] - \omega_i^2 [I]) \{\gamma_i\} = 0 \quad (3.3)$$

in which  $\omega_i$  is the  $i$ th critical speed of the system and  $\{\gamma_i\}$  is its corresponding normal mode. The normal modes, or the eigenvectors of the system, can be shown to be orthogonal with respect to the mass and stiffness matrices as follows. Equation (3.2) for the  $i$ th mode can be written as

$$\left\{ -\omega_i^2 [M] + [K] \right\} \{\gamma_i\} = 0 \quad (3.4)$$

Premultiply by  $\{\gamma_j\}^T$

$$\{\gamma_j\}^T [K] \{\gamma_i\} - \omega_i^2 \{\gamma_j\}^T [M] \{\gamma_i\} = 0 \quad (3.5)$$

Premultiply the equation of  $j^{\text{th}}$  mode by  $\{\gamma_i\}^T$  with the result

$$\{\gamma_i\}^T [K] \{\gamma_j\} - \omega_j^2 \{\gamma_i\}^T [M] \{\gamma_j\} = 0 \quad (3.6)$$

If the stiffness matrix  $K$  is symmetric such that

$$\{\gamma_i\}^T [K] \{\gamma_j\} = \{\gamma_j\}^T [K] \{\gamma_i\} \quad (3.7)$$

Equation (3.5) and (3.6) can be reduced to

$$(\omega_i^2 - \omega_j^2) \{\gamma_i\}^T [M] \{\gamma_j\} = 0 \quad (3.8)$$

Thus, the orthogonality conditions are

$$\{\gamma_i\}^T [M] \{\gamma_j\} = 0, \quad i \neq j \quad (3.9)$$

$$\{\gamma_i\}^T [K] \{\gamma_j\} = 0, \quad i \neq j \quad (3.10)$$

Now a set of orthonormal modes is defined such that

$$\{\phi_i\}^T [M] \{\phi_j\} = \begin{cases} 0, & i \neq j \\ 1, & i = j \end{cases} \quad (3.11)$$

Thus  $\{\phi_i\}$  can be calculated as

$$\{\phi_i\} = \frac{\{\gamma_i\}}{\sqrt{\{\gamma_i\}^T [M] \{\gamma_i\}}} \quad (3.12)$$

Substituting the above relationships into equation (3.4), we have

$$\{\phi_i\}^T [K] \{\phi_j\} = \begin{cases} 0, & i \neq j \\ \omega_i^2, & i = j \end{cases} \quad (3.13)$$

which are the orthogonality conditions for the orthonormal modes  $\{\phi_i\}$ .

### 3.1.2 Uncoupled Modal Equations of Motion

The general assumption used in modal analysis is that the generalized displacements of the system can be represented by a linear combination of the mode shapes (or eigenvectors) of the system. In this analysis, the generalized displacements are discretized into mass stations which can be represented by a set (or sets) of discretized orthonormal modes  $[\Phi]$  as

$$\{X(z, t)\} = \sum_{i=1}^n q_i(t) \{\phi_i(z)\} \quad (3.14)$$

Using this representation, equation (3.1) can now be transformed into

$$[M] [\Phi] \{\ddot{q}(t)\} + [C] [\Phi] \{\dot{q}(t)\} + [K] [\Phi] \{q(t)\} = \{f(t)\} \quad (3.15)$$

where

$$[\Phi] = [\{\phi_1\}, \{\phi_2\}, \{\phi_3\}, \dots, \{\phi\}]$$

$$\text{and } \{q(t)\} = \begin{Bmatrix} q_1(t) \\ q_2(t) \\ \vdots \\ q_n(t) \end{Bmatrix}$$

Equation (3.12) is then premultiplied by  $[\phi]^T$  as

$$\begin{aligned} [\phi]^T [M] [\phi] \ddot{q}(t) + [\phi]^T [C] [\phi] \dot{q}(t) + [\phi]^T [K] [\phi] q(t) \\ = [\phi]^T \{f(t)\} \end{aligned} \quad (3.16)$$

Using the orthogonal condition of (3.9) and (3.10), we have

$$[\phi]^T [M] [\phi] = [I] \quad (3.18)$$

$$[\phi]^T [K] [\phi] = [\Lambda] \quad (3.18)$$

where  $[\Lambda]$  is a diagonal matrix composing of the squares of the undamped critical speeds  $\omega_i$ . Thus equation (3.16) can be simplified as

$$\ddot{q}_i(t) + \sum_{j=1}^n c_{ij} \dot{q}_j(t) + \omega_i^2 q_i(t) = F_i(t) \quad \text{for } i = 1, 2, \dots, n \quad (3.19)$$

where

$$c_{ij} = \{\phi_i\}^T [C] \{\phi_j\}$$

$$F_i = \{\phi_i\}^T \{F(t)\}$$



It was shown by Caughey [54] that if  $[C]$  is linearly proportional to  $[M]$  and  $[K]$  or

$$[C] [M]^{-1} [K] = [K] [M]^{-1} [C] \quad (3.20)$$

Then  $[C]$  can also be uncoupled by the normal modes as

$$\{\phi_i\}^T [C] \{\phi_j\} = \begin{cases} 0, & i \neq j \\ C_i, & i = j \end{cases} \quad (3.21)$$

Using this orthogonality condition, equation (3.19) can be written as

$$\ddot{q}_i(t) + C_{ii} \dot{q}_i(t) + \omega_i^2 q_i(t) = F_i(t) \quad \text{for } i = 1, 2, \dots, n \quad (3.22)$$

This assumption uncouples the modal equations of motion which are relatively easy to analyze but often not accurate for turbomachinery with fluid film bearings or seals. Bishop and Parkinson [27] used this approach of proportional damping in their balancing schemes. However, this procedure fails when large damping is presented in the system. This justification will be verified in the next chapter.

### 3.1.3 Damped Natural Frequencies and Forced Response of Uncoupled System

Using the assumption of proportional damping, the modal equations can be reduced to the standard form [27, 48] as follows

$$\ddot{q}_i + 2\xi_i \omega_i \dot{q}_i + \omega_i^2 q_i = F_i$$

where

$$\xi_i = \frac{C_{ii}}{C_{ci}} = \text{modal damping ratio}$$

$C_{ci}$  = critical modal damping for the  $i^{\text{th}}$  mode

Assuming a solution of the form

$$q_i = \bar{A}_i e^{\lambda t}, \quad \lambda = \text{Complex eigenvalue}$$

the homogeneous solution yields the complex eigenvalues

$$\lambda_{1,2} = P_i \pm i \omega_{di} = -\xi_i \omega_i \pm i \omega_i \sqrt{1 - \xi_i^2} \quad (3.26)$$

where  $P_i$  is the growth factor and  $\omega_{di}$  is the damped critical speed.

If  $F_i$  is a sinusoidal forcing function due to unbalance, a synchronous response solution is easily found. It can be shown that the peak rotor unbalance response does not occur at the undamped critical speed  $\omega_i$  or at the damped critical speed  $\omega_{di}$  but at a speed  $\omega_{ui}$  given by [18] similar to that for a single mass rotor.

$$\omega_{ui} = \frac{\omega_i}{\sqrt{1 - 2\xi_i^2}} \quad (3.25)$$

or if the complex eigenvalues for the damped system are known

$$\omega_{ui} = \frac{\omega_{di}^2 + p_i^2}{\sqrt{\omega_{di}^2 - p_i^2}} \quad (3.26)$$

The rotor amplification factor for the peak rotor unbalance response is given by [18]

$$A_{ui} = \frac{1}{2\xi_i \sqrt{1 - \xi_i^2}} \quad (3.27)$$

or

$$A_{ui} = \frac{\omega_{di}^2 + p_i^2}{-2p_i \omega_{di}} \quad (3.28)$$

Therefore, it is seen for the case of the uncoupled modal analysis that if the modal damping or complex eigenvalues can be calculated and the damping is proportional, then the speed at which the maximum unbalance response occurs can be predicted along with the rotor amplification factor.

Although the above equations for the prediction of the rotor peak unbalance response speeds and amplification factors provide insight into rotor behavior, for realistic turborotors with fluid film bearings and gyroscopic moment coupling, the modal equations of motion cannot be simply uncoupled, as Bishop and Parkinson have done, [27, 48], but the modal equations must be simultaneously considered for both the x-z and y-z planes of motion as Childs [40 - 44] or Lund [51] has demonstrated. The general coupled modal analysis to determine the stability of the damped natural frequencies (eigenvalues) is discussed in the following chapters.

### 3.2 Modal Analysis Using Damped Modes

#### 3.2.1 Reduction to Standard Form

Another approach to uncouple the equations of motion of a damped system is the damped modal analysis [39, 51]. In order to apply the damped modes of the system, the set of equations of motion in (3.1) has to be reduced to standard form. It is assumed that the displacement vector  $\{X\}$  may be represented by

$$\{X\} = \{A\} e^{\lambda t} \quad (3.29)$$

such that

$$\dot{\{X\}} = \lambda \{X\} = (P + i\omega_d) \{X\}$$

In order to solve for the eigenvalues of the system and develop the orthogonality conditions for the general damped rotor, the system must first be reduced from a set of  $N$  coupled second order differential equations to a set of  $2N$  first-order equations. This can be done by adding an equation of the form

$$\dot{\{X\}} - \dot{\{X\}} = 0$$

into equation (3.1) which gives

$$\begin{bmatrix} [M] & [0] \\ [0] & [I] \end{bmatrix} \begin{Bmatrix} \ddot{X} \\ \dot{X} \end{Bmatrix} + \begin{bmatrix} [C] & [K] \\ [-I] & [0] \end{bmatrix} \begin{Bmatrix} \dot{X} \\ X \end{Bmatrix} = 0 \quad (3.30)$$

Let  $V$  be defined such that

$$V = \begin{Bmatrix} \dot{X} \\ X \end{Bmatrix} = \begin{Bmatrix} \lambda X \\ X \end{Bmatrix} \text{ and } \dot{V} = \begin{Bmatrix} \ddot{X} \\ \dot{X} \end{Bmatrix} = \begin{Bmatrix} \lambda^2 X \\ \lambda X \end{Bmatrix}$$

Then equation (3.30) can be reduced to a standard eigenvalue problem

$$\begin{bmatrix} [M] & [0] \\ [0] & [I] \end{bmatrix} \{ \dot{V} \} + \begin{bmatrix} [C] & [K] \\ [-I] & [0] \end{bmatrix} \{ V \} = 0 \quad (3.31)$$

or in another form as

$$[D] \{ V \} - \lambda \{ V \} = 0 \quad (3.32)$$

where

$$[D] = \begin{bmatrix} [-M^{-1}C] & [-M^{-1}K] \\ [I] & [0] \end{bmatrix}$$

The iteration of equation (3.32) for the determination of the complex eigenvalue will converge to the highest eigenvalue of the system. If the eigenvalue problem is formulated with the inverse matrix of  $[D]$ , the iterative procedure of Hurty and Roberstein [67] will converge to the lowest system eigenvalues.

### 3.2.2 Orthogonality of Eigenvectors

Solving the eigenvalue problem in equation (3.32), there exists a set of eigenvalues with their corresponding eigenvectors which will satisfy the following homogeneous equations.

$$[D] - \lambda_i [I] \cdot \{\psi_{di}\} = 0 \quad (3.33)$$

$$\text{where } \{\psi_{di}\} = \begin{pmatrix} \lambda_i \phi_{di} \\ \phi_{di} \end{pmatrix}$$

is the complex eigenvector of the ith mode for the damped system.

In order to derive the orthogonal conditions for the damped eigenvectors, the transpose of the matrix  $[D]$  is considered. In general,  $[D]^T$  is not equal to  $[D]$  but  $|D^T| = |D|$ ; that is, the determinant of the transpose matrix is equal to the original matrix.

Let  $\bar{\psi}_{dj}$  satisfy the equation

$$[D]^T - \lambda_j [I] \cdot \{\bar{\psi}_{dj}\} = 0 \quad (3.34)$$

where

$$\{\bar{\psi}_{dj}\} = \begin{pmatrix} \lambda_j \bar{\phi}_{dj} \\ \bar{\phi}_{dj} \end{pmatrix}$$

is the left-hand eigenvector of the ith mode.

To develop the orthogonality condition, multiply equation (3.33) by the transposed left-handed eigenvector,  $\{\bar{\psi}_{di}\}$ , such that

$$\{\bar{\psi}_{dj}\}^T \left[ [D] - \lambda_i [I] \right] \{\psi_{di}\} = 0 \quad (3.35)$$

or by expanding out into

$$\{\bar{\psi}_{dj}\}^T [D] \{\psi_{di}\} - \lambda_i \{\bar{\psi}_{dj}\}^T \{\psi_{di}\} = 0 \quad (3.36)$$

Similarly, premultiply equation (3.34) by the transpose of  $\{\psi_{di}\}$  which becomes

$$\{\psi_{di}\}^T [D]^T \{\bar{\psi}_{dj}\} - \lambda_j \{\psi_{di}\}^T \{\bar{\psi}_{dj}\} = 0 \quad (3.37)$$

Taking the transpose of equation (3.37) and subtracting equation (3.36) results in

$$\{\lambda_j - \lambda_i\} \{\bar{\psi}_{dj}\}^T \{\psi_{di}\} = 0 \quad (3.38)$$

Thus, the orthogonal condition can be stated as

$$\{\bar{\psi}_{dj}\}^T \{\psi_{di}\} = \lambda_i \lambda_j \{\bar{\phi}_{dj}\}^T \{\phi_{di}\} + \{\bar{\phi}_{dj}\}^T \{\phi_{di}\} = 0 \quad \text{for } i \neq j \quad (3.39)$$

or



$$\left\{ \bar{\phi}_{dj} \right\}^T \left\{ \phi_{di} \right\} = 0, \text{ for } i \neq j \quad (3.40)$$

Thus, the left handed eigenvector generated for the jth mode is orthogonal to the right vector of the ith mode. This represents the most general case of orthogonality for an arbitrary unsymmetrical [D] matrix.

The above developed orthogonality condition can be further expanded for general use. Note that

$$\psi_{di} = \begin{Bmatrix} \lambda \phi_{di} \\ \phi_{di} \end{Bmatrix}$$

where  $\psi_{di}$  is of the order  $2N$  where  $\phi_{di}$  is of the order  $N$ . Assume  $\phi_{di}$  satisfies the equation

$$\left[ \lambda_i^2 M + \lambda_i C + K \right] \phi_{di} = 0 \quad (3.41)$$

and that  $\bar{\phi}_{di}$  satisfies the following equation

$$\left[ \lambda_j^2 M^T + \lambda_j C^T + K^T \right] \bar{\phi}_{di} = 0 \quad (3.42)$$

Taking the transpose of the above and premultiplying by  $\lambda_i \{ \phi_{di} \}$

$$\bar{\phi}_{dj}^T \left[ \lambda_i^2 M + \lambda_j C + K \right] \lambda_i \phi_{di} = 0 \quad (3.43)$$

Postmultiplying equation (3.41) by  $\lambda_j \bar{\phi}_{dj}^T$  gives

$$\lambda_j \bar{\phi}_{dj}^T \left[ \lambda_i^2 M + \lambda_i C + K \right] \phi_{di} = 0 \quad (3.44)$$

Subtracting equation (3.44) from (3.43) we obtain

$$\lambda_j \lambda_i \bar{\phi}_{dj}^T [M] \phi_{di} (\lambda_j - \lambda_i) + (\lambda_i - \lambda_j) \phi_{dj}^T [K] \phi_{di} = 0 \quad (3.45)$$

Dividing out the constant  $\lambda_i - \lambda_j$  we obtain

$$\bar{\phi}_{dj}^T (\lambda_i \lambda_j M - K) \phi_{di} = 0 \quad (3.46)$$

Eliminating  $\bar{\phi}_{dj}^T [K] \phi_{di}$  from equation (3.43) results in

$$(\lambda_i + \lambda_j) \left[ \bar{\phi}_{dj}^T [M] \phi_{di} \right] + \bar{\phi}_{dj}^T [C] \phi_{di} = 0 \quad (3.47)$$

When  $i = j$ , the above orthogonality condition equation (3.46) reduces to

$$\lambda_i^2 M_i = K_i \quad (3.48)$$

where

$$M_i = \bar{\phi}_{di}^T [M] \phi_{di}$$

$$K_i = \bar{\phi}_{di}^T [K] \phi_{di}$$

And the orthogonality condition of equation (3.47) reduces to

$$C_i = -2\lambda_i M_i \quad (3.49)$$

where

$$C_i = \bar{\phi}_{di}^T [C] \phi_{di}$$

### 3.2.3 Forced Response Using Damped Modes

Modal response of a complex system using damped modes has been extensively investigated by Foss [39] and Lund [51]. The general equations of motion in (3.1) are uncoupled and solved independently. To uncouple the equations of motion, they are reduced to the standard form from equation (3.1) as (note that this form is somewhat different from the formulation of equation 3.31 such that the symmetry of the matrices is retained if  $[M]$ ,  $[C]$  and  $[K]$  are symmetric)

$$[R] \dot{\{V\}} + [B] \{V\} = \{F(t)\} \quad (3.50)$$

where

$$[R] = \begin{bmatrix} [0] & [M] \\ [M] & [C] \end{bmatrix}$$

$$[B] = \begin{bmatrix} -[M] & [0] \\ [0] & [K] \end{bmatrix}$$

$$\{F(t)\} = \begin{Bmatrix} \{0\} \\ \{f(t)\} \end{Bmatrix}$$

$$\{V\} = \begin{Bmatrix} \dot{\{x\}} \\ \{x\} \end{Bmatrix}$$

The orthogonality conditions are similar to equation (3.47) as

$$(\lambda_i - \lambda_j) \left\{ \bar{\psi}_{dj} \right\}^T [R] \left\{ \psi_{di} \right\} = 0, \quad \text{for } i \neq j \quad (3.51)$$

and

$$\left\{ \bar{\psi}_{di} \right\}^T \left[ \lambda_j [R] + [B] \right] \left\{ \psi_{di} \right\} = 0, \quad \text{for } i \neq j \quad (3.52)$$

In modal analysis, it is assumed that the  $2N$  vector  $\{V\}$  can be expressed by a combination of the modes as

$$\{V\} = \sum_{j=1}^N q_j(t) \left\{ \psi_{dj} \right\} \quad (3.53)$$

Substituting equation (3.53) into (3.50) and premultiplying by  $\{\bar{\psi}_{di}\}^T$  gives

$$\begin{aligned} \{\bar{\psi}_{di}\}^T [R] \sum_{j=1}^n \dot{q}_j(t) \{\psi_{dj}\} + \{\bar{\psi}_{di}\}^T [B] \sum_{j=1}^n q_j(t) \{\psi_{dj}\} \\ = \{\bar{\psi}_{di}\}^T \{F(t)\} \end{aligned} \quad (3.54)$$

Applying the orthogonality conditions in equations (3.51) and (3.52), the above matrix equation can be uncoupled into  $2N$  equations of the form

$$\begin{aligned} R_i \dot{q}_i(t) - \lambda_i R_i q_i(t) &= \{\bar{\psi}_{di}\}^T \{F(t)\} \\ R_i^* \dot{q}_i(t) - \lambda_i^* R_i^* q_i(t) &= \{\bar{\psi}_{di}^*\}^T \{F(t)\} \end{aligned} \quad (3.55)$$

where superscript  $*$  denotes the complex conjugates and

$$\begin{aligned} R_i &= \{\bar{\psi}_{di}\}^T [R] \{\psi_{di}\} \\ B_i &= \{\bar{\psi}_{di}\}^T [B] \{\psi_{di}\} = -\lambda_i R_i \end{aligned} \quad (3.56)$$

or expanding out the matrix to obtain  $R_i$ , which is a complex number

$$R_i = 2\lambda_i \{\bar{\phi}_{di}\}^T [M] \{\phi_{di}\} + \{\bar{\phi}_{di}\}^T [C] \{\phi_{di}\} \quad (3.57)$$

In the case where the mass matrix  $[M]$ , the damping matrix  $[C]$  and the stiffness matrix  $[K]$  are symmetric, the left-hand eigenvector  $\{\bar{\phi}_{di}\}$ , equals to the right-hand eigenvector  $\{\phi_{di}\}$ , then

$$R_i = \{\phi_{di}\}^T [2\lambda[M] + [C]] \{\phi_{di}\} \quad (3.58)$$

The forced response of the system can be evaluated by the decoupled equations in (3.55) through the use of the convolution integral.

$$\{v(t)\} = \sum_{i=1}^{2N} \left[ \frac{1}{R_i} \int_0^t e^{\lambda_i(t-\tau)} \{\bar{\psi}_{di}\}^T \{F(\tau)\} d\tau \right] \{\psi_{di}\} \quad (3.59)$$

or

$$\{x(t)\} = \sum_{i=1}^{2N} \left[ \frac{1}{R_i} \int_0^t e^{\lambda_i(t-\tau)} \{\bar{\phi}_{di}\}^T \{f(\tau)\} d\tau \right] \{\phi_{di}\}$$

If  $f(t)$  is a sinusoidal forcing function such as unbalance forces that

$$\{f(t)\} = \{me\} \omega^2 e^{i\omega t} \quad (3.61)$$

then

$$x(t) = \sum_{i=1}^{2N} \frac{1}{R_i} \int_0^t e^{\lambda_i(t-\tau)} U_i \omega^2 e^{i\omega\tau} d\tau \{\phi_{di}\} \quad (3.62)$$

where

where

$$U_i = \{\bar{\phi}_{di}\}^T \{me_i\}$$

$$\{me_i\} = \text{mass eccentricity vector of the system}$$

For zero initial conditions, the convolution integral can be integrated to give

$$\begin{aligned} \{X(t)\} = & \sum_{i=1}^N \left\{ \frac{U_i \omega^2}{R_i} e^{\lambda_i t} \left[ \frac{e^{-\lambda_i t + i\omega t} - 1}{(i\omega - \lambda_i)} \right] \{\phi_{di}\} \right. \\ & \left. + \frac{U_i^* \omega^2}{R_i^*} e^{\lambda_i^* t} \left[ \frac{e^{-\lambda_i^* t + i\omega t} - 1}{(i\omega - \lambda_i^*)} \right] \{\phi_{di}^*\} \right\} \end{aligned} \quad (3.63)$$

where the upper superscript \* designates the conjugate of the variable. If  $t$  is very large, the transient response goes into steady state where

$$\{X(t)\} = \sum_{i=1}^N \left[ \frac{U_i \omega^2}{R_i} \frac{e^{i\omega t}}{(i\omega - \lambda_i)} \{\phi_{di}\} + \frac{U_i^* \omega^2}{R_i^*} \frac{e^{i\omega t}}{(i\omega - \lambda_i^*)} \{\phi_{di}^*\} \right] \quad (3.64)$$

For zero or small damping, the following values are valid.

$$\lambda_i = i\omega_i \quad , \quad \lambda_i^* = -i\omega_i$$

$$\{\phi_{di}^*\} = \{\phi_{di}\} = \{\gamma_i\} \quad , \quad \{\bar{\phi}_{di}\} = \{\phi_{di}\}$$

$$M_i = \{\gamma_i\}^T [M] \{\gamma_i\} = \text{modal mass for undamped system}$$

$$R_i = 2 \omega_i M_i, \quad R_i^* = -2 \omega_i M_i$$

$$U_i = \{\lambda_i^T\} \{m_i e_i\}$$

$$E_i = \frac{U_i}{m_i} = \text{modal eccentricity for the undamped system}$$

Thus

$$\{X(t)\} = \sum_{i=1}^N \frac{\omega_i^2 E_i}{\omega_i^2 - \omega^2} \{\gamma_i\} \quad (3.65)$$

or

$$\{X(t)\} = \sum_{i=1}^N \frac{f_i^2 E_i}{1 - f_i^2} \{\gamma_i\} \quad (3.66)$$

where

$$f_i = \frac{\omega}{\omega_i}$$

Note that equation (3.66) is just the equation for modal excitation of an undamped system. If we define the modal amplification factor to be  $A_i$  such that



$$(X) = \sum_{i=1}^N A_i E_i (\gamma_i) \quad (3.67)$$

then

$$A_i = \frac{f_i^2}{1 - f_i^2} \quad (3.68)$$

which goes to infinity when  $f_i$  equals to 1 or  $\omega = \omega_i$ . Similarly, for the lightly damped system, assuming  $U_i = U_i^*$  the modal amplification will be

$$A_i = \omega_i^{2M_i} \left[ \frac{1}{R_i(i\omega - \lambda_i)} + \frac{1}{R_i^*(i\omega - \lambda_i^*)} \right] \quad (3.69)$$

Applying equation (3.28) to (3.69), the modal amplification of the system at resonance speed ( $\omega = \omega_{ui}$ ) becomes

$$A_{ui} = \omega_{ui}^{2M_i} \left[ \frac{1}{R_i(i\omega_{ui} - \lambda_i)} + \frac{1}{R_i^*(i\omega_{ui} - \lambda_i^*)} \right] \quad (3.70)$$

Where  $\omega_{ui}$  is given by equation (3.25) as  $\omega_{ui} = \frac{\omega_{di} + P_i^2}{\sqrt{\omega_{di}^2 - P_i^2}}$

Another form of representing the modal equations of motion is in the form of uncoupled second order differential equation [29] as follows

$$\ddot{\tau}_i + 2P_i \dot{\tau}_i + \omega_i^2 \tau_i = 2\text{Re} \left[ \frac{\{\bar{\phi}_i\}^T \{\dot{f}(t)\} - \lambda_i^* \{\bar{\phi}_i\}^T \{f(t)\}}{R_i} \right]$$

$$\ddot{\eta}_i + 2p_i \dot{\eta}_i + \omega_i^2 \eta_i = 2IM \left[ \frac{\{\phi_i\}^T \{\dot{f}(t)\} - \lambda_i^* \{\phi_i\}^T \{f(t)\}}{R_i} \right]$$

where

$$\tau_i = q_i + q_i^* \quad (3.71)$$

$$\eta_i = -i(q_i - q_i^*)$$

The above equations are a more efficient way of modal representation which involves no complex number calculation in obtaining the forced response solution.

It can be seen from the above analysis that the rotor equations of motion can be decoupled and force response can be calculated from integration the modal equation directly. But there are several drawbacks of this approach. First, damped natural frequencies and mode shapes of a large system are more difficult and time consuming to obtain; and secondly, the equations of motion cannot be completely decoupled if rotor acceleration and nonlinear bearing forces exist in the system. In this case, the same kind of coupled equations have to be solved, and the complex mode shapes in the damped system makes it more difficult. Thus, it may be more efficient to resort to a set of coupled modal equations transformed by the undamped modes, which will be discussed in the next section.

### 3.3 Coupled Undamped Modal Analysis

The use of undamped modes in solving dynamical equations of motion has been extensively investigated by Dennis [45], Black [46], Childs [40], Morton [52], and other researchers. Different approaches have been used by these investigators to give satisfactory results. The analysis based on using "free-free" modes alone simplifies the equation and the modes are relatively easy to obtain, but a lot of higher modes have to be incorporated in order to give accurate results. A better approach is the addition of two rigid body (rotational and translational) modes along with the "free-free" modes. This would give better results even when less higher modes are used. The drawback of this approach is that the sets of mode shapes used does not provide the designers a real "feeling" of the system. Another approach is the incorporation of the "Pin-pin" jointed modes at the main bearing in addition to the set of "free-free" modes used. This approach will give very accurate results, but the two sets of modes, the free-free and the pin-pin, are not orthogonal to each other; and thus, further complicating the problem.

The use of planar modes, where bearing stiffness is incorporated, seems to be a better way. The mode shapes calculated can give the designer a better "feel" of the bending of the system, and the results of using planar modes are in good accuracy even when only a few modes are used. A comparison of using the planar modes to the free-free plus rigid-body modes will be discussed in the next chapter.

### 3.3.1 Orthogonality of Planar Modes

It is desired to obtain a single set of planar undamped modes incorporating an average bearing stiffness for modal analysis. The shaft is assumed symmetric, rotor gyroscopic effects are neglected, bearing damping is neglected, and only an average bearing principal stiffness term is considered. The equations for the planar undamped mode shapes are

$$\begin{bmatrix} [M] & 0 & 0 & 0 \\ 0 & [I_t] & 0 & 0 \\ 0 & 0 & [M] & 0 \\ 0 & 0 & 0 & [I_t] \end{bmatrix} \begin{bmatrix} \ddot{x} \\ \ddot{\theta} \\ \ddot{y} \\ \ddot{\psi} \end{bmatrix} +$$

$$\begin{bmatrix} [k_{xx}] & [k_{x\theta}] & 0 & 0 \\ [k_{\theta x}] & [k_{\theta\theta}] & 0 & 0 \\ 0 & 0 & [k_{xx}] & [k_{x\theta}] \\ 0 & 0 & [k_{\theta x}] & [k_{\theta\theta}] \end{bmatrix} \begin{bmatrix} x \\ \theta \\ y \\ \psi \end{bmatrix} +$$

$$\begin{bmatrix}
 \begin{bmatrix} K_{xx} \\ 0 \end{bmatrix} & 0 & \begin{bmatrix} K_{xy} \\ 0 \end{bmatrix} & 0 \\
 0 & 0 & 0 & 0 \\
 \begin{bmatrix} K_{yx} \\ 0 \end{bmatrix} & 0 & \begin{bmatrix} K_{yy} \\ 0 \end{bmatrix} & 0 \\
 0 & 0 & 0 & 0
 \end{bmatrix}_B
 \begin{bmatrix}
 (x) \\
 (\theta) \\
 (y) \\
 (\psi)
 \end{bmatrix}
 =
 \begin{bmatrix}
 F(t)
 \end{bmatrix}
 \quad (3.72)$$

where

$$\begin{bmatrix} K_b \end{bmatrix} = \frac{\begin{bmatrix} K_{xx} \end{bmatrix}_B + \begin{bmatrix} K_{yy} \end{bmatrix}_B}{2}$$

is the average bearing stiffness taken from  $K_{bxx}$  and  $K_{byy}$  which is evaluated for a single speed in the operating speed range.

Eliminating the cross-coupling bearing stiffness and the difference in the direct stiffness terms, equation (3.72) becomes symmetrical in the x-y, y-z planes.

$$\begin{bmatrix}
 \begin{bmatrix} M \\ 0 \end{bmatrix} & 0 \\
 0 & \begin{bmatrix} I_t \end{bmatrix}
 \end{bmatrix}
 \begin{Bmatrix}
 \ddot{(x)} \\
 \ddot{(\theta)}
 \end{Bmatrix}
 +
 \begin{bmatrix}
 \begin{bmatrix} k_{xx} + K_b \\ k_{\theta x} \end{bmatrix} & \begin{bmatrix} k_{x\theta} \\ k_{\theta\theta} \end{bmatrix}
 \end{bmatrix}
 \begin{Bmatrix}
 (x) \\
 (\theta)
 \end{Bmatrix}
 = 0
 \quad (3.73)$$

and

$$\begin{bmatrix} [M] & 0 \\ 0 & [I_z] \end{bmatrix} \begin{Bmatrix} \ddot{(Y)} \\ \ddot{(\psi)} \end{Bmatrix} + \begin{bmatrix} [k_{xx} + K_b] & [k_{x\theta}] \\ [k_{\theta\theta}] & [k_{\theta\theta}] \end{bmatrix} \begin{Bmatrix} (Y) \\ (\psi) \end{Bmatrix} = 0 \quad (3.74)$$

let  $\omega_i$  be the  $i$ th natural frequency of the system and  $\{A_i\}$  be its corresponding orthonormal mode shape such that

$$A_i = \begin{bmatrix} A_{ei} \\ -A_{\beta i} \end{bmatrix}$$

where  $[A_{ei}]$  = translational orthonormal mode

$$[A_{\beta i}] = \text{rotational orthonormal mode} = \left( \frac{\partial A_{ei}}{\partial z} \right)$$

and

$$\begin{bmatrix} A_e \\ A_\beta \end{bmatrix} = \frac{(\phi_1), (\phi_2), (\phi_3), \dots, (\phi_n)}{(\phi_1), (\phi_2), (\phi_3), \dots, (\phi_n)} = [A]$$

The orthogonality conditions of the orthonormal modes require that

$$\begin{aligned} \{A_{ej}\}^T [M] \{A_{ei}\} + \{A_{\beta j}\}^T [I_t] \{A_{\beta i}\} &= 1, \text{ for } i = j \\ &= 0, \text{ for } i \neq j \end{aligned} \quad (3.75)$$

and

$$\begin{aligned} &\{A_{ej}\}^T [k_{xx} + K_b] \{A_{ei}\} + \{A_{ej}\}^T [k_{xe}] \{A_{\beta i}\} + \{A_{\beta j}\}^T [k_{\theta x}] \{A_{ei}\} \\ &+ \{A_{\beta j}\}^T [k_{\theta e}] \{A_{\beta i}\} = \omega_i^2, \text{ for } i = j \\ &= 0, \text{ for } i \neq j \end{aligned} \quad (3.76)$$

### 3.3.2 Planar Modal Analysis

In modal analysis, it is assumed that the response of the system can be represented by a combination of the planar modes. Therefore, the generalized displacement vector  $\{U\}$  is represented by the expansion of the undamped modes obtained from a solution of equation (3.72) as

$$\{U\} = \sum_{i=1}^n \begin{pmatrix} q_{xi} \{\phi_i\} \\ q_{yi} \{\psi_i\} \end{pmatrix} \quad (3.77)$$

where

$$\{U\} = \begin{Bmatrix} (x) \\ (\theta) \\ (y) \\ (\psi) \end{Bmatrix}$$

or in another form as

$$\begin{bmatrix} \{X\} \\ \{\theta\} \\ \{Y\} \\ \{\psi\} \end{bmatrix} = \sum_{i=1}^n \left\{ \frac{\begin{matrix} q_{xi} & \{\phi_i\} \\ q_{yi} & \{\phi_i\} \end{matrix}}{\begin{matrix} q_{xi} & \{\phi_i\} \\ q_{yi} & \{\phi_i\} \end{matrix}} \right\} = \sum_{i=1}^n \left\{ \frac{\begin{matrix} q_{xi} & \{\phi_i\} \\ q_{yi} & \{\phi_i\} \end{matrix}}{\begin{matrix} q_{xi} & \{\phi_i\} \\ q_{yi} & \{\phi_i\} \end{matrix}} \right\} \quad (3.78)$$

Premultiply equation (2.17) by  $\{\phi_i\}^T$  and apply orthogonality condition of the mode shapes, the equations of motion can be written into a set of compact equations using the Eienstein summation convention as

$$\ddot{q}_{xi} + \omega_i^2 q_{xi} + C_{ij}^x \dot{q}_{xj} + B_{ij}^x q_{xj} + D_{ij}^x \dot{q}_{yj} + E_{ij}^x q_{yj} = P_{xi} \quad (3.79)$$

and there is a similar set of equations for the y-z plane as follows

$$\ddot{q}_{yi} + \omega_i^2 q_{yi} + C_{ij}^y \dot{q}_{yj} + B_{ij}^y q_{yj} + D_{ij}^y \dot{q}_{xj} + E_{ij}^y q_{xj} = P_{yi} \quad (3.80)$$

and

$$\begin{aligned} P_{xi} &= (\phi_i)^T Me[\omega^2 \cos(\omega t + \alpha) + \dot{\omega} \sin(\omega t + \alpha)] \\ &+ (\phi_i')^T \tau(I_p - I_t) [\omega^2 \cos(\omega t + \beta) + \dot{\omega} \sin(\omega t + \beta)] \end{aligned} \quad (3.81)$$



where  $B_{ij}$ ,  $C_{ij}$ ,  $D_{ij}$ , and  $E_{ij}$  are modal cross-coupling terms from from disc gyroscopic, bearing cross-coupling stiffness and damping effects. For example, the modal damping coefficient  $C_{ij}^x$  can be calculated as

$$C_{ij}^x = \{\phi_i\}^T [C_{xx}] \{\phi_j\} + \{\phi_i\}^T [C_{x\theta}] \{\phi_j'\} + \{\phi_i'\}^T [C_{\theta x}] \{\phi_j\} + \{\phi_i'\}^T [C_{\theta\theta}] \{\phi_j'\} \quad (3.82)$$

or in matrix form, equation (3.79) and (3.80) can be combined as

$$\begin{Bmatrix} \ddot{q}_x \\ \ddot{q}_y \end{Bmatrix} + \begin{bmatrix} [C^x] & [D^x] \\ [D^y] & [C^y] \end{bmatrix} \begin{Bmatrix} \dot{q}_x \\ \dot{q}_y \end{Bmatrix} + \begin{bmatrix} [B^x] & [E^x] \\ [E^y] & [B^y] \end{bmatrix} \begin{Bmatrix} q_x \\ q_y \end{Bmatrix} + \begin{bmatrix} [\Lambda] & [0] \\ [0] & [\Lambda] \end{bmatrix} \begin{Bmatrix} q_x \\ q_y \end{Bmatrix} = \begin{Bmatrix} (P_x) \\ (P_y) \end{Bmatrix} \quad (3.83)$$

It should be clear that this general modal formulation is not restricted to the particular set of mode shapes obtained by solving equation (3.72). Equation (3.82) can now be solved for damped eigenvalues and eigenvectors, stability analysis, and forced response of the system. The solution procedures for them is given in the following chapters.

#### IV. STABILITY ANALYSIS USING MODAL APPROACH

##### 4.1 Modal Equations for Stability Analysis

The stability and damped modes of a multi-mass rotor system can be obtained by solving the homogeneous modal equations of motion. Using the undamped modes of the system can greatly reduce the number of equations to be solved as compared to a finite element formulation. The matrix dynamic equation of (3.1) can be expanded into homogeneous form as

$$[\bar{M}] (\ddot{U}) + \left[ [C]_G + [C]_B \right] (\dot{U}) + \left[ [K]_S + [K]_B + [K]_A \right] (U) = 0 \quad (4.1)$$

where

$[C]_G$  = Gyroscopic damping matrix

$[C]_B$  = Bearing damping matrix

$[K]_S$  = Shaft and bearing stiffness matrix

$[K]_B$  = Bearing stiffness matrix

$[K]_A$  = Acceleration stiffness matrix

By principles of modal expansion [39-55], the rotor translational and rotational response amplitudes can be represented by a summation of the modes. That is

$$\begin{Bmatrix} (x) \\ (\theta) \end{Bmatrix} = \begin{bmatrix} [A_e] \\ [A_\beta] \end{bmatrix} \{q_x\} \quad (4.2)$$

$$\begin{Bmatrix} (y) \\ (\psi) \end{Bmatrix} = \begin{bmatrix} [A_e] \\ [A_\beta] \end{bmatrix} \{q_y\} \quad (4.3)$$

where  $\{q_x\}$  and  $\{q_y\}$  are time dependent vectors. Using the above modal expansions, the dynamic equations of motion in the x-z plane from equation (3.79) can be written as

$$\begin{aligned} & \begin{bmatrix} [M] & 0 \\ 0 & [I_t] \end{bmatrix} \begin{bmatrix} [A_e] \\ [A_\beta] \end{bmatrix} \begin{Bmatrix} \ddot{q}_x \\ \ddot{q}_x \end{Bmatrix} + \begin{bmatrix} [c_{xx}] & [c_{x\theta}] \\ [c_{\theta x}] & [c_{\theta\theta}] \end{bmatrix} \begin{bmatrix} [A_e] \\ [A_\beta] \end{bmatrix} \begin{Bmatrix} \dot{q}_x \\ \dot{q}_x \end{Bmatrix} + \\ & \begin{bmatrix} [k_{xx} + K_b] & [k_{x\theta}] \\ [k_{\theta x}] & [k_{\theta\theta}] \end{bmatrix} \begin{bmatrix} [A_e] \\ [A_\beta] \end{bmatrix} \begin{Bmatrix} q_x \\ q_x \end{Bmatrix} + \begin{bmatrix} [K_{xx} - K_b] & [K_{x\theta}] \\ [K_{\theta x}] & [K_{\theta\theta}] \end{bmatrix} \begin{bmatrix} [A_e] \\ [A_\beta] \end{bmatrix} \begin{Bmatrix} q_x \\ q_x \end{Bmatrix} + \\ & \begin{bmatrix} [c_{xy}] & [c_{x\psi}] \\ [c_{\theta y}] & [c_{\theta\psi}] \end{bmatrix} \begin{bmatrix} [A_e] \\ [A_\beta] \end{bmatrix} \begin{Bmatrix} \dot{q}_y \\ \dot{q}_y \end{Bmatrix} + \begin{bmatrix} 0 & 0 \\ 0 & [-\omega I_{p_z}] \end{bmatrix} \begin{bmatrix} [A_e] \\ [A_\beta] \end{bmatrix} \begin{Bmatrix} q_y \\ q_y \end{Bmatrix} + \\ & \begin{bmatrix} [K_{xy}] & [K_{x\psi}] \\ [K_{\theta y}] & [K_{\theta\psi}] \end{bmatrix} \begin{bmatrix} [A_e] \\ [A_\beta] \end{bmatrix} \begin{Bmatrix} q_y \\ q_y \end{Bmatrix} = 0 \quad (4.4) \end{aligned}$$

To apply the orthogonality condition to the dynamic equations of motion, equation (4.4) is premultiplied by  $\begin{bmatrix} A_e \\ A_\beta \end{bmatrix}^T$  which leads to the following equation

$$\begin{aligned}
 & \{\ddot{q}_x\} + \{[A_e]^T [C_{xx}] [A_e] + [A_e]^T [C_{x\theta}] [A_\beta] + [A_\beta]^T [C_{\theta x}] [A_e] \\
 & + [A_\beta]^T [C_{\theta\theta}] [A_\beta]\} \{\dot{q}_x\} + [\omega_i^2] \{q_x\} + \{[A_e]^T [K_{xx} - K_B] [A_e] \\
 & + [A_e]^T [K_{x\theta}] [A_\beta] + [A_\beta]^T [K_{\theta x}] [A_e] + [A_\beta]^T [K_{\theta\theta}] [A_\beta]\} \{q_x\} \\
 & + \{[A_e]^T [C_{xy}] [A_e] + [A_e]^T [C_{x\psi}] [A_\beta] + [A_\beta]^T [C_{\theta y}] [A_e] \\
 & + [A_\beta]^T [C_{\theta\psi}] [A_\beta]\} \{\dot{q}_y\} + \{[A_\beta]^T [\omega I_p] [A_\beta]\} \{\dot{q}_y\} \\
 & + \{[A_e]^T [K_{xy}] [A_e] + [A_e]^T [K_{x\psi}] [A_\beta] + [A_\beta]^T [K_{\theta y}] [A_e] \\
 & + [A_\beta]^T [K_{\theta\psi}] [A_\beta]\} \{q_y\} = 0
 \end{aligned} \tag{4.5}$$

Equation (4.5) can be simplified in compact form as

$$\{\ddot{q}_x\} + [C_x] \{\dot{q}_x\} + [K_x] \{q_x\} + [D_x] \{\dot{q}_y\} + [CM_x] \{\dot{q}_y\} + [E_x] \{q_y\} = 0$$

(4.6)

There is also a similar set of equations corresponding to the y-z plane for the stability analysis of the system. Let

$$(q_x) = (Q_x) e^{\lambda t}$$

and

$$(q_y) = (Q_y) e^{\lambda t}$$

such that

$$(\ddot{q}_x) = \lambda(\dot{q}_x) = \lambda^2(q_x)$$

$$(\ddot{q}_y) = \lambda(\dot{q}_y) = \lambda^2(q_y) \quad (4.6)$$

Substitution of these relationships into Equation (4.6) yields

$$\begin{aligned} & \left( \lambda^2 [I_x] + \lambda [C_x] + [A_x] + [K_x] \right) (q_x) + \left( \lambda [D_x] + \lambda [CM_x] \right. \\ & \left. + [E_x] \right) (q_y) = 0 \end{aligned} \quad (4.7)$$

There is a similar set of matrix equations for the y-z plane

$$\begin{aligned}
 & \left( \lambda^2 [\mathbf{I}_x] + \lambda [\mathbf{C}_y] + [\mathbf{A}] + [\mathbf{K}_y] \right) (\mathbf{q}_y) + \left( \lambda [\mathbf{D}_y] + \lambda [\mathbf{CM}_y] \right. \\
 & \left. + [\mathbf{E}_y] \right) (\mathbf{q}_x) = 0
 \end{aligned} \tag{4.8}$$

The above two sets of coupled matrix equations can be combined into a set of  $2n$  second-order matrix equations as

$$\begin{bmatrix}
 \lambda^2 [\mathbf{I}] + \lambda [\mathbf{C}_x] + [\mathbf{A}] + [\mathbf{K}_x] & \lambda [\mathbf{D}_y] + \lambda [\mathbf{CM}_y] + [\mathbf{E}_y] \\
 \lambda [\mathbf{D}_x] + \lambda [\mathbf{CM}_x] + [\mathbf{E}_x] & \lambda^2 [\mathbf{I}] + \lambda [\mathbf{C}_y] + [\mathbf{A}] + [\mathbf{K}_y]
 \end{bmatrix}
 \begin{Bmatrix}
 (\mathbf{q}_x) \\
 (\mathbf{q}_y)
 \end{Bmatrix} = 0 \tag{4.9}$$

The above matrix equation can be solved for  $\lambda_i$  and  $\mathbf{q}_{xi}$  and  $\mathbf{q}_{yi}$ , which are the damped natural frequencies of the system and their corresponding eigenvectors.

#### 4.2 Solution Procedures for Modal Stability Analysis

The stability and the damped modes of the system can be obtained by solving the set of homogeneous modal equations of motion in (4.9). This can be accomplished by expanding the set of  $2n$  second order equations into the standard eigenvalues form of a set of  $4n$  first order equations as follows.

$$\begin{bmatrix} \lambda[I] & 0 & 0 & 0 \\ 0 & \lambda[I] & 0 & 0 \\ 0 & 0 & \lambda[I] & 0 \\ 0 & 0 & 0 & \lambda[I] \end{bmatrix} \begin{Bmatrix} \lambda(q_x) \\ \lambda(q_y) \\ (q_x) \\ (q_y) \end{Bmatrix} - \begin{bmatrix} -[C_x] & -[D_x + CM_x] & -[K_x + \Lambda] & -[E_x] \\ -[D_y + CM_y] & -[C_y] & -[E_y] & -[K_y + \Lambda] \\ [I] & 0 & 0 & 0 \\ 0 & [I] & 0 & 0 \end{bmatrix} \begin{Bmatrix} \lambda(q_x) \\ \lambda(q_y) \\ (q_x) \\ (q_y) \end{Bmatrix} = 0 \quad (4.10)$$

or in compact form as

$$\det [\lambda[I] - [A]] = 0$$

The set of equations in (4.10) can now be solved using various eigenvalue search procedures such as the power method, the Q-R algorithm, or the Leverrier's algorithm. Since for most rotor systems only the first several modes are of importance, it is more profitable to use a solution procedure which only searches for the lower modes instead of searching for all the modes of the system. In this particular study, the Leverrier's algorithm [65] is used. The matrix homogeneous equations can be expanded into a polynomial equation of the form as follows:

$$\lambda^{4n} + p_1 \lambda^{4n-1} + p_2 \lambda^{4n-2} + \dots + p_{4n-1} \lambda + p_{4n} = 0 \quad (4.11)$$

where

$$p_1 = - \text{trace } [A]$$

$$p_k = - \frac{1}{k} \text{trace } [AB_{k-1}] \quad k = 2, 3, 4, \dots, 4n$$

$$[B_1] = [A] + p [I]$$

$$[B_k] = [A] [B_{k-1}] + p_k [I] \quad k = 2, 3, 4, \dots, 4n$$



The damped natural frequencies of the system can now be obtained as the roots of the polynomial equation of (4.11). A powerful procedure for obtaining these complex roots is the Newton-Raphson iteration [11] approach, by which the smaller roots can be calculated relatively rapidly. Assuming an initial value  $\lambda_0$

$$\Delta = \Delta_0 + (\lambda - \lambda_0) \left( \frac{d\Delta}{d\lambda} \right)_0 = 0 \quad (4.12)$$

$$\Delta = \lambda^{4n} + p_1 \lambda^{4n-1} + \dots + p_{4n-1} \lambda + p_{4n} = 0$$

and

$$\Delta_0 = \lambda_0^{4n} + p_1 \lambda_0^{4n-1} + \dots + p_{4n-1} \lambda_0 + p_{4n}$$

Solving equation (4.12) for a new estimate of the eigenvalue  $\lambda$  yields

$$\lambda = \lambda_0 - \Delta_0 / \left( \frac{d\Delta}{d\lambda} \right)_0 \quad (4.13)$$

In order to avoid the recalculation of the already obtained roots, a sweeping condition has to be included by rewriting equation (4.13) as

$$\lambda = \lambda_0 - \Delta_0 \left[ \left( \frac{d\Delta}{d\lambda} \right)_0 - \Delta_0 \sum_{j=1}^M \frac{1}{\lambda_0 - \lambda_j} \right]^{-1} \quad (4.14)$$

where  $M$  is the number of roots has been previously calculated. The convergence using the Newton-Raphson technique is less than 10 iterations in most cases.

With the calculation of the damped natural frequencies  $\lambda_i$ , the stability of the system can be obtained by

$$\lambda_i = P_i \pm i\omega_d i \quad (4.15)$$

where  $P$  is the real part or growth factor indicating the stability (negative values are stable), while the imaginary part  $\omega_d$  is the damped critical speed of the system. Further, the modal coordinates of the system can also be obtained using Leverrier's algorithm as

$$\begin{bmatrix} q^{(i)} \end{bmatrix} = B_1 + \lambda_i B_2 + \lambda_i^2 B_3 + \dots + \lambda_i^{n-1} B_n \quad (4.16)$$

where  $B_i$  is defined as in equation (4.11). The matrix  $\begin{bmatrix} q^{(i)} \end{bmatrix}$  combines of  $n$  column vectors of mode shapes in which each column is proportional to each other. Thus only one column of the matrix is necessary for the determination of the eigenvector of the corresponding material frequency  $\lambda_i$ . Since the  $[B_i]$  matrices are obtained during the expansion of the polynomial as in equation (4.11), the eigenvector

(or mode shapes) of the system can be obtained with little extra computation. It can be seen that the element in the  $[B_i]$  matrix and also the value of  $\lambda_i$  may be very large. Initial scaling of the vector may be a necessity when using this procedure.

To compute the eigenvector of the corresponding  $\lambda_i$  of the system, the modal coordinate calculated are multiplied to the orthogonal mode shapes such that

$$\begin{Bmatrix} \phi_i \\ \phi_i \end{Bmatrix} = \begin{Bmatrix} \phi_i \\ \phi_i \end{Bmatrix} = \begin{bmatrix} A_e \\ A_B \end{bmatrix} \begin{Bmatrix} q^{(i)} \end{Bmatrix}$$

Since for every eigenvalue  $\lambda_j$  there exists a set of modal coordinate vector  $\{q^{(i)}\}$  such that the damped eigenvector for every  $\lambda_j$  can readily be obtained by the above modal treatment.

#### 4.3 Applications and Comparisons of Different Modal Methods

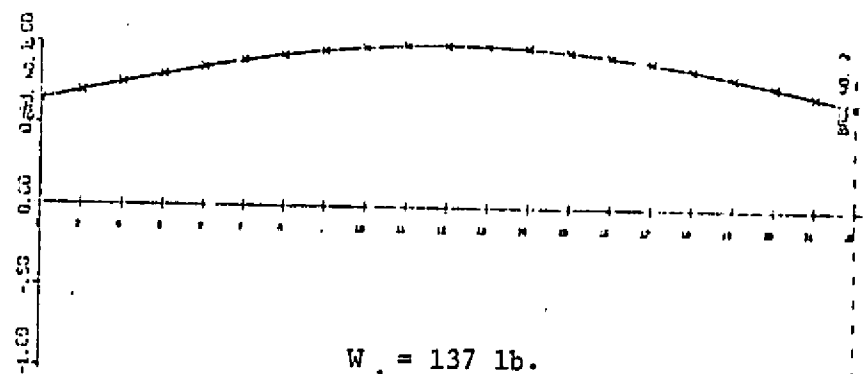
To illustrate the use of modal approach in calculating damped modes, a simple rotor model is used as an example. Consider a uniform rotor of 50 inches long and 4 inches in diameter supported by two symmetric bearings with stiffness of 60,000 lb/in. and damping of 100 lb-sec/in. The undamped critical speeds of the system are calculated by a transfer matrix computer program to be 4,193 RPM, 8,230 RPM, 19,806 RPM, and 48,000 RPM, and their corresponding mode shapes are given in Figure 4.1.

Table 4.1 represents the comparison of the undamped, damped critical speeds and the speeds at which maximum unbalance response was determined for the uniform rotor. The undamped critical speeds were calculated in this case to be 4,193 RPM and 8,230 RPM as shown in Figure 4.1, and the amplification factor for the first and second modes using the single mass theory such that  $A_c = \frac{1}{2\xi}$  predicts that the first and second amplification factors will be 2.936 and 0.38 respectively for the first and second modes. This equation is based on the common assumption used in structural vibration theory that the modal damping cross coupling terms can be ignored and that each modal amplification factor can be calculated independently. It will be shown that even for the case of bearing damping  $C_b = 200$  lb-sec/in. that this computation is greatly in error.

A matrix transfer stability program based on the theory as outlined by Lund [11] was programmed and the damped eigenvalues were calculated as shown in table 4.1. The damped natural frequencies

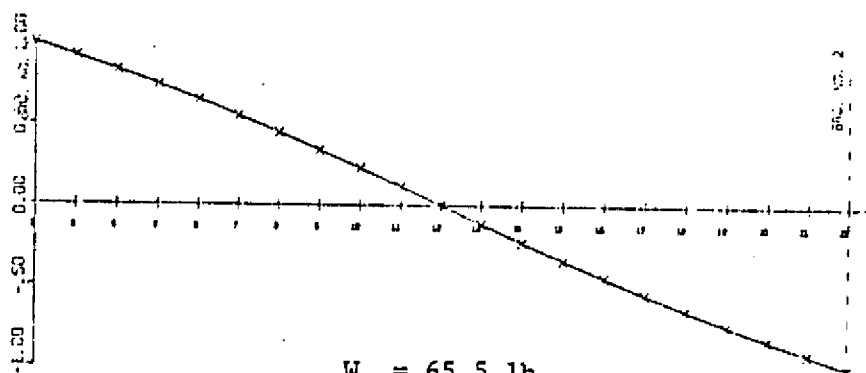
Figure 4.1

CRITICAL SPEED OF UNIFORM LUND  
ROTOR FOR  $k_b = 60,000$  LB/IN



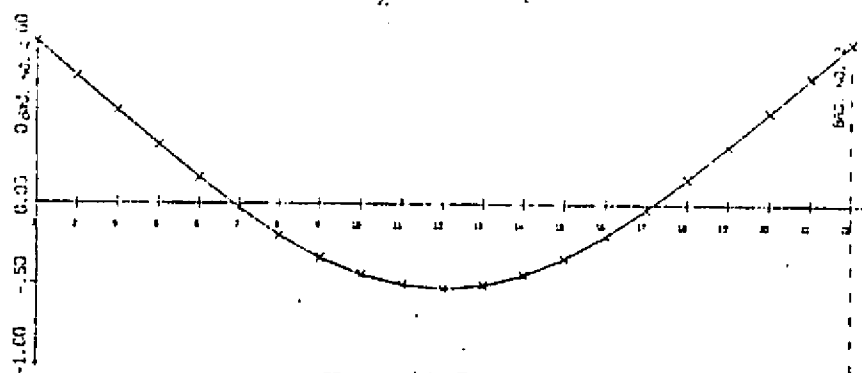
$W_1 = 137$  lb.

$N_1 = 70$  cps



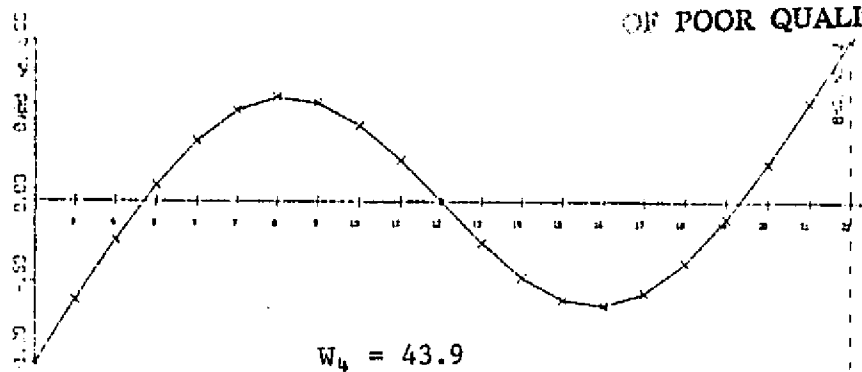
$W_2 = 65.5$  lb.

$N_2 = 137$  cps



$W_3 = 41.7$  lb.

$N_3 = 330.1$  cps



$W_4 = 43.9$

$N_4 = 800$  cps

ORIGINAL PAGE IS  
OF POOR QUALITY

TABLE 4.1

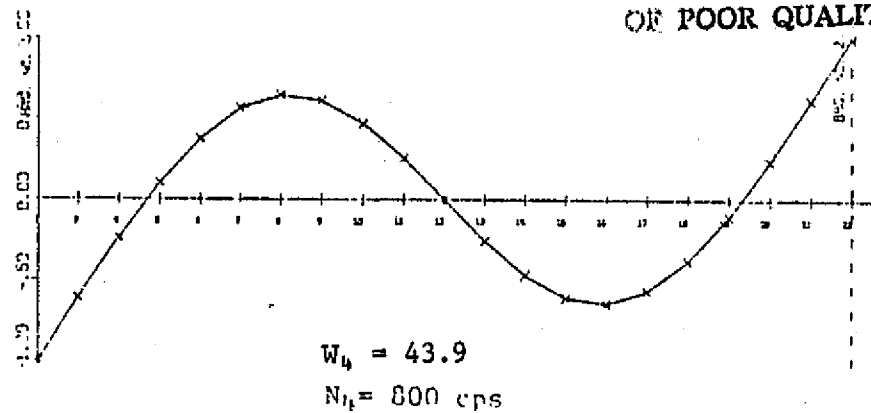
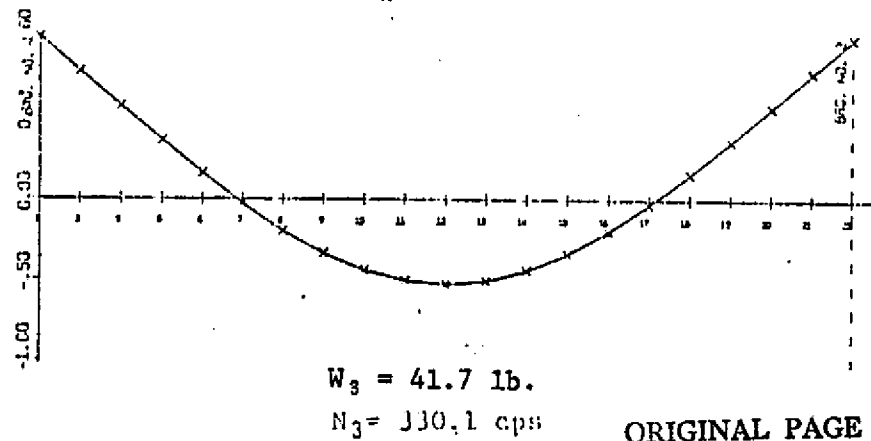
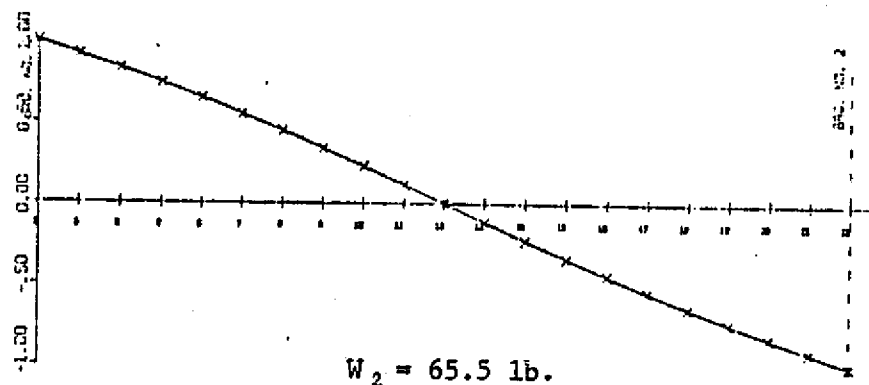
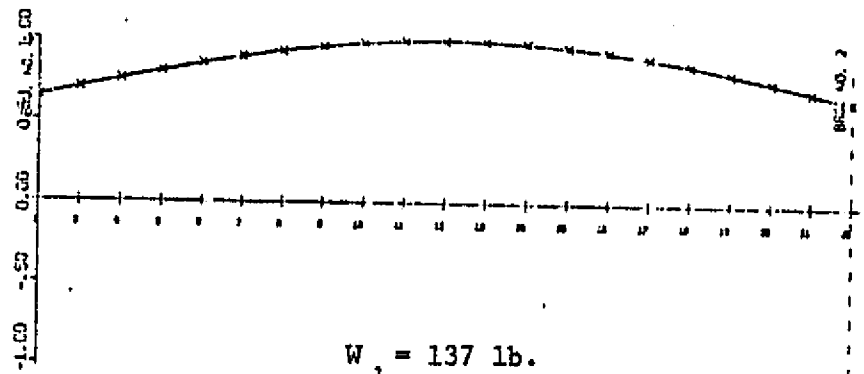
COMPARISON OF DAMPED AND UNDAMPED  
CRITICAL SPEEDS AND AMPLIFICATION FACTORS

$C_b = 200 \text{ lb-sec/in}$        $K_b = 60,000 \text{ lb/in}$

	MODE	
	1	2
$N_c$ (undamped)	4,193 RPM (69.84 Hz)	8,230 RPM (137.2 Hz)
$A_c$ (undamped)	0.936	0.38
$N_d$ (trans. matrix)	5,713 RPM (95.2 Hz)	35,040 RPM (584 Hz)
P	-283 rad/sec	-1199 rad/sec
$N_c$ (calc)	6,319 RPM (105 Hz)	36,863 RPM (614.4 Hz)
$A_u$	1.29 ( $\xi = .427$ )	1.69
$N_d$ (modal)	5,667 RPM (94.46 Hz)	37,403.6 RPM (623 Hz)
P	-307	-1145.9
$N_c$	6,380 RPM (106.3 Hz)	42,463 RPM (707.7 Hz)
$A_u$	1.23	1.85

Figure 4.1

CRITICAL SPEED OF UNIFORM LUND  
ROTOR FOR  $k_b = 60,000 \text{ LB/IN}$



ORIGINAL PAGE IS  
OF POOR QUALITY

TABLE 4.1

COMPARISON OF DAMPED AND UNDAMPED  
CRITICAL SPEEDS AND AMPLIFICATION FACTORS

$$C_b = 200 \text{ lb-sec/in} \quad K_b = 60,000 \text{ lb/in}$$

	MODE	
	1	2
$N_c$ (undamped)	4,193 RPM (69.84 Hz)	8,230 RPM (137.2 Hz)
$A_c$ (undamped)	0.936	0.38
$N_d$ (trans. matrix)	5,713 RPM (95.2 Hz)	35,040 RPM (584 Hz)
P	-283 rad/sec	-1199 rad/sec
$N_c$ (calc)	6,319 RPM (105 Hz)	36,863 RPM (614.4 Hz)
$A_u$	1.29 ( $\xi = .427$ )	1.69
$N_d$ (modal)	5,667 RPM (94.46 Hz)	37,403.6 RPM (623 Hz)
P	-307	-1145.9
$N_c$	6,380 RPM (106.3 Hz)	42,463 RPM (707.7 Hz)
$A_u$	1.23	1.85



were calculated to be approximately 5,713 RPM for the first mode and 35,040 RPM for the second mode. The values of  $P_1 = -283$  rad/sec and  $P_2 = -1199$  rad/sec are the damping exponents of the system indicating the stability of the system.

The equivalent undamped critical speed as illustrated by single mass theory is

$$\omega_i = \sqrt{\omega_d^2 + p^2}$$

Thus using the real and imaginary components, the undamped natural frequency is calculated to be 6,319 RPM and 36,863 RPM for the second mode. The modal amplification factors for each mode are calculated in the following example to be 1.29 and 1.69.

Using the modal approach, if  $N$  natural modes of motion are assumed, there will be  $N$  simultaneous equations to be solved for the determination of the coefficients  $A_i$ . As an example of this procedure, the undamped mode shapes for the uniform rotor were used to determine the first and second damped natural frequencies. It can be assumed that due to rotor symmetry the second and fourth modes will not contribute to the formulation of the first or third mode shape due to the symmetry of the mode shapes. The first and third modal equations were solved simultaneously as follows:

$$\ddot{A}_1 + C_{11} \dot{A}_1 + C_{13} \dot{A}_3 + \omega_1^2 A_1 = 0 \quad (4.17)$$

C-2

$$\ddot{A}_3 + C_{31} \dot{A}_1 + C_{33} \dot{A}_3 + \omega_3^2 A_3 = 0 \quad (4.18)$$

Assuming a solution of the form

$$A = \bar{A} e^{\lambda t} = \bar{A} e^{(p \pm i\omega d)t} \quad (4.19)$$

We can write the result in matrix form as follows

$$\begin{bmatrix} \lambda^2 + \omega_1^2 + \lambda C_{11} & \lambda C_{13} \\ \lambda C_{31} & \lambda^2 + \omega_3^2 + \lambda C_{33} \end{bmatrix} \begin{Bmatrix} \bar{A}_1 \\ \bar{A}_3 \end{Bmatrix} = \begin{Bmatrix} 0 \\ 0 \end{Bmatrix} \quad (4.20)$$

The corresponding frequency equation is

$$\begin{aligned} & \lambda^4 + \lambda^3(C_{11} + C_{33}) + \lambda^2(\omega_1^2 + \omega_3^2 - C_{13}C_{31} + C_{11}C_{33}) \\ & + \lambda(C_{11}\omega_3^2 + C_{33}\omega_1^2) + \omega_1^2\omega_3^2 = 0 \end{aligned} \quad (4.21)$$

$$\begin{aligned} \text{With } C_{11} &= 468, & C_{13} &= 726 \\ C_{31} &= 2388, & C_{33} &= 3704 \end{aligned}$$

Equation (4.21) can be solved as

$$\lambda^4 + 4172\lambda^3 + 4.49 \times 10^5\lambda^2 + 2.73 \times 10^9\lambda + 8.29 \times 10^{11} = 0$$

with the solution

$$\lambda_1 = -307 \pm 1593.5 \text{ rad/sec}$$

This value is in close agreement with the value calculated by the transfer matrix method as shown in Table 4.1. The amplification factor predicted from the transfer matrix method was 1.29 whereas the value calculation based on the first mode is only 0.93 (as given in Table 4.1).

This value is in close agreement to the value calculated by transfer matrix method as shown in Table 4.1.

In a similar fashion, using only the second and the fourth undamped modes, the second complex eigenvalue is predicted to be

$$\lambda_2 = -1145.9 \pm 13916.9 \text{ rad/sec}$$

The resulting second response speed amplification factor is calculated to be

$$A_{u2} = 1.85$$

Comparing the calculations of the damped natural frequencies for the first and second modes, the modal method compares favorably with the calculated numerical values based on the matrix transfer stability program. Because of the simplicity of the system, the

first and second damped modes may be accurately calculated by applying the conditions of symmetry; that is, only the first and third modes are necessary for the accurate calculation of the first damped mode and only the second and fourth modes are necessary for the calculation of the damped second critical speed. In complex multistage turborotors, however, there is usually not the convenient condition of symmetry as it exists in this sample problem. However, the first damped mode can often be accurately calculated by using the first three undamped critical speeds.

In addition to the calculation of the damped natural frequency by means of the modal method, the damped mode shapes can also be determined. This also provides considerable insight into the elastic shaft deformation behavior of the rotor at resonance. By applying the complex eigenvalue to equation (4.17)

$$A_3 = - \frac{(\lambda^2 + C_{11} \lambda + \omega_1^2)}{C_{13} \lambda} A_1$$

and normalizing the first coefficient  $A_1 = 1$ , the coefficient  $A_3$  can be calculated as follows.

$$A_3 = \frac{-(4.46 \times 10^5 \angle 125.3^\circ + 3.13 \times 10^5 \angle 117.3^\circ + 1.92 \times 10^5 \angle 0^\circ)}{4.848 \times 10^5 \angle 117.4^\circ}$$

$$= 0.47 \angle 85.19^\circ$$

Therefore, it can be seen that the complex first damped mode is a function of both the first and the third mode. The third mode is approximately  $90^\circ$  leading the first mode and its magnitude is approximately one half of the first mode. Therefore, we conclude that with a bearing damping of  $C_b = 200$  lb-sec/in, the complex first mode is composed of the normalized first mode plus 50% of the third mode leading the first mode by  $90^\circ$ .

In summary, it can be seen that the introduction of bearing damping of 200 lb-sec/in into the simple model will cause a considerable shift of the rotor natural frequencies. From the standpoint of examining the peak response of the rotor, it can be shown that if an undamped modal expansion is used, the rotor amplitude may be calculated with less than approximately 5% error when undamped modes up to approximately five times running speed are incorporated.

To further illustrate the application of the method, modal calculations were performed for an 8-stage centrifugal compressor as discussed by Lund [11] where the damped natural frequencies were calculated. The rotor weighs about 1,400 lbs and is 102 inches in length. The center of gravity of the rotor is almost midway between the two identical journal bearings of 5 inches diameter, 1.5 inch length, and 0.0035 inch clearance. A description of the rotor shaft geometric properties is given in Table 4.2 and the bearing characteristics are given in Table 4.3. An undamped critical speed analysis with the average bearing stiffness of 609,550 lb/in. at the left bearing and 558,100 lb/in. at the right bearing indicates that the critical

STATION NO.	WEIGHT (LP)	LENGTH (IN.)	SHAFT DIA. OUTSIDE	SHAFT DIA. INSIDE	I (IN**4)	IP-POLAR MOM. (LP-IN**2)	IT-TRANS. MOM. (LB-IN**2)
1	108.172	.800	2.750	0.000	2.81	0.000	0.000
2	13.982	6.300	4.360	0.000	17.74	0.000	0.000
3	21.009	1.400	5.000	0.000	30.68	0.000	0.000
4	12.225	1.600	5.000	0.000	30.68	0.000	0.000
5	19.660	3.240	6.500	0.000	97.62	0.000	0.000
6	24.955	2.000	6.620	0.000	94.28	0.000	0.000
7	25.814	3.300	6.620	0.000	94.28	0.000	0.000
8	34.292	3.180	7.180	0.000	130.46	0.000	0.000
9	29.694	2.300	6.700	0.000	98.92	0.000	0.000
10	66.943	2.900	6.700	0.000	98.92	617.000	309.000
11	28.753	2.300	6.700	0.000	98.92	33.900	17.800
12	66.943	2.900	6.700	0.000	98.92	617.000	309.000
13	28.753	2.300	6.700	0.000	98.92	33.900	17.800
14	66.943	2.900	6.700	0.000	98.92	617.000	309.000
15	28.753	2.300	6.700	0.000	98.92	33.900	17.800
16	81.859	5.890	6.700	0.000	98.92	617.000	309.000
17	58.770	5.890	6.700	0.000	98.92	0.000	0.000
18	83.606	2.650	6.700	0.000	98.92	617.000	309.000
19	34.034	3.350	6.700	0.000	98.92	49.100	27.100
20	70.934	2.650	6.700	0.000	98.92	617.000	309.000
21	34.034	3.350	6.700	0.000	98.92	49.100	27.100
22	70.934	2.650	6.700	0.000	98.92	617.000	309.000
23	34.034	3.350	6.700	0.000	98.92	49.100	27.100
24	81.061	4.680	6.700	0.000	98.92	617.000	309.000
25	50.018	2.700	6.700	0.000	98.92	164.000	121.000
26	25.233	2.160	7.000	0.000	117.86	0.000	0.000
27	27.933	3.320	6.620	0.000	94.28	0.000	0.000
28	25.911	2.000	6.620	0.000	94.28	0.000	0.000
29	24.861	3.220	6.500	0.000	87.62	0.000	0.000
30	19.566	1.600	5.000	0.000	30.68	0.000	0.000
31	8.335	1.400	5.000	0.000	30.68	0.000	0.000
32	16.840	5.320	4.680	0.000	23.55	0.000	0.000
33	41.897	1.750	3.740	0.000	9.60	0.000	0.000
34	41.590	5.150	3.680	0.000	9.00	0.000	0.000
35	12.643	0.000	3.680	0.000	9.00	0.000	0.000
-----		-----					
1420.984		102.800					

ORIGINAL PAGE IS  
OF POOR QUALITY

Table 4.2 GEOMETRIC PROPERTIES OF LUND [11] COMPRESSOR

Table 4.3  
BEARING CHARACTERISTICS USED FOR SIMULATION  
OF THE 8-STAGE COMPRESSOR

Stiffness and damping coefficients.	Bearing Number	
	1	2
$K_{xx}$ (lb/in)	441,000	415,300
$K_{xy}$ (lb/in)	83,330	88,540
$K_{yx}$ (lb/in)	-853,500	-792,400
$K_{yy}$ (lb/in)	778,100	700,900
$C_{xx}$ (lb-sec/in)	786.3	758.7
$C_{xy}$ (lb-sec/in)	-716.4	-674.3
$C_{yx}$ (lb-sec/in)	-716.4	-674.3
$C_{yy}$ (lb-sec/in)	2,196.0	2,196.0

speeds will occur at 3,270 RPM, 7,527 RPM, 9,018 RPM, 14,092, and 27,921 RPM. Note that the effects of bearing cross-coupled stiffness and rotor polar moments of inertia are neglected. The undamped mode shapes for this compressor are typical flexible rotor modes due to high stiffness of the bearings. Normalized mode shapes for the first five critical speed are given in Figures 4.2 and 4.3.

In order to illustrate the use of the modal equation derived in the previous section, the damped natural frequencies of the system were calculated with bearing cross-coupling stiffness and damping effects. A computer program was set up to formulate the standard eigenvalue matrix as given in equation (4.10) and the  $4N$  degree polynomial equation of 4.11 was solved by Leverrier's Algorithm. A rotor speed of 2,000 RPM is assumed for first critical speed calculation of disc gyroscopic calculations and 4,000 RPM for the second critical speed. Using the modal approach discussed in section 4.2, the damped natural frequencies were calculated to be: 2,962 RPM ( $P = -0.43$  rad/sec) for the forward mode and 3,633 RPM ( $P = -19.5$  rad/sec) for the backward whirl mode where  $P$  is the damping exponent of the corresponding critical speed. The mode shapes for the corresponding forward and backward modes of the first critical speed are given in Figure 4.4 and 4.5. Note that the first critical speed backward mode shape given in Figure 4.5 is quite similar to the conventional free-free undamped critical speed mode. (Lund [11] pointed out that the first two backward modes were damped out and the third backward mode appears to be the first.) But this



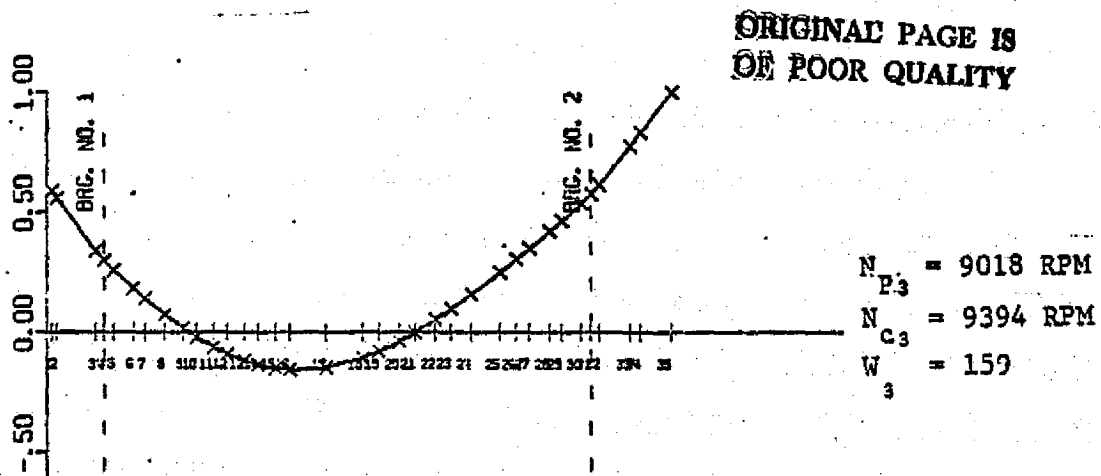
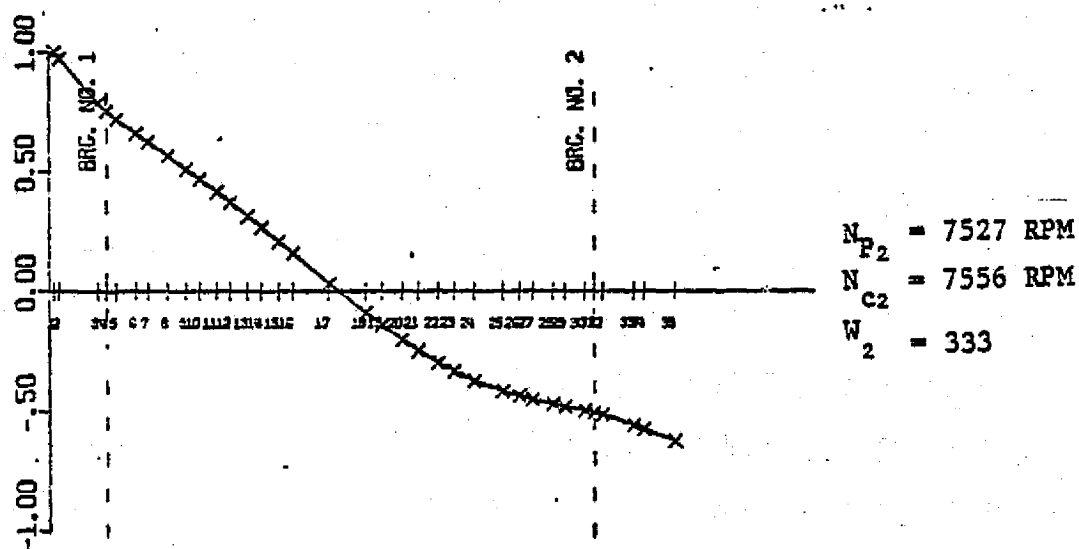
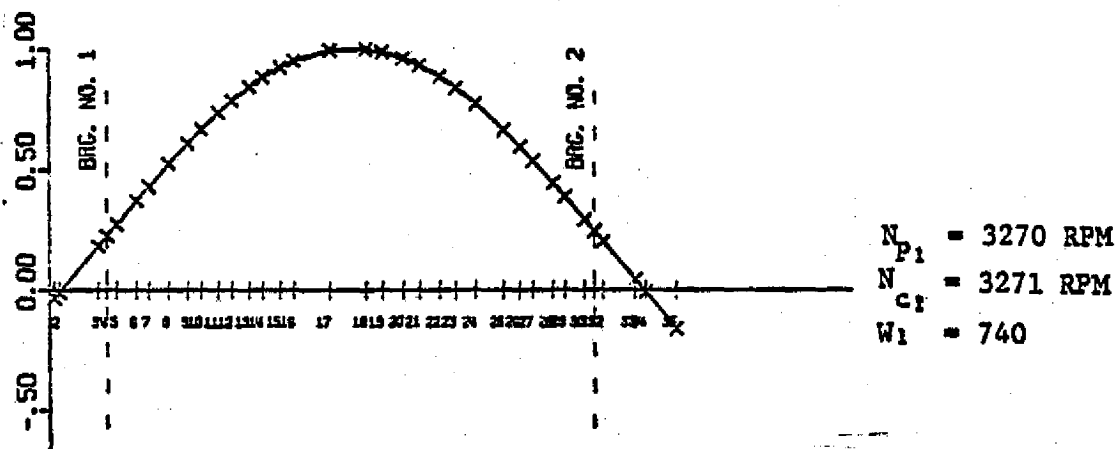
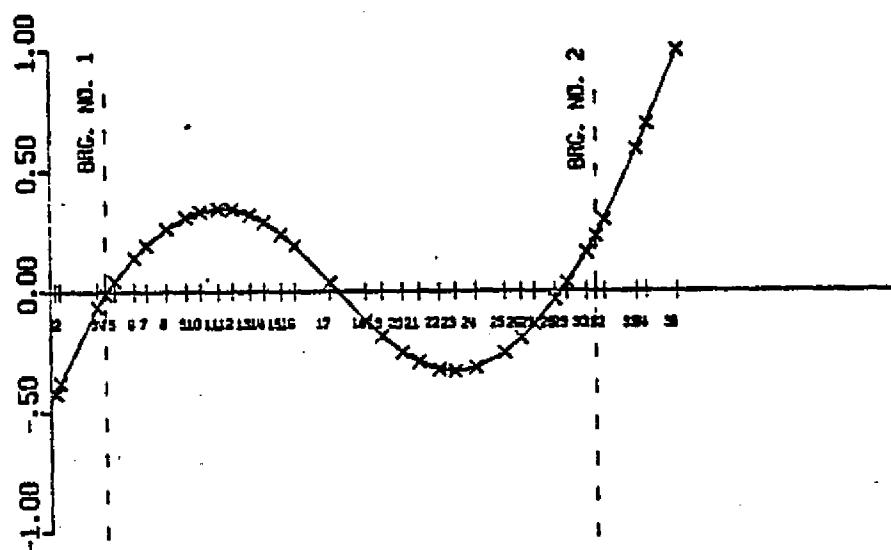
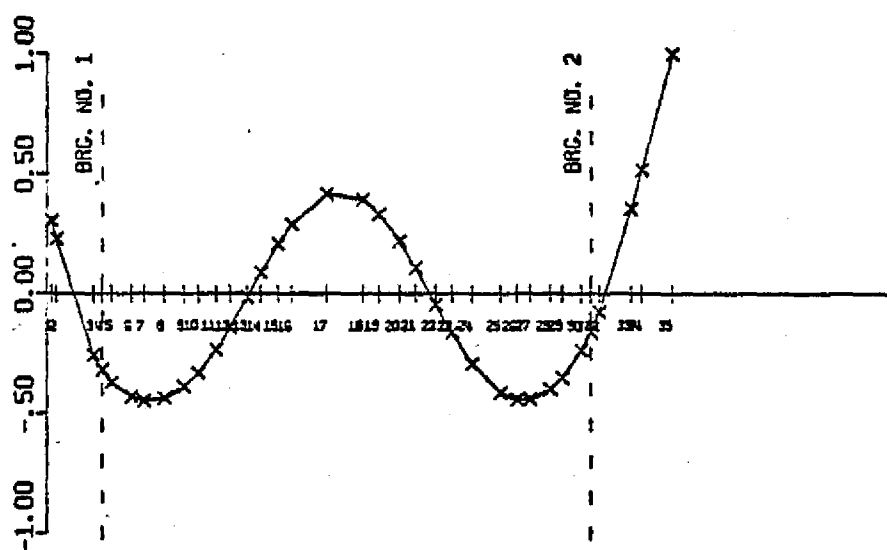


FIGURE 4.2 FIRST THREE UNDAMPED COMPRESSOR PLANAR MODE SHAPES



$N_{C4} = 14092 \text{ RPM}$   
 $N_{C4} = 14763 \text{ RPM}$   
 $W_4 = 144 \text{ LB}$



$N_{P5} = 27921 \text{ RPM}$   
 $N_{C5} = 29822 \text{ RPM}$   
 $W_5 = 151 \text{ LB}$

FIGURE 4.3 4th AND 5th UNDAMPED COMPRESSOR PLANAR MODE SHAPES

ORIGINAL PAGE IS  
OF POOR QUALITY

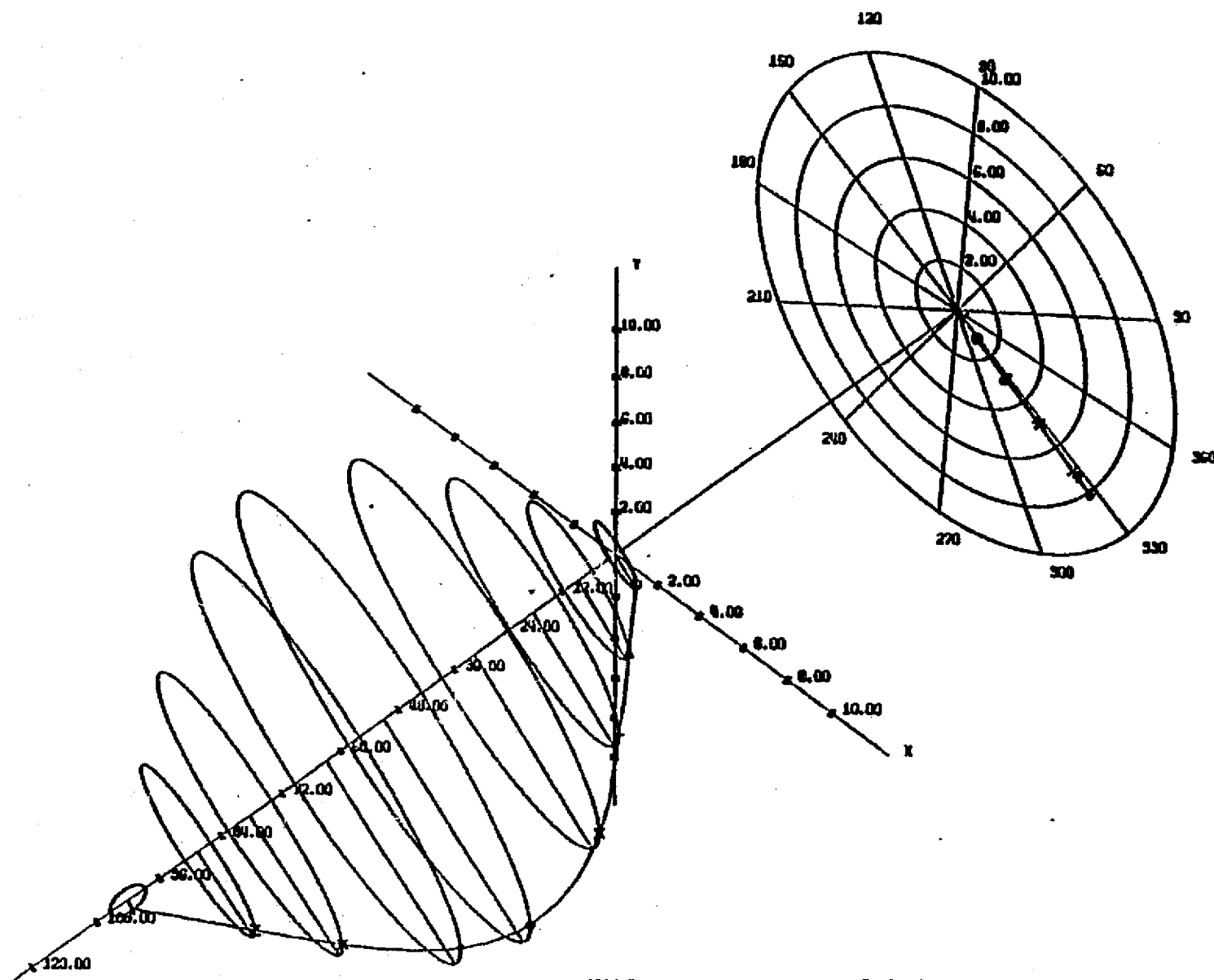


FIGURE 4.4 FIRST DAMPED FORWARD COMPRESSOR MODE SHAPE

$N = 2962 \text{ RPM}$

$P = -0.43 \text{ rad/sec}$

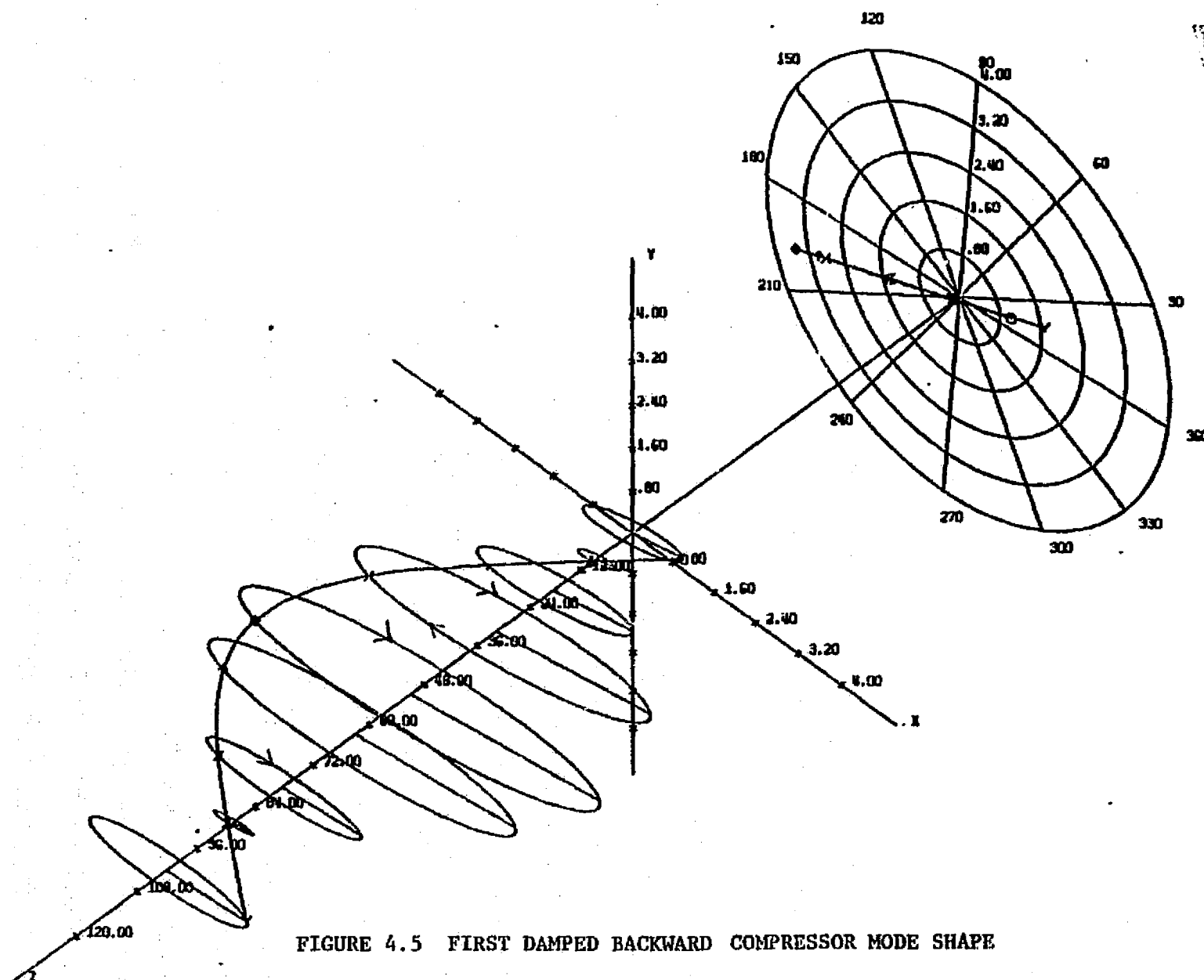


FIGURE 4.5 FIRST DAMPED BACKWARD COMPRESSOR MODE SHAPE

$N = 3633 \text{ RPM}$

$P = -19.5 \text{ rad/sec}$

ORIGINAL PAGE IS  
OF POOR QUALITY

mode will not be easily excited due to its high damping exponent values while the first forward mode with  $P$  almost zero is close to the stability threshold. This means that the rotor is marginally stable and has a very high rotor amplification factor, and hence may cause a large rotor unbalance response at the first critical speed. Similarly, the rotor backward resonance speed and amplification factor are computed to be  $N_{u_1}^b = 3,651$  RPM and  $A_{u_1}^b = 9.64$ . Thus, it can be seen that the forward mode has a much higher amplification factor than the backward mode and will be very easy to excite.

Similar modal calculations show that the second damped natural frequency will have a forward critical speed at 4,933 RPM ( $P = -104.7$  rad/sec). In this case, the backward critical speed occurs at a speed of 13,910 RPM, which is much higher than the forward critical speed (the third forward damped critical speed is 6,730 RPM). The forward and backward mode shapes of the second damped critical speed are given in Figures 4.6 and 4.7. Note that in Figure 4.7, the second backward mode shape is similar to a conventional fourth bending mode because the second and third backward critical modes are critically damped over their critical speed range [11].

A further justification of the planar modal analysis is the comparisons of results of modal analysis using different sets of undamped mode. Modal stability calculations of the same compressor were performed using (a) four undamped planar modes (from average bearing stiffness), (b) four free-free undamped modes, (c) two

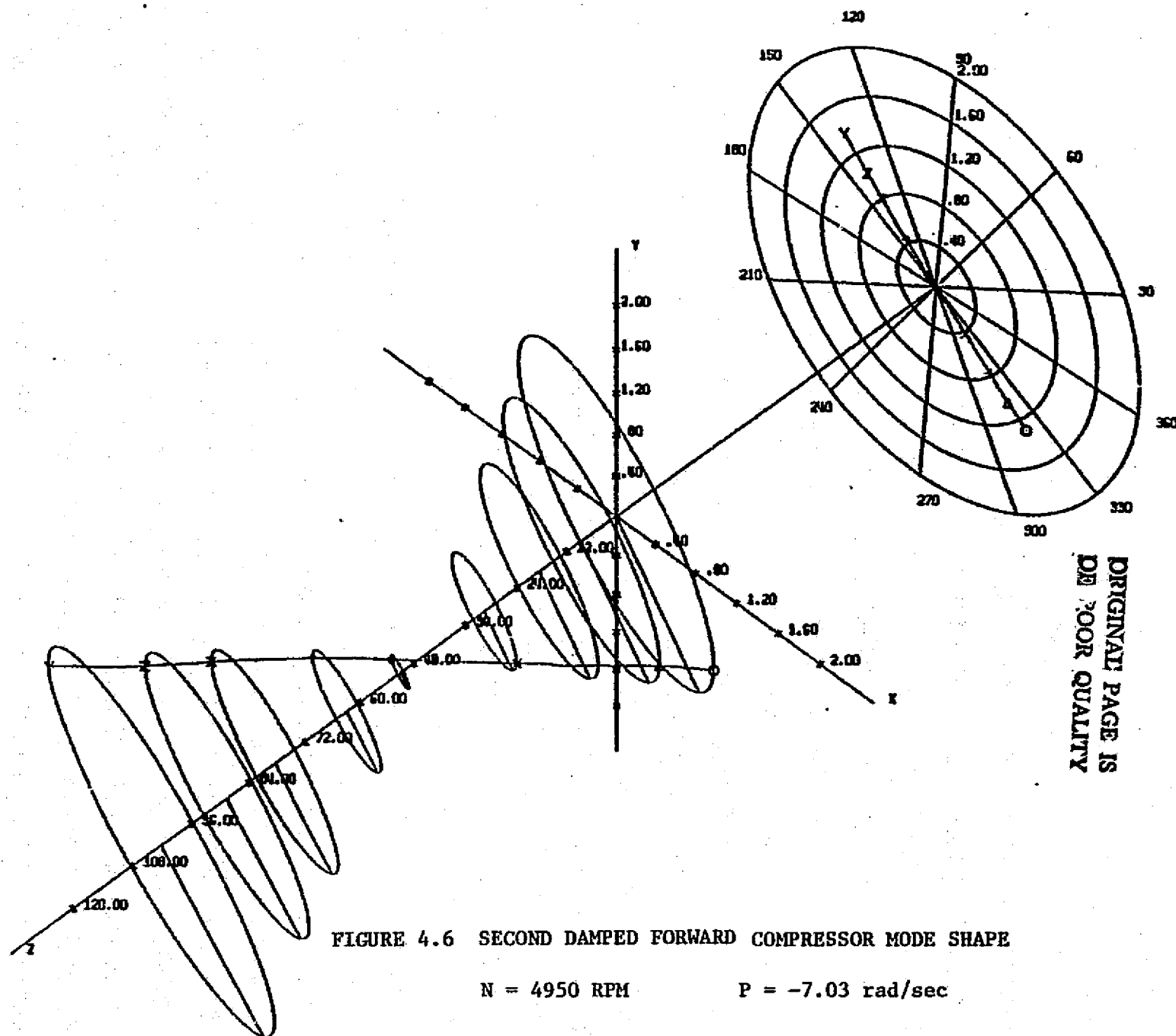


FIGURE 4.6 SECOND DAMPED FORWARD COMPRESSOR MODE SHAPE

$N = 4950 \text{ RPM}$

$P = -7.03 \text{ rad/sec}$

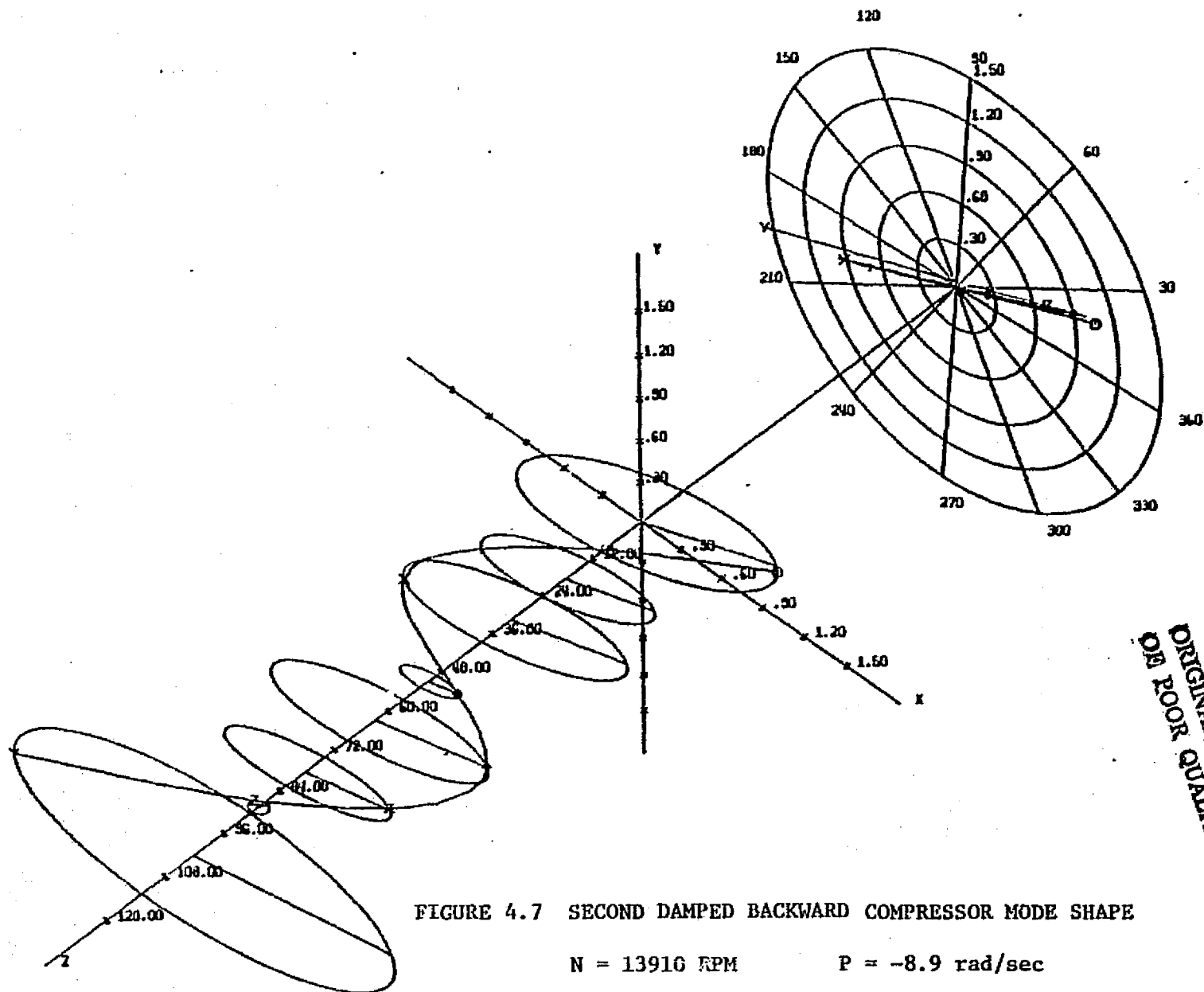


FIGURE 4.7 SECOND DAMPED BACKWARD COMPRESSOR MODE SHAPE

$N = 13916 \text{ RPM}$

$P = -8.9 \text{ rad/sec}$

ORIGINAL PAGE IS  
OF POOR QUALITY

free-free undamped modes plus two rigid body (rotational and translational) modes, (d) four free-free modes plus two rigid body modes, and the corresponding results are given in Table 4.4. A set of values calculated from transfer matrix method are also given in the table. The damped natural frequencies calculated from planar modes and the free-free plus rigid body modes are in very close agreement to each other, and their accuracy is verified by the values predicted by the matrix transfer calculations.

In the case of using only four planar modes, eight damped natural frequencies are resulted from solving the frequency equation of (4.11). The complex frequencies calculated are in good agreement with the matrix transfer method, especially for the lower frequencies. Including the computation of the planar modes, the computer time used (central processor time of the Cyper 172 system) is the least of all cases (23.2 seconds as given in Table 4.4). In the case of using 4 free-free modes of the system, the solution is quite misleading. The two lowest and the two zero frequencies of the system are missing due to the lack of basic rigid-body mode contributions. The computer time consumed is higher than the previous case of using planar modes because more computer time has been consumed in calculating the free-free modes. The complex frequencies calculated by the 2 free-free plus 2 rigid body modes are also in good agreement with those by the transfer matrix method. Comparing these results with those of the planar modes, it seems that the planar mode calculation has better accuracy in the lower frequencies while the free-free plus rigid body mode calculation has more accuracy



TRANSFER MATRIX		4 AVERAGE STIFFNESS MODES		4 FREE-FREE MODES		2 FREE-FREE PLUS 2 RIGID BODY MODES		4 FREE-FREE PLUS 2 RIGID BODY MODES	
P rad/sec	$\omega_d$ RPM	P rad/sec	$\omega_d$ RPM	P rad/sec	$\omega_d$ RPM	P rad/sec	$\omega_d$ RPM	P rad/sec	$\omega_d$ RPM
-6,630	0	-2,074	0	-	-	-2,457	0	-3,712	0
-834	0	-921	0	-	-	-2,070	0	-838.8	0
-0.36	2,955	-0.49	2,967	-	-	-0.65	2,978	-2.33	2,969
-18.5	3,623	-20.5	3,639	-	-	-18.5	3,659	-16.5	3,633
-108.7	4,835	-104.7	4,933	-93.1	6,362	-112.0	4,836	-108.7	4,834
-149.7	6,687	-139.2	6,779	-101.5	6,680	-153	6,637	150.8	6,650
-8.9	13,885	-6.8	13,912	-5.37	14,050	-6.28	13,906	-8.02	13,896
-5.8	14,032	-5.3	14,037	-21.2	14,077	-5.8	14,033	-5.8	14,036
-382	24,600	-	-	-381	28,252	-	-	-221	24,997
-95.1	27,600	-	-	-93.4	27,520	-	-	-93.5	27,440
-1,360	42,500	-	-	-327	40,385	-	-	-958	31,822
-340	42,500	-	-	-1,679	40,383	-	-	-330	42,005
C.P. TIME 33.8 sec.		23.2 sec.		27.4 sec.		27 sec.		56.8 sec.	

Table 4.4 Comparisons of The Complex Eigenvalues Calculated by the Modal and Matrix Transfer Methods

in the higher frequencies. Again the computer time used in this case is slightly higher than using the planar modes. For further investigation, the system complex frequencies were also computed using 4 free-free plus 2 rigid body modes of the system. As shown in Table 4.4, this use of two additional free-free modes did not improve the results significantly, but the computer time consumed has increased over 100 percent (from 27 seconds to 56.8 seconds). Thus it can be concluded that if only the lower frequencies of the system are required, the use of a few basic system undamped modes can give very good results. However, there is a drawback in this modal analysis such that the damping exponents (real part of the complex frequencies) of the system may sometimes be inaccurate due to the lack of the higher mode contributions. When the number of modes used is restricted by computational time and cost consideration, the use of planar (average stiffness) modes will be a better approach.

## V. FORCED RESPONSE ANALYSIS USING MODAL ANALYSIS

### 5.1 Solutions of Modal Equations of Motion

In solving for the forced response of the rotor-bearing system, the matrix equation of motion in (3.1) is transformed into modal coordinates using a set of undamped orthogonal modes. With the effects of unbalance, disc skew, shaft bow, and rotor acceleration, the set of modal equations in the x-z plane can be written as follows

$$\begin{aligned}
 & \begin{bmatrix} [M] & 0 \\ 0 & [I_t] \end{bmatrix} \begin{bmatrix} [A_e] \\ [A_\beta] \end{bmatrix} \begin{bmatrix} \ddot{q}_x \\ \ddot{q}_x \end{bmatrix} + \begin{bmatrix} [c_{xx}] & [c_{x\theta}] \\ [c_{\theta x}] & [c_{\theta\theta}] \end{bmatrix} \begin{bmatrix} [A_e] \\ [A_\beta] \end{bmatrix} \begin{bmatrix} \dot{q}_x \\ \dot{q}_x \end{bmatrix} \\
 & + \begin{bmatrix} [k_{xx} + K_b] & [k_{x\theta}] \\ [k_{\theta x}] & [k_{\theta\theta}] \end{bmatrix} \begin{bmatrix} [A_e] \\ [A_\beta] \end{bmatrix} \begin{bmatrix} q_x \\ q_x \end{bmatrix} - \begin{bmatrix} [k_{xx}] & [k_{x\theta}] \\ [k_{\theta x}] & [k_{\theta\theta}] \end{bmatrix} \begin{bmatrix} x_d \\ \theta_d \end{bmatrix} \\
 & + \begin{bmatrix} [K_{xx} - K_b] & [K_{x\theta}] \\ [K_{\theta x}] & [K_{\theta\theta}] \end{bmatrix} \begin{bmatrix} [A_e] \\ [A_\beta] \end{bmatrix} \begin{bmatrix} q_x \\ q_x \end{bmatrix} + \begin{bmatrix} [c_{xy}] & [c_{x\psi}] \\ [c_{\theta y}] & [c_{\theta\psi}] \end{bmatrix} \begin{bmatrix} [A_e] \\ [A_\beta] \end{bmatrix} \begin{bmatrix} \dot{q}_y \\ \dot{q}_y \end{bmatrix} \\
 & + \begin{bmatrix} 0 & 0 \\ 0 & [\omega I_p] \end{bmatrix} \begin{bmatrix} [A_e] \\ [A_\beta] \end{bmatrix} \begin{bmatrix} \dot{q}_y \\ \dot{q}_y \end{bmatrix} + \begin{bmatrix} [K_{xy}] & [K_{x\psi}] \\ [K_{\theta y}] & [K_{\theta\psi}] \end{bmatrix} \begin{bmatrix} [A_e] \\ [A_\beta] \end{bmatrix} \begin{bmatrix} q_y \\ q_y \end{bmatrix}
 \end{aligned}$$

ORIGINAL PAGE IS  
OF POOR QUALITY

ORIGINAL PAGE IS  
OF POOR QUALITY

$$+ \begin{bmatrix} 0 & 0 \\ 0 & \frac{1}{2} \dot{\omega} I_p \end{bmatrix} \begin{bmatrix} [A_e] \\ [A_\beta] \end{bmatrix} \begin{bmatrix} q_x \\ q_y \end{bmatrix}$$

$$= \begin{bmatrix} (M_e [\omega^2 \cos(\omega t + \alpha) + \dot{\omega} \sin(\omega t + \alpha)]) \\ \tau(I_p - I_t) [\omega^2 \cos(\omega t + \beta) + \dot{\omega} \sin(\omega t + \beta)] \end{bmatrix} \quad (5.1)$$

Note that all the terms in the left-hand side of the equation are represented by generalized coordinates ( $q_x, q_y$ ) except for the bow of the shaft. In the modal approach as discussed in the previous sections, it was noted that for general cases, the shaft stiffness matrix of the shaft is not required after the modal transformation while equation (5.1) has to retain the stiffness matrix in order to include the shaft bow effects. To avoid the derivation of the stiffness matrix and to save computer time and core memory space, the bow of the shaft can also be transformed into modal coordinates as follows:

$$\begin{Bmatrix} (x_d) \\ (\theta_d) \end{Bmatrix} = \begin{bmatrix} [A_e] \\ [A_\beta] \end{bmatrix} \begin{Bmatrix} R_x \end{Bmatrix}$$

$$\begin{Bmatrix} (y_d) \\ (\psi_d) \end{Bmatrix} = \begin{bmatrix} [A_e] \\ [A_\beta] \end{bmatrix} \begin{Bmatrix} R_y \end{Bmatrix}$$

(5.2)

and

$$\begin{bmatrix} [k_{xx}] & [k_{x\theta}] \\ [k_{\theta x}] & [k_{\theta\theta}] \end{bmatrix} \begin{Bmatrix} (x_d) \\ (\theta_d) \end{Bmatrix} = \begin{bmatrix} [k_{xx} + K_b] & [k_{x\theta}] \\ [k_{\theta x}] & [k_{\theta\theta}] \end{bmatrix} \begin{bmatrix} [A_e] \\ [A_\beta] \end{bmatrix} \begin{Bmatrix} R_x \end{Bmatrix}$$

$$- \begin{bmatrix} [K_b] & 0 \\ 0 & 0 \end{bmatrix} \begin{bmatrix} [A_e] \\ [A_\beta] \end{bmatrix} \begin{Bmatrix} R_x \end{Bmatrix}$$

(5.3)

and  $(R_x)$  can be represented by

$$\begin{bmatrix} [A_e] \\ [A_\beta] \end{bmatrix}^T \begin{bmatrix} [M] & 0 \\ 0 & [I_T] \end{bmatrix} \begin{Bmatrix} (x_d) \\ (\theta_d) \end{Bmatrix} = \begin{bmatrix} [A_e] \\ [A_\beta] \end{bmatrix}^T \begin{bmatrix} [M] & 0 \\ 0 & [I_T] \end{bmatrix} \begin{bmatrix} [A_e] \\ [A_\beta] \end{bmatrix} \begin{Bmatrix} R_x \end{Bmatrix} = \begin{Bmatrix} R_x \end{Bmatrix}$$

(5.4)

and therefore

$$\begin{Bmatrix} R_x \end{Bmatrix} = \begin{bmatrix} [A_e] \\ [A_\beta] \end{bmatrix}^T \begin{bmatrix} [M] & 0 \\ 0 & [I_t] \end{bmatrix} \begin{Bmatrix} (x_d) \\ (\phi_d) \end{Bmatrix} = \begin{Bmatrix} [A_e]^T [M] \{x_d\} + [A_\beta]^T [I_t] \{\theta_d\} \end{Bmatrix}$$

(5.5)

Substituting this relationship into Equation (5.1) and premultiplying the equation by  $\begin{bmatrix} [A_e] \\ [A_\beta] \end{bmatrix}^T$  gives the following matrix equation.

$$\begin{aligned} & \{\ddot{q}_x\} + \{[A_e]^T [C_{xx}] [A_e] + [A_e]^T [C_{x\theta}] [A_\beta] + [A_\beta]^T [C_{\theta x}] [A_e] \\ & + [A_\beta]^T [C_{\theta\theta}] [A_\beta]\} \{\dot{q}_x\} + [\omega_1^2] \{q_x\} + \{[A_e]^T [K_{xx} - K_B] [A_e] \\ & + [A_e]^T [K_{x\theta}] [A_\beta] + [A_\beta]^T [K_{\theta x}] [A_e] + [A_\beta]^T [K_{\theta\theta}] [A_\beta]\} \{q_x\} \\ & + \{[A_e]^T [C_{xy}] [A_e] + [A_e]^T [C_{x\psi}] [A_\beta] + [A_\beta]^T [C_{\theta y}] [A_e] \\ & + [A_\beta]^T [C_{\theta\psi}] [A_\beta]\} \{\dot{q}_y\} + \{[A_\beta]^T [-\omega I_p] [A_\beta]\} \{\dot{q}_y\} \\ & + \{[A_e]^T [K_{xy}] [A_e] + [A_e]^T [K_{x\psi}] [A_\beta] + [A_\beta]^T [K_{\theta y}] [A_e] \\ & + [A_\beta]^T [K_{\theta\psi}] [A_\beta]\} \{q_y\} + \{[A_\beta]^T [-\omega I_p] [A_\beta]\} \{q_y\} \end{aligned}$$

$$\begin{aligned}
&= [A_e]^T \{F_x\} + [A_\beta]^T \{m_x\} + \{[\omega_1^2] - [A_e]^T [K_b] [A_e]\} \{[A_e]^T [M] \{x_d\} \\
&+ [A_\beta]^T [I_T] \{\theta_d\}\}
\end{aligned} \tag{5.6}$$

The equations can be written in the compact form as

$$\begin{aligned}
&\{\ddot{q}_x\} + [C_x] \{\dot{q}_x\} + [\Lambda] \{q_x\} + [K_x] \{q_x\} + [D_x] \{\dot{q}_y\} + [CM_x] \{\dot{q}_y\} \\
&+ [E_x] \{q_y\} + [EA_x] \{q_y\} = \{xF\} + \{xB\}
\end{aligned} \tag{5.7}$$

Similarly, the equation for the y-z plane can be written as

$$\begin{aligned}
&\{\ddot{q}_y\} + [C_y] \{\dot{q}_y\} + [\Lambda] \{q_y\} + [K_y] \{q_y\} + [D_y] \{\dot{q}_x\} + [CM_y] \{\dot{q}_x\} \\
&+ [E_y] \{q_x\} + [EA_y] \{q_x\} = \{yF\} + \{yB\}
\end{aligned} \tag{5.8}$$

Combining Equation (5.7) with (5.8) and rearranging the terms, we have

$$\begin{aligned}
&\begin{Bmatrix} \{\ddot{q}_x\} \\ \{\ddot{q}_y\} \end{Bmatrix} = \begin{Bmatrix} \{xF\} + \{xB\} \\ \{yF\} + \{yB\} \end{Bmatrix} - \begin{bmatrix} [C_x] & [D_x + CM_x] \\ [D_y + CM_y] & [C_y] \end{bmatrix} \begin{Bmatrix} \{\dot{q}_x\} \\ \{\dot{q}_y\} \end{Bmatrix} \\
&- \begin{bmatrix} [\Lambda + K_x] & [E_x + EA_x] \\ [E_y + EA_y] & [\Lambda + K_y] \end{bmatrix} \begin{Bmatrix} \{q_x\} \\ \{q_y\} \end{Bmatrix}
\end{aligned} \tag{5.9}$$

Thus, the modal acceleration terms can be calculated from the above equation with initial conditions for the modal displacement given by the following relations

$$\begin{Bmatrix} \langle\langle x(0) \rangle\rangle \\ \langle\langle \theta(0) \rangle\rangle \end{Bmatrix} = \begin{bmatrix} [A_e] \\ [A_\beta] \end{bmatrix} \begin{Bmatrix} q_x(0) \end{Bmatrix} \quad (5.10)$$

or

$$\begin{Bmatrix} q_x(0) \end{Bmatrix} = \begin{bmatrix} [A_e] \\ [A_\beta] \end{bmatrix}^T \begin{bmatrix} [M] & 0 \\ 0 & [I_t] \end{bmatrix} \begin{Bmatrix} \langle\langle x(0) \rangle\rangle \\ \langle\langle \theta(0) \rangle\rangle \end{Bmatrix} \quad (5.11)$$

Similarly, the modal velocity is given by

$$\begin{Bmatrix} \dot{q}_x(0) \end{Bmatrix} = \begin{bmatrix} [A_e] \\ [A_\beta] \end{bmatrix}^T \begin{bmatrix} [M] & 0 \\ 0 & [I_t] \end{bmatrix} \begin{Bmatrix} \langle\langle \dot{x}(0) \rangle\rangle \\ \langle\langle \dot{\theta}(0) \rangle\rangle \end{Bmatrix} \quad (5.12)$$

With the modal acceleration and velocity terms calculated as above, the modal transient motion can be computed by numerical integration in time. The rotor forced response motion can be obtained by back substitution of the modal coefficients into the following equation:



$$\begin{Bmatrix} U(t) \end{Bmatrix} = \begin{Bmatrix} x(t) \\ \theta(t) \\ y(t) \\ \psi(t) \end{Bmatrix} = \begin{Bmatrix} [A_e] \begin{Bmatrix} q_x(t) \end{Bmatrix} \\ [A_\beta] \begin{Bmatrix} q_y(t) \end{Bmatrix} \end{Bmatrix} \quad (5.13)$$

If steady state synchronous unbalance response motion of the rotor is assumed such that

$$\{\ddot{q}_x\} = i\omega \{\dot{q}_x\} = -\omega^2 \{q_x\} \quad (5.14)$$

$$\{\ddot{q}_y\} = i\omega \{\dot{q}_y\} = -\omega^2 \{q_y\} \quad (5.15)$$

Equation (5.7) can be rewritten as

$$\begin{aligned} & \left[ (\omega_1^2 - \omega^2) + i\omega [C_x] + [K_x] \right] \{q_x\} + \left[ i\omega [D_x] + i\omega [CM_x] \right. \\ & \left. + [E_x] + [EA_x] \right] \{q_y\} = \{xF\} + \{xB\} \end{aligned} \quad (5.16)$$

Similarly, equation (5.8)

$$\begin{aligned} & \left[ (\omega_1^2 - \omega^2) + i\omega [C_y] + [K_y] \right] \{q_y\} + \left[ i\omega [D_y] + i\omega [CM_y] \right. \\ & \left. + [E_y] + [EA_y] \right] \{q_x\} = \{yF\} + \{yB\} \end{aligned} \quad (5.17)$$

These two sets of simultaneous equations are coupled, and by solving the  $2n$  system of equations,  $q_x$  and  $q_y$  can be calculated. Thus, the unbalance response of the system at the operating speed of  $\omega$  (rad/sec) can be computed as

$$\begin{bmatrix} U \end{bmatrix} = \begin{bmatrix} (x) \\ (\theta) \\ (y) \\ (\psi) \end{bmatrix}$$

$$= \begin{bmatrix} [A_e] & 0 \\ [A_\beta] & 0 \\ 0 & [A_e] \\ 0 & [A_\beta] \end{bmatrix} \begin{bmatrix} [-\omega_1^2 - \omega^2] + i\omega [C_x] + [K_x] & i\omega [D_x + CM_x] + [E_x + EA_x] \\ i\omega [D_y + CM_y] + [E_y + EA_y] & [-\omega_1^2 - \omega^2] + i\omega [C_y] + [K_y] \end{bmatrix} \begin{bmatrix} \{x_F + x_B\} \\ \{y_F + y_B\} \end{bmatrix} \quad (5.18)$$

The solutions of  $x$  and  $y$  from the complex equation (5.13) are complex. They can be expressed as

$$x = \text{Re} \left[ (x_r + ix_i) e^{i\omega t} \right] \quad (5.19)$$

$$y = \text{Re} \left[ (y_r + iy_i) e^{i\omega t} \right] \quad (5.20)$$

The subscript r denotes the real part of the solution and i denotes the imaginary part of the solution. Thus, the maximum amplitude in x and y coordinate directions are given by

$$|x| = \sqrt{x_r^2 + x_i^2} \quad (5.21)$$

$$|y| = \sqrt{y_r^2 + y_i^2} \quad (5.22)$$

or expanding equations (5.19) and (5.20) that

$$x = x_r \cos \omega t - x_i \sin \omega t \quad (5.23)$$

$$y = y_r \cos \omega t + y_i \sin \omega t \quad (5.24)$$

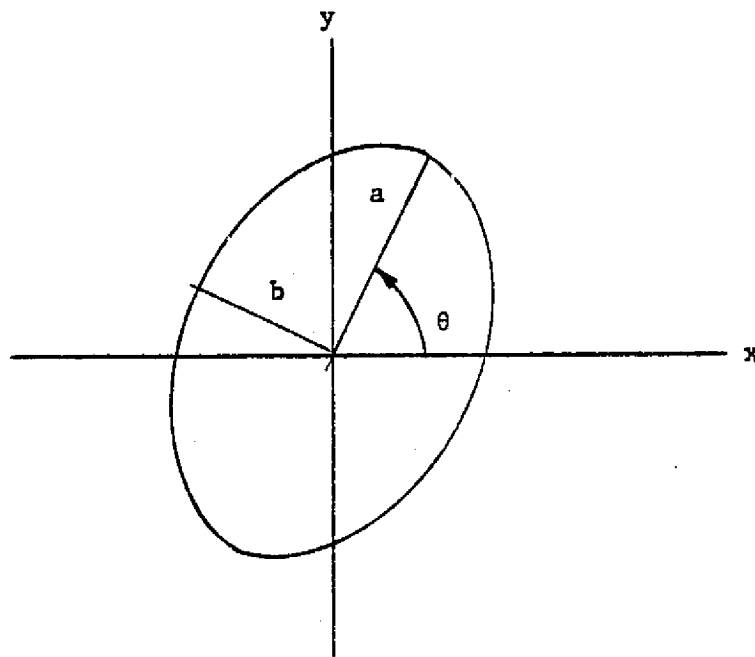
The results of the above equations can be expressed by major and minor elliptical semi-axis [17, 38] a and b as shown in figure 5.1 that

$$a = \sqrt{\frac{1}{2}\eta + \frac{1}{2}\sqrt{\eta^2 + 4\beta^2}} \quad (5.25)$$

$$b = \sqrt{\frac{1}{2}\eta - \frac{1}{2}\sqrt{\eta^2 + 4\beta^2}} \quad (5.26)$$

$$\text{where } \eta = x_r^2 + x_i^2 + y_r^2 + y_i^2$$

$$\beta = x_r y_i - x_i y_r$$



### 5.1 ORIENTATION OF ELLIPTICAL ORBIT MOTION

The orientation angle for the elliptical major axis is given by

$$\theta = \frac{1}{2} \arctan \left( \frac{2(x_r y_r + x_i y_i)}{x_r^2 + x_i^2 - y_r^2 - y_i^2} \right) \quad (5.27)$$

An alternate representation of the rotor motion is to write the x, y components of motion as

$$x = \bar{x} \cos (\omega t - \beta_x) \quad (5.28)$$

$$y = \bar{y} \sin (\omega t - \beta_y) \quad (5.29)$$

The amplitude and phase angle are similar to those obtained from experimental results as indicated in figure 5.2. For the probe to be in the same line as the positive x-axis, the timing mark is at an angle  $\beta_x$  such that

$$\beta_x = \arctan \left( \frac{-x_i}{x_r} \right) \quad (5.30)$$

and similarly for the probe at y axis

$$\beta_y = \arctan \left( \frac{-y_r}{-y_i} \right) \quad (5.31)$$

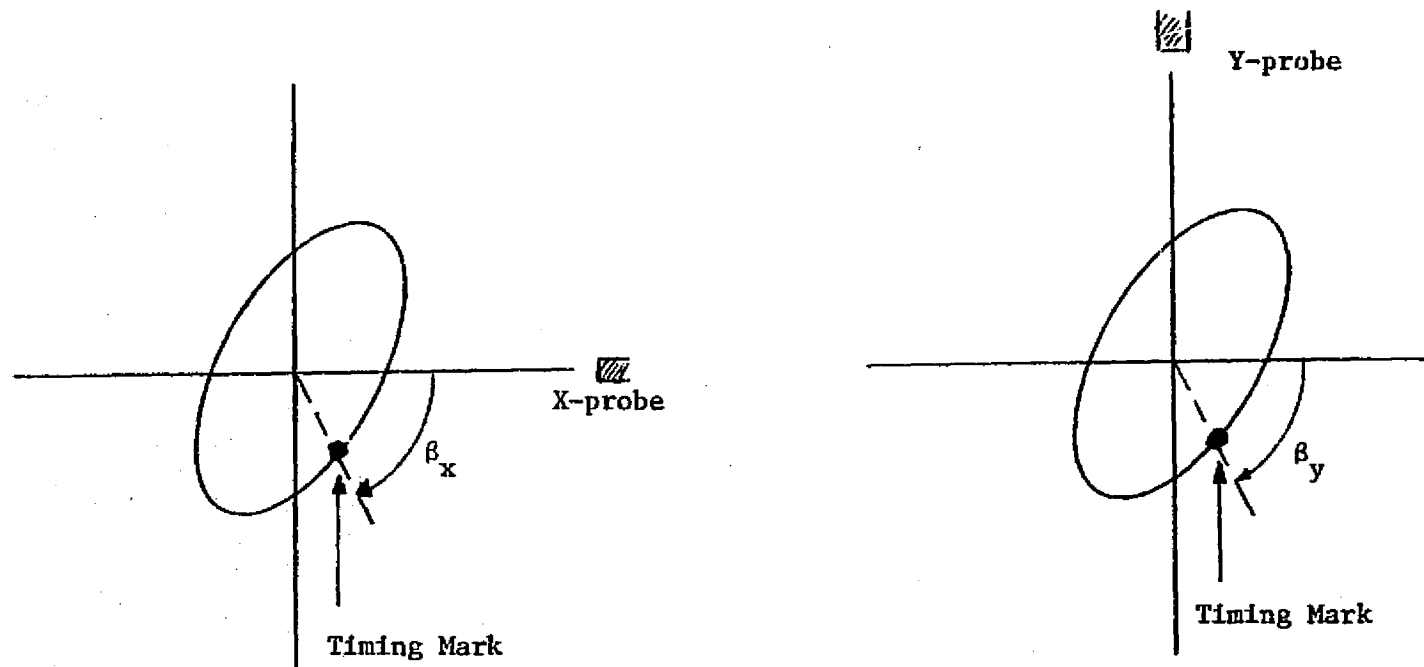


Figure 5.2 Phase Angle Relationship in Rotor Elliptical Orbit

For a symmetrical system,

$$x = R \cos (\omega t - \beta) \quad (5.32)$$

$$y = R \sin (\omega t - \beta) \quad (5.33)$$

Then it can be deduced that

$$x_r = -iy_i, \quad x_i = y_r \quad (5.34)$$

and

$$\overline{y} = i\overline{x} \quad (5.35)$$

or

$$(y_r + iy_i) = i(x_r + ix_i) \quad (5.36)$$

Hence, the rotor symmetrical whirl orbit is circular and the outlined calculation procedure can be much simplified using the above relationships.

## 5.2 Applications and Comparisons of Steady State Solutions

In order to illustrate the use of the modal equations derived in the previous section, the same example of an centrifugal compressor discussed in section 4.3 is used. The modal method was applied to compute the unbalance response of the compressor. An unbalance of 1 oz-in. was placed in the mid-span between the bearings to simulate a first-mode excitation using the modal approach discussed in section 5.1. The rotor unbalance response was calculated for an operating speed range of 500 RPM to 4,500 RPM. For validation purposes, unbalance response calculations based on the matrix transfer method [17] were also performed. Figure 5.3 shows the comparisons of unbalance response calculated by both methods at the left bearing station, and Figure 5.4 shows the unbalance response at the mid-rotor span. It can be seen from the figures that the results from both methods are in very good agreement. Note from figure 5.4 that the peak of the curve occurs at 2,995 RPM with an amplitude of 29 mils. This peak response speed is very close to the calculation of  $N_{u1} = 2,963$  RPM using equation (3.26). A closer investigation at the unbalance response of the system passing through its first critical speed by both transfer matrix and modal methods is given in Table 5.1. Note that the modal method can predict the peak response speed quite closely to the one by transfer matrix method with a peak magnitude of response of about 22 mils. Note that the accuracy in the results does not improve significantly by using 6 planar modes instead of 4 planar modes.



ORIGINAL PAGE IS  
OF POOR QUALITY

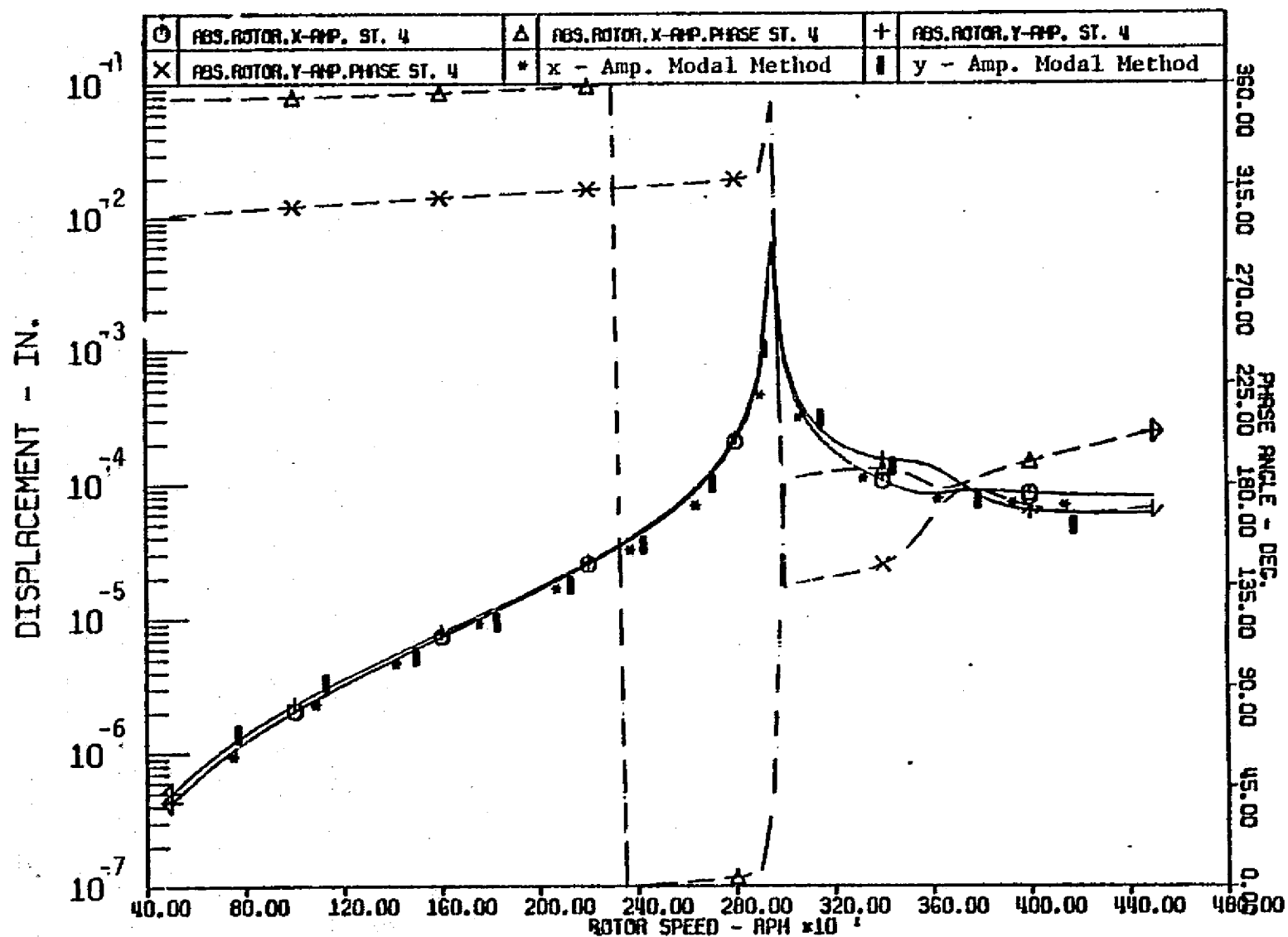


Figure 5.3 UNBALANCE RESPONSE PLOT OF THE COMPRESSOR BEARING STATION  
WITH FIRST MODE EXCITATION

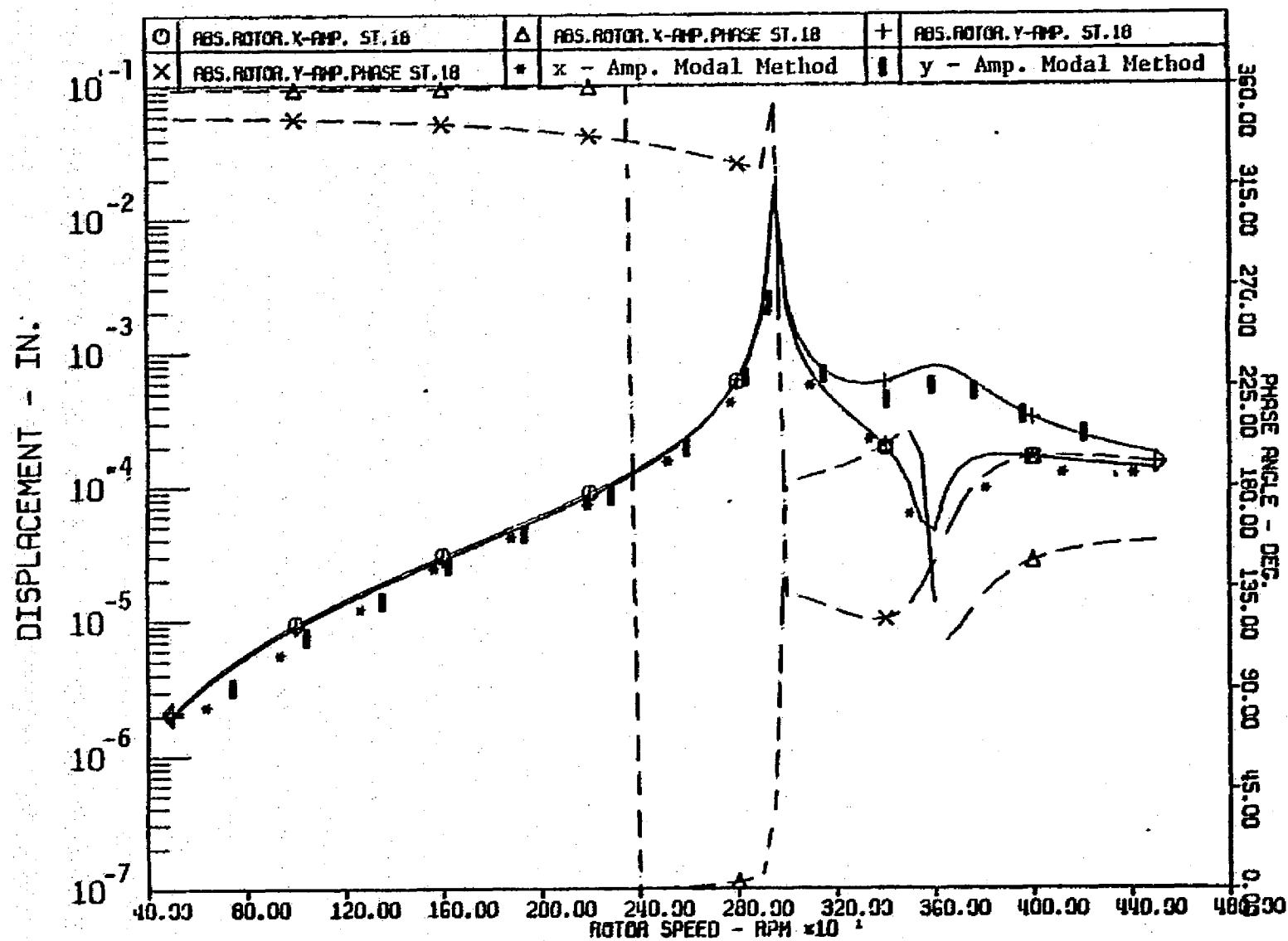


Figure 5.4 UNBALANCE RESPONSE PLOT OF THE MID-SPAN OF COMPRESSOR ROTOR WITH FIRST MODE EXCITATION

ORIGINAL PAGE IS  
OF POOR QUALITY

SPEED	MATRIX TRANSFER (mils)	6 PLANAR MODES (mils)	4 PLANAR MODES (mils)
2,940	6.41	4.19	3.63
2,942	7.32	4.55	3.9
2,944	8.52	4.95	4.22
2,946	10.17	5.43	4.59
2,948	12.5	5.99	5.05
2,950	15.95	6.67	5.59
2,952	21.05	7.52	6.25
2,954	26.9	8.65	7.08
2,956	27.71	10.18	8.15
2,958	22.27	12.27	9.55
2,960	16.86	15.05	11.44
2,962	13.13	18.1	14.01
2,964	10.62	19.43	17.36
2,966	8.86	17.57	20.79
2,968	7.59	14.44	22.01
2,970	6.63	11.72	19.69
2,972	5.88	9.67	16.11
2,974	5.28	8.18	13.05
2,976	4.79	7.06	10.75
2,978	4.38	6.2	9.06
C.P. TIME		7.32 sec.	11.5 sec.

Table 5.1 COMPARISON OF UNBALANCE RESPONSE  
OF COMPRESSOR BY MODAL AND TRANSFER MATRIX METHODS

Another aspect of this analysis is that for a lightly damped system such as this compressor, the unbalance response curve always gives a very sharp rising slope near the resonance speed, or, in other words, the speed range in which the peak resonance speed will occur is very narrow. For accurate calculations, the unbalance response of the system has to be calculated for very small speed increments so as to insure the peak response amplitude will not occur between two consecutive speed increments. Since each unbalance response calculation is quite time consuming, this will make the analysis quite expensive. However, there is a fast method of approximating the maximum unbalance response amplitude using the amplification factors discussed previously. Using the concept that the peak response amplitude  $Z_1$  is

$$Z_1 = e_1 A_{ui} = 0.085 \times 430 = 36 \text{ mils}$$

where

$$\text{Modal eccentricity } e_1 = \frac{1 \text{ oz-in} \times 1,000 \text{ mils/in}}{16 \text{ oz/lb} \times 740 \text{ lbs}} = 0.085 \text{ mils}$$

In this calculation, a modal weight of 740 lbs. for the first mode is used instead of the rotor weight of 1,400 lbs.

The maximum amplitude of 36 mils calculated from the rotor amplification factor is higher than the 29 mils calculated from the unbalance response computer program. It appears that in this case even a speed increment of 1 RPM is still not small enough to catch the real peak of the resonance motion. The amplification factor can provide compressor designers with information of the maximum rotor motion in a simplified manner.

To further illustrate the calculation of steady state forced response, the results from the modal method were compared to experimental data. A uniform rotor of 21 in. long, 1 in. diameter with 3 large disks located at the mid span was used as the model for analysis. The rotor is supported by two plain journal bearings at each end. A schematic of the rotor system is given in figure 5.5. A noncontacting probe is set up in the position x2 as in the diagram monitoring the horizontal rotor motion. The solid lines in figure 5.5 indicate the rotor synchronous response from experimental data [56]. The dotted line represents the unbalance response calculation using only the first undamped mode of the system. In this particular case, the unbalance of the system is measured to be 0.2 oz-in at 0 degree located at the center dial of the rotor. The rotor has a residual run out of 0.7 mils at the center disk and 0.6 mils at the other disks and are 175 degrees out of phase with the rotor unbalance. The rotor geometry and bearing characteristics used in this analysis are shown in Table 5.2. The dotted line of modal calculations in figure 5.5 shows very good agreement with the experimental results. Note

ORIGINAL PAGE IS  
OF POOR QUALITY

STATION NO.	WEIGHT (LP)	LENGTH (IN.)	SHAFT DIA. OUTSIDE	SHAFT DIA. INSIDE	I (IN**4)	IP-POLAR MOM. (LP-IN**2)	IT-TRANS. MOM. (LB-IN**2)
1	.000	.100	1.000	0.000	.05	0.000	0.000
2	.000	1.500	1.000	0.000	.05	0.000	0.000
3	.000	1.500	1.000	0.000	.05	0.000	0.000
4	.000	1.500	1.000	0.000	.05	0.000	0.000
5	.000	1.500	1.000	0.000	.05	0.000	0.000
6	.000	1.500	1.000	0.000	.05	0.000	0.000
7	.000	1.500	1.000	0.000	.05	0.000	0.000
8	9.810	1.500	1.000	0.000	.05	0.000	0.000
9	9.810	1.500	1.000	0.000	.05	0.000	0.000
10	9.810	1.500	1.000	0.000	.05	0.000	0.000
11	.000	1.500	1.000	0.000	.05	0.000	0.000
12	.000	1.500	1.000	0.000	.05	0.000	0.000
13	.000	1.500	1.000	0.000	.05	0.000	0.000
14	.000	1.500	1.000	0.000	.05	0.000	0.000
15	.000	1.500	1.000	0.000	.05	0.000	0.000
16	.000	.100	1.000	0.000	.05	0.000	0.000
17	.000	.100	1.000	0.000	.05	0.000	0.000
-----		-----					
		29.430	21.300				

#### LINEAR SUPPORT BEARING STIFFNESS CHARACTERISTICS

BEARING NUMBER	BEARING LOCATION	KXX (LB/IN)	KXY (LB/IN)	KYX (LB/IN)	KYY (LB/IN)
1	2	58000.0	400000.0	-400000.0	39000.0
2	16	58000.0	400000.0	-400000.0	39000.0

#### LINEAR SUPPORT BEARING DAMPING CHARACTERISTICS

DAMPING NUMBER	DAMPING LOCATION	CXX (LB-SEC/IN)	CXY (LB-SEC/IN)	CYX (LB-SEC/IN)	CYY (LB-SEC/IN)
1	2	1400.0	-15.0	-15.0	1400.0
2	16	1400.0	-15.0	-15.0	1400.0

Table 5.2 ROTOR GEOMETRY AND BEARING CHARACTERISTICS OF THE THREE-MASS ROTOR

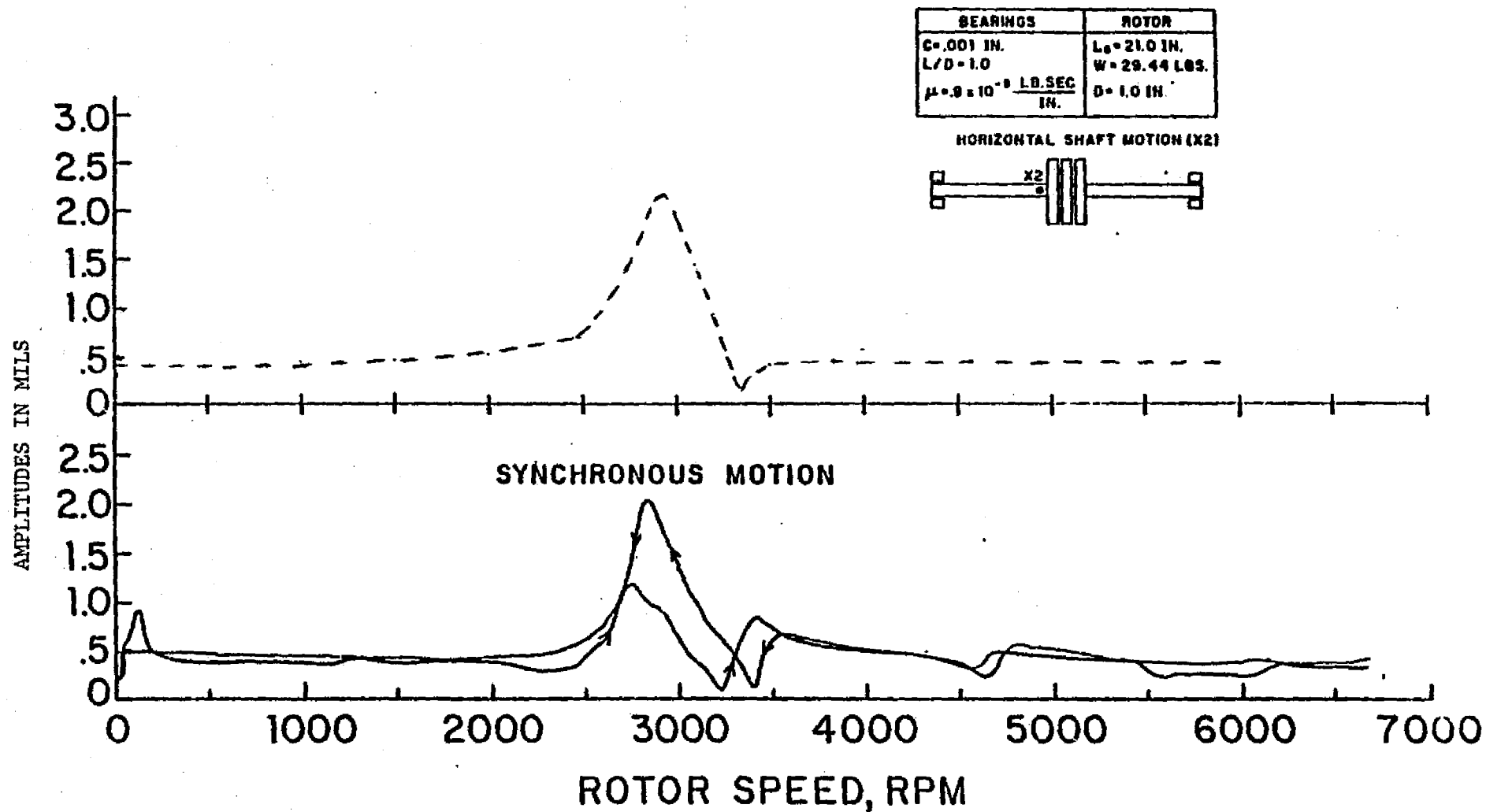


Figure 5.5. COMPARISON OF EXPERIMENTAL AND THEORETICAL RESULTS OF A THREE-MASS ROTOR [56]

that there are differences in response during up and down speed of the rotor while the unbalance response calculation predicts the average between them. Also, there occurs a dip in the response after the resonance peak, which indicates eccentricity in the rotor [21]. It can also be seen that the dip in the rotor response did not go to zero, which indicates that the bow and the unbalance is less than 180 degrees out of phase with each other.



### 5.3 Verification of Transient Response Solutions

In order to illustrate the application of the modal method discussed in the previous sections, a computer code was set up to predict the forced response of rotor systems and compared those of known solutions or published works. The first case of this study is the single-mass Jeffcott rotor. It consists of a single mass of 100 lbs on a uniform rotor of 100 in long and 4 in diameter supported by rigid bearings as shown in figure 5.6. The system also has a damper of 13.7 lb-sec/in acting at the central mass of the rotor. The undamped critical speed of the system is calculated to be at 2,525 RPM. Since there was no instability mechanism existing in the rotor, the system is stable. This implies that the forced response of the system will go from the initial transient motion into the steady state unbalance response as time increases.

In this particular study, a rotor unbalance of 1 oz-in. is assumed to be located at the center mass. From unbalance response calculations using the transfer matrix approach or the modal method discussed, it was found that the rotor will have a magnitude of 3.07 mils with a phase change of 84.3 degrees when the rotor operating speed is 2,500 RPM. Note that the rotor response orbit should be circular due to symmetry at the bearings, and the large phase change (near to 90 degrees) indicates that the rotor is operating near its critical speed. Figure 5.7 and 5.8 show the transient response motion of the rotor center mass starting with zero initial conditions.

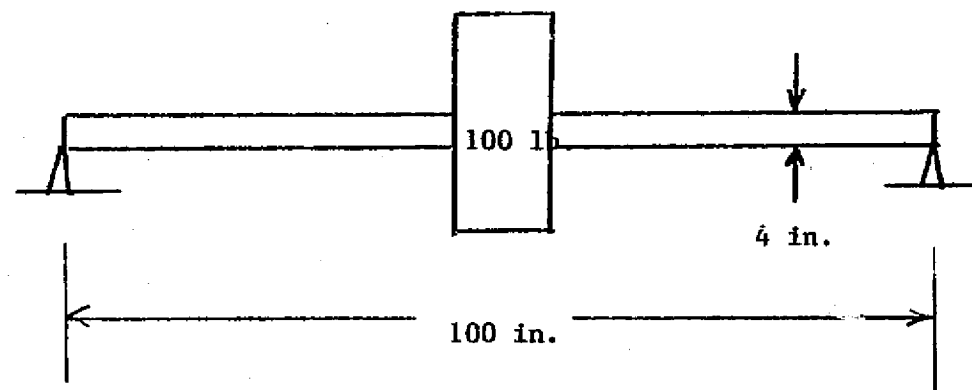


Figure 5.6 SCHEMATIC OF JEFFCOTT ROTOR

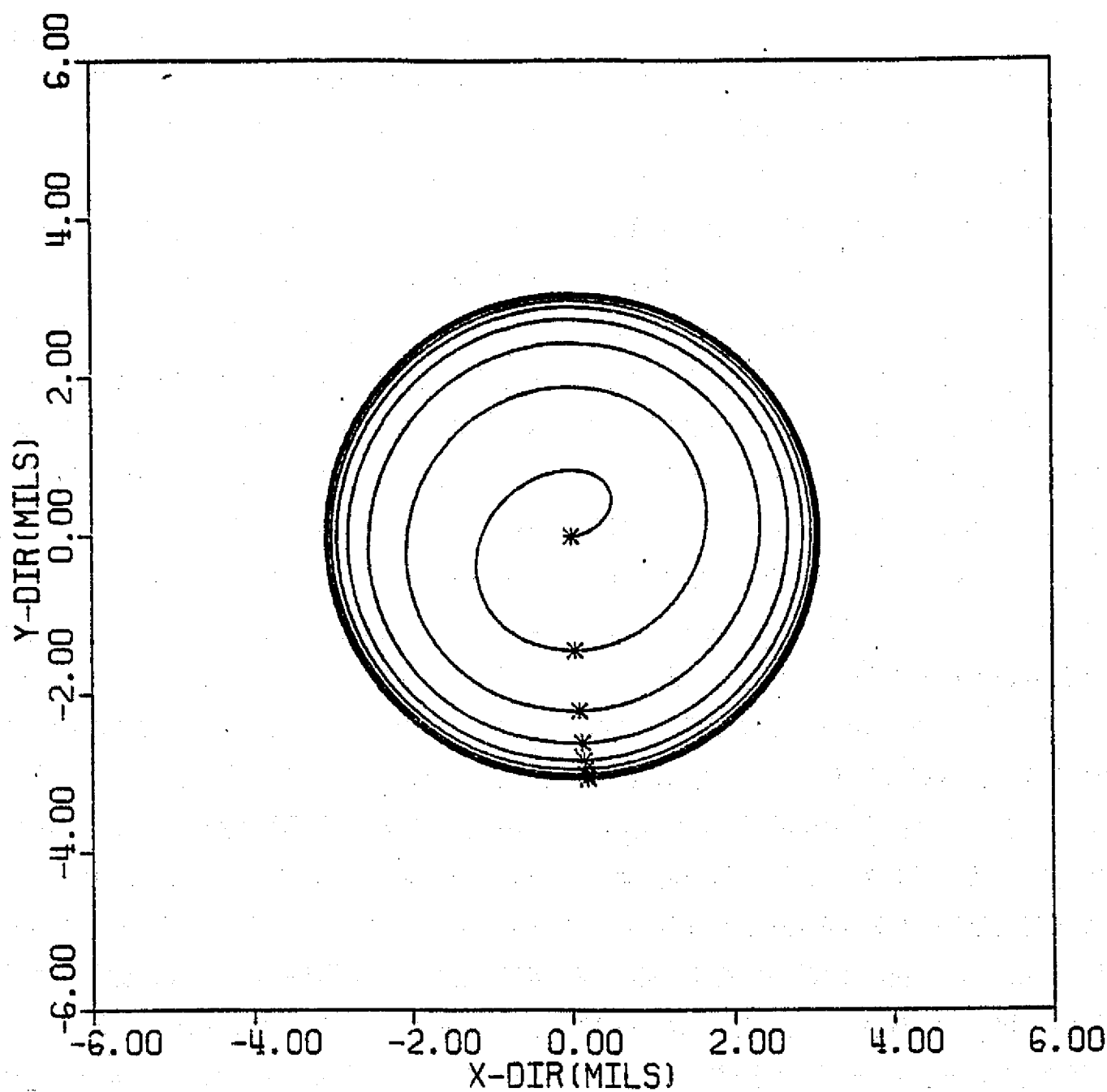


Figure 5.7 TEST CASE WITH SINGLE MASS ROTOR WITH RIGID SUPPORTS

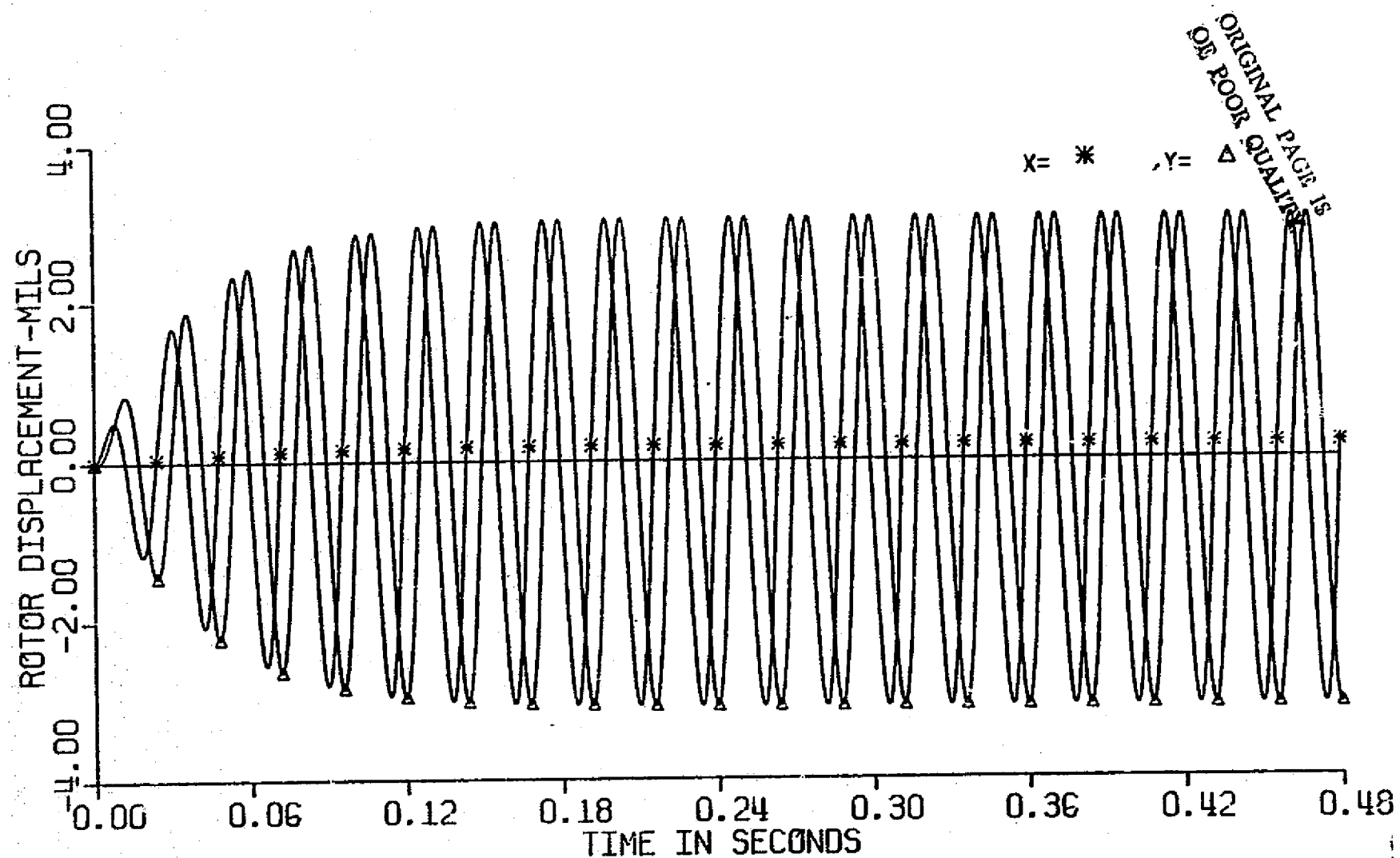


Figure 5.8 TEST CASE WITH SINGLE MASS ROTOR WITH RIGID SUPPORTS

Note that the rotor transient motion dies out and gradually assumes the steady state orbits as predicted by the unbalance response calculation. A further illustration is the comparison of this transient results with some exact solutions, namely, the convolution integral. Since the rotor model considered is a Jeffcott type, the transient solution can be readily obtained through analytical integration of the convolution integral. Table 5.3 shows the comparison of results from both the modal method and the convolution integral. These results are in very good agreement with an error less than 0.5% as both solutions go into steady state motion. This further illustrates the validity and accuracy of the modal approach of transient response analysis.

Another example of verification is the comparison of results from published works. A rotor single-mass rotor model on flexible bearings with internal damping effects similar to the one analyzed by Gunter [9] was introduced. The rotor model consists of a mass  $M = 0.25 \text{ lb-sec}^2/\text{in}$ ,  $K_y$  (vertical bearing stiffness) =  $K_2$  (shaft effective stiffness) =  $250,000 \text{ lb/in}$ ,  $K_x$  (horizontal bearing stiffness) =  $125,000 \text{ lb/in}$ ,  $C_1$  (bearing damping) =  $50 \text{ lb-sec/in}$ , and  $C_2$  (internal damping acting on mass) =  $50 \text{ lb-sec/in}$ . The rotor system has two critical speeds (vertical and horizontal) occurring at  $577 \text{ rad/sec}$  and  $707 \text{ rad/sec}$ . Assuming a rotor mass imbalance of  $1 \text{ oz-in}$  exists in the rotor mass, the forced response of the system was calculated at two different speeds. Figure 5.9 and 5.10 show the

Table 5.3 COMPARISON OF TRANSIENT RESPONSE  
RESULTS OF JEFFCOTT ROTOR

TIME	ABSOLUTE AMPLITUDE (MILS)	
SECOND	MODAL ANALYSIS	CONVOLUTION INTEGRAL
0.0012	0.02986	0.02987
0.0084	0.74902	0.74921
0.0168	1.0636	1.0642
0.0240	1.4426	1.4431
0.0420	2.07041	2.07017
0.6000	2.4448	2.4462
0.078	2.6894	2.6913
0.096	2.8328	2.8346
0.108	2.8992	2.9011
0.126	2.9687	2.9708
0.18	3.0504	3.0525
0.30	3.0755	3.0777

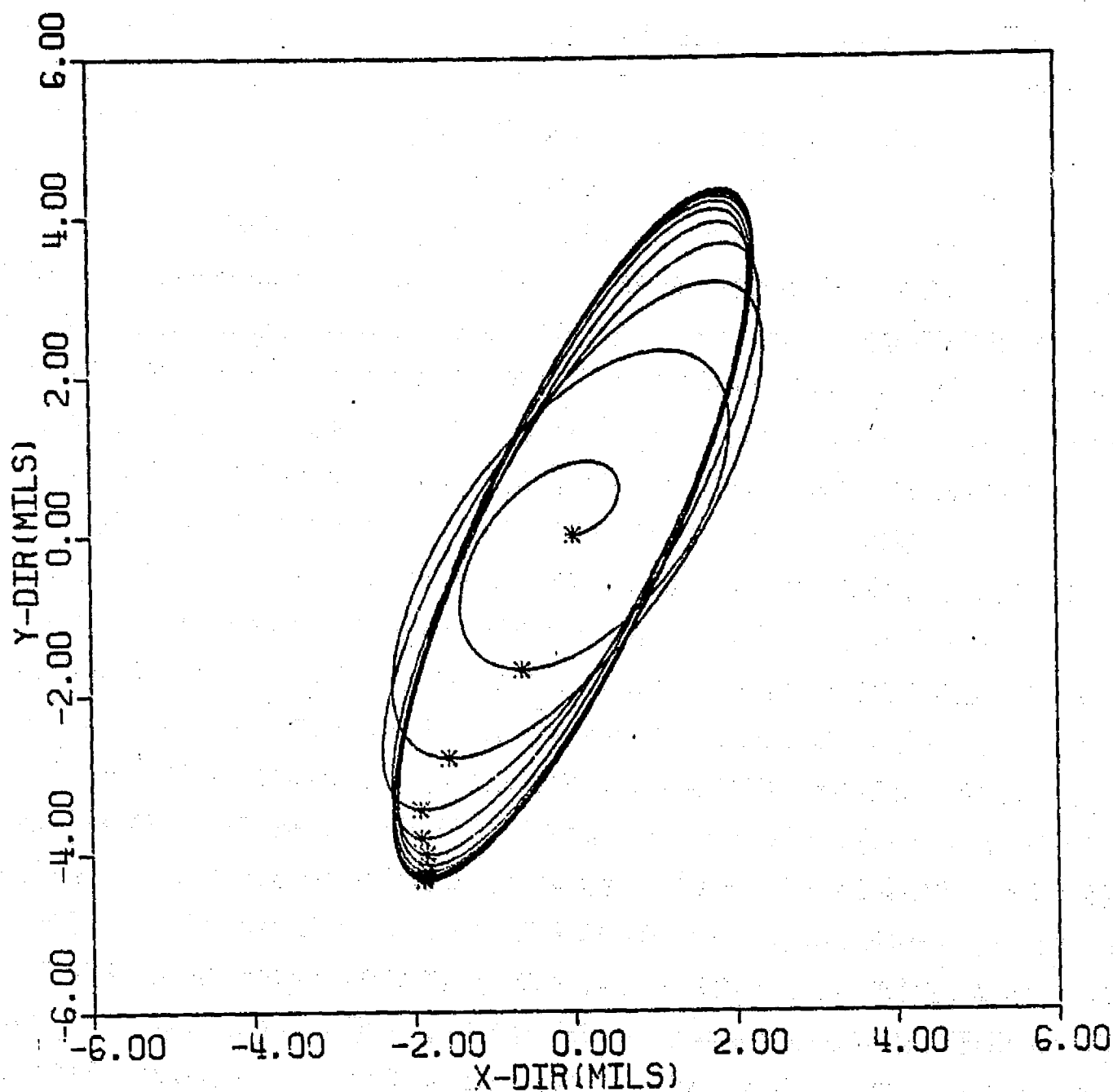


Figure 5.9 TRANSIENT ANALYSIS OF SINGLE MASS ROTOR  
USING MODAL METHOD - SPEED = 707 RAD/SEC

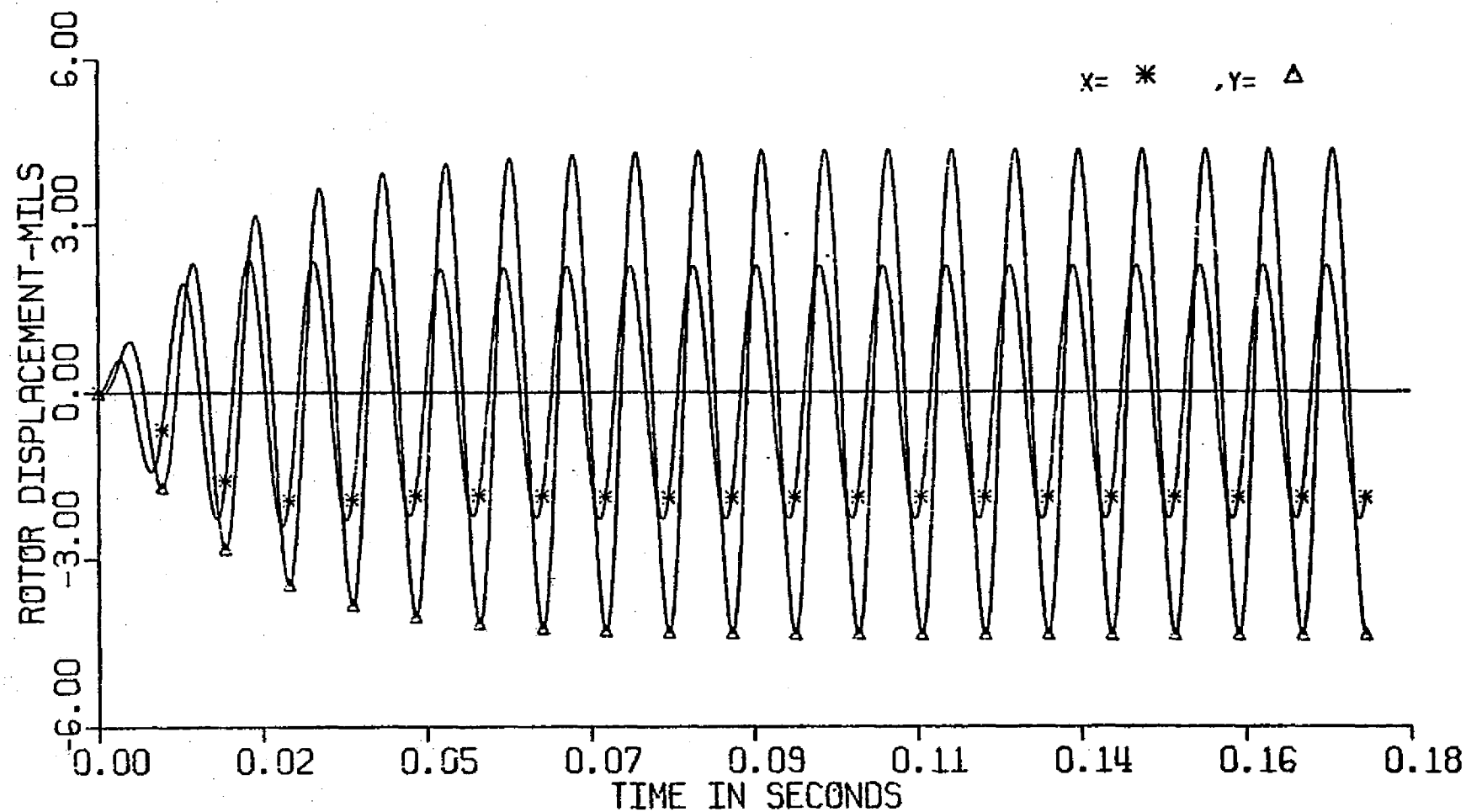


Figure 5.10 TRANSIENT ANALYSIS OF SINGLE MASS ROTOR USING MODAL METHOD - SPEED = 707 RAD/SEC



transient orbit and time-displacement plot of the rotor running at 707 rad/sec with zero initial conditions. It can be seen from these figures that the rotor eventually goes into the steady state motion because the system is stable (far below the stability threshold speed). The elliptical orbit motion of the rotor shows that there is bearing assymetry in the system, and the 90-degree phase change indicates that the rotor is operating near a critical speed. Figure 5.11 shows the results from Gunter [9] calculated with an analog computer. Examining the figures, it can be seen that the orbits and motion from both calculations are in good agreement. Thus it further verifies the use of modal transient response analysis.

When the rotor running speed is changed to 3,200 rad/sec, the rotor transient motion changes dramatically. Figure 5.12 and 5.13 shows the rotor orbit motion and time-displacement plots at 3,200 rad/sec operating speed. The presence of the inside loops in the rotor response orbits indicates the existance of non-synchronous rotor motion components. This effect is due to the fact that the rotor is operating near the stability threshold (threshold speed of 3,230 rad/sec). In this case, the non-synchronous motion components are more easily excited than when operating at a much lower speed of 7.7 rad/sec (vertical critical speed) in which the first critical speed component has completely dominated the rotor motion. Figure 5.16 shows the rotor transient response orbits by Gunter obtained with an analog computer. From the figure, it can be seen that the

CONDITIONS:

$M = 0.25 \text{ LB SEC}^2/\text{IN.}$

$K_y = K_z = 250,000 \text{ LB/IN.}$

$K_x = 125,000 \text{ LB/IN.}$

$D_1 = D_2 = 200 \text{ RAD/SEC}$

$\omega_s = 3230 \text{ RAD/SEC}$

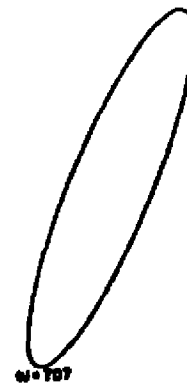
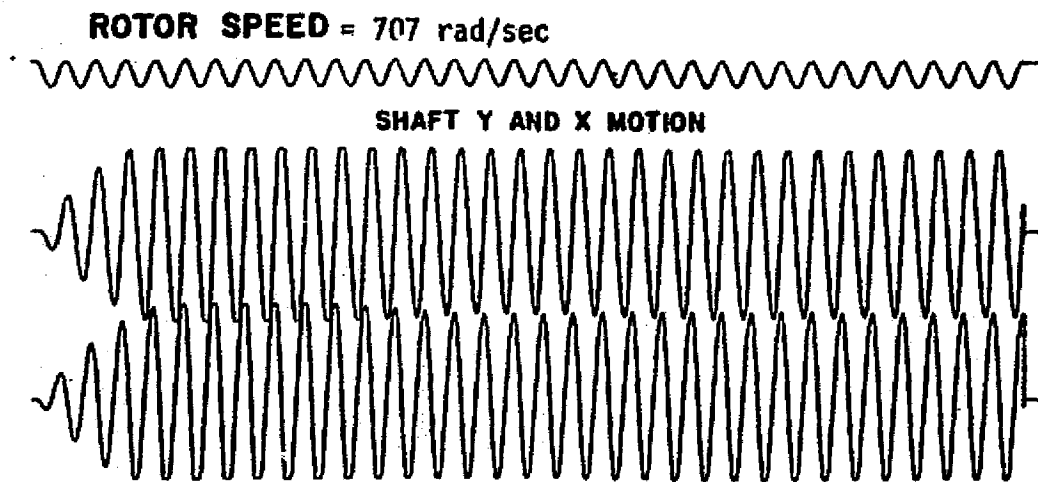


Figure 5.11 FORCED RESPONSE OF SINGLE MASS ROTOR FROM ANALOG PROGRAM

Ref. Gunter [ 9 ]

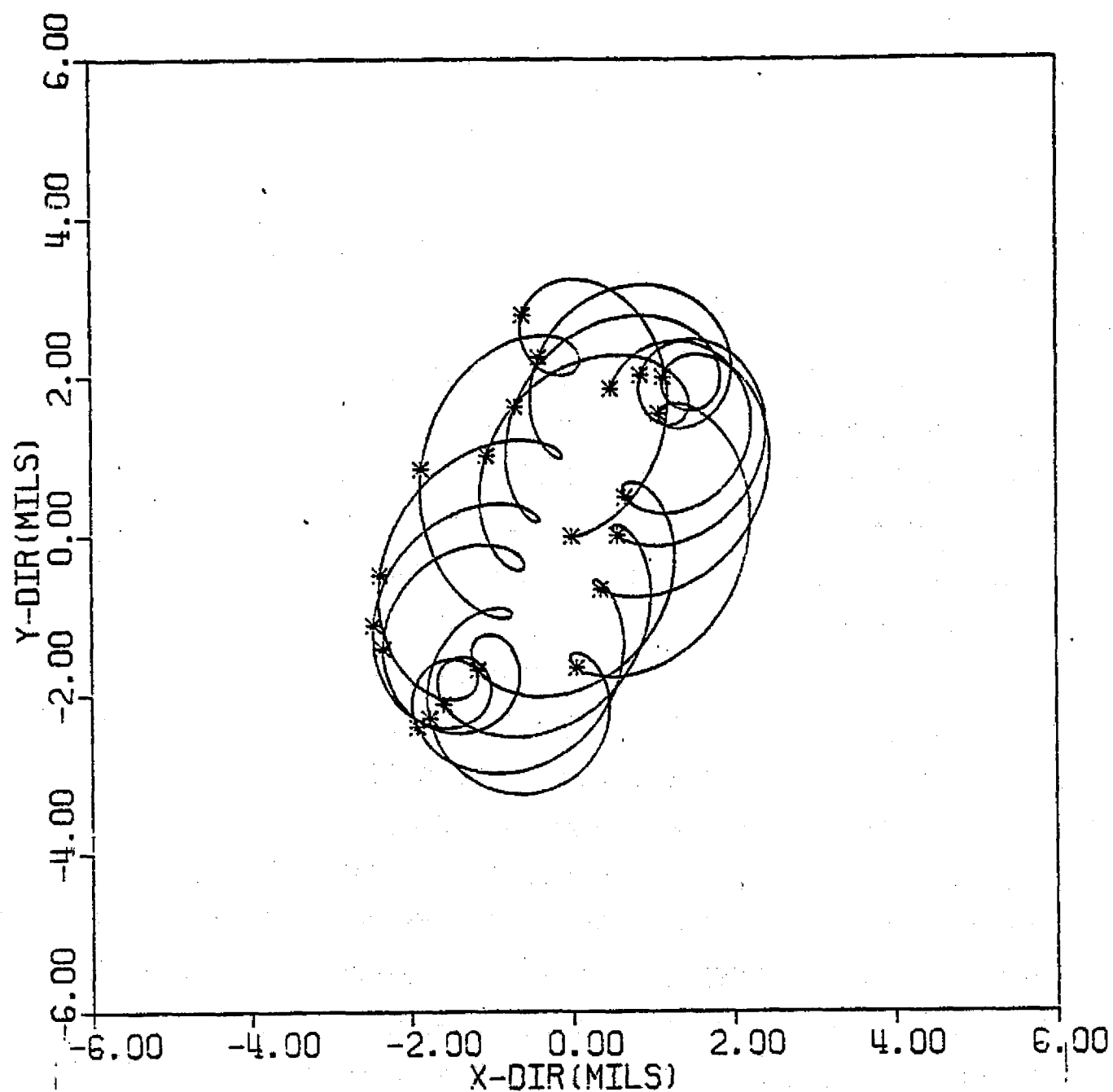


Figure 5.12 TRANSIENT RESPONSE OF SINGLE MASS ROTOR -  
MODAL METHOD AT 3,200 RAD/SEC

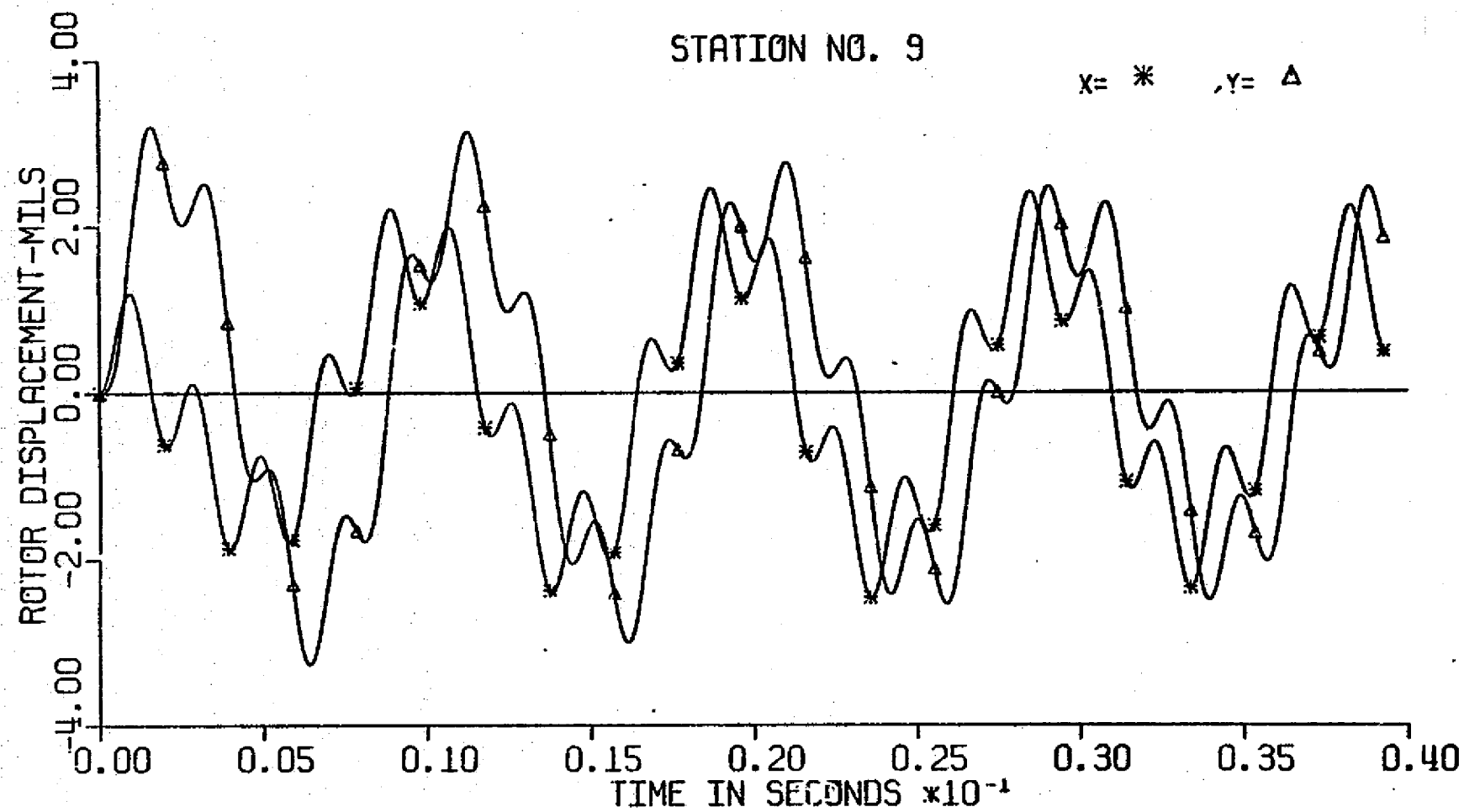


Figure 5.13 TRANSIENT RESPONSE OF SINGLE MASS ROTOR - MODAL METHOD AT 3,200 RAD/SEC

# WHIRL ORBIT OF AN UNBALANCED ROTOR AT THE THRESHOLD OF STABILITY

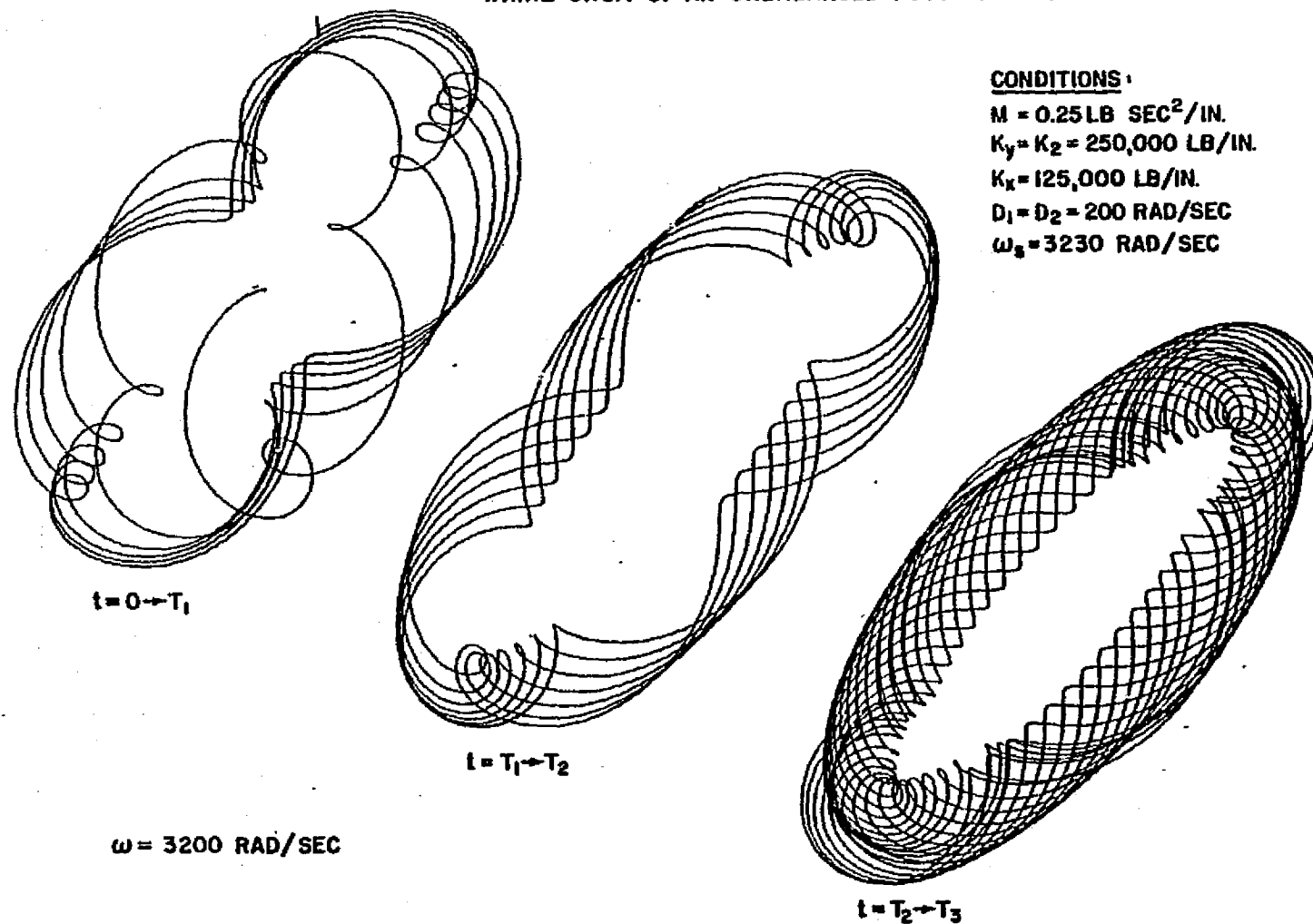


Figure 5.14 TRANSIENT RESPONSE OF SINGLE MASS ROTOR  
BY ANALOG COMPUTER - Ref. Gunter [9]

rotor transient orbits by both approaches are very similar and, thus, verifies the application and accuracy of the modal forced response analysis.

## VI. NON-LINEAR MODAL TRANSIENT ANALYSIS

### 6.1 Application of Numerical Integration Procedures

In transient analysis of most mechanical structures, the accelerations obtained by solving the equations of motion are integrated directly to evaluate the dynamic transient response of the system. In this particular analysis, the modal equations of motion (5.9) with modal excitations are solved, and the modal accelerations are integrated directly by numerical integration. The stability and accuracy of different types of numerical integration procedures have been extensively discussed [57 - 61]. These considerations are beyond the scope of this research. In this study, the main concern is the application of simple, accurate numerical integration schemes in nonlinear transient response analysis of turbomachinery, especially when a large number of integration steps are necessary. For direct integration of the equations of motion using the point mass stiffness formulation, equation (5.9) can be rewritten in the following form.

$$\left\{ \ddot{U} \right\} = \begin{Bmatrix} (\ddot{x}) \\ (\ddot{\theta}) \\ (\ddot{y}) \\ (\ddot{\psi}) \end{Bmatrix} = - \left[ \bar{M}^{-1} \right] \left\{ \left[ C \right] \left\{ \dot{U} \right\} + \left[ K \right] \left\{ U \right\} - \left\{ F(t) \right\} \right\} \quad (6.1)$$

With this equation, the acceleration quantities  $U$  may be calculated starting from the initial conditions. Using the summation notation convention, the coupled equations may be written as

$$\ddot{u}_i = -\bar{C}_{ij} \dot{u}_j - \bar{K}_{ij} u_j + F_i(t, \dot{u}_i, u_i)$$

There are numerous procedures that have been proposed for numerical integration of this type of equation, and three of the commonly used methods will be stated.

### 1. Modified Euler Method

This is one of the simplest procedures and has been found to work well with a relatively small number of degrees of freedom. It is based upon a Taylor series expansion of the motion for a small time step about the previous step. It has the advantage of simplicity and requires no starting solution and is usually stable [58, 61] for small step sizes (in the absence of highly nonlinear forces). According to the Taylor series expansion, we may find the velocity and displacement at time  $t_{n+1} (=t_n + \Delta t)$ .

$$\dot{y}_{n+1} = \frac{dy}{dt}_{n+1} = \dot{y}_n + \Delta t \ddot{y}_n + \frac{(\Delta t)^2}{2!} \dddot{y}_n + \dots \quad (6.3)$$

$$y_{n+1} = y_n + \Delta t \dot{y}_n + \frac{(\Delta t)^2}{2} \ddot{y}_n + \frac{(\Delta t)^3}{3!} \dddot{y}_n + \dots \quad (6.4)$$

This procedure can be carried out to cover the whole range of time for which computation is required.

### 2. Runge-Kutta-Gill Method

This is a more complex procedure which is accurate to the fourth order. In this approach, the second order differential equation [67]



$$\ddot{y} = f(t, y, v) \quad (6.5)$$

is replaced by two simultaneous first order equations

$$\dot{v} = \ddot{y} = f(t, y, v) \quad (6.6)$$

and

$$v = \dot{y} = g(t, y, v) \quad (6.7)$$

Usually, this method has a greater accuracy than the Euler method, and larger time steps can be used to save computer time for integration. Also, its accuracy up to the fourth order makes it more applicable to nonlinear transient analysis. One drawback of this method is that it may develop numerical instability when a coulomb friction type of damper support is encountered. A step by step procedure is as follows:

$$y_{n+1} = y_n + \frac{\Delta t}{6} (K_0 + 2K_1 + 2K_2 + K_3) \quad (6.8)$$

$$v_{n+1} = v_n + \frac{\Delta t}{6} (M_0 + 2M_1 + 2M_2 + M_3) \quad (6.9)$$

where

$$K_0 = g(t_n, y_n, v_n)$$

$$K_1 = g(t_n + \frac{\Delta t}{2}, y_n + \frac{\Delta t}{2} K_0, v_n + \frac{\Delta t}{2} M_0)$$

$$K_2 = g(t_n + \frac{\Delta t}{2}, y_n + \frac{\Delta t}{2} K_1, v_n + \frac{\Delta t}{2} M_1)$$

$$K_3 = g(t_n + \Delta t, y_n + \Delta t K_2, v_n + \Delta t M_2)$$

$$M_0 = f(t_n, y_n, v_n)$$

$$M_1 = f(t_n + \frac{\Delta t}{2}, y_n + \frac{\Delta t}{2} K_0, v_n + \frac{\Delta t}{2} M_0)$$

$$M_2 = f(t_n + \frac{\Delta t}{2}, y_n + \frac{\Delta t}{2} K_1, v_n + \frac{\Delta t}{2} M_1)$$

$$M_3 = f(t_n + \Delta t, y_n + \Delta t K_2, v_n + \Delta t M_2)$$

### 3. Newmark's $\beta$ -parameter Method

The method originated by Newmark introduces a parameter  $\beta$  which can be changed to suit the requirements of the problem at hand.

The second order differential equation can be solved as

$$\dot{y}_{n+1} = \dot{y}_n + \frac{\Delta t}{2} (\ddot{y}_n + \ddot{y}_{n+1}) \quad (6.10)$$

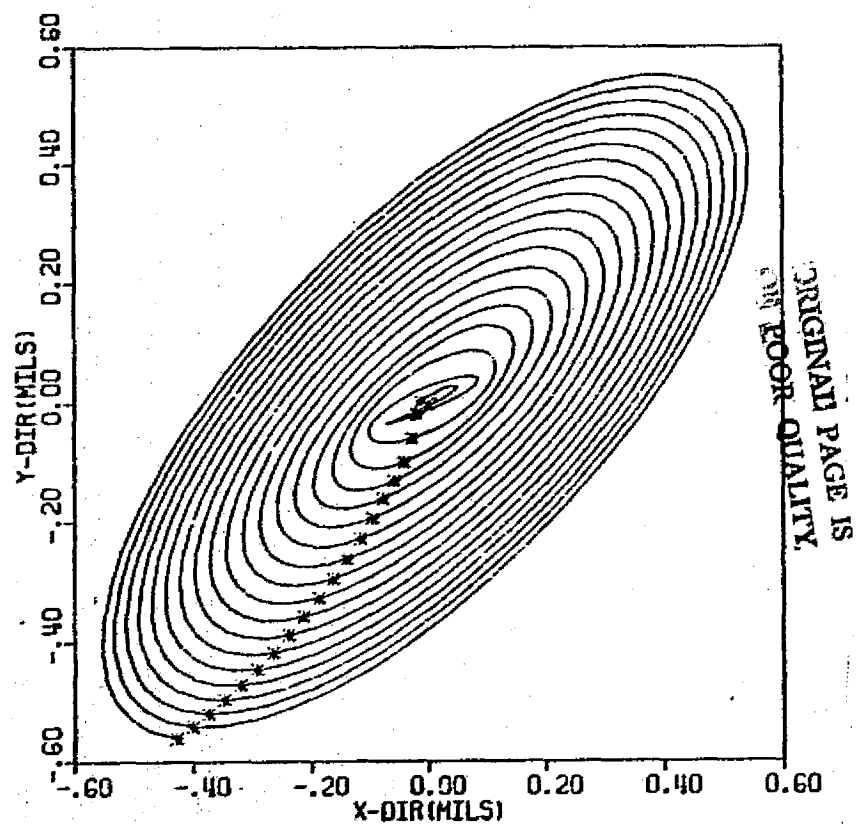
$$y_{n+1} = y_n + \Delta t \dot{y}_n + \frac{(\Delta t)^2}{2} \ddot{y}_n + \beta (\Delta t)^2 (\ddot{y}_{n+1} - \ddot{y}_n) \quad (6.11)$$

The net effect of  $\beta$  is to change the form of the variation of acceleration during the time interval  $\Delta t$ . By letting  $\beta = 0$ , the acceleration is constant and equal to  $\ddot{y}_n$  during each interval. If  $\beta = 1/8$ , the acceleration is constant from the beginning as  $\ddot{y}_n$  and then changes to  $\ddot{y}_{n+1}$  at the middle of the interval. The value  $\beta = 1/6$  assumes that acceleration changes linearly from  $\ddot{y}_n$  to  $\ddot{y}_{n+1}$ ;  $\beta = 1/4$  corresponds to assuming that the acceleration remains constant at an average value of  $(\ddot{y}_n + \ddot{y}_{n+1})/2$ .

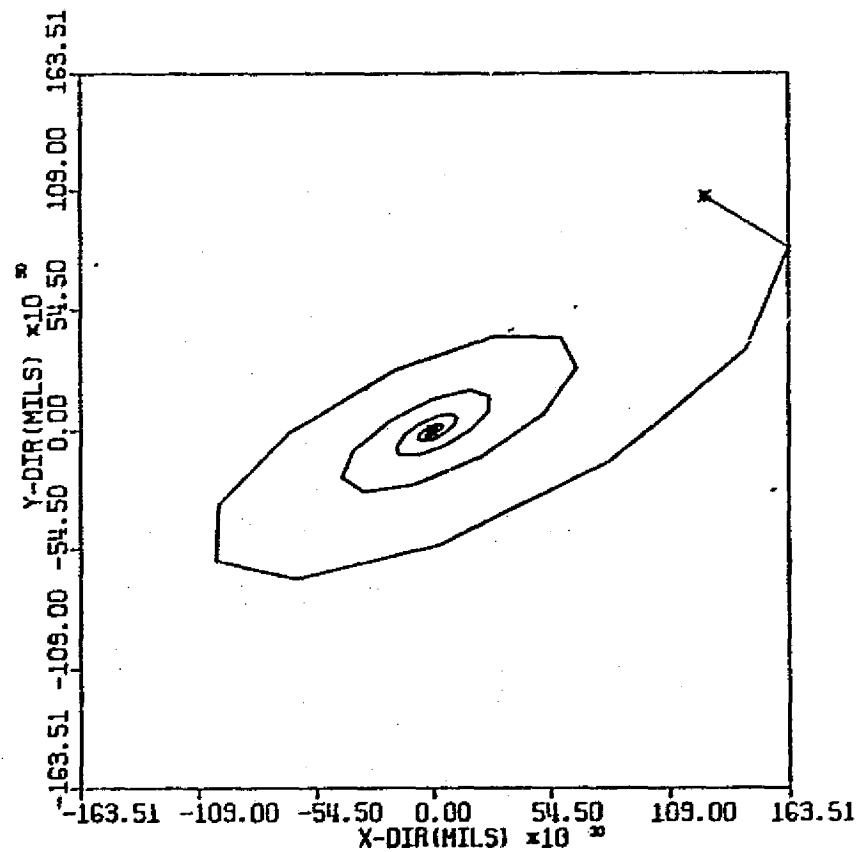
This method is fast in comparison with the Runge-Kutta-Gill method and is usually numerically stable. The introduction of the  $\beta$ -parameter allows this method to handle complicated nonlinear problems in a simple fashion while maintaining good accuracy. A problem encountered in this method is that the proper choice of  $\beta$ -parameter value can significantly affect the accuracy of the integration. When a  $\beta$  value of  $1/4$  is chosen, the integration scheme is unconditionally stable [61], but the solution may not be as accurate as  $\beta = 1/6$ .

To illustrate the choice of integration procedures used in transient response analysis, the industrial 8-stage compressor discussed in section 4.3 is chosen as an example. The compressor is supported by two hydrodynamic bearings, and the bearing characteristics are similar to those given in table 4.2. An unbalance of 1 oz-in. is assumed to be located at one of the compressor stages. The rotor model is running at 3,000 RPM, which is at the stability

threshold speed of the system. The transient response of the system is evaluated using two different integration procedures; namely, the modified Euler integration procedures and the Newmark Beta integration procedure. A time step of 48 integration steps per rotor revolution cycle is used. Figure 6.1a is the response calculated by Newmark Beta which shows that the rotor is unstable at the operating speed, and the magnitude of the rotor response is increasing with time without approaching a limit cycle. The curve in the orbit is relatively smooth, which shows that smaller time steps of integration is not necessary. Figure 6.1b is the transient response orbit of the same condition with modified Euler integration scheme. Note that the transient response solution suddenly grows very rapidly and the procedure is numerically unstable. The large response in the figure ( $10^{30}$  mils) proves the numerical instability of the scheme as well as the roughness of the curve. A much smaller time step is necessary. Figure 6.2 shows the time-displacement plot of the same station, which provides further ground for this statement. Figure 6.3 and 6.4 shows the transient orbits and time-displacement plot of the compressor stage at which the rotor imbalance is located. Again, it indicates that the modified Euler procedure is numerically unstable, while the Newmark Beta method gives much better results. Comparing the computer time consumed in both procedures, it was found that the Newmark Beta integration procedure only requires 5% more time than the Modified Euler scheme. Thus, it can be concluded that the Newmark Beta integration procedure is by far superior to the modified Euler

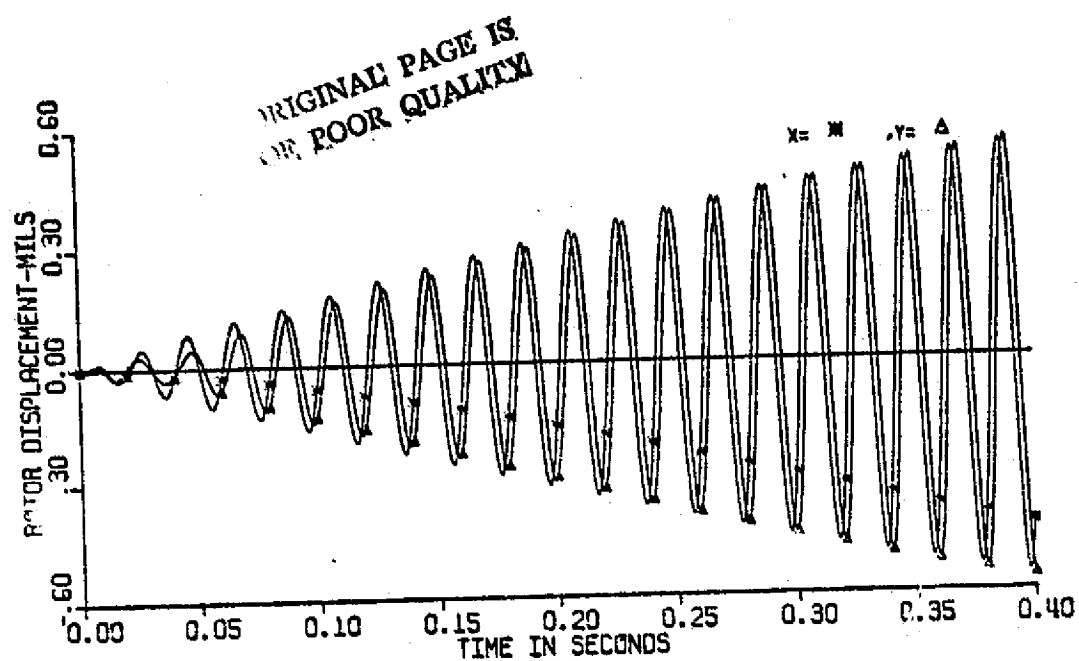


a) By Newmark Beta Integration Procedure

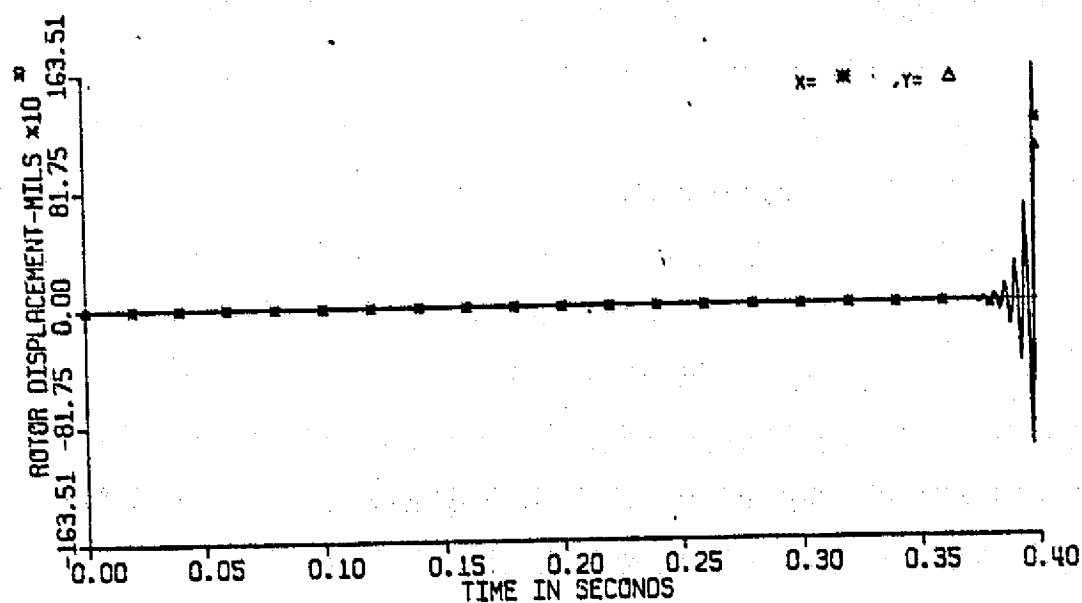


b) By Modified Euler Integration Procedure

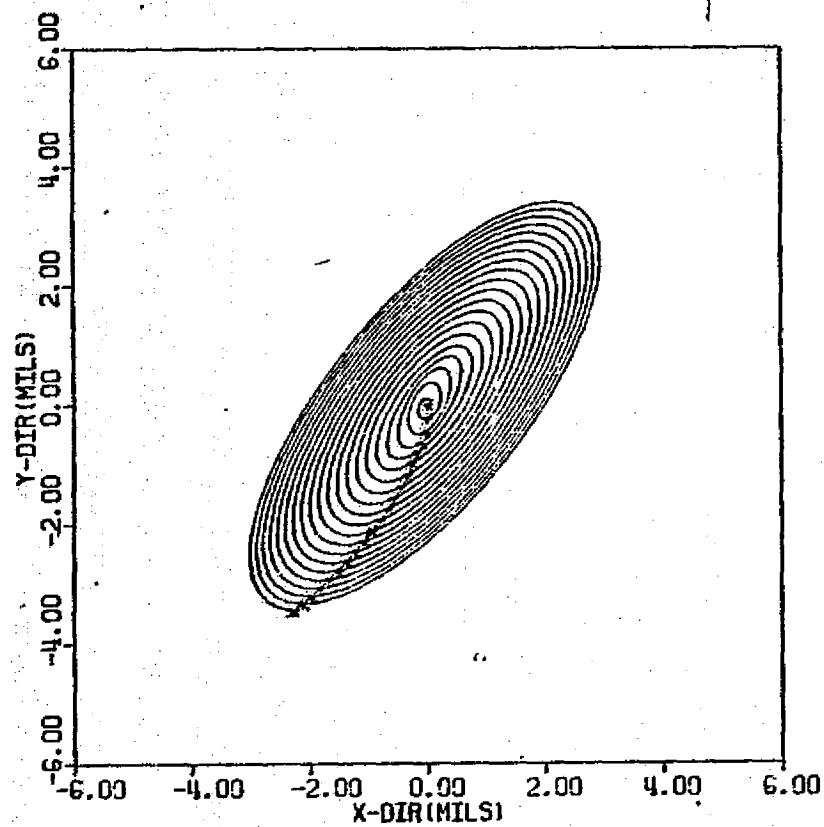
Figure 6.1 TRANSIENT ORBIT AT LEFT BEARING LOCATION OF THE 8-STAGE COMPRESSOR



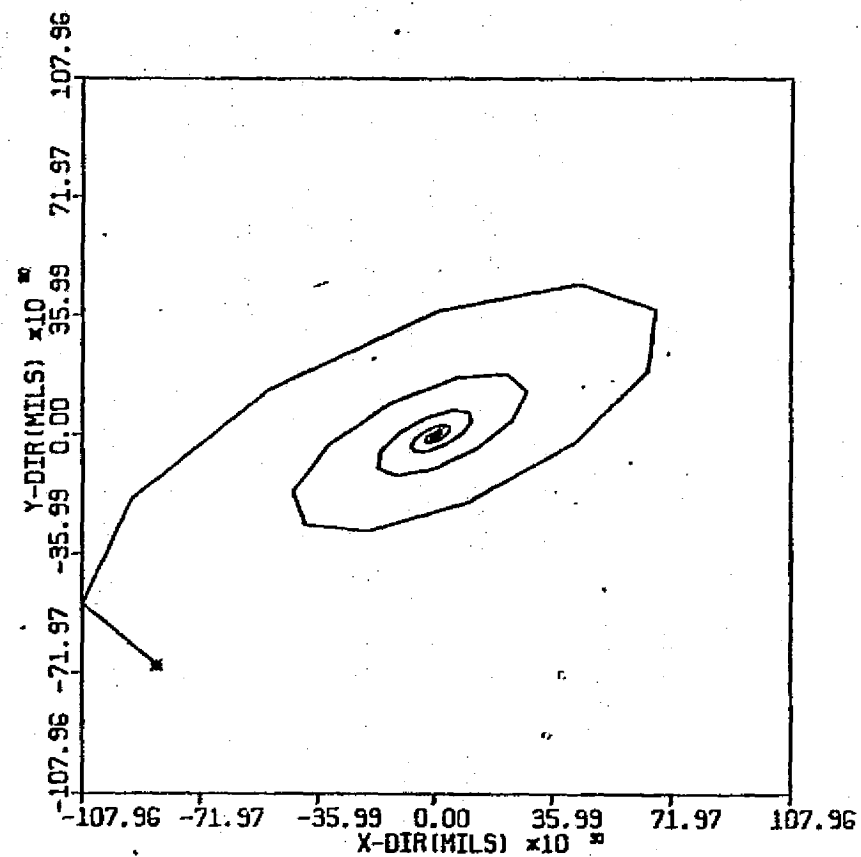
6.2a TRANSIENT MOTION AT LEFT BEARING OF 8-STAGE COMPRESSOR  
(NEWMARK BETA PROCEDURE)



6.2b TRANSIENT MOTION AT LEFT BEARING OF 8-STAGE COMPRESSOR  
(MODIFIED EULER PROCEDURE)

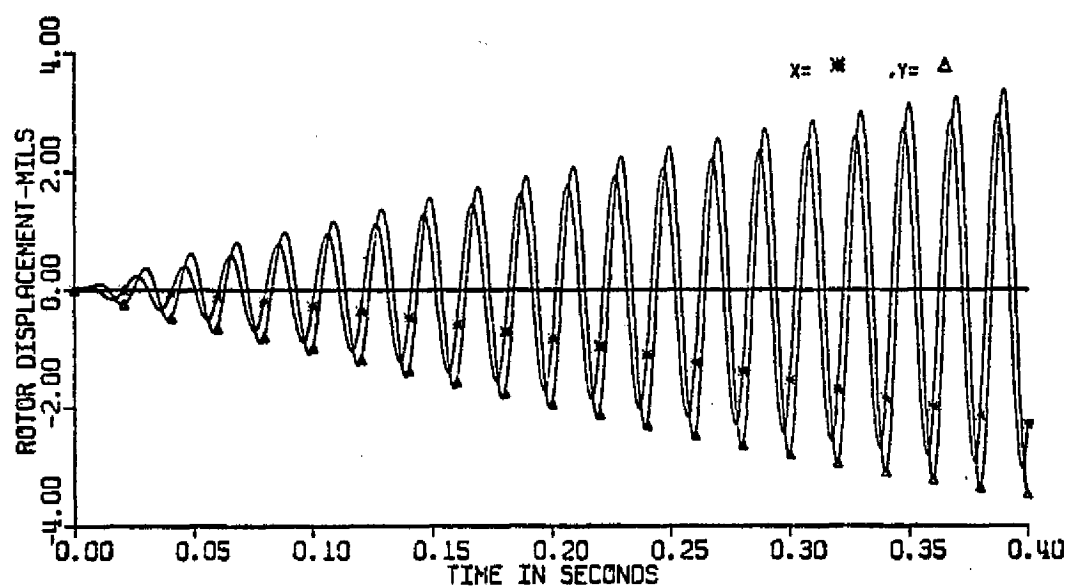


a) By Newmark Beta Procedure

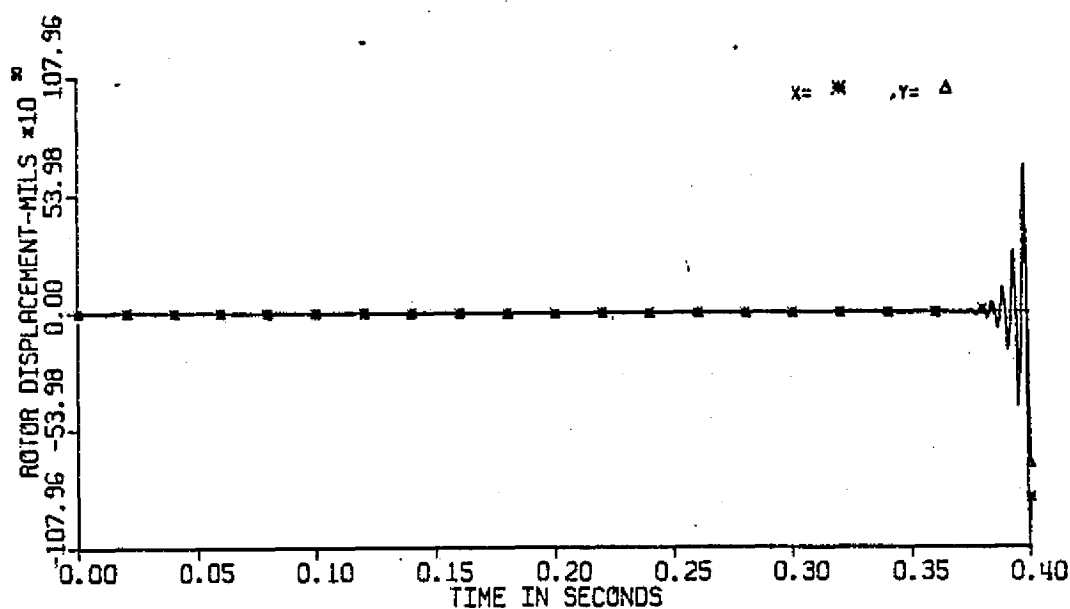


b) By Modified Euler Procedure

Figure 6.3 TRANSIENT RESPONSE ORBIT AT UNBALANCE LOCATION OF 8-STAGE COMPRESSOR



6.4a TRANSIENT MOTION AT UNBALANCE LOCATION OF 8-STAGE COMPRESSOR  
(NEWMARK BETA PROCEDURE)



6.4b TRANSIENT MOTION AT UNBALANCE LOCATION OF 8-STAGE COMPRESSOR  
(MODIFIED EULER PROCEDURE)



schemes. A complete solution procedure and a computer flow chart of the Newmark Beta integration procedure with integration for nonlinear transient motion is given in Appendix C.

## 6.2 Effects of Nonlinear Bearing Supports

In the dynamic analysis of rotating machinery, rotor system dynamic behavior has been either studied with flexible rotors on spring and dashpot supports [1, 2, 8] or as a rigid or point mass body with nonlinear fluid film bearings [36, 58, 61]. Both approaches may be inaccurate for flexible rotors undergoing large displacements when the bearing forces become nonlinear in nature. In this analysis, the coupled rotor modal equations of motion are solved similar to those discussed in the previous chapter while additional bearing forces and moments are calculated and incorporated for each time increment during integration. The bearing forces and moments are calculated using the integrated rotor displacements and velocities and are iterated through each time step.

In modal analysis, the bearing forces of the system are incorporated into the modal equations of motion as modal forces  $F_{bx}$  and  $F_{by}$ , (Equation 5.7). These modal forces are combined together with other excitations such as rotor unbalance, disk skew, and shaft bow to form the total modal excitation of the system. The modal bearing forces can be calculated by

$$\{F_{bx}\} = [A_e]^T \{F_x\} \quad (6.12)$$

$$\{F_{by}\} = [A_e]^T \{F_y\} \quad (6.13)$$

where  $F_x$  and  $F_y$  are the bearing force vectors at the mass stations. Thus equations 5.7 and 5.8 with nonlinear bearing forces effects can be written as

$$\begin{aligned} & \{\ddot{q}_x\} + [C_x] \{\dot{q}_x\} + [\Lambda] \{q_x\} + [k_x] \{q_x\} + [D_x] \{\dot{q}_y\} + [CM_x] \{q_y\} \\ & + [E_x] \{q_y\} + [EA_x] \{q_y\} = \{xF\} + \{xB\} + \{FBx\} \end{aligned} \quad (6.14)$$

and

$$\begin{aligned} & \{\ddot{q}_y\} + [C_y] \{\dot{q}_y\} + [\Lambda] \{q_y\} + [k_y] \{q_y\} + [D_y] \{\dot{q}_x\} + [CM_y] \{\dot{q}_x\} \\ & + [E_y] \{q_x\} + [EA_y] \{q_x\} = \{yF\} + \{yB\} + \{F_{By}\} \end{aligned} \quad (6.15)$$

In this particular analysis, the effects of non-linear bearing forces can be illustrated using short journal bearings whose bearing forces can be represented by an analytical expression. Assuming isothermal fluid film, the Reynolds equation for short journal bearings [58] in nondimensional form can be written as  $\left(\frac{L}{D} = 0\right)$

$$\frac{\partial}{\partial \xi} \left( h^3 \frac{\partial P}{\partial \xi} \right) = (1 - 2\phi) \frac{\partial h}{\partial \theta} + 2\dot{\epsilon} \cos \theta \quad (6.16)$$

where

$$P = \frac{\bar{p}}{6\mu\omega \left(\frac{R}{C}\right)^2}$$

$$h = \frac{\bar{h}}{C} = 1 + \epsilon \cos \theta$$

$$\xi = \frac{z}{R}$$

Using the boundary conditions of pressure  $P = 0$  at  $\xi = 0$  and  $\xi = 1$ , we have

$$P = \frac{1}{2} \left[ \left( \frac{L}{D} \right)^2 - \xi^2 \right] \frac{1}{h^3} \left[ \epsilon(1 - 2\dot{\phi}) \sin\theta - 2\dot{\epsilon} \cos\theta \right] \quad (6.17)$$

Integrating the pressure using the half sommerfeld condition as given by Lund [58], the bearing forces are calculated to be

$$f_r = \epsilon(1 - 2\dot{\phi}) \left( -2 \int_{\theta_1}^{\theta_2} \frac{\cos\theta \sin\theta}{h^3} d\theta \right) + 2\dot{\epsilon} \left( 2 \int_{\theta_1}^{\theta_2} \frac{\cos^2\theta}{h^3} d\theta \right) \quad (6.18)$$

$$f_t = \epsilon(1 - 2\dot{\phi}) \left( 2 \int_{\theta_1}^{\theta_2} \frac{\sin^2\theta}{h^3} d\theta \right) + 2\dot{\epsilon} \left( -2 \int_{\theta_1}^{\theta_2} \frac{\cos\theta \sin\theta}{h^3} d\theta \right) \quad (6.19)$$

where  $\frac{F}{W} = \sigma f$ ,  $\sigma = \frac{1}{8} \frac{\mu \omega D L}{W} \left( \frac{L}{C} \right)^2$

The integral can be evaluated as

$$-2 \int_{\theta_1}^{\theta_2} \frac{\cos\theta \sin\theta}{h^3} d\theta = \pm 4 \frac{\epsilon \cos^3\theta_1}{[1 - \epsilon^2 \cos^2\theta_1]^2} \begin{cases} + \text{ for } (1 - 2\dot{\phi}) > 0 \\ - \text{ for } (1 - 2\dot{\phi}) < 0 \end{cases} \quad (6.20)$$

$$2 \int_{\theta_1}^{\theta_2} \frac{\cos^2\theta}{h^3} d\theta = \frac{\pi(1 + 2\epsilon^2)}{(1 - \epsilon^2)^{5/2}} \pm \left\{ \frac{2(1 + 2\epsilon^2)}{(1 - \epsilon^2)^{5/2}} \tan^{-1} \alpha \right.$$

$$\left. - \frac{u}{(1 - \epsilon^2)^2} \left[ \frac{(3 - 5a^2) u^2 + (5 - 3a^2) a^2}{(u^2 + a^2)^2} + \frac{(3 - 5a^2) + (5 - 3a^2) a^2 u^2}{(1 + a^2 u^2)^2} \right] \right\} \quad (6.21)$$

and

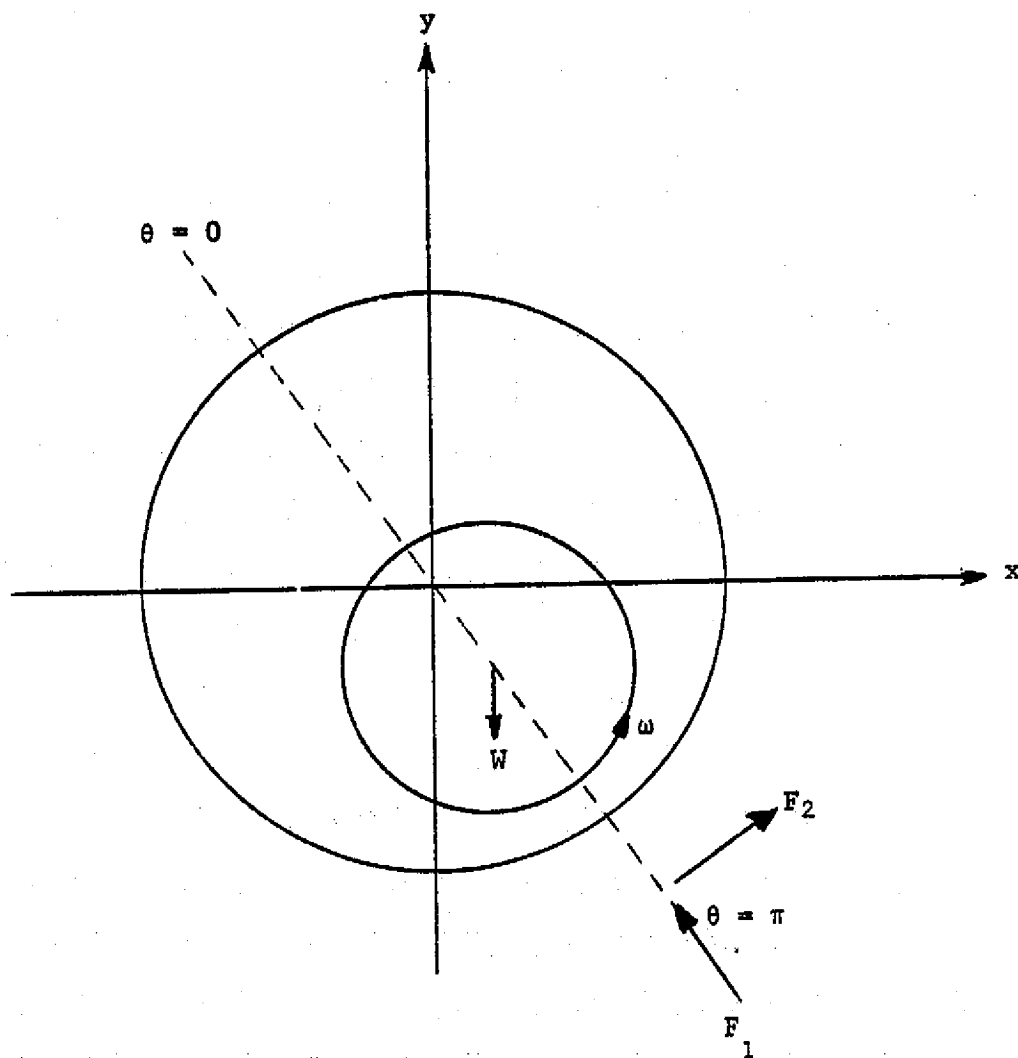


Figure 6.5 SHORT JOURNAL BEARING WITH 180° CAVITATION FLUID FILM

$$2 \int_{\theta_1}^{\theta_2} \frac{\sin^2 \theta}{h^3} a \theta = \frac{2}{(1 - \epsilon^2)^{3/2}} \left\{ \frac{\pi}{2} \pm \left[ \tan^{-1} \alpha - \frac{a u (u^2 - a^2)}{(u^2 + a^2)^2} - \frac{a u (1 - a^2 u^2)}{(1 + a^2 u^2)^2} \right] \right\} \begin{cases} + \text{ for } \dot{\epsilon} > 0 \\ - \text{ for } \dot{\epsilon} < 0 \end{cases} \quad (6.22)$$

where

$$u = \sqrt{\frac{1 - \cos \theta}{1 + \cos \theta}} \quad \cos \theta_0 = \frac{\epsilon |1 - 2\phi|}{\sqrt{\epsilon^2 (1 - 2\phi)^2 + (2\epsilon)^2}}$$

$$a^2 = \frac{1 + \epsilon}{1 - \epsilon}$$

$$\alpha = \left( \frac{u}{a} \right) \left( \frac{a^2 - 1}{1 + u^2} \right)$$

The bearing forces can be transformed into fixed  $x, y$  coordinates by

$$F_x = \left[ -(f_r x + f_t y) / \sqrt{x^2 + y^2} \right] \sigma \quad (6.23)$$

$$F_y = \left[ (-f_r y + f_t x) / \sqrt{x^2 + y^2} \right] \sigma \quad (6.24)$$

In order to verify the use of the above bearing force equations, a short journal bearing of  $L/D = 0.5$  illustrated by Kirk [61] is used as an example. The bearing used is 1 in long, 2 in diameter, 0.005 in clearance, and with lubricant viscosity of  $1.0 \times 10^{-5}$  reyns. When the bearing is located horizontally, the journal has a weight of 50 lbs.

Figure 6.6 shows the transient orbits of a balanced rotor in the bearing calculated by the bearing force equations discussed. Note that the journal finally reached its equilibrium position where  $F_x$  vanishes and  $F_y$  equals the journal load of 50 lbs. Figure 6.7 shows the transient motion in the same bearing calculated by Kirk [61] in non-dimensional form. The transient response from the two independent approaches are in very good agreement, and thus the bearing force equations are verified. Another example is the transient orbit of the same bearing located vertically with an unbalance eccentricity ratio of 0.2 running at 4,000 RPM. Figure 6.8 shows the transient orbits from the bearing force equations and figure 6.9 from Kirk [61]. Again they are in very good agreement and thus further verifies the equations and computer program.

STATION NO. 1

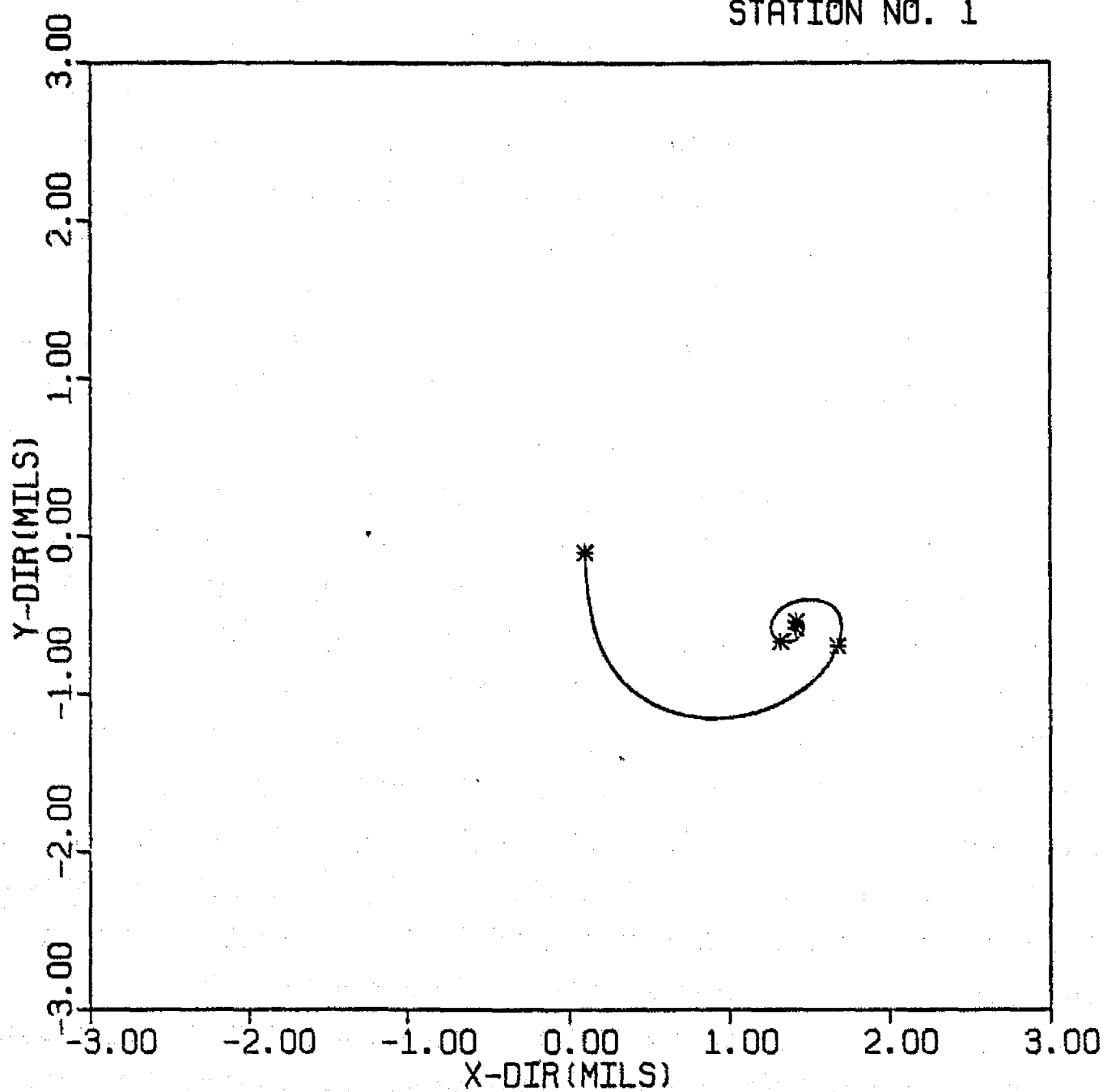
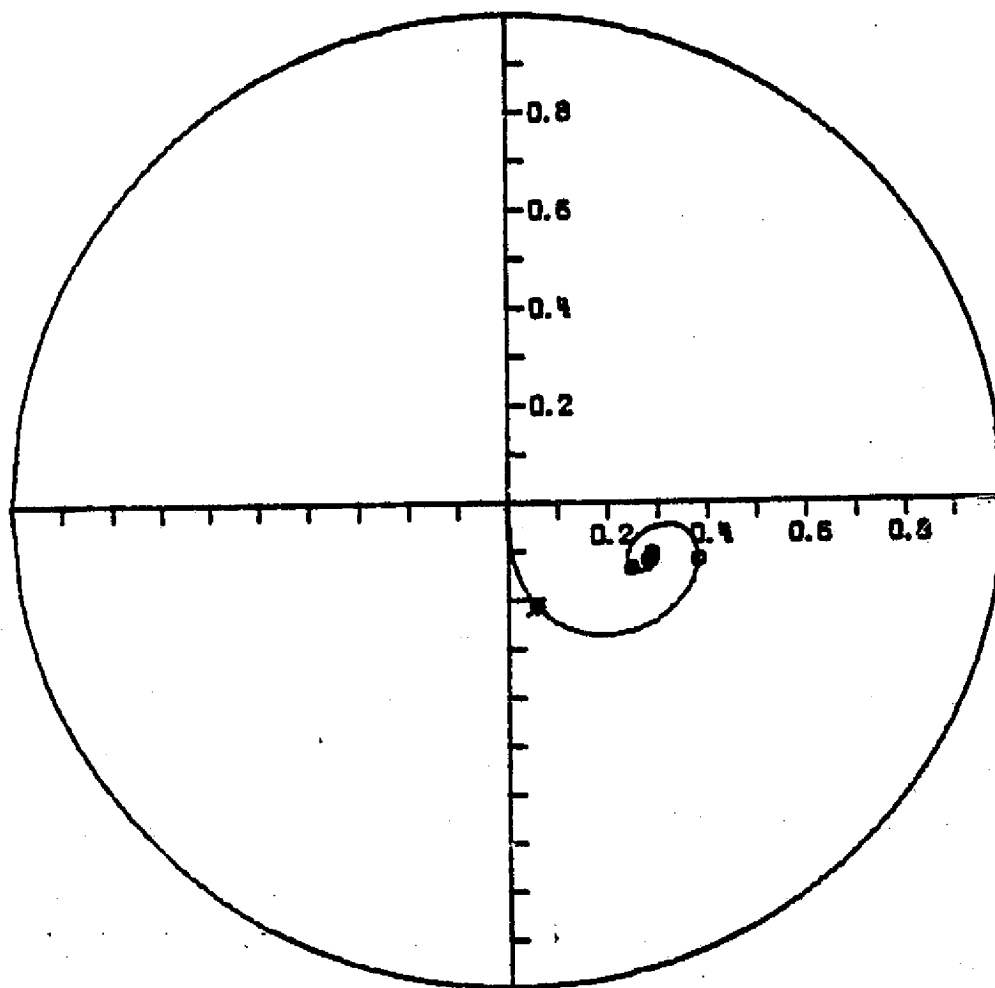


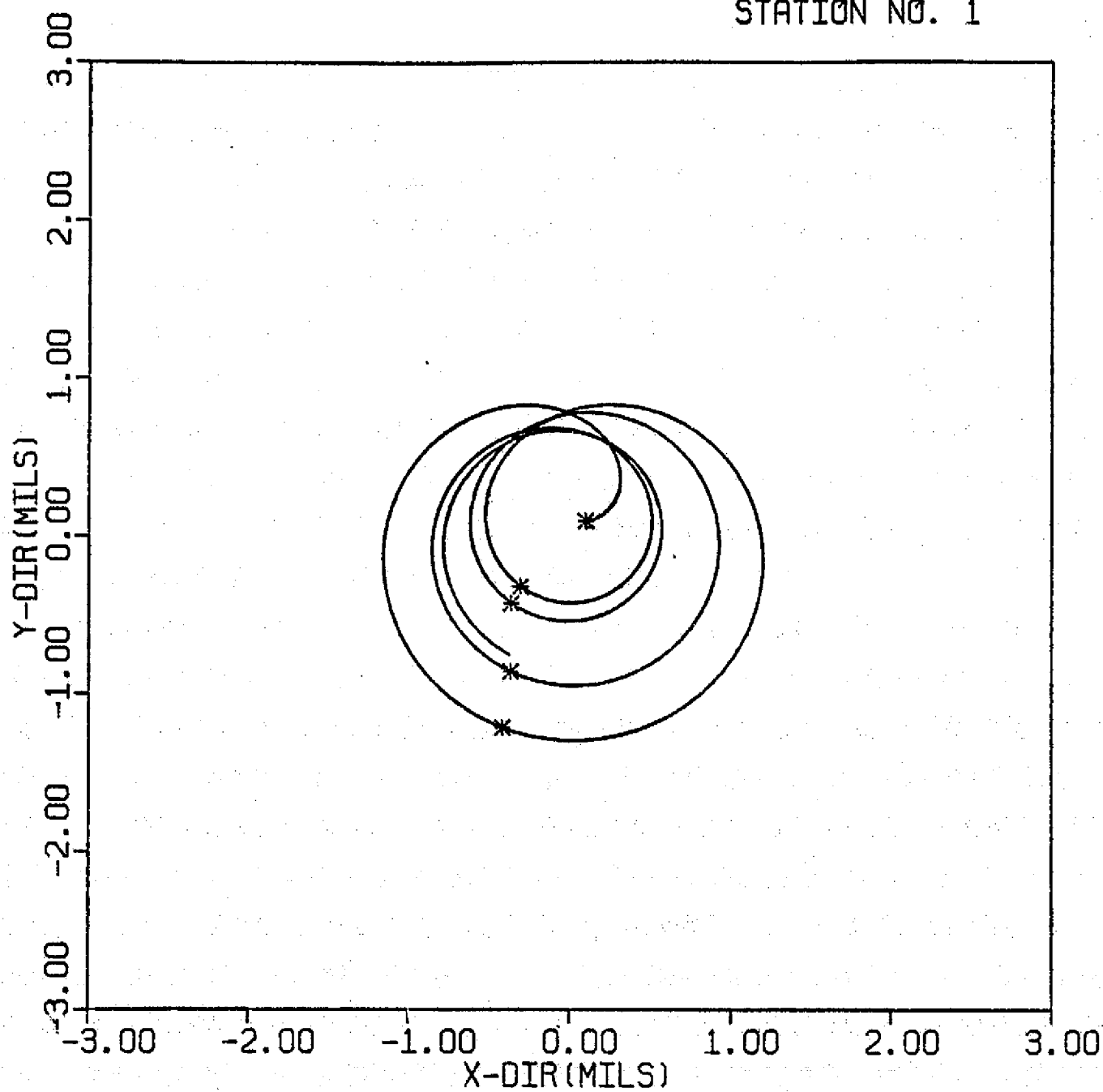
Figure 6.6 TRANSIENT MOTION OF A BALANCED HORIZONTAL ROTOR  
FROM BEARING FORCE EQUATIONS





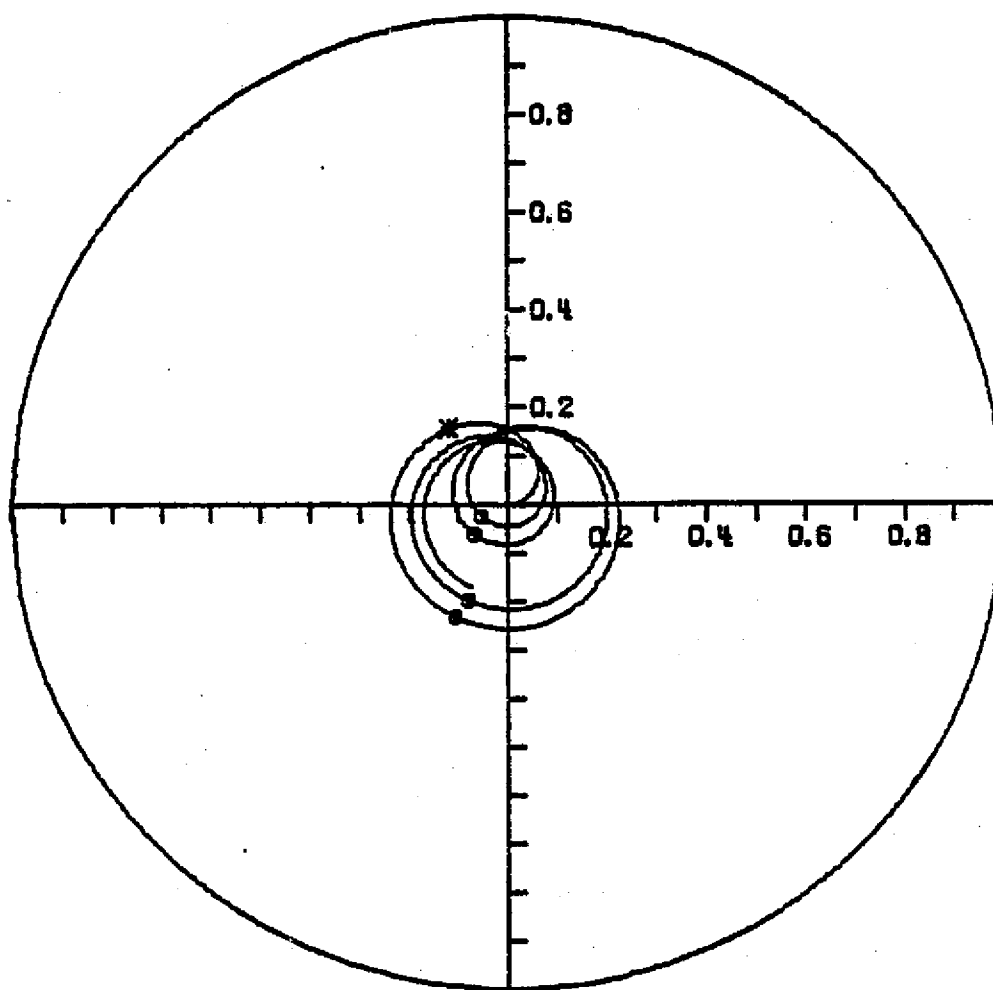
6.7 JOURNAL ORBIT OF A BALANCED HORIZONTAL ROTOR FROM KIRK [61]

STATION NO. 1



6.8 TRANSIENT MOTION OF UNBALANCE ROTOR

FROM BEARING FORCE EQUATIONS



6.9 JOURNAL ORBIT OF AN UNBALANCED VERTICAL ROTOR FROM KIRK [61]

### 6.3 Frequency Analysis of Transient Response Using Discrete Fast Fourier Transformation

In the analysis of transient response of rotor-bearing systems, it may sometimes be difficult to interpret results from transient response orbits or from time-displacement plots, especially for a complex rotor system. The use of Fourier Transformation simulating a "spectrum analyzer" numerically by digital computer is likely to be a powerful technique in transient response analysis. It also provides information concerning the non-linear stability of the system.

In applying the Fourier transformation, the response of the system in the time domain is transformed into the frequency domain as

$$\bar{F}(\omega) = \int_{-\infty}^{\infty} f(t) e^{i\omega t} dt \quad (6.25)$$

Since the transient response calculated in the particular study is in discrete time steps, a discrete Fourier transformation is necessary.

$$\bar{F}_m(\omega) = \sum_{n=0}^{N-1} f_n e^{-i(2\pi m n/N)} \quad m = 0, 1, 2, \dots, N-1 \quad (6.26)$$

where  $m$  = frequency index

$N$  = total number of sample

$f_n$  =  $n^{\text{th}}$  sample of  $f(t)$

Using the above equations, the transient response of the system is transformed into discrete frequency responses which are the "densities" or "excitations" of the corresponding frequencies. In other words, the

responses after the transformation are the magnitudes which these frequencies will be excited.

A more efficient algorithm is the fast Fourier transformation [76, 78] by which the repetitions in the discrete Fourier transformation calculations are eliminated. With  $N$  is a multiple of  $P$ , the frequency responses of the system are given by

$$\bar{F}_m = \bar{A}_m + W_N^m \bar{B}_m \quad m = 0, 1, 2, \dots, P-1 \quad (6.27)$$

where

$$\bar{A}_m = \sum_{n=0}^{P-1} f_{2n} W_P^{mn}$$

$$\bar{B}_m = \sum_{n=0}^{P-1} f_{2n+1} W_P^{mn}$$

$$W_P = e^{-i\left(\frac{2\pi}{P}\right)} = \left( e^{-i\left(\frac{2\pi}{N}\right)} \right)^2$$

$$W_N = \sqrt{W_P}$$

Since the Fourier transformation is applied to periodic functions, it is necessary to use the whole series of real time transient motion as sample input for one sample period. Also, in order to avoid overlapping of the periodic motions, a series of zeros may be attached at the rear part of the sample input such that each period is separated and will not affect each other.

To illustrate the use of Fourier transformation in transient analysis, the transient motion of the simple mass model discussed in section 5.3 was used as an example. The rotor is run through a series of speeds ranging from 10,000 RPM to 35,000 RPM. The bearing coefficients and the internal damping values for each speed are given in Table 6.1. The bearing stiffness and damping coefficients are kept constant while the internal damping of the system varies with operating speed. Figures 6.10 through 6.15 show the transient motion of the rotor with various operating speeds. When the rotor is operating under 30,000 RPM, it can be seen from the figure that the transient response of the system decays with time until it settles into steady state motion. When the rotor is running at 30,000 RPM, Figure 6.14 shows that the rotor motion does not decrease with time and is almost constant. It means that the rotor is operating near its stability threshold speed, and the transient motion orbit is whirling near a limit cycle. The inside loop in the transient motion indicates the existence of large nonsynchronous components. When the operating speed is raised, for example, to 35,000 RPM as shown in figure 6.15, it can be seen that the rotor system is unstable. The transient response is increasing with time and the response orbit is growing.

Using the Fourier transformation as discussed previously, the rotor transient motion can be transformed into frequency components and can be expressed in a Campbell or "waterfall" diagram as shown in Figure 6.16. From this Campbell diagram, one can visualize more easily the stability, component response, and resonance speeds of the system.

SPEED	BEARING COEFFICIENTS			INTERNAL DAMPING COEFFICIENTS		
RPM	$K_x$ lb/in	$K_y$ lb/in	$C$ lb-sec/in	$C_x$ $\omega$ -sec/in	$Q$ lb/in	$C_y$
10,000	62,500	125,000	25	22.2	10,000	12.5
15,000	62,500	125,000	25	22.2	15,000	12.5
20,000	62,500	125,000	25	22.2	20,000	12.5
25,000	62,500	125,000	25	22.2	25,000	12.5
30,000	62,500	125,000	25	22.2	30,000	12.5
35,000	62,500	125,000	25	22.2	35,000	12.5

Table 6.1 BEARING & INTERNAL DAMPING COEFFICIENTS  
FOR A SINGLE MASS ROTOR MODEL

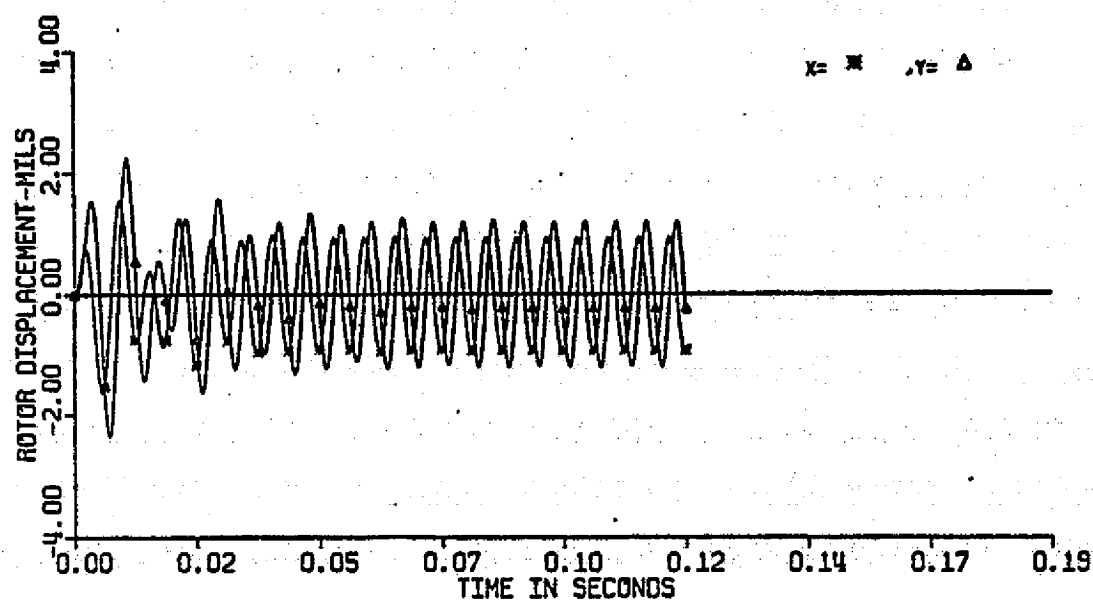
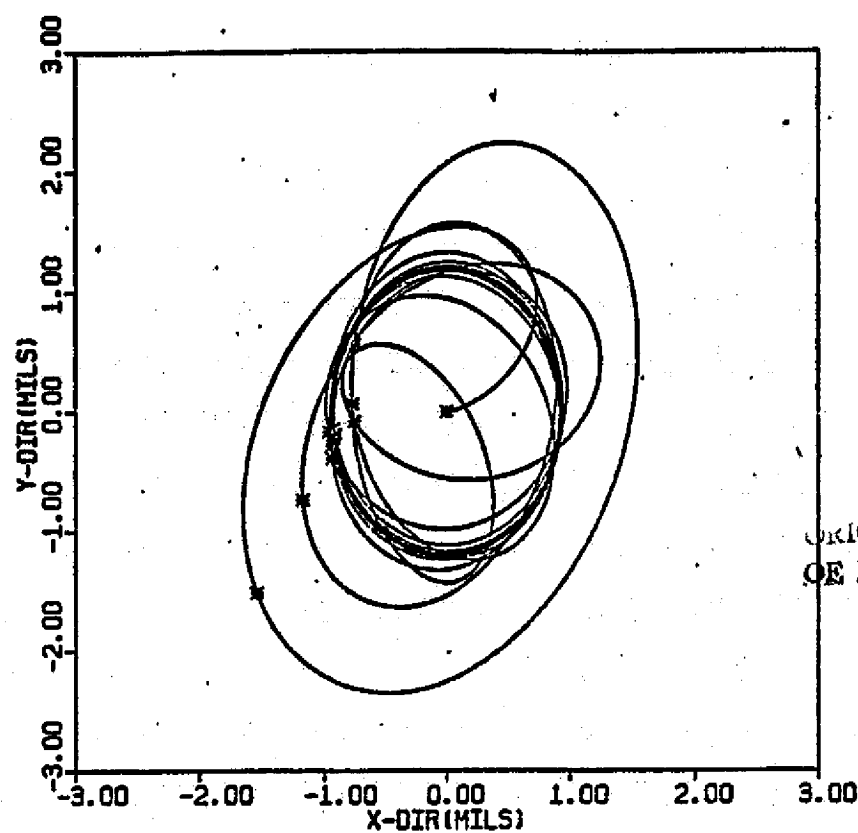


Figure 6.10 TRANSIENT MOTION OF A SINGLE MASS ROTOR AT 10,000 RPM



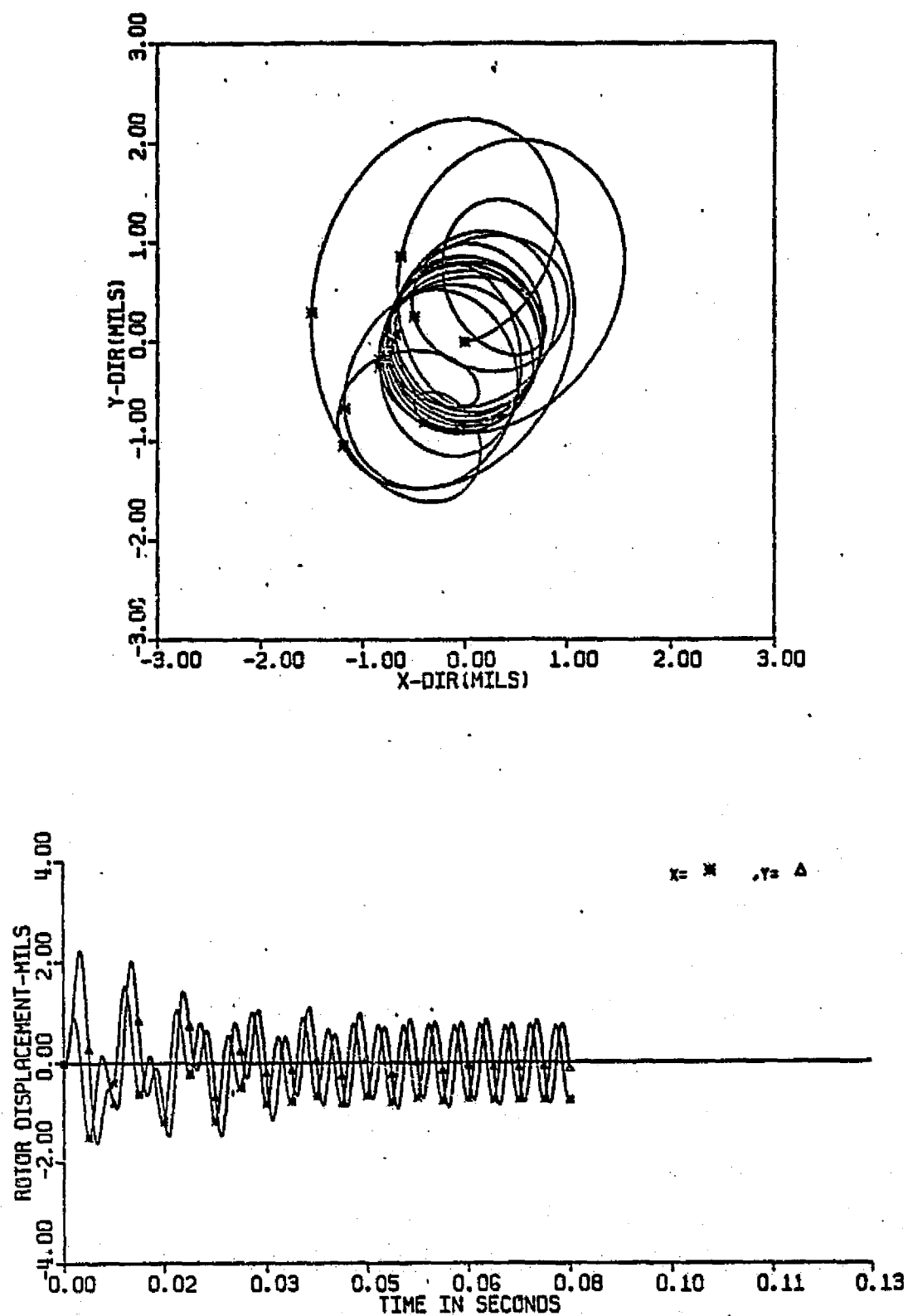


Figure 6.11 TRANSIENT MOTION OF A SINGLE MASS ROTOR AT 15,000 RPM

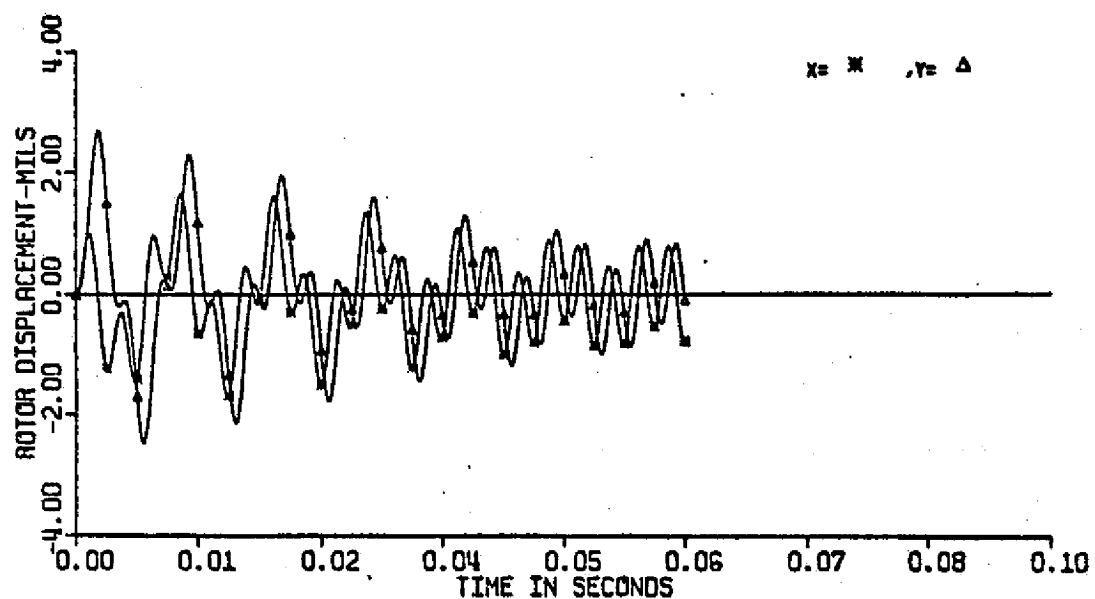
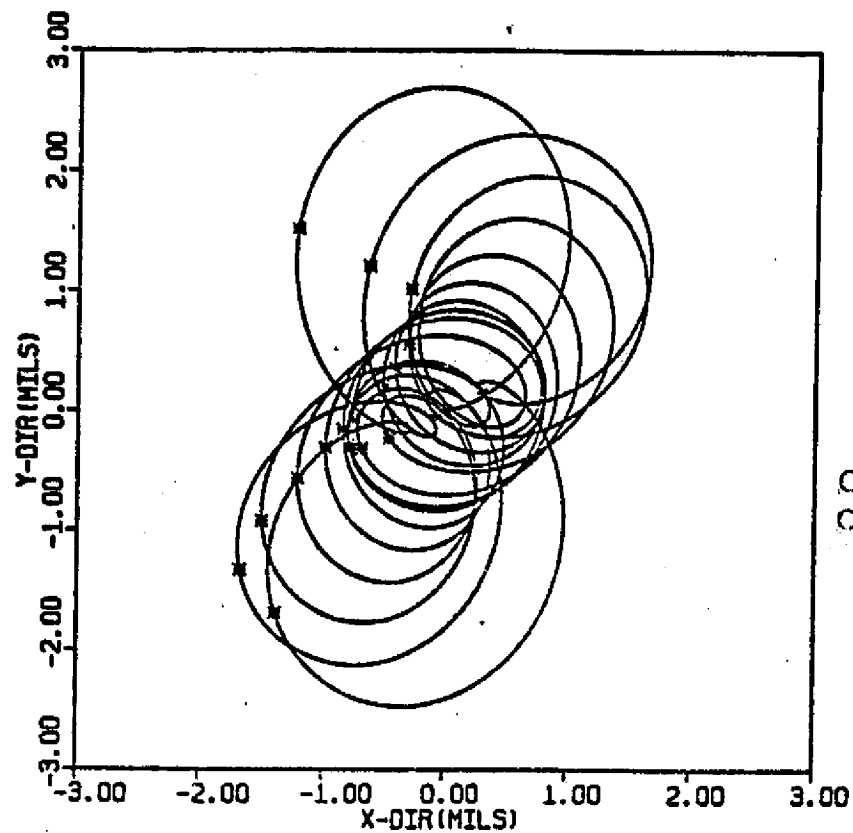


Figure 6.12 TRANSIENT MOTION OF A SINGLE MASS ROTOR AT 20,000 RPM

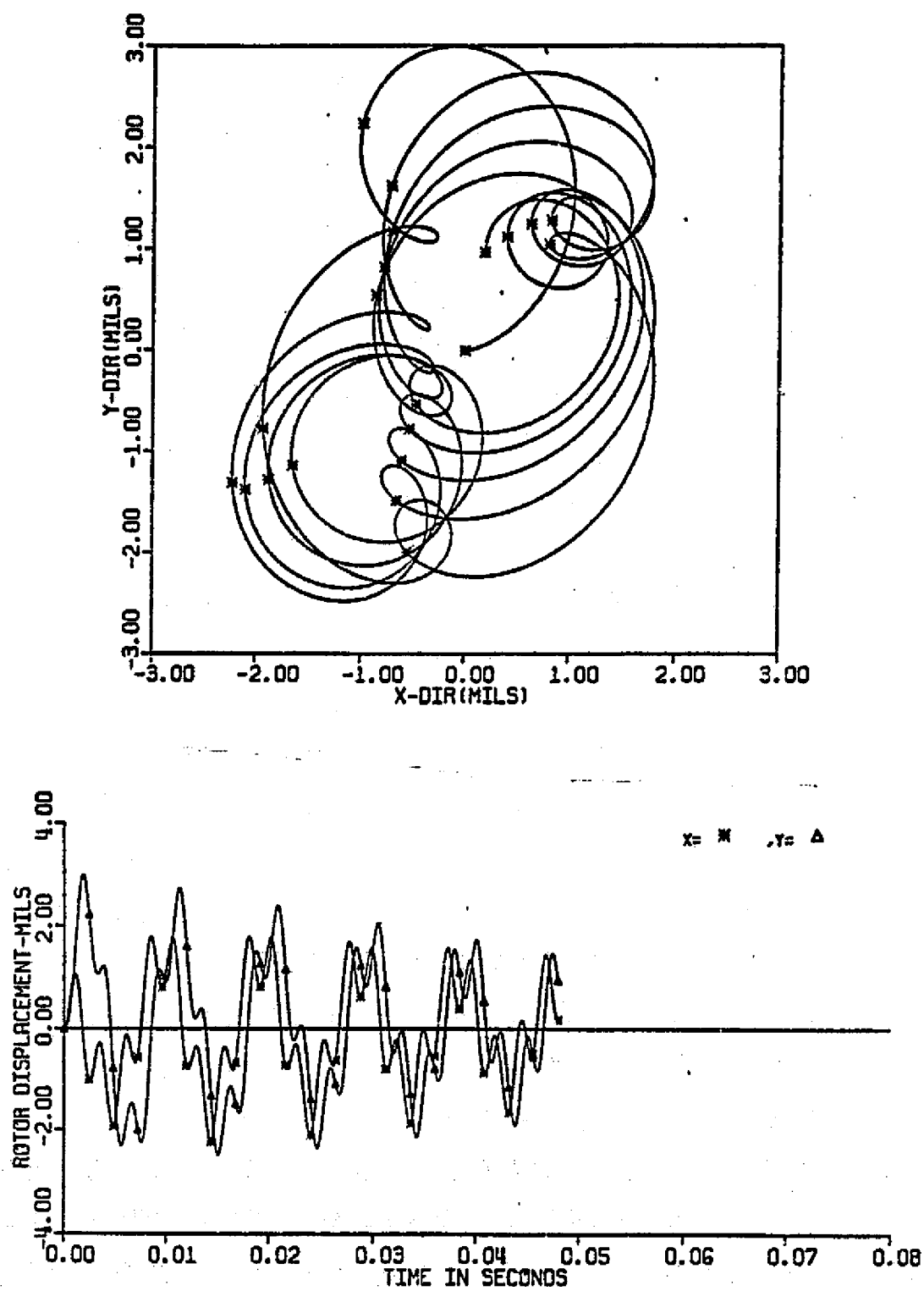


Figure 6.13 TRANSIENT MOTION OF A SINGLE MASS ROTOR AT 25,000 RPM

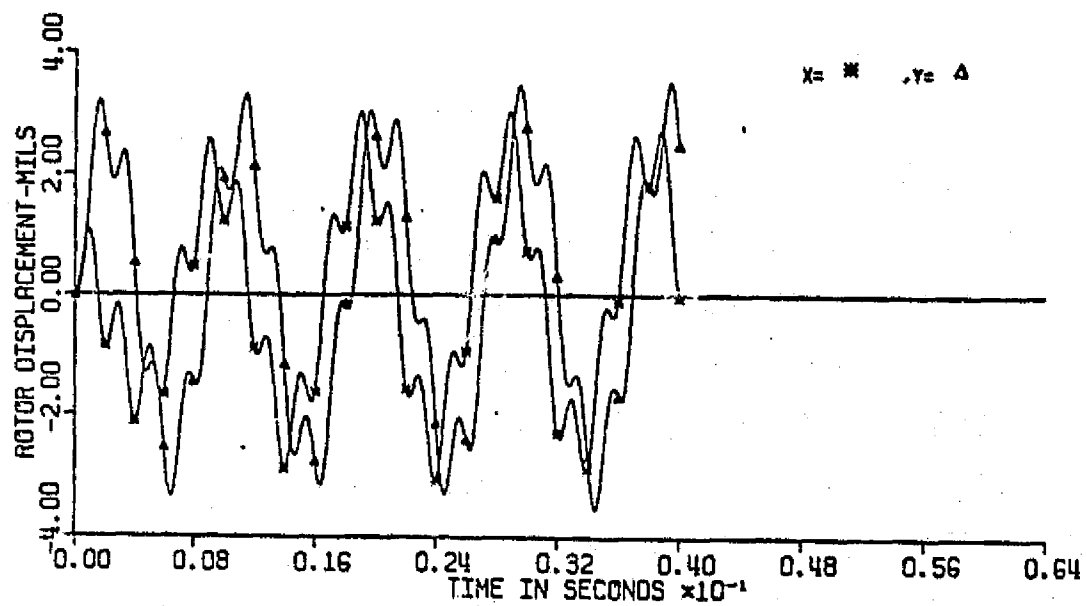
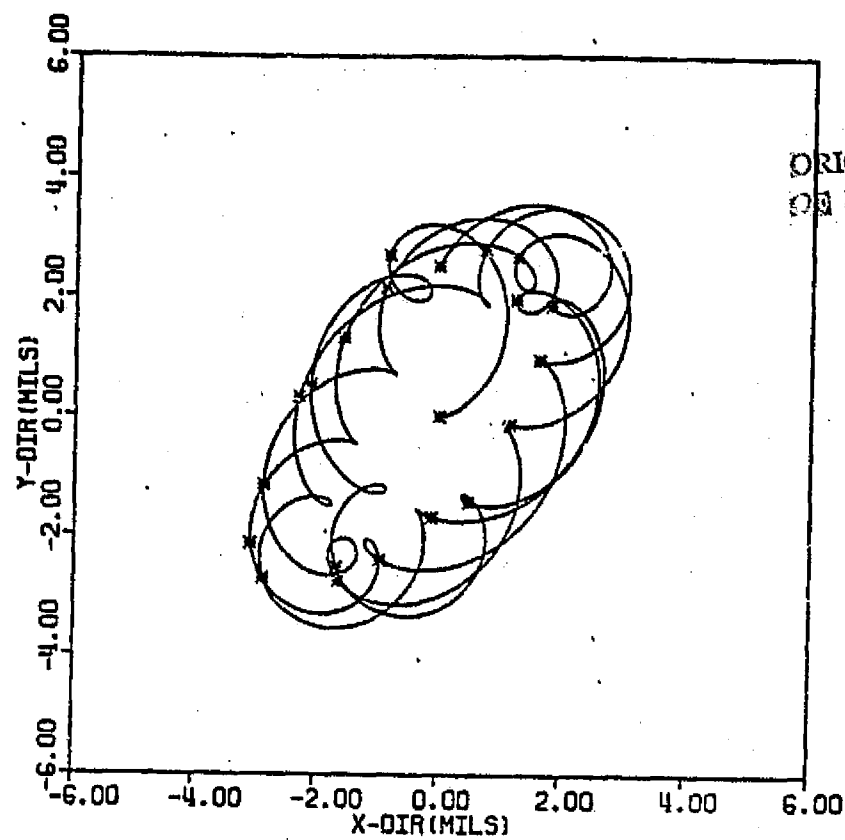


Figure 6.14 TRANSIENT MOTION OF A SINGLE MASS ROTOR AT 30,000 RPM

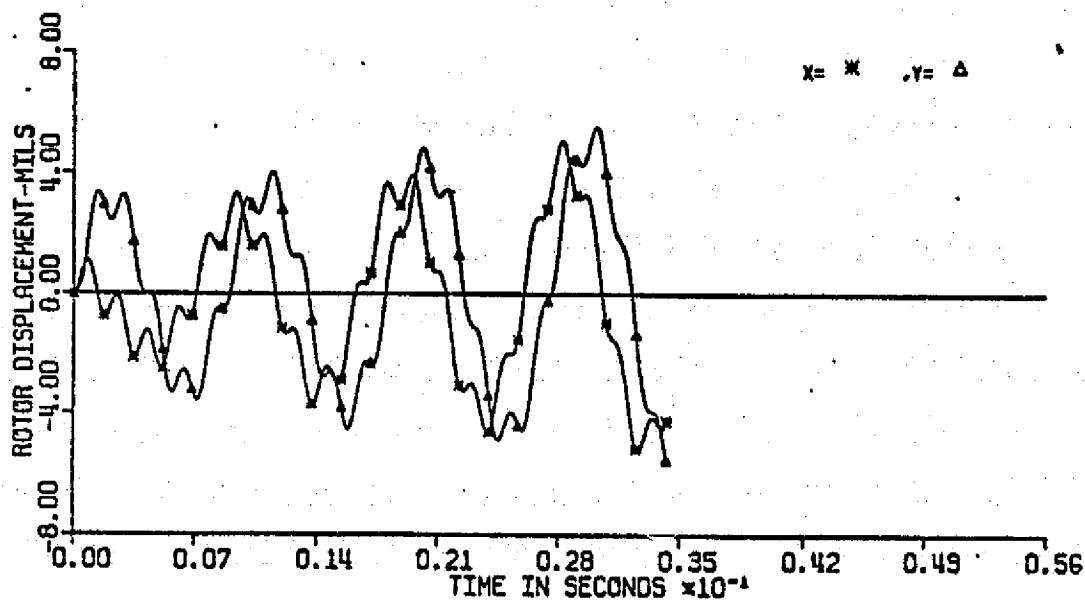
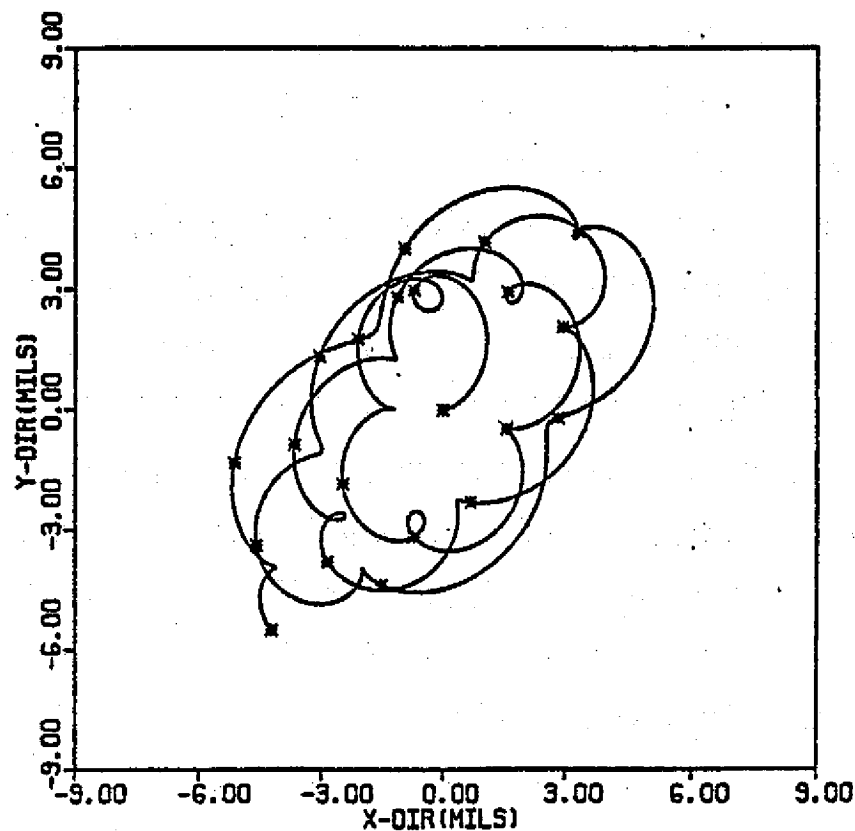


Figure 6.15 TRANSIENT MOTION OF A SINGLE MASS ROTOR AT 35,000 RPM

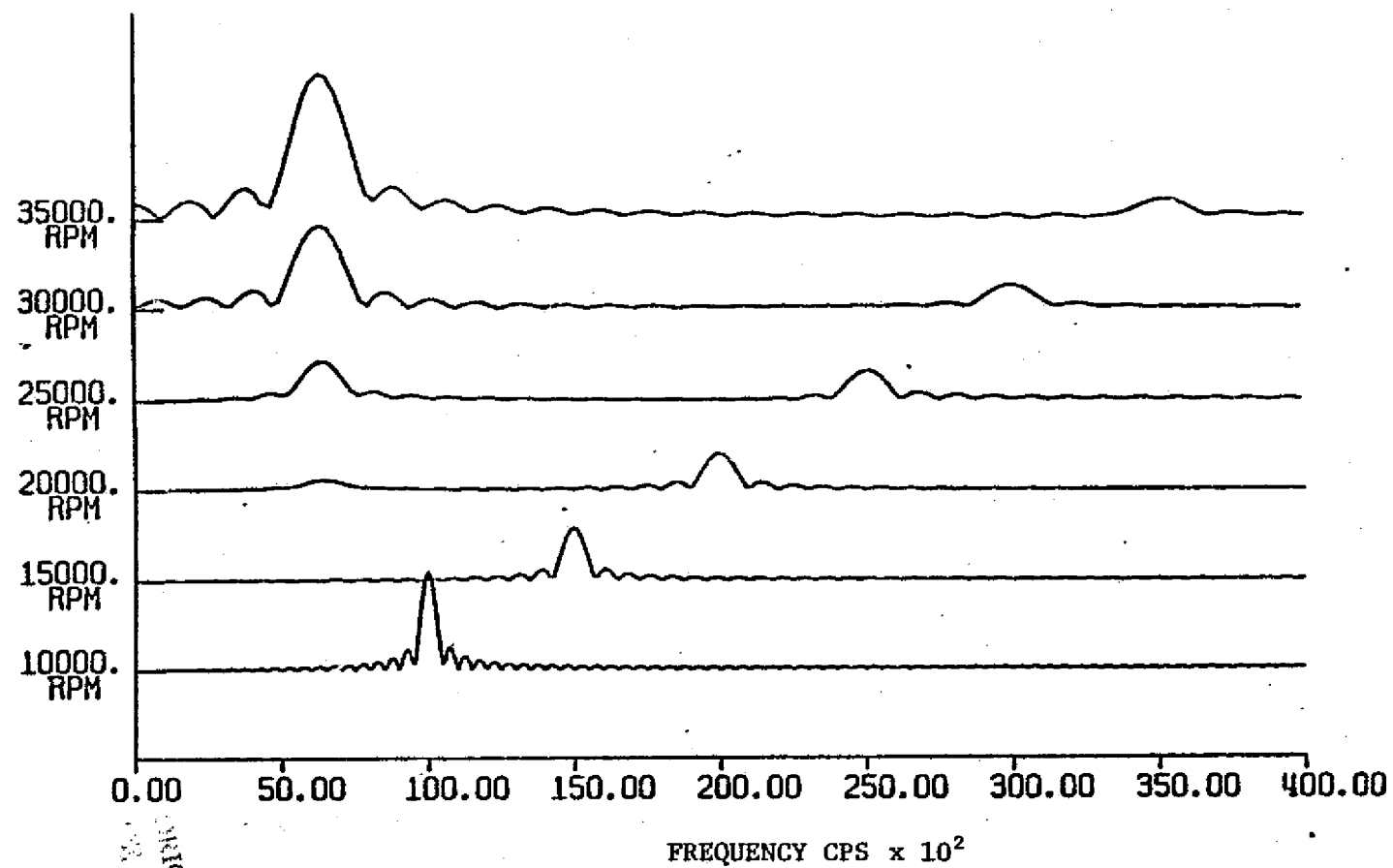


Figure 6.16 FREQUENCY CAMPBELL DIAGRAM OF A SINGLE MASS ROTOR  
WITH EFFECTS OF INTERNAL FRICTION

ORIGINAL PAGE IS  
OF POOR QUALITY

It can be seen that the large response component occurs at a synchronous operating speed of 10,000 RPM. This indicates that it is near one of the critical speeds of the system (707 rad/sec for first critical). The decrease in magnitudes of the synchronous component and increase in magnitude of the non-synchronous components with speed indicates that the stability decreases with the increase of speed. The large non-synchronous component at 30,000RPM occurs near 7,000 RPM, which is at a multiple of one of the critical speeds of the system, shows the instability excited by the first critical speed frequency ( $N_{c_1} = 6,751 \text{ RPM or } 707 \text{ rad/sec}$ ).

The above example demonstrates the use of Fourier transformation in frequency analysis of rotor transient motion. Similarly, this stability analysis can be applied when non-linear bearings or other non-linear forces exist in the system while linear stability analysis of the system fails. The further application of this technique will be discussed with real machinery in the next section. (The computer subroutines used in this fast Fourier transformation analysis were provided by Dr. Jethro Meek, visiting professor in the University of Virginia.)

#### 6.4 Correlation of Experimental Data with Modal Analysis

As to correlate results of modal analysis to experimental data, the three-mass rotor discussed in section 5.2 is used as an example. The experimental rotor consists of three 9-pound disks located on the center span of an uniform shaft supported by two identical journal bearings. The shaft has a diameter of 1 in., and the span between the bearings is 21 inches long. The journal bearing has a clearance of 0.001 in.,  $L/D = 1$ , and a lubricant viscosity of  $0.9 \times 10^{-5}$  lb-sec/in. A schematic of the rotor is given in Figure 5.5. Using linear bearing stiffness, the rotor has a first undamped critical speed near 3000 RPM. Since all the masses are lumped near the center of the rotor, the second critical speed of the rotor is very high compared to the first critical (over 20,000 RPM). Figure 6.17 shows the experimental Campbell (waterfall) diagram of the system at various operating speeds. It can be seen that the critical speed of the system comes in near 2500 RPM, and the dip of the response due to the mechanical bow of the system occurs at 3200 RPM (as discussed in section 5.2). Figure 6.8 shows both the synchronous and transient response of the rotor at various speeds [56].

It is also noted that the subsynchronous component grows significant beyond 6000 RPM, which is near the stability threshold speed of the system. The instability of the system is due to the half-whirl motion of the supporting journal bearings.

In using modal analysis, the rotor is modelled into 17 mass stations. Since the second critical speed is much higher than the first and is far beyond the operating speed range, only the first



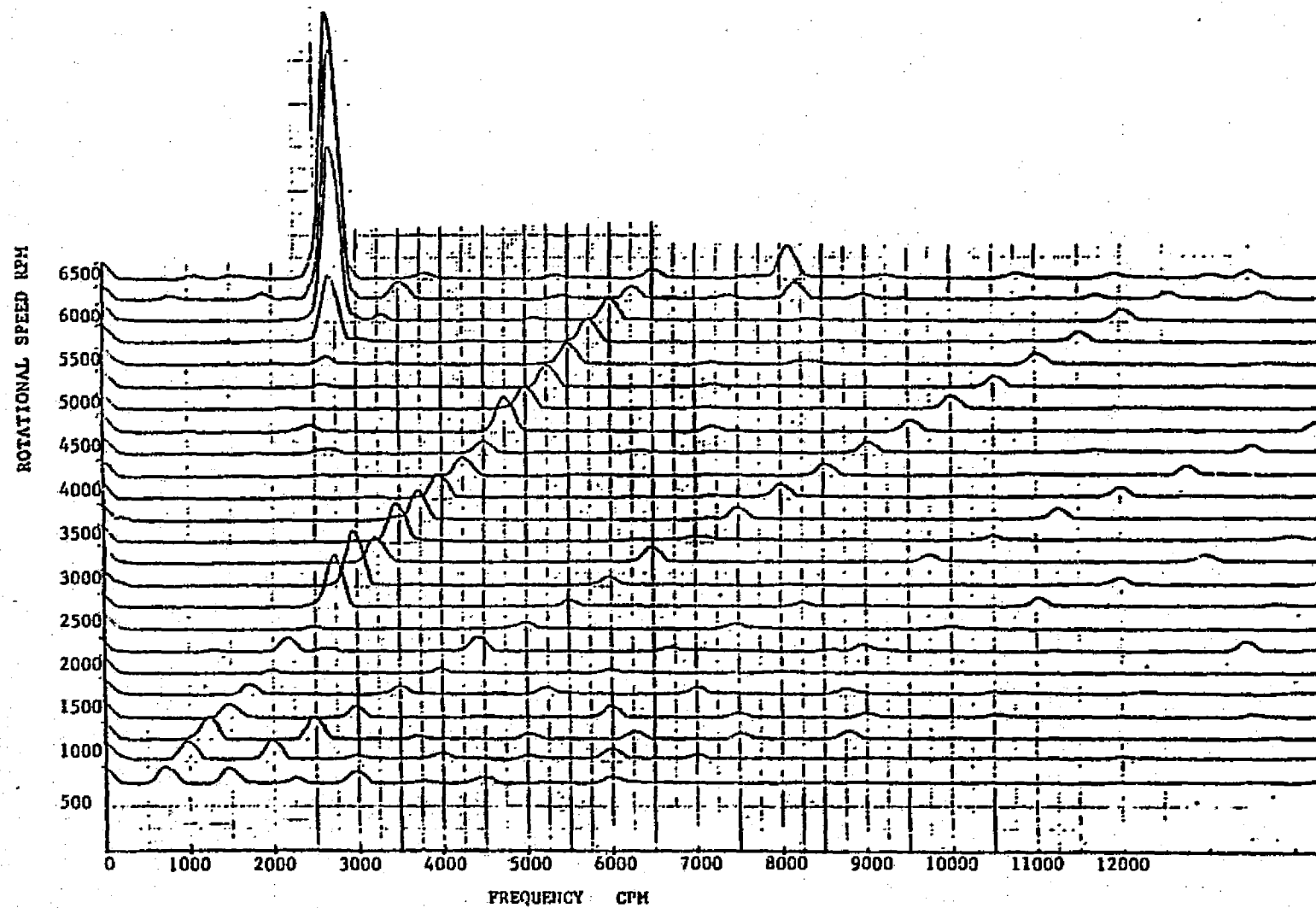


Figure 6.17 EXPERIMENTAL CAMBELL DIAGRAM OF THE 3-MASS ROTOR

ORIGINAL PAGE IS  
OF POOR QUALITY

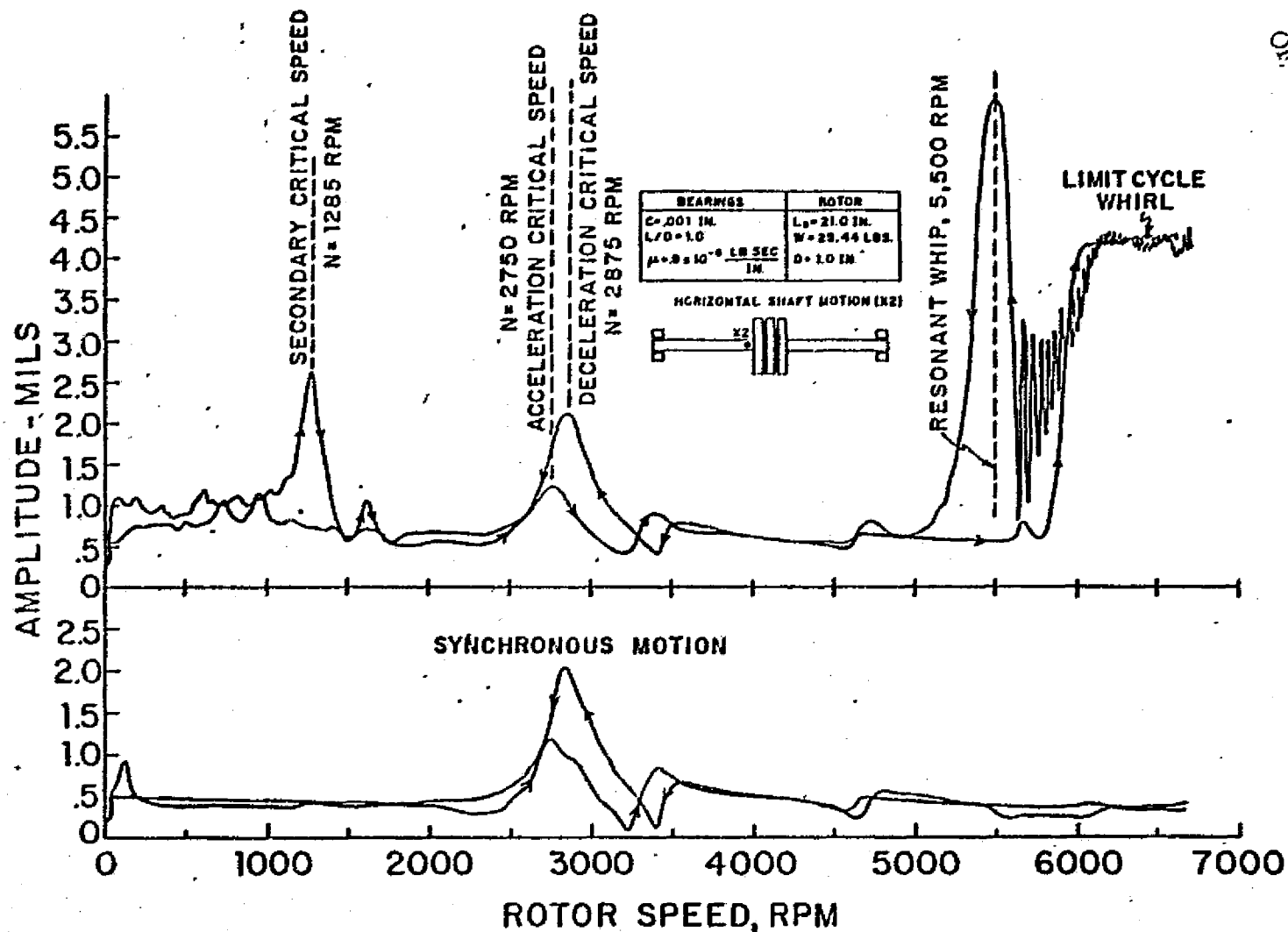


Figure 6.18 TRANSIENT AND SYNCHRONOUS RESPONSE OF THE 3-MASS ROTOR

critical speed mode is used in this analysis. Transient responses of the system are calculated with nonlinear journal bearing forces (as discussed in the previous sections). Figure 6.19 shows the transient motion of the rotor center mass near the first critical speed at 2550 RPM. The rotor is stable at this operating speed and the transient response of the system goes into steady state motion. Figure 6.20 shows the transient motion of the rotor near the stability threshold speed (6350 RPM). The occurrence of an inside loop in the transient response orbit indicates the half-whirl motion of the system. Figure 6.21 shows the transient motion of the system beyond the stability threshold speed (at 7000 RPM). The rotor response is growing and does not settle into steady state motion. Note that the existence of the inside loop type of transient orbit at the beginning gradually becomes a 2 in 1 whirl ratio motion. For a purpose of further understanding, the transient motion was simulated for another 160 cycles of transient motion. Figure 6.22 shows the transient motion of the center mass after 160 cycles and the transient orbit is settling into a form of limit cycle while the system is unstable. This phenomenon can only be predicted with the effect of nonlinear bearing force. With the presence of this limit cycle, the stability of the system may sometimes be very difficult to interpret from transient orbits, and a frequency spectrum analysis of the transient response will be very useful.

The Fourier transformation discussed in the previous section is applied to the transient motion calculated. A Campbell diagram using the results of the transformation is given in Figure 6.23. Note that

ORIGINAL PAGE IS  
OF POOR QUALITY

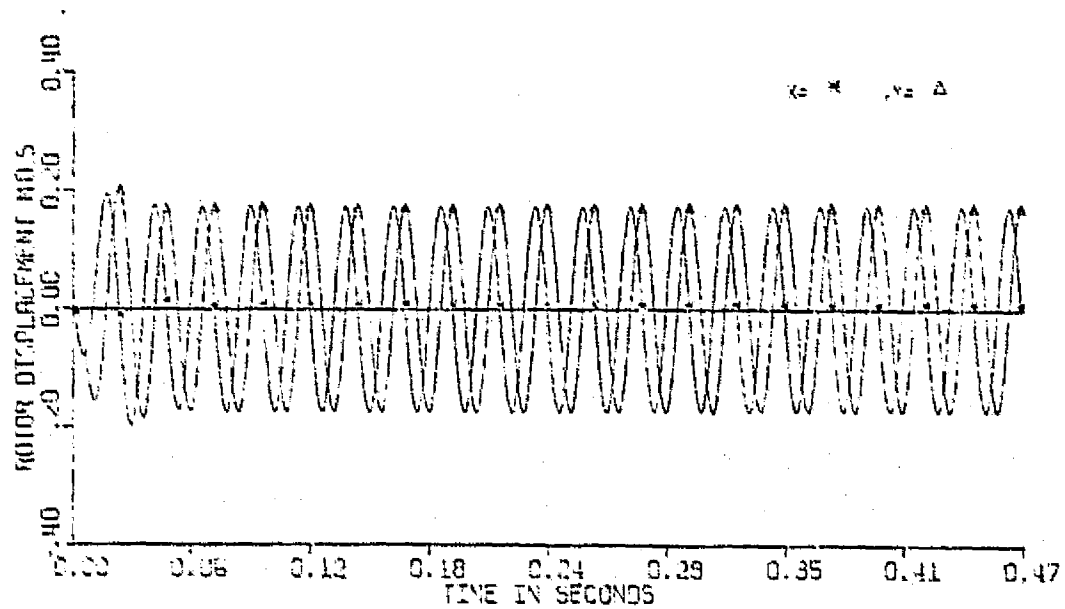
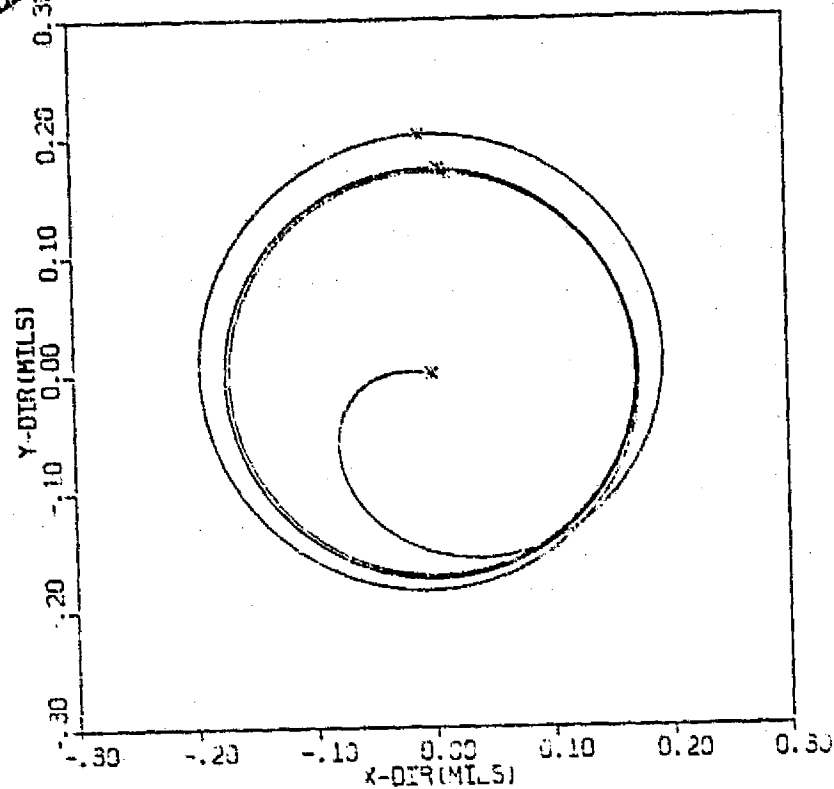


Figure 6.19 TRANSIENT MOTION OF CENTER MASS AT 2550 RPM

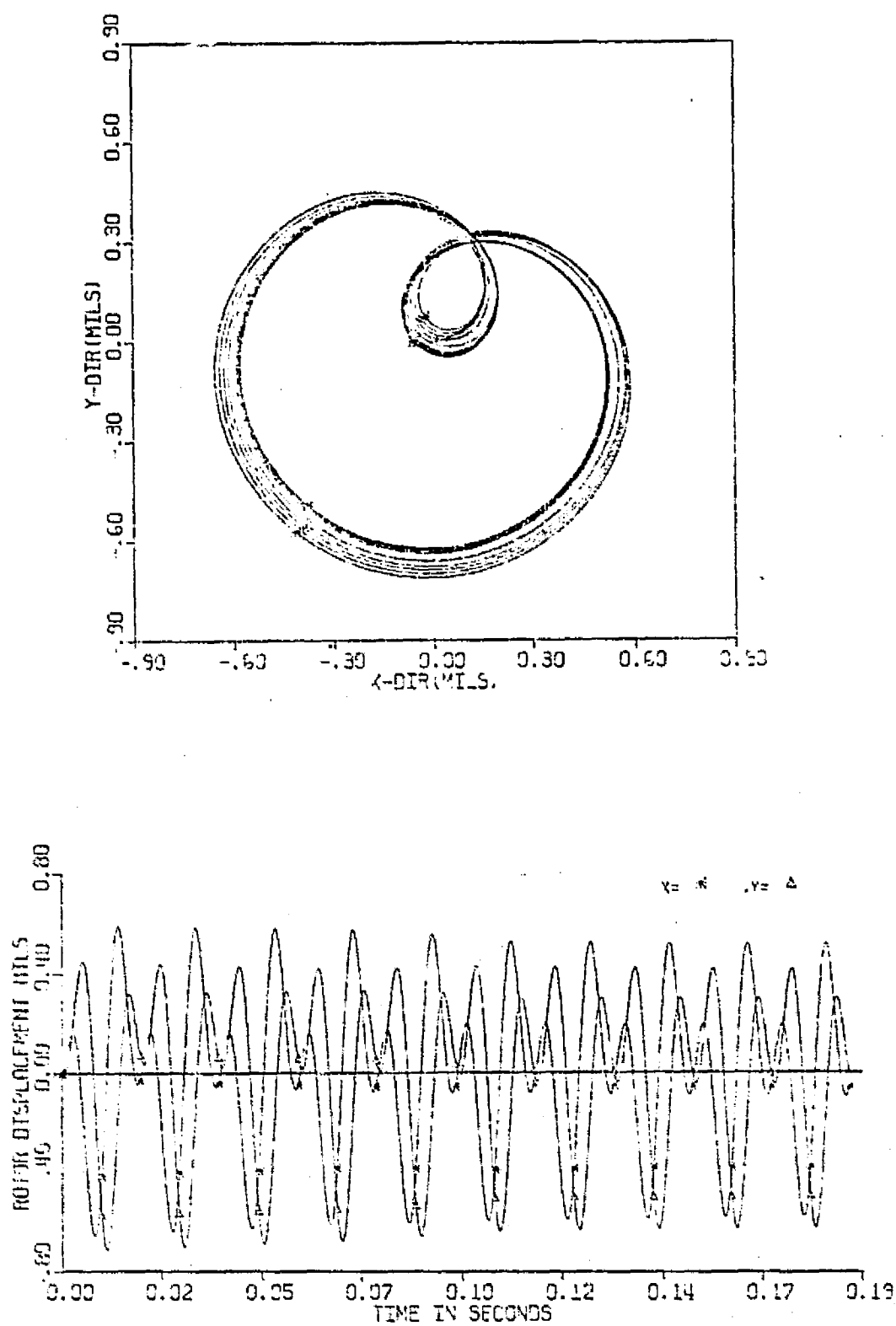


Figure 6.20 TRANSIENT MOTION OF THE CENTER MASS AT 6350 RPM

ORIGINAL PAGE IS  
OF POOR QUALITY

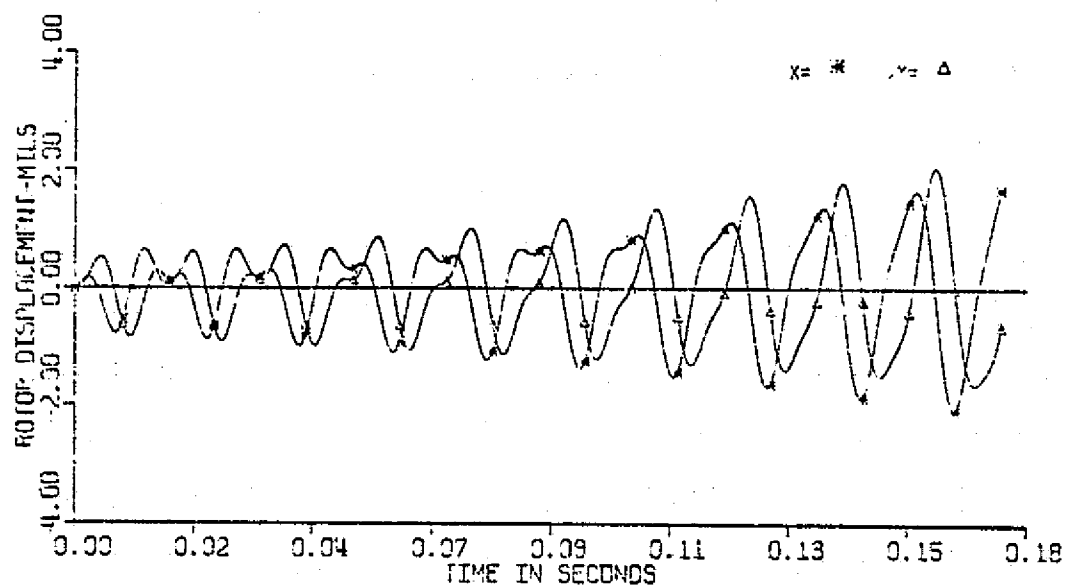
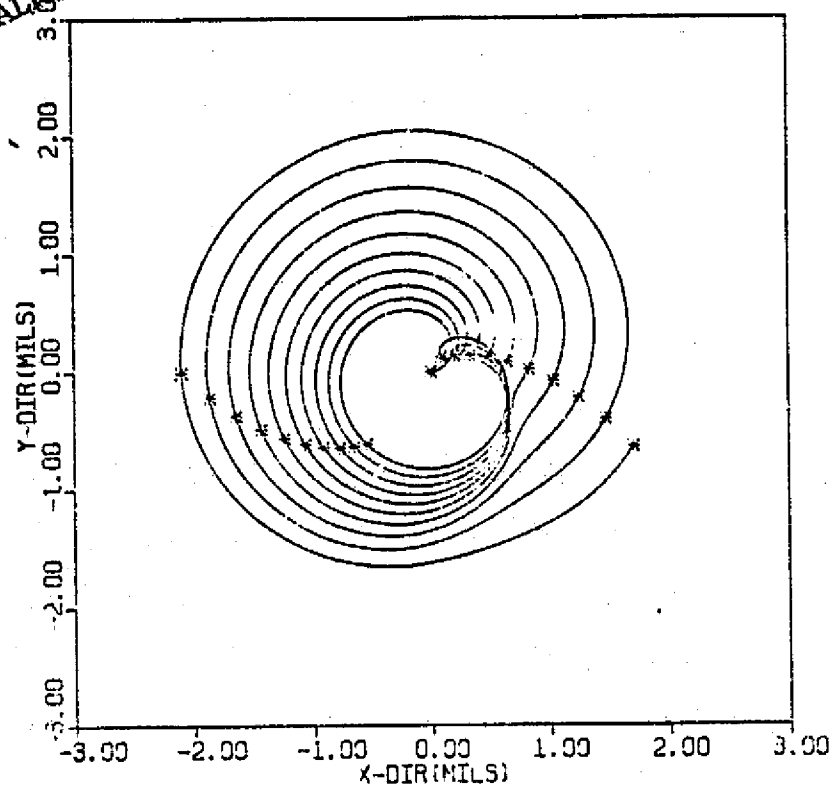


Figure 6.21 TRANSIENT MOTION OF THE CENTER MASS AT 7000 RPM

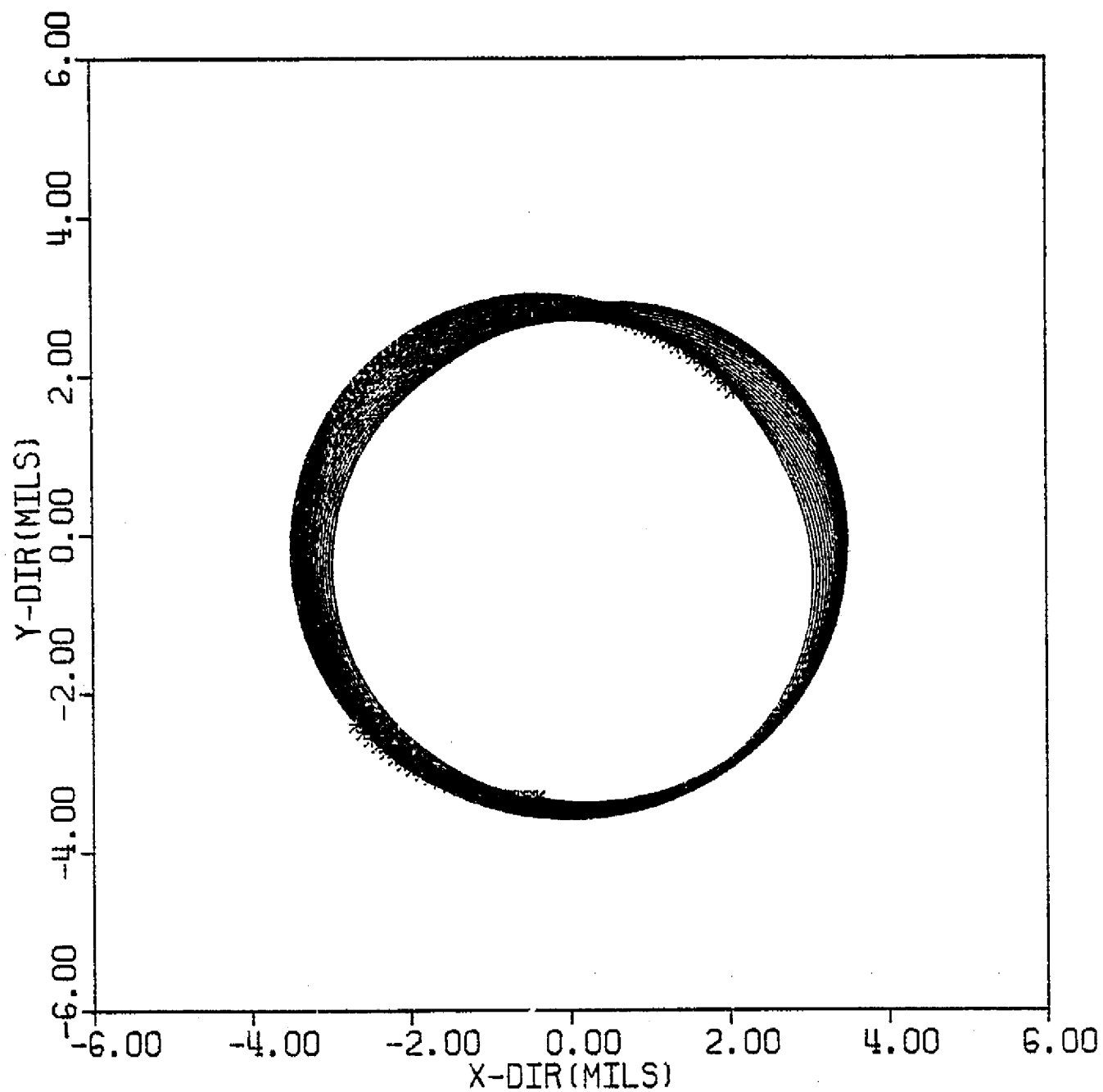


Figure 6.22 TRANSIENT MOTION OF ROTOR CENTER AFTER 160 CYCLES OF MOTION

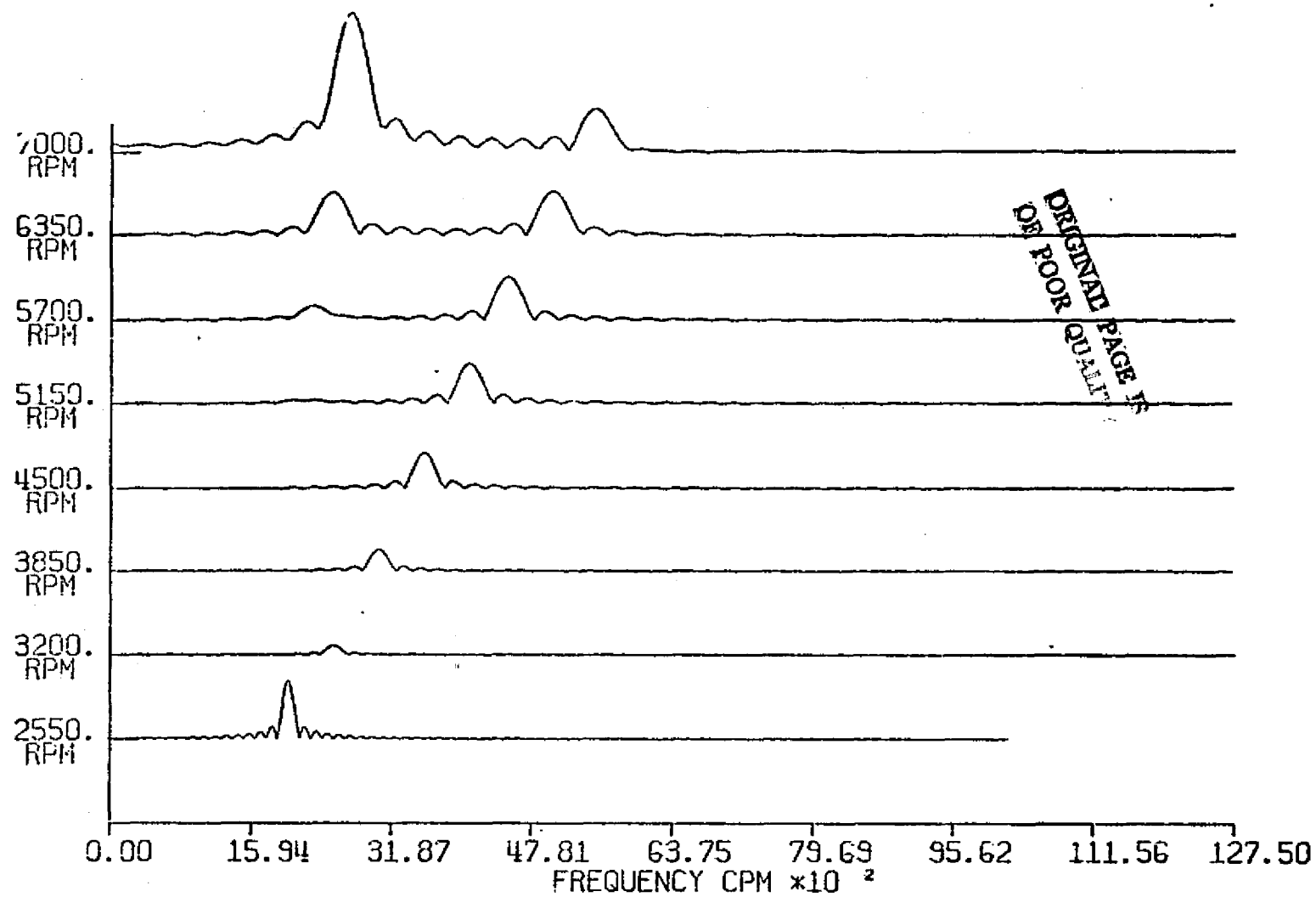


Figure 6.23 CAMPBELL DIAGRAM OF THREE-MASS ROTOR USING FOURIER TRANSFORMATION



the diagram is very similar to the experimental data (critical speed occurs near 2550 RPM). The lack of higher nonsynchronous components (2 or 3 times running speed components) in Cambell diagram as compared to the experimental data is due to the fact that perfect symmetrical rotor is assumed, and only one basic critical speed mode is used in this simulation. If more higher modes can be incorporated in the analysis, a more accurate simulation will be obtained. From the above investigation, it can be concluded that the modal approach discussed in this study can be a fast and powerful technique in predicting dynamic behavior of rotor-bearing systems.

## VII. APPLICATION OF MODAL ANALYSIS ON SPACE SHUTTLE OXYGEN PUMP

### 7.1 Undamped Modes of Oxygen Pump

The SSME turbopumps are presently under development by Rocketdyne division of Rockwell International. The oxygen pump consists of a single rotating shaft mounted in flexibly supported rolling element bearings. The overall rotor length is 21.8 in and weighs about 78 lbs. The rotor consists of a two-stage turbine drive section and a pump section with an overhung boost impeller that supplies high-pressure liquid oxygen to the Space Shuttle Main Rocket Engine at a full power level (FPL) speed of approximately 31,200 RPM. The oxygen pump rotating assembly is illustrated in Figure 7.1. The minimum, nominal, and emergency operating speeds for this turbopump are 20,890, 29,250, and 31,160 RPM respectively.

In order to simulate the dynamics of the pump, the rotor is divided into a 24-mass-station shaft. The rotor weights and their mass inertia effects are lumped at the mass stations. Figure 7.2 shows the computer simulation of the oxygen pump rotating assembly. The rotor geometric properties used in this study is given in Table 7.1. In this simulation, bearing 1 and 4 are the locations of the seals while bearing 2 and 3 are the supporting ball bearing locations. For critical speed analysis, a combined seal stiffness of 25,000 lb/in is used in bearing 1 and 40,000 lb/in in bearing 4. The pump bearing (bearing 2) is assumed a stiffness of 2,200,000 lb/in and turbine bearing (bearing 3) of 3,200,000 lb/in. The critical speeds calculated are 13,266, 47,787, and 58,769 RPM. A set of the critical speed mode shapes is given in Figure 7.3. Table 7.2, 7.3, and 7.4 show the

C-3

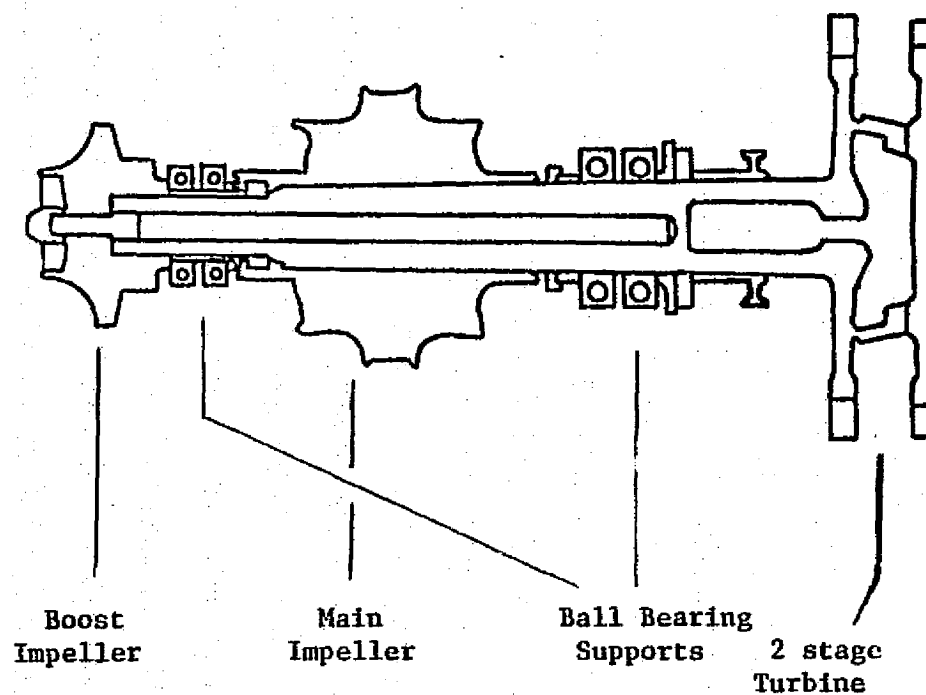


Figure 7.1 Rotating Assembly of Space Shuttle Main Engine Oxygen Pump

ORIGINAL PAGE IS  
OF POOR QUALITY

STATION NO.	WEIGHT (LP)	LENGTH (IN.)	SHAFT DIA. OUTSIDE	SHAFT DIA. INSIDE	I (IN**4)	IP-PULAR MOM. (LP-IN**2)	IT-TRANS. MOM. (LB-IN**2)
1	3.045	.510	2.100	.610	.95	6.211	3.710
2	.000	.560	2.810	.750	3.04	0.000	0.000
3	3.041	.620	2.620	.750	2.30	4.327	2.571
4	.000	.938	2.000	.750	.77	0.000	0.000
5	1.290	.773	2.000	.750	.77	.758	.444
6	.000	.750	1.450	.750	.20	0.000	0.000
7	.000	.375	1.720	.750	.41	0.000	0.000
8	2.540	.315	2.020	.750	.80	2.386	2.230
9	.000	.370	2.300	.750	1.36	0.000	0.000
10	3.085	1.310	2.620	2.000	1.53	12.851	6.808
11	8.825	1.330	3.600	2.000	7.46	36.767	20.254
12	6.695	1.600	3.600	2.000	7.46	35.594	18.420
13	5.901	2.110	2.620	2.000	1.53	14.487	10.086
14	2.702	.740	2.080	.750	.90	2.746	2.810
15	.000	1.360	2.600	.750	2.23	0.000	0.000
16	3.356	1.490	2.600	.750	2.23	3.248	1.924
17	4.195	2.000	2.620	1.050	2.25	6.572	4.640
18	2.348	1.600	2.460	1.050	1.74	3.278	1.941
19	.000	.770	2.460	1.050	1.74	0.000	0.000
20	13.467	.580	2.860	2.060	2.40	158.962	80.104
21	3.414	1.200	3.300	2.650	3.40	15.688	8.407
22	.000	.450	4.000	3.640	3.95	0.000	0.000
23	13.825	.100	4.000	3.640	3.95	157.768	79.438
24	.000	0.000	4.000	3.640	3.95	0.000	0.000
	77.729	21.850					

Table 7.1 Rotor Geometry of the Space Shuttle Oxygen Pump

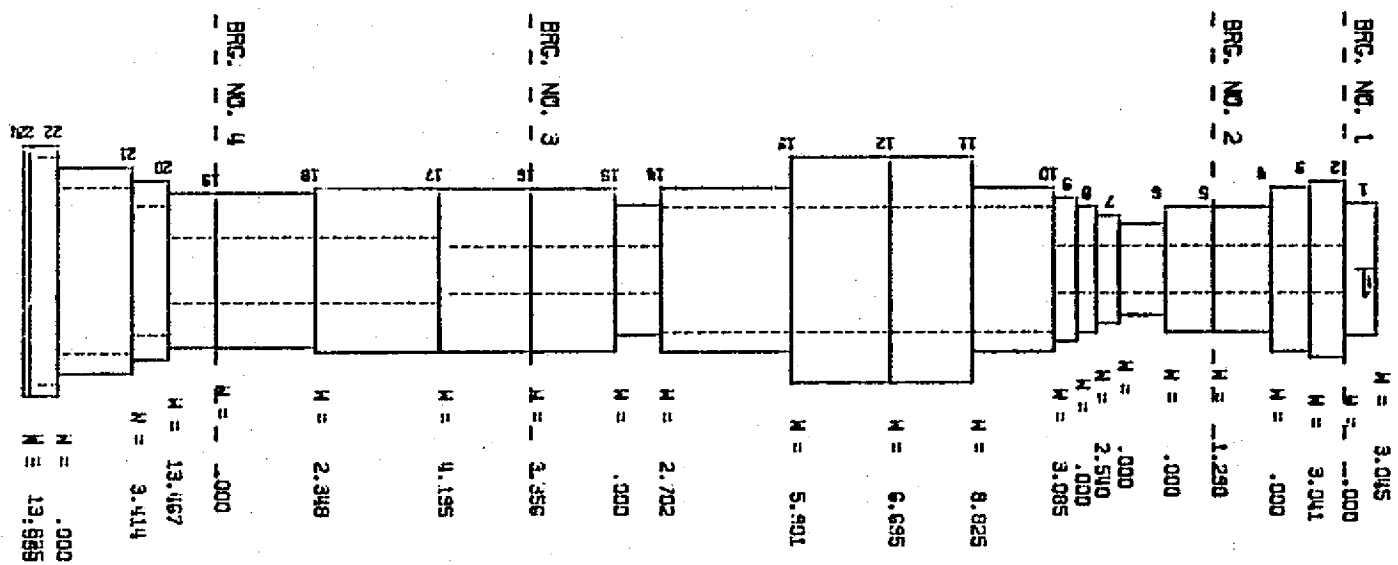
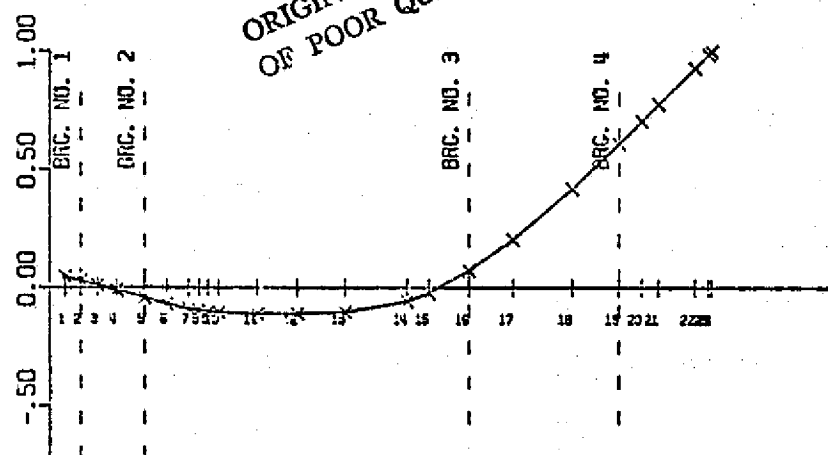


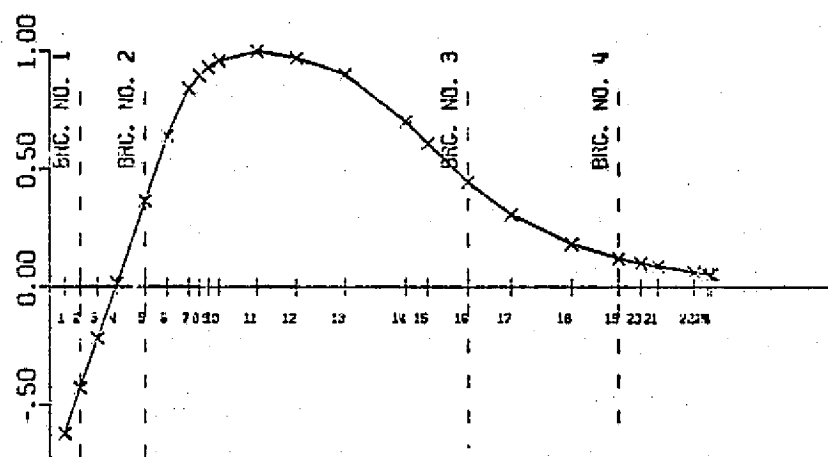
Figure 7.2 Computer Simulation of the Oxygen Pump Rotating Assembly

ORIGINAL PAGE IS  
OF POOR QUALITY

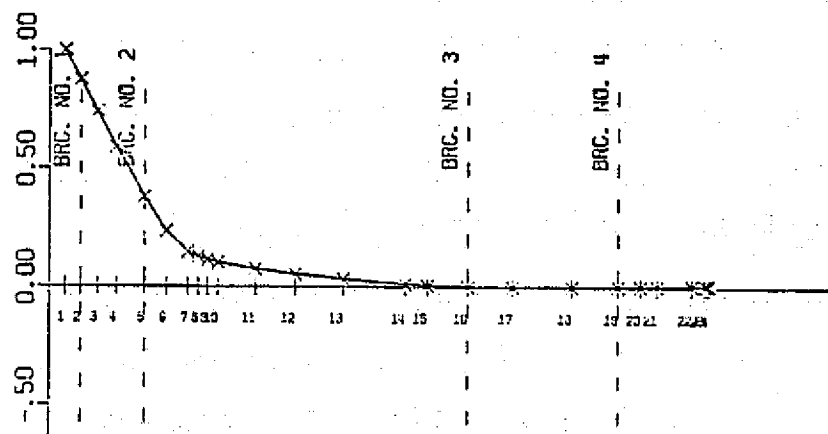
ORIGINAL PAGE IS  
OF POOR QUALITY



$N1 = 13266$  RPM



$N2 = 47787$  RPM



$N3 = 58769$  RPM

Figure 7.3 Undamped Mode Shapes of Oxygen Pump

ORIGINAL PAGE IS  
OF POOR QUALITY

CRITICAL SPEED NO. 1 13266.1RPM  
MODAL MASS = .067 LB-SEC\*\*2/IN

THE ORTHONORMAL MODE SHAPES

STATION	TRANSLATIONAL	ROTATIONAL
1	.18449	-.13232
2	.11702	-.13226
3	.04296	-.13224
4	-.03901	-.13218
5	-.16282	-.13194
6	-.26346	-.12709
7	-.34146	-.07534
8	-.36633	-.05667
9	-.38269	-.04696
10	-.39866	-.03913
11	-.42969	-.00608
12	-.43172	.00345
13	-.41484	.01825
14	-.25331	.13974
15	-.11931	.22343
16	.23036	.29216
17	.72150	.36468
18	1.52897	.43864
19	2.27647	.49244
20	2.66306	.51077
21	2.96115	.51686
22	3.58517	.52256
23	3.82057	.52358
24	3.87293	.52358

Table 7.2 Oxygen Pump Orthonormal Mode of the First Critical Speed

ORIGINAL PAGE IS  
OF POOR QUALITY

CRITICAL SPEED NO. 2 47787.0RPM  
MODAL MASS = .079 LB-SEC\*\*2/IN

THE ORTHONORMAL MODE SHAPES

STATION	TRANSLATIONAL	ROTATIONAL
1	3.56663	-1.68785
2	2.70823	-1.67735
3	1.77043	-1.67157
4	.73853	-1.65623
5	-.77008	-1.55589
6	-1.92483	-1.42248
7	-2.72865	-.68049
8	-2.94259	-.45560
9	-3.06913	-.34635
10	-3.18226	-.26397
11	-3.33644	.03791
12	-3.24133	.10456
13	-3.01773	.17147
14	-2.37919	.38562
15	-2.08771	.39075
16	-1.59233	.32211
17	-1.19617	.21716
18	-.85277	.13643
19	-.66471	.10603
20	-.58324	.10735
21	-.52104	.10744
22	-.39072	.11048
23	-.34058	.11242
24	-.32934	.11242

Table 7.3 Oxygen Pump Orthonormal Mode of the Second Critical Speed



ORIGINAL PAGE IS  
OF POOR QUALITY

CRITICAL SPEED NO. 3 58769.1RPM  
MODAL MASS= .016 LB-SEC\*\*2/IN

THE ORTHONORMAL MODE SHAPES

STATION	TRANSLATIONAL	ROTATIONAL
1	7.81703	-1.79822
2	6.90474	-1.77582
3	5.91414	-1.76081
4	4.83445	-1.71840
5	3.35961	-1.40304
6	2.39056	-1.11893
7	1.85655	-.35230
8	1.75079	-.21748
9	1.68986	-.17121
10	1.63122	-.14724
11	1.46329	-.12233
12	1.29803	-.12729
13	1.08770	-.13562
14	.77327	-.15217
15	.66630	-.13413
16	.50256	-.10279
17	.37980	-.06535
18	.27746	-.04141
19	.21521	-.03955
20	.18277	-.04544
21	.15589	-.04736
22	.09707	-.05092
23	.07383	-.05238
24	.06859	-.05238

Table 7.4 Oxygen Pump Orthonormal Mode of the Third Critical Speed

orthonormal translational and rotational modes of the pump. These critical speeds and modes calculated are very similar to those provided by Rocketdyne and Childs [42, 43, 44]. Since the second critical speed is far above the full-power level operating speed range, the prime concern of this study will be on the dynamics of the rotor operating through the first critical speed and the stability of the system. From the mode shapes given in Figure 7.3, it can be predicted that large response will occur at the turbine end of the rotor when operating through the first critical speed. It was also believed that the ball bearings used will not provide adequate damping to the system such that a very high amplification factor will result or possibly instability problems. The stability and forced response analysis of the oxygen pump will be discussed in the next section.

## 7.2 Stability Analysis of Oxygen Pump

The stability of the system is found by examining the real part of the calculated eigenvalues which govern the growth and decay rate of the rotor motion. As being discussed in Chapter 4, a positive real part of an eigenvalue indicates an unstable rotor whereas a negative real part indicates a stable one. The relative stability of a given mode is given by the magnitude of the real part, which is based mainly on the magnitude of effective damping in the system. For stable modes, an estimate of the peak response speed and amplification factor can be calculated through modal resolution of that particular mode.

In the analysis of the space shuttle main engine oxygen pump (SSME-HPOTP), because of the lack of damping contributions from the ball bearing supports, stability of the system becomes one of the major concerns of design. A large part of the damping in the system is obtained from the seals, which are the main design parameters in the stabilization of the machine. Childs [44] modelled these axial-flow seals in 7 different locations in the system. To simplify calculation, the seals were lumped into 3 major groups in this stability analysis. Without the consideration of any effects from the turbine and impeller of the system, the damped natural frequency of the pump was found to be  $-5.49 \pm 1494.3 \text{ rad/sec}$ , which indicates that the system is stable. The damped mode shape of the system is given in Figure 7.4. Note that extremely high amplitude of response occurs at the turbine end of the system which agrees with the large values in the calculated modal

ORIGINAL PAGE IS  
POOR QUALITY

	Seal Group	1	2	3
Original Seal Design	$K_{xx}$	156,700	146,000	3,024
	$K_{xy}$	29,590	1,100	528
	$K_{yx}$	-29,590	-1,100	-528
	$K_{yy}$	156,700	146,000	3,024
	$C_{xx}$	18.4	1.0	0.5
	$C_{yy}$	18.4	1.0	0.5
Modified Seal Design	$K_{xx}$	156,700	380,900	28,150
	$K_{xy}$	29,590	66,730	4,854
	$K_{yx}$	-29,590	-12,330	-2,454
	$K_{yy}$	156,700	309,900	59,050
	$C_{xx}$	18.4	10.2	1.68
	$C_{yy}$	18.4	32.0	3.36

\*Modified Seal Design with Seal 4 Extended at

$\Delta P = 3,200$  psi and Seal 6 as 3-step Seal at  $\Delta P = 581$  psi. ( $\epsilon = .9$ )

Table 7.5 SEAL COEFFICIENT USED IN SSME-HPOTP ANALYSIS

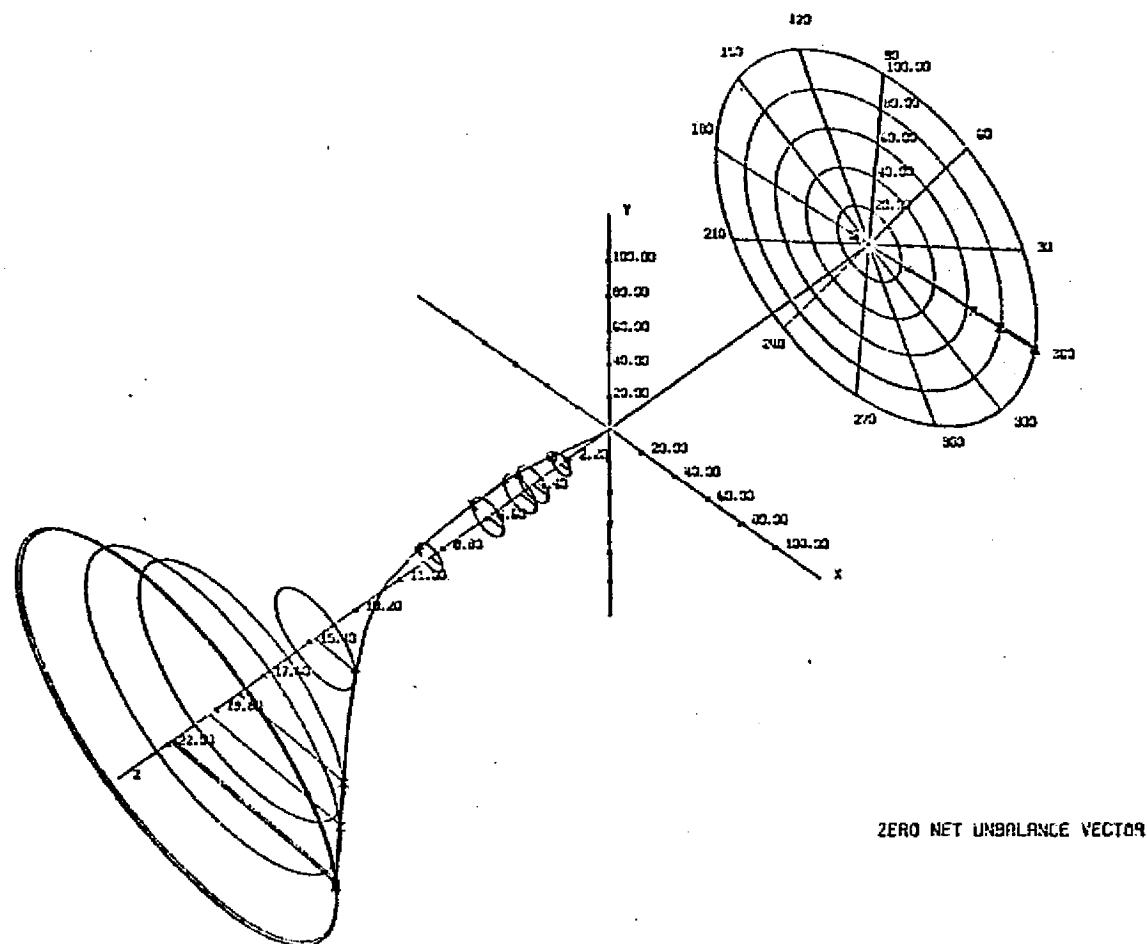


Figure 7.4 DAMPED MODE SHAPE OF THE OXYGEN PUMP AT FIRST CRITICAL SPEED

ORIGINAL PAGE IS  
OF POOR QUALITY

amplification factor of 136. Further investigation of rotor response through the first critical speed will be discussed in the next section.

To simulate a more realistic situation in the system, a turbine cross coupling effect of 4000 lb/in is assumed. Damped critical speed calculations showed that the system is unstable with a natural frequency of  $14 \pm i 1475.3$  rad/sec. This calculation shows that the system is marginally stable without any turbine effects, and even with a small instability driving force from the turbine, the system is unstable. In order to stabilize the system, a change of seal design is necessary. The redesign of No. 4 seal (group 2) with extended seals near the turbine and seal No. 6 (group 3) with modified 3-step seals at the turbine seems to be a more stable design. The seal coefficients used in the original design and the modified design are given in Table 7.5. Using the above modified seal design and with the turbine forces, the damped frequency calculated is  $-67 \pm i 2342.5$  rad/sec, which indicates a stable system. Thus it can be concluded that a major redesign of the seals in the system can significantly change the stability conditions of the pump.

### 7.3 Forced Response Analysis of Oxygen Pump

A simulation study has been performed to examine the steady state and transient rotor dynamics of the space shuttle oxygen pump. This simulation confirms the previous results of modal amplification factor and stability analysis. The rotor model used is similar to the one discussed in the previous section. Using the original seal design discussed by Childs [44] and without considering turbine force, a steady state unbalance response study was performed for a range of operating speeds from 0 to FPL (full power level) speed of 32,000 RPM. With rigid ball bearing supports (2,200,000 lb/in stiffness for pump bearing and 3,200,000 lb/in stiffness for turbine bearing) and an unbalance of 6 gm-in at the turbine, the rotor experiences a very high level amplitude of vibration at its first critical speed. Table 7.6 shows the results of the steady state unbalance response analysis at various operating speeds. As discussed in the last section, the turbine end of the pump has the most violent vibration problem with 54 mils of steady state response at the first resonance. In this case, the response of the second resonance speed (over 40,000 RPM) is not considered because it is well beyond the operating speed range. However, the magnitude of the steady state unbalance response at FPL of 32,000 RPM is within an acceptable range, and thus the problem lies in the operation of the pump through its first critical speed.

A further study of the problem is the transient analysis of the rotor at its first critical speed. Since it is a common occurrence that a rotor may exhibit a higher magnitude of vibration during deceleration than

<div> <div>SPEED (RPM)</div> <div>LOCATION</div> </div>	14,200 1st RESONANCE	20,890 (MINIMUM)	29,250 (NOMINAL)	31,160 (EMERGENCY)
Seal No. 1	0.25	0.005	0.003	0.003
Pump bearing	3.26	0.06	0.042	0.040
Turbine bearing	5.33	0.10	0.069	0.065
Seal No. 2	36.6	0.67	0.47	0.45
Turbine	54	1.03	0.73	0.68

Table 7.6 STEADY STATE UNBALANCE RESPONSE (in mils)  
OF OXYGEN PUMP WITH 6 gm. in. UNBALANCE AT TURBINE



acceleration, a transient response study of the pump during deceleration through its first critical speed was performed. With the same model used in steady state analysis, transient motion of the pump was calculated at 14,500 RPM with a deceleration rate of  $940 \text{ rad/sec}^2$ . In order to have a closer simulation of the real situation, rotor steady state motion with small perturbation is used as the initial conditions. Figure 7.6 and 7.7 are the transient simulations at the pump and the turbine bearings respectively. Figure 7.5 and 7.8 are the transient simulations at the seal locations. Figure 7.9 is the transient simulation at the turbine end of the rotor. Note that the turbine undergoes a very large amplitude of response of 24 mils at its resonance speed. Figure 7.8 also predicts very large transient motion at the seal location when going through the first critical speed of the system. This large motion at the turbine end of the pump will cause rubbing at the floating ring seal or even pump failure. Figure 7.10 shows the forced response of the pump at the turbine from both steady state and transient solution. Note that the amplitude of the steady state response is about 80 percent higher than the transient. Thus with steady state unbalance response analysis alone, the simulation may be quite misleading. However, in this case, both solutions predict very high amplitude of vibration at the turbine, which may cause pump failure.

With the above analysis of the oxygen pump, it can be concluded that a redesign of the system is necessary. The introduction of extended seals or 3-step seals may add more damping to the system and thus reduce the amplitude of vibration in the system. The rubbing condition indicated

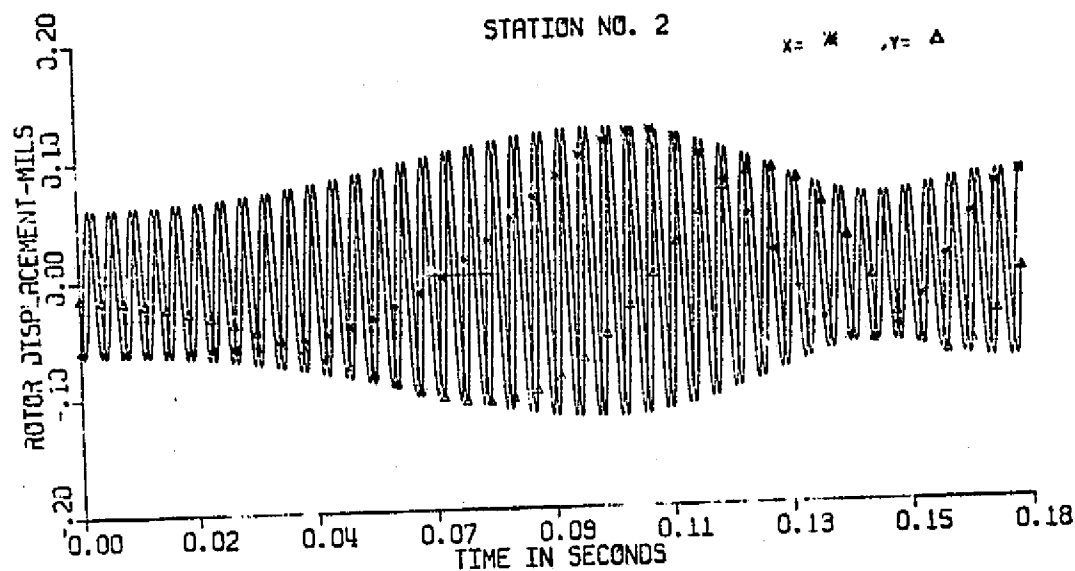


Figure 7.5 TRANSIENT MOTION AT THE FIRST SEAL LOCATION

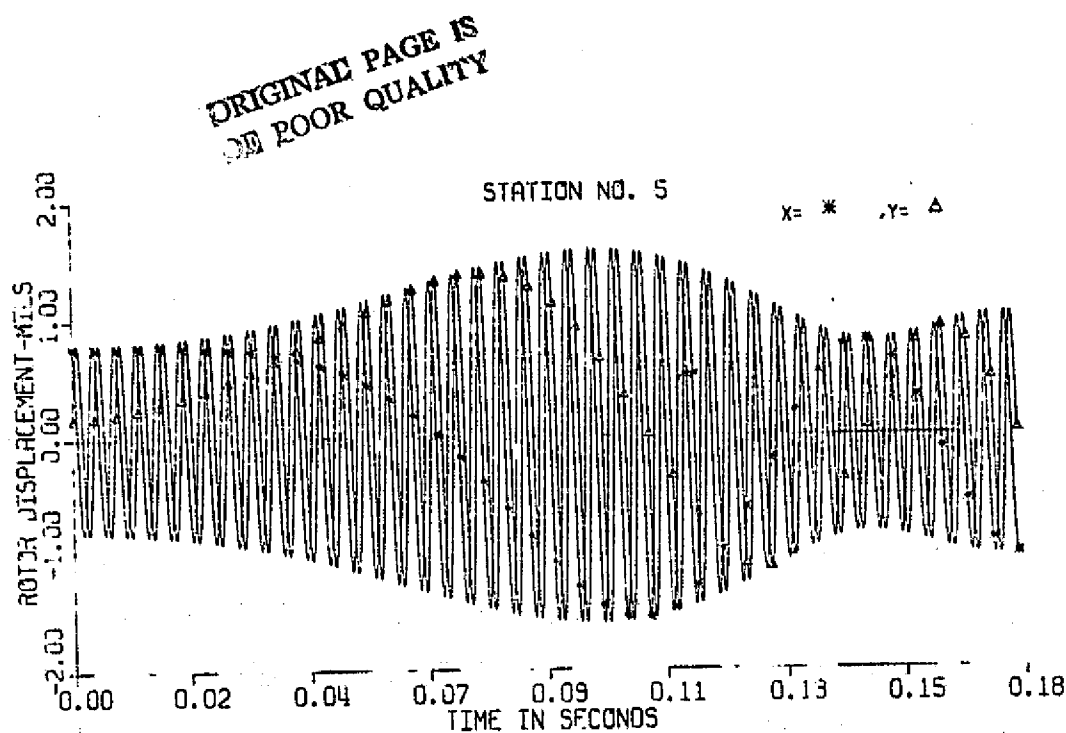


Figure 7.6 TRANSIENT MOTION AT THE PUMP BEARING

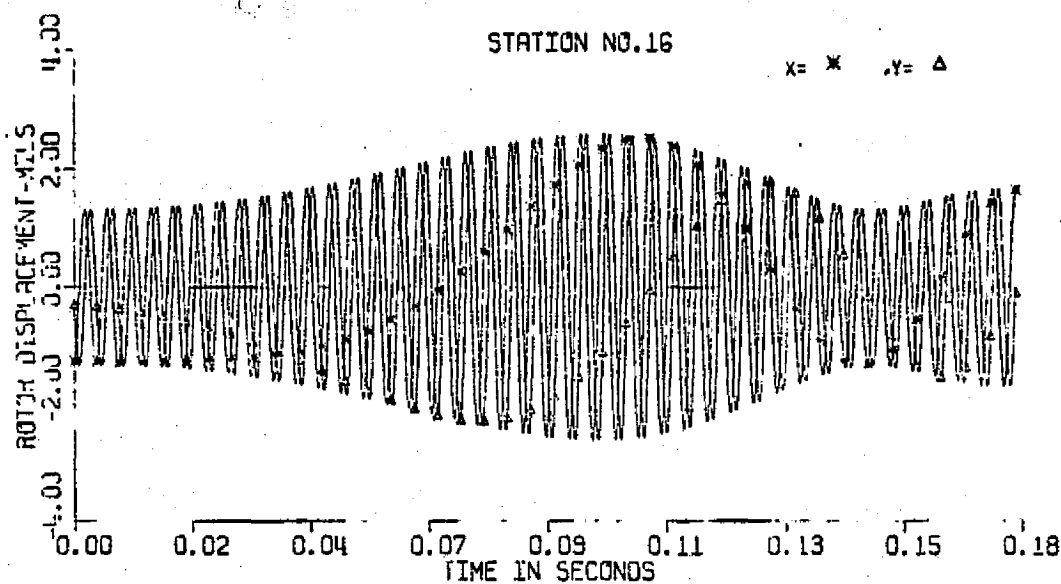
ORIGINAL PAGE IS  
POOR QUALITY

Figure 7.7 TRANSIENT MOTION AT THE TURBINE BEARING

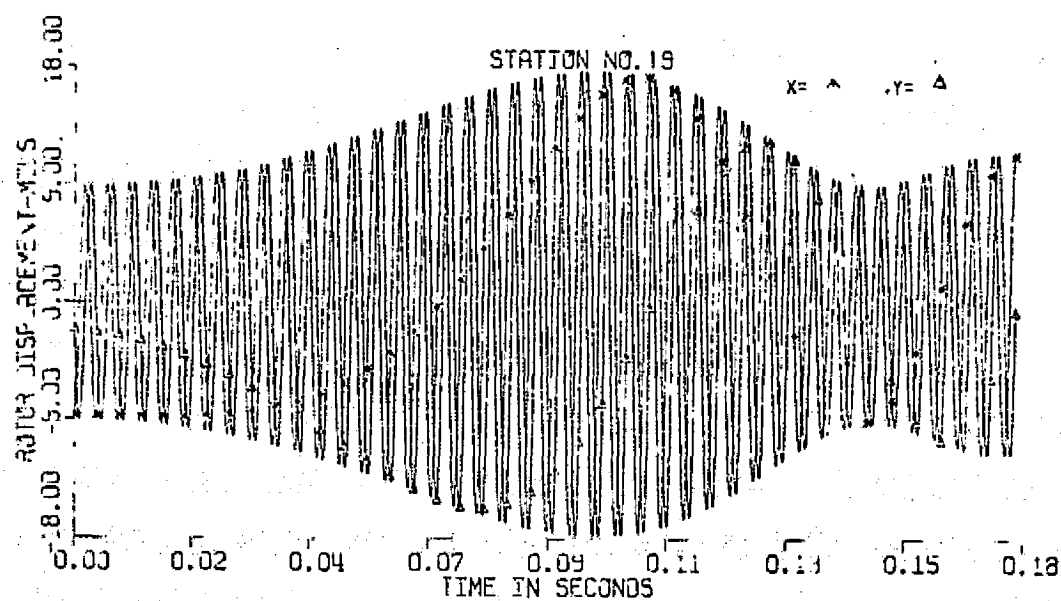


Figure 7.8 TRANSIENT MOTION AT THE SECOND SEAL LOCATION

ORIGINAL PAGE IS  
POOR QUALITY

STATION NO.22

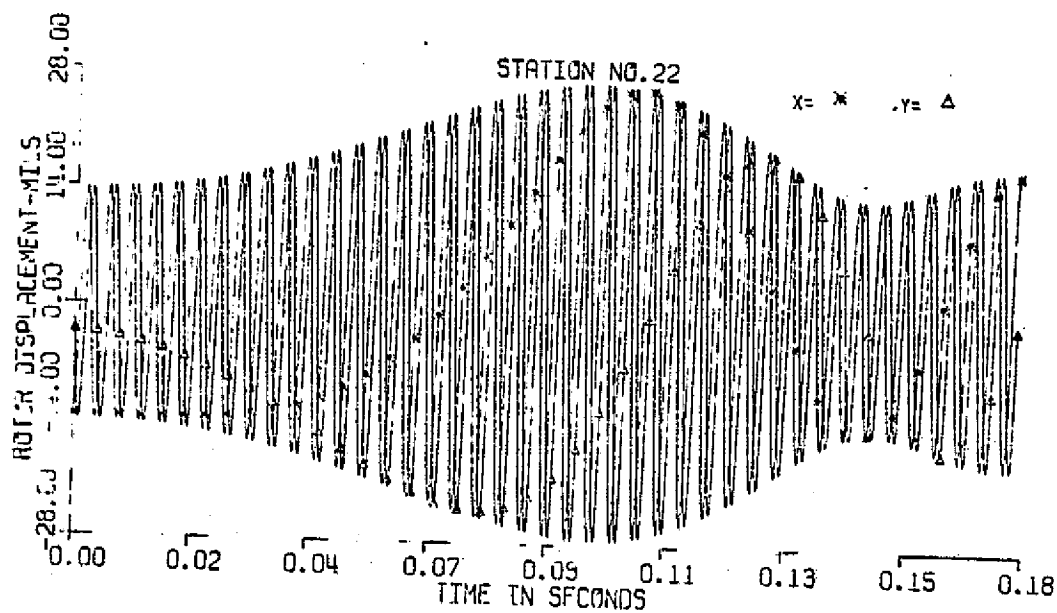
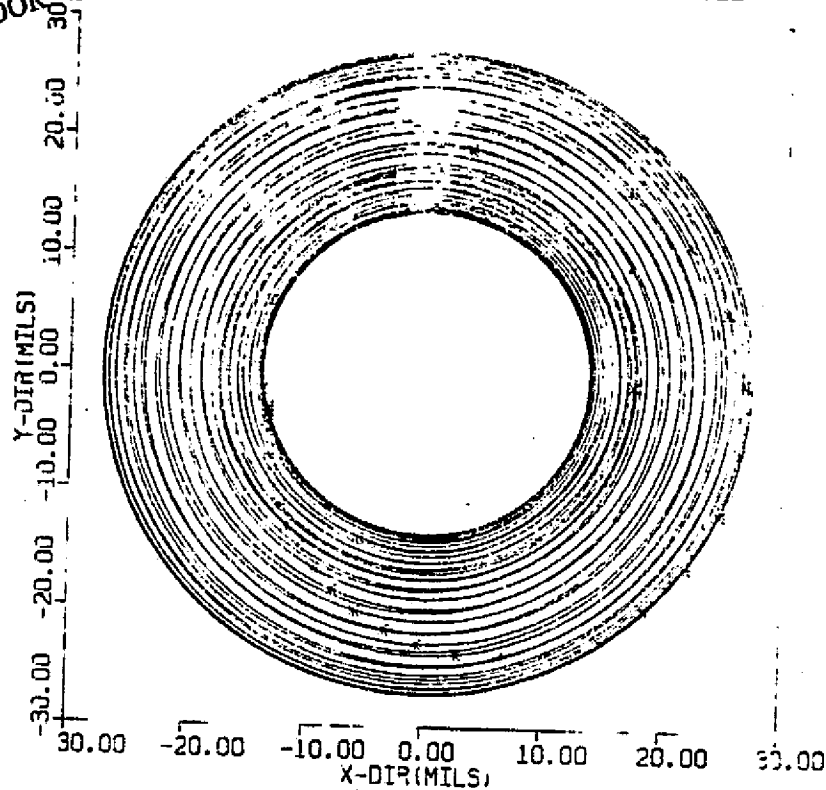


Figure 7.9 TRANSIENT MOTION AT THE TURBINE END

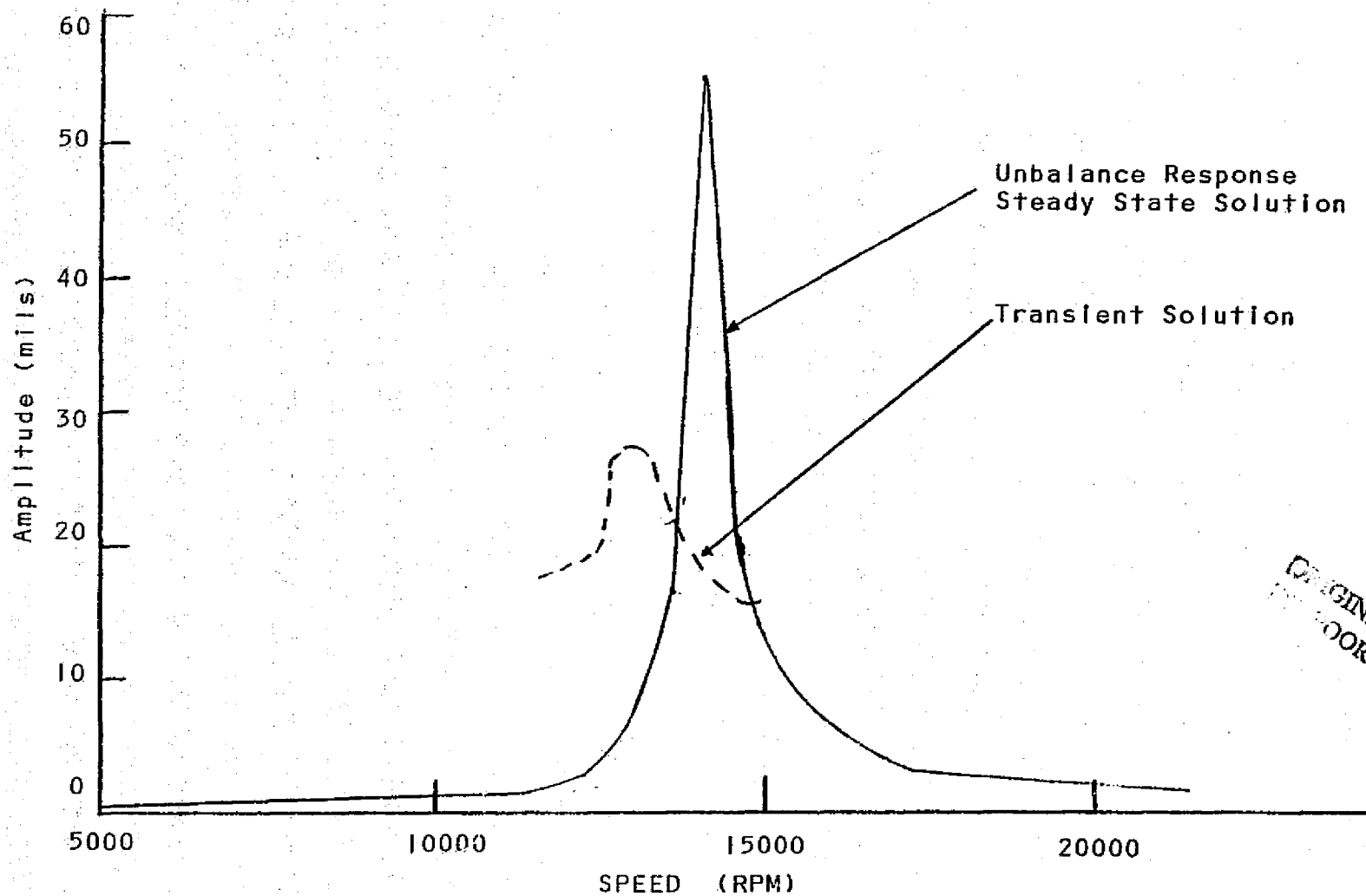


Figure 7.10 FORCED RESPONSE OF SSME-HPOTP AT THE TURBINE END

ORIGINAL PAGE IS  
OF POOR QUALITY

is now under investigation by both NASA and Rocketdyne personnel. A test program is developed to determine whether this rubbing condition will arise and whether it will affect the integrity of the operation of the pump.

## VIII. CONCLUSIONS

### 8.1 Summary and Conclusions

This analysis presents and develops a compact modal analysis which can be used to determine its results of steady state response, transeint simulation, and stability of flexible rotors on flexible supports. The transient and stability models developed included both linear and nonlinear bearing and support characterisitcs. The transient results were also presented in the form of frequency spectrum. The results and conclusions may be summarized as follows:

1. A modal method has been developed using undamped modes to approximate the dynamic behavior of rotor-bearing systems. Modal transformation of the generalized equations of motion into modal equations of motion using the undamped modes can significantly reduce the number of equations to be solved without losing the generalities of bearing cross-coupling effects and influence of gyroscopic moments. This reduction of degrees of freedom can greatly reduce the computational effort and cost and, thus, make possible the transient analysis of large, complex rotor systems.
2. The generalized equations of motion for an  $n$ -mass rotor are derived by the direct stiffness method including the effects of nonlinear bearing characteristics, shaft bow, skewed discs, rotor unbalance, and acceleration. The generalized shaft stiffness matrix is given in terms of the individual shaft sectional geometry and material properties. This procedure is more direct than the finite element type of formulation as the stiffness submatrixes are directly and uniquely given and may be easily stated for any rotor.

3. Since the shaft stiffness matrixes are completely defined for a given rotor, the shaft potential energy function  $V$  may be obtained. The ability to write an explicit formulation of the shaft elastic potential energy function thus allows one to readily derive the dynamical equations of motion of multi-level rotor systems, such as two spool gas turbines or rotors mounted in flexible casings.

4. Chapter 2 states the use of Guyan Reduction to eliminate all rotational coordinates in which rotational inertia effects are not present. This procedure is necessary for direct integration of the equations of motion.

5. The shaft mass and stiffness matrices of the system can be uncoupled using the orthonormal modes of the undamped system. The modal coupling terms result from the bearing cross coupling and damping and gyroscopic effects. The other external effects, such as shaft bow and unbalance and bearing nonlinearity can be placed in the right-hand side of the modal equations. This eliminates the formulation and storage of large blocks of shaft mass and stiffness matrices which are required in other direct integration methods.

6. Uncoupled modal analysis based on the assumption of proportional damping may further simplify the modal equations of motion, but it is often not accurate for rotor systems with seals or hydrodynamic bearings.

7. The incorporation of moderate amounts of bearing damping in the rotor system can cause a considerable shift of the rotor resonance speeds from the values predicted by the undamped critical speed calculations.



8. Damped complex eigenvalues, stability, and steady state unbalance response of the rotor system can be rapidly determined using the undamped modes which are essential for design and are relatively easy to obtain by the designers.

9. The use of modal analysis offers a new approach to balancing rotors with shaft bow and skewed disc effects. This can be achieved by equating the modal excitation by unbalance eccentricities, shaft bow, and disc skew for the particular mode that needs to be balanced.

10. The calculation of rotor peak unbalance response speed and its corresponding amplification factor using the simple single-mass equation can provide the designers good design parameters in a simple manner.

11. The accuracy of modal analysis can be improved by using a larger number of modes. As a general rule, an error of less than 5% can be achieved if mode shapes of 5 times the operating speed are incorporated into the system.

12. If a large number of modes are incorporated into the system, the use of either the average support stiffness modes or the free-free plus two rigid body modes will give very good results. When the number of modes used are restricted by computational time or cost, the use of average support stiffness modes seems to be a better selection.

13. In the transient analysis of multimass rotor by the direct integration of the point mass stations, numerical instability can occur, this problem is greatly alleviated by the modal method while reduces the number of equations of motion. The Newmark Beta

method, which is unconditionally stable at  $\beta = 1/4$ , is proven to be superior especially when nonlinear forces are presented in the system than the traditional modified Euler integration procedure.

14. The phenomenon of passing through regions of instability has been demonstrated by the stability analysis of flexible rotor-bearing models and verified by transient simulation.

15. Steady-state response information will be essential for large complex rotor simulation to avoid costly, undesired transient behavior. Zero initial conditions may be acceptable for impact unbalance studies, but instabilities due to aerodynamic excitation, internal damping, and fluid film bearings are best studied from steady state initial conditions with small perturbations.

16. The existence of non-linear support bearing forces can change the transient response motion of the system considerably from those with linear support forces. The half-whirl transient motion of the system with journal bearing supports verifies the above conclusion.

17. The use of numerical fast Fourier transformation provides a new way of interpretation of numerical transient response results. This transformation of transient motion into a frequency spectrum makes the stability analysis of nonlinear systems possible.

18. The correlation of experimental data with modal analysis not only verifies the use of modal analysis and numerical Fourier transformation, it also provides deeper understanding of the excitations of different modes and the accuracy of system simulation.

## 8.2 Suggestions for Future Research

This analysis has developed computer codes for the simulation of large, complex rotor-bearing systems. Additional design criteria can be produced from the modal method presented and will be of great interest to compressor, turbine, and jet engine manufacturers. Some areas that require further investigation are as follows:

1. With appropriate boundary conditions and mode shapes, the modal approach in predicting dynamic behavior of rotor systems can be easily expanded into the analysis of multi-level rotor systems.
2. The coupling of the corresponding axial modes into the system can make possible the analysis of rotor wrapping and torsional problems. This also provides further research in the effects of incorporating axial and rotational resisting bearings such as a balance piston.
3. The effect of squeeze film dampers on stability and transient response of the system.
4. Further extension on the use of numerical fast Fourier transformation in interpretation of transient motion.
5. The incorporation of base motion effect in the transient analysis of the system. This can be further used to simulate seismic effects on rotor-dynamic behavior such as nuclear water pumps.
6. Extensive study of the effects of change of acceleration rate to forces transmitted and transient response of the system.
7. The inclusion of thermal effects in stability and forced response analysis of the system.

8. A more extensive study of the correlation of experimental data to theoretical simulation of rotor-bearing systems.

## BIBLIOGRAPHY

## Critical Speed Analysis

1. Rankine, W. A. "On Centrifugal Force of Rotating Shaft." Engineer, London, Vol. 27, 1869.
2. Jeffcott, H. H. "The Lateral Vibration of Loaded Shafts in the Neighborhood of a Whirling Speed - The Effect of Want of Balance." Philosophical Magazine, Vol. 37, Series 5, 1919.
3. Newkirk, B. L. "Shaft Whipping." Gen. Elec. Rev., Vol. 27, 1924, pp. 169.
4. Prohl, M. Z. "A General Method for Calculating Critical Speeds of Flexible Rotors." Trans ASME, Vol. 67, 1945, Journal of Applied Mechanics, Vol. 12, P. A - 142.
5. Yamamoto, T. "On the Critical Speeds of a Shaft." Memoirs of the Faculty of Engineering, Nagaya University, Japan, November 1954.
6. Gunter, E. J., Choy, K., and Allaire, P. E. "Effects of Bearing Damping on Critical Speeds and Unbalance Response of Turbo-rotors." RLES Report No. ME76-138, University of Virginia, December 1976.
7. Choundbury, P. D., et. al. "Effect of Damping on the Lateral Critical Speeds of Rotor Bearing Systems." Trans. ASME, Journal of Engineering for Industry, Paper No. 75-DET-38.

## Stability Analysis

8. Dunkerley, S. "On the Whirling and Vibration of Shafts." Phil. Trans. A., Vol. 185, 1894.
9. Gunter, E. J. "Dynamic Stability of Rotor-Bearing System." NASA Report SP-113, 1965.
10. Lund, J. W. "The Stability of an Elastic Rotor in Journal Bearings With Flexible Damped Supports." Journal of Applied Mechanics, Trans. ASME, December 1965.
11. Lund, J. W. "Stability and Damped Critical Speeds of a Flexible Rotor in Fluid-Film Bearings." Journal of Engineering for Industry, Trans. ASME, May 1974, pp. 509-517.

12. Bansal, P. N. and Kirk, R. G. "Stability and Damped Critical Speeds of Rotor-Bearing Systems." Journal of Engineering for Industry, Paper No. 75-DET-57.
13. Choudhury, P. De, Zsolcsak, S. J., and Barth, E. W., "Effect of Damping on the Lateral Critical Speeds of Rotor-Bearing Systems." Journal of Engineering for Industry, Trans. ASME, Paper No. 75-DET-38.
14. Ruhl, R. L. and Booker, J. F. "A Finite Element Model for Distributed Parameter Turborotor Systems." Journal of Engineering for Industry, Trans. ASME, Series B, Vol. 94, No. 1, February 1972, pp. 126-132.
15. Black, H. F. "Calculation of Forced Whirlpool Stability of Centrifugal Pump Rotor System." ASME, Paper No. 73-DET-131.

#### Unbalance Response Analysis

16. Kikuchi, K. "Analysis of Unbalance Vibration of Rotating Shaft System with Many Bearings and Disks." Bulletin of ASME, Vol. 13, No. 61, pp. 864-872, June 1969.
17. Lund, J. W. and Orcutt, F. K. "Calculations and Experiments on the Unbalance Response of a Flexible Rotor." Journal of Engineering for Industry, Trans. ASME, Series B, Vol. 89, No. 4, November 1967, pp. 785-796.
18. Barrett, L., Allaire, P., and Gunter, E. "Unbalance Response of Flexible Rotors: Effect and Design of Flexible Damped Bearings." Report No. ME-543-106-74, May 1974, Department of Mechanical Engineering, University of Virginia, Charlottesville, Virginia.
19. Choy, K. and Gunter, E. J. "Unbalance Response and Modal Balancing of a Uniform Rotor." Report No. ME-543-125-75, August 1975, Department of Mechanical Engineering, University of Virginia, Charlottesville, Virginia.
20. Barrett, L. E. and Gunter, E. J. "Steady-State and Transient Analysis of a Squeeze Film Damper Bearing for Rotor Stability." NASA CR-254, May 1975.
21. Nicholas, J. C., Gunter, E. J., and Allaire, P. E. "Effect of Residual Shaft Bow on Unbalance Response and Balancing of a Single-Mass Rotor-Part 1 Unbalance Response." Journal of Engineering for Power, Trans. ASME, April 1976.
22. Nelson, H. D. and McVaugh, J. M. "The Dynamics of Rotor-Bearing System Using Finite Elements." Journal of Engineering for Industry, ASME Paper No. 75-WA/DE-19.

23. Kirk, R. G. and Gunter, E. J. "The Effect of Support Flexibility and Damping on the Synchronous Response of a Single-Mass Flexible Rotor." Journal of Engineering for Industry, Trans. ASME, February 1972.
24. Gunter, E. J. "Influence of Flexibly Mounted Rolling Element Bearings on Rotor Response-Part 1 Linear Analysis." Journal of Lubrication Technology, Trans. ASME, January 1970.
25. Rieger, N. F. "Unbalance Response of An Elastic Rotor in Damped Flexible Bearings at Supercritical Speeds." Journal of Engineering for Power, Trans. ASME, April 1971.
26. Benson, R. C. "The Dynamical Response of an Overhung, Unbalance, Skewed Rotor on Two Flexible Supports." Master Thesis, Department of Mechanical Engineering, University of Virginia, 1976.

#### Balancing of Flexible Rotors

27. Bishop, R. E. D. and Parkinson, A. G., "Vibration and Balancing of Flexible Shafts." Applied Mechanics Reviews, May 1968, pp. 439-493.
28. Thearle, E. L. "Dynamic Balancing of Rotating Machinery in the Field." Journal of Applied Mechanics, APM-56-19, 1934, pp. 745-753.
29. Black, H. F. and Nuttall, S. M. "Modal Resonance and Balancing of Synchronous Vibrations in Flexible Rotors with Nonconservative Cross Coupling." Conference on Vibrations in Rotating Machinery, Instn. Mechanical Engineering, September 1976, pp. 151-158.
30. Lund, J. W. and Tonnesen, J. "Analysis and Experiments on Multi-Plane Balancing of a Flexible Rotor." Journal of Engineering for Industry, Trans. ASME, Paper No. 71-WDT-74.
31. Lund, J. W. "A Method for Using the Free Shaft Modes in Rotor Balancing." Conference on Vibrations in Rotating Machinery, Instn. Mechanical Engineering, September 1976, pp. 65-72.
32. Nicholas, J. C., Gunter, E. J., and Allaire, P. E. "Effect of Residual Bow on Unbalance Response and Balancing of a Single-Mass Rotor-Part 1 Balancing." Journal of Engineering for Power, Trans. ASME, April 1976.

#### Transient Response Analysis

33. Kirk, R. G. and E. J. Gunter. "Transient Response of Rotor-Bearing Systems." Journal of Engineering for Industry, Trans. ASME, May 1974.
34. Shen, F. A., "Transient Flexible Dynamic Analysis-Part 1 Theory." Journal of Engineering for Industry, May 1972.

35. Breed, D. and Castelli, V. "Time Transient Approach to the Solution of Shaft Dynamic Problems." Columbia University Ph.D. Dissertation, 1970.
36. Falkenhagen, G. L. and Gunter, E. J. "Non-Linear Transient Analysis of a Rigid Rotor Supported by Non-Circular Bearing." NASA Report NGR-47-005-050, Report No. ME-4040-102-70U, Department of Mechanical Engineering, University of Virginia.
37. Hitching, D. and Dance, S. H. "Response of Nuclear Structural Systems to Transient and Random Excitations Using Both Deterministic and Probabilistic Methods." Nuclear Engineering and Design 29 (1974), pp. 311-337.
38. Kirk, R. G. and Gunter, E. J. "Nonlinear Transient Analysis of Multi-mass Flexible Rotors" RLES Report No. ME-4040-112-72U, University of Virginia, June 1, 1972.

#### Modal Transient Analysis

39. Foss, K. "Co-Ordinates Which Uncouple the Equations of Motion of Damped Linear Dynamic Systems." Journal of Applied Mechanics, Trans. ASME, September 1958.
40. Childs, D. W. "A Rotor-Fixed Modal Simulation Model for Flexible Rotating Equipment." Journal of Engineering for Industry, Trans. ASME, Series B, Vol. 96, No. 2, May 1974, pp. 459-669.
41. Childs, D. "A Modal Transient Simulation Model for Flexible Asymmetric Rotors." Journal of Engineering for Industry, Trans. ASME, Paper No. 75-DET-34.
42. Childs, D. W. "Two Jeffcott-Based Modal Simulation Models for Flexible Rotating Equipment." Journal of Engineering for Industry, ASME Paper No. 74-WA/DE-17.
43. Childs, D. W. "Transient Rotor Dynamic Analysis for the Space Shuttle Main Engine High-Pressure Oxygen Turbopump." Journal of Space Craft, Vol. 12, No. 1, January 1975.
44. Childs, D. W. "SSME Turbopump Technology Improvements Via Transient Rotor Dynamic Analysis." NASA Report Contract No. NAS8-31233, December 1975.
45. Dennis, A. J., Erisksson, R. H., and Seitelman, L. H. "Transient Response Analysis of Damped Rotor System by the Normal Mode Method." ASME Paper No. 75-GT-58.
46. Kirk, R. G. and Hibner, D. H. "A Note on Blade Loss Dynamics of Rotor Bearing Systems." ASME Paper No. 75-DET-56.



47. Black, H. F. and Nuttall, S. M. "Modal Resolution and Balancing of Synchronous Vibrations in Flexible Rotors with Non-Conservative Cross Coupling." Conference on Vibrations in Rotating Machinery, Instn. Mechanical Engineering, September 1976, pp. 263-278.
48. Parkinson, A. G. "The Modal Interpretation of the Vibration of a Damped Rotating Shaft." Conference on Vibrations in Rotating Machinery, Instn. Mechanical Engineering, September 1976, pp. 263-278.
49. Black, H. F. "Calculation of Forced Whirling and Stability of Centrifugal Pump Rotor Systems." Journal of Engineering for Industry, Trans. ASME; Paper No. 73-DET-131.
50. Nelson, F. C. "Shock and Seismic Excitation of Mechanical Equipment." ASME Paper No. 74-DE-3.
51. Lund, J. W. "Modal Response of a Flexible Rotor in Fluid Film Bearings." Journal of Engineering for Industry, Trans. ASME, May 1974.
52. Morton, P. G. "Analysis of Rotors Supported Upon Many Bearings." Journal of Mechanical Engineering Science, Vol. 14, No. 1, 1972.
53. Klosterman, A. L. "On the Experimental Determination and Use of Modal Representations of Dynamic Characteristics." Ph.D. Thesis, University of Cincinnati, 1971.
54. Caughey, T. K. and O'Kelly, M. E. J. "Classical Normal Modes in Damped Linear Dynamic Systems." Journal of Applied Mechanics, Trans. ASME, September 1965.
55. Choy, K., Gunter, E. J., Barrett, L. E., and Allaire, P. E. "Transient and Stability Analysis Using the Modal Method." RLES Report No. UVA1464761/ME76/137, University of Virginia, December 1976.

#### Lubrication Analysis

56. Leader, M. E., et al., "The Experimental Dynamic Response of a Single Mass Rotor in 3 different Bearings", Report No. UVA/464761/ME76/141, December 1976, University of Virginia.
57. Poritsky, H. "Contribution to the Theory of Oil Whip." Trans. ASME, 1953.
53. Lund, J. W. "Self-Excited, Stationary Whirl Orbits of a Journal in a Sleeve Bearing." Ph. D. Thesis, Rensselaer Polytechnic Institute, 1966.
59. Myrick, S. T., Jr. and Rylander, H. G. "Analysis of Flexible Rotor Whirl and Whip Using a Realistic Hydrodynamic Journal Bearing Model." Trans. ASME, Journal of Engineering for Industry, Paper No. 75-DET-68.

60. Childs, D., Moes, H., and Leeuwen, H. Van. "Journal Bearing Impedance Description for Rotordynamic Applications," Journal of Lubrication Technology, Trans. ASME Paper, April 1977, pp. 88 - 214.
61. Kirk, R. and Gunter, E. J. "Transient Journal Bearing Analysis." NASA Report No. CR-154, June 1970.

#### Numerical Integration Procedures

62. Fu, C. C. "A Method for the Numerical Integration of the Equations of Motion Arising from a Finite Element Analysis." Journal of Applied Mechanics, Trans. ASME, September 1970.
63. Durham, R. S., Nickell, R. E., and Stickler, D. C. "Integration Operators for Transient Structural Response. Computers & Structures, Vol. 2, pp. 1-15, Pergamon Press, 1972.
64. Stricklin, J. A. and Haisler, W. E. "Survey of Solution Procedures for Nonlinear Static and Dynamics Analyses." Proc. of International Conference on Vehicle Structural Mechanics Finite Element Application to Vehicle Design, SAE, 1974, pp. 1-17.
65. Nickell, R. E. "Nonlinear Dynamics by Modal Superposition." Presented at the AZAA/ASME/SAE 15th Structures, Structural Dynamics and Materials Conference, Las Vegas, Nevada, April 1974.
66. Nickell, R. E. "Direct Integration Methods in Structural Dynamics." J. Engineering Mechanics Division, ASCE99 (1973), pp. 303-317.

#### General References

67. Hurty, W. C. and Rubinstein, M. F. "Dynamics of Structures." Prentice Hall, 1967.
68. Pestel, E. C. and Leckie, F. A. "Matrix Methods in Elasto-mechanics, McGraw Hill, New York, 1963.
69. Hildebrand, F. B. "Advanced Calculus for Application." Prentice-Hall, 1962.
70. Barnett, S. and Storey, C. "Matrix Methods in Stability Theory." Barnes & Noble, Inc., New York, 1970.
71. Wilkinson, J. H. "The Algebraic Eigenvalue Problem." Oxford University Press, 1965.

72. Acton, F. S. "Numerical Methods That Work." Harper & Row Publishers, New York, 1970.
73. Sneddon, I. N. "The Use of Integral Transforms." McGraw-Hill Publisher, 1974.
74. Thompson, W. T. "Theory of Vibration with Applications." Prentice-Hall, Inc., 1972.
75. Tondl, A. "Some Problems of Rotor Dynamics." Chapman & Hall, London, 1965.

#### Fast Fourier Transformation

76. Cooley, J. W., Lewis, P. A., and Welch, P. D. "Application of the Fast Fourier Transformation to Computation of Fourier Integrals, Fourier Series, and Convolution Integrals." IEEE Trans. Vol. AU-15, No. 2, June 1967.
77. Stearns, S. D. "Digital Signal Analysis." Hayden Book Company, Inc., New Jersey, 1975.
78. Rabiner, L. R. and Rader, C. M. "Digital Signal Processing." IEEE Press, 1972.

APPENDIX ADisc Rotational Equations of Motion - Langrangian Approach

Consider a massive disc attached to a massless shaft with

- $\phi$  = precession angle about z-axis
- $\theta$  = inclination of the shaft away from z-axis
- $\Omega$  = rotation about the axis of the shaft

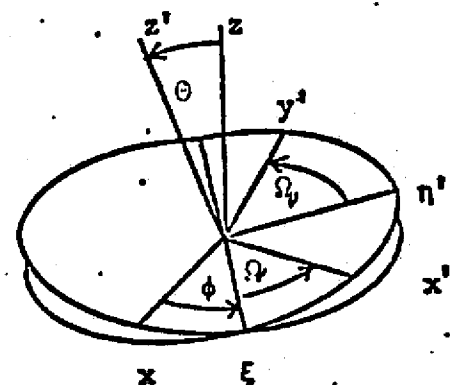
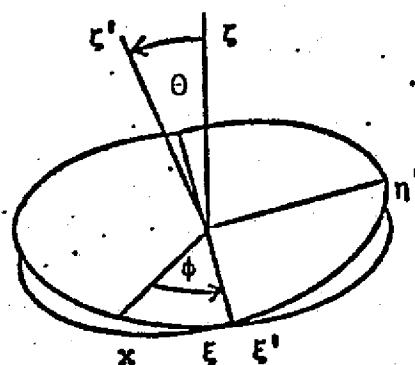
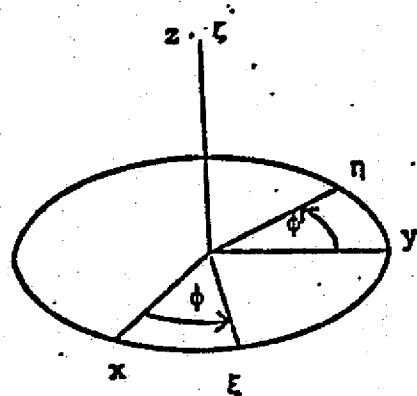
The rotation of the disc can be described by standard Euler angles, however, it is shown later in the section that small deflections may be replaced by more physically obvious angles,  $\theta$  and  $\psi$ .  $\theta$  is the inclination of the shaft away from z-axis projected into the x-z plane.  $\psi$  is a similar projection into the y-z plane.

Considering only the rotational effects of the disc, it is not immediately obvious how rotation can be represented by the  $\theta$  and  $\psi$  coordinates. In order to apply the Euler angles  $\phi$ ,  $\theta$ , and  $\Omega$ , the following transformations are necessary.

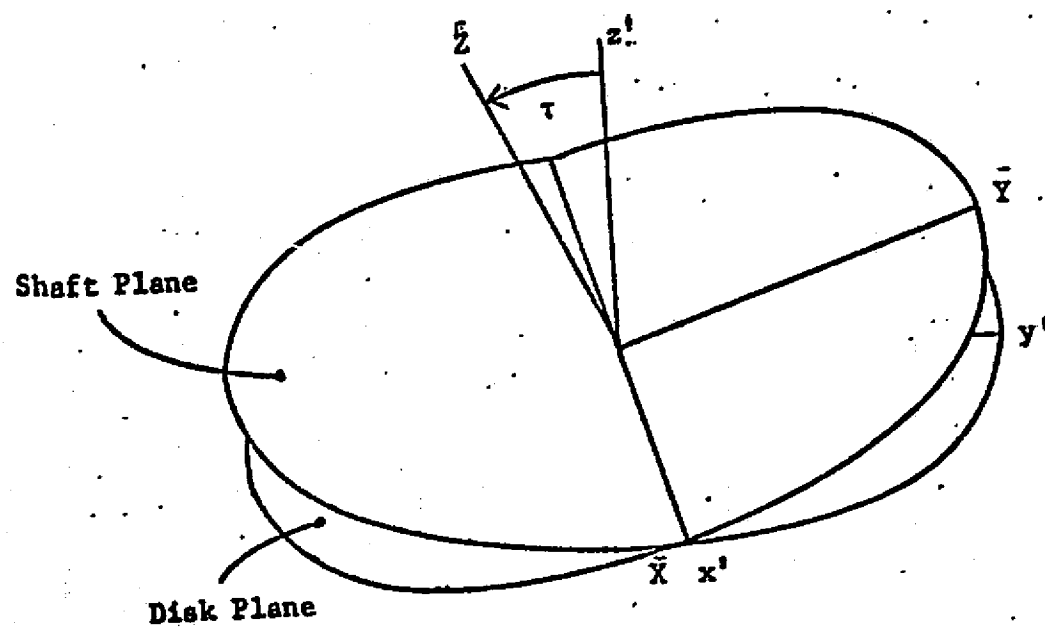
$$\begin{aligned} \begin{Bmatrix} \xi \\ \eta \\ \phi \end{Bmatrix} &= \begin{bmatrix} \cos \phi & \sin \phi & 0 \\ -\sin \phi & \cos \phi & 0 \\ 0 & 0 & 1 \end{bmatrix} \begin{Bmatrix} x \\ y \\ z \end{Bmatrix} \\ \begin{Bmatrix} \xi' \\ \eta' \\ \phi' \end{Bmatrix} &= \begin{bmatrix} 1 & 0 & 0 \\ 0 & \cos \theta & \sin \theta \\ 0 & -\sin \theta & \cos \theta \end{bmatrix} \begin{Bmatrix} \xi \\ \eta \\ \phi \end{Bmatrix} \\ \begin{Bmatrix} x' \\ y' \\ z' \end{Bmatrix} &= \begin{bmatrix} \cos \Omega & \sin \Omega & 0 \\ -\sin \Omega & \cos \Omega & 0 \\ 0 & 0 & 1 \end{bmatrix} \begin{Bmatrix} \xi' \\ \eta' \\ \phi' \end{Bmatrix} \end{aligned}$$

ORIGINAL PAGE IS  
OF POOR QUALITY

# Disk Rotation



# Permanent Skew



ORIGINAL PAGE IS  
OF POOR QUALITY

The physical rotational transformation is given in Figure A.1.

In addition to these rotations, the permanent skew of the disc,  $\tau$ , can also be represented by a fourth transformation

$$\begin{Bmatrix} \bar{x} \\ \bar{y} \\ \bar{z} \end{Bmatrix} = \begin{bmatrix} 1 & 0 & 0 \\ 0 & \cos \tau & \sin \tau \\ 0 & -\sin \tau & \cos \tau \end{bmatrix} \begin{Bmatrix} x' \\ y' \\ z' \end{Bmatrix}$$

where  $\tau$  is in the opposite direction of  $\theta$  and  $\psi$  in the  $x$ - $z$  and  $y$ - $z$  plane as given in Figure A.2. Note that the  $xyz$  (inertia) frame is fixed in space while the  $x'y'z'$  (shaft) frame is fixed with the end of shaft, and  $\bar{x}\bar{y}\bar{z}$  (disc) frame is fixed with the disc.

Using Euler angles, the angular rotation of the disc can be given by

$$\begin{aligned} \omega &= \dot{\phi} \hat{n}_{\phi} + \dot{\theta} \hat{n}_{\theta} + \dot{\Omega} \hat{n}_{\Omega} \\ &= (\dot{\theta} \cos \Omega + \dot{\phi} \sin \theta \sin \Omega) \hat{n}_x \\ &\quad + (-\dot{\theta} \sin \Omega + \dot{\phi} \sin \theta \cos \Omega) \hat{n}_y \\ &\quad + (\dot{\Omega} + \dot{\phi} \cos \theta) \hat{n}_z \\ &= \omega_1 + \omega_2 + \omega_3 \end{aligned}$$

The moment of inertia matrix in the disc frame is

$$[\bar{I}]_{\bar{x}\bar{y}\bar{z}} = \begin{bmatrix} I_t & 0 & 0 \\ 0 & I_t & 0 \\ 0 & 0 & I_p \end{bmatrix}$$

ORIGINAL PAGE IS  
OF POOR QUALITY

and in shaft frame

$$[I]_{x'y'z'} = \begin{bmatrix} I_t & 0 & 0 \\ 0 & I_t \cos^2 \tau + I_p \sin^2 \tau & (I_t - I_p) \sin \tau \cos \tau \\ 0 & (I_t - I_p) \sin \tau \cos \tau & I_t \sin^2 \tau + I_p \cos^2 \tau \end{bmatrix}$$

The kinetic energy due to rotation is

$$\begin{aligned} T_R &= \frac{1}{2} \begin{Bmatrix} \dot{\omega} \end{Bmatrix}^T [I]_{x'y'z'} \begin{Bmatrix} \dot{\omega} \end{Bmatrix} \\ &= \frac{1}{2} \omega_1^2 I_t + \frac{1}{2} (\omega_2^2 I_t + \omega_3^2 I_p) \cos^2 \tau + \frac{1}{2} (\omega_2^2 I_p + \omega_3^2 I_t) \sin^2 \tau \\ &\quad + \omega_2 \omega_3 (I_t - I_p) \cos \tau \sin \tau \end{aligned}$$

Assume that  $\tau$  is small and linearized by

$$\cos \tau = 1$$

$$\sin \tau = \tau$$

$$\sin^2 \tau = 0$$

and the kinetic energy expression reduces to

$$T_R = \frac{1}{2} (\omega_1^2 + \omega_2^2) I_t + \frac{1}{2} I_p \omega_3^2 + \tau (I_t - I_p) \omega_2 \omega_3$$



Also using the small angle approximation to

$$\cos \theta \approx 1 - \frac{\theta^2}{2}$$

$$\sin \theta \approx \theta$$

Then

$$\begin{aligned} T_R = & \frac{1}{2} I_t (\dot{\theta}^2 + \dot{\phi}^2 + \dot{\Omega}^2) + \frac{1}{2} I_p (\dot{\Omega} + \dot{\phi}) (\dot{\Omega} + \dot{\phi} - \dot{\phi} \theta^2) \\ & + \tau (I_t - I_p) (\dot{\Omega} + \dot{\phi}) (\dot{\phi} \cos \Omega - \dot{\Omega} \sin \Omega) \end{aligned}$$

Also, the Euler angles can be transformed into the generalized coordinates by the small angle approximations as the inclination projection of the shaft can be represented by

$$\theta = \Theta \cos \phi$$

$$\psi = \Theta \sin \phi$$

For small  $\Theta$ , the angle  $\phi$  and  $\Omega$  almost lie in the same plane and can be approximated as

$$\phi + \Omega = \omega t + \beta + \pi$$

where  $\beta$  is the angle between the maximum disc skew and the shaft reference mark.

Using the above relationship, the following identities exists

$$\Theta^2 = \theta^2 + \psi^2$$

$$\Theta^2 \dot{\phi} = \theta \dot{\psi} + \dot{\theta} \psi$$

$$\dot{\Theta}^2 + \Theta^2 \dot{\phi}^2 = \dot{\theta}^2 + \psi^2$$

$$\Theta \dot{\phi} \cos \Omega - \dot{\Theta} \sin \Omega = \dot{\theta} \sin (\omega t + \beta) - \dot{\psi} \cos (\omega t + \beta)$$

and using this expression, the kinetic energy can be written as

$$\begin{aligned} T_R = & \frac{1}{2} \omega^2 I_p + \frac{1}{2} I_t (\dot{\theta}^2 + \dot{\psi}^2) + \frac{1}{2} \omega I_p (\dot{\theta} \psi - \dot{\psi} \theta) \\ & + \tau \omega (I_p - I_t) (\dot{\psi} \cos (\omega t + \beta) - \dot{\theta} \sin (\omega t + \beta)) \end{aligned}$$

From Lagrange's equation,

$$\frac{d}{dt} \left( \frac{\partial T_R}{\partial \dot{\theta}} \right) - \frac{\partial T_R}{\partial \theta} = 0$$

the  $\theta$  equation becomes

$$\begin{aligned} I_t \ddot{\theta} + \omega I_p \dot{\psi} + \frac{1}{2} \omega I_p \psi = & \tau (I_p - I_t) [\omega^2 \cos (\omega t + \beta) \\ & + \dot{\omega} \sin (\omega t + \beta)] + F_\theta \end{aligned}$$

and the  $\psi$  equation

$$\begin{aligned} I_t \ddot{\psi} - \omega I_p \dot{\theta} - \frac{1}{2} \omega I_p \theta = & \tau (I_p - I_t) [\omega^2 \sin (\omega t + \beta) \\ & - \dot{\omega} \cos (\omega t + \beta)] + F_\psi \end{aligned}$$

ORIGINAL PAGE IS  
OF POOR QUALITY

## APPENDIX B

## BASIC EQUATIONS OF MOTION FOR A BOW SHAFT

The effects of shaft mechanical bow can be easier to understand by the study on a simple rotor-bearing system. A three-mass rotor with spring and damper supports given as in Figure B1 is used as an example. The equations of motion of the system can be written as follows

$$\begin{aligned}
 & \begin{bmatrix} M_1 & 0 & 0 \\ 0 & M_2 & 0 \\ 0 & 0 & M_3 \end{bmatrix} \begin{Bmatrix} \dot{x}_1 \\ \dot{x}_2 \\ \dot{x}_3 \end{Bmatrix} + \begin{bmatrix} C_1 & 0 & 0 \\ 0 & 0 & 0 \\ 0 & 0 & C_3 \end{bmatrix} \begin{Bmatrix} \dot{x}_1 \\ \dot{x}_2 \\ \dot{x}_3 \end{Bmatrix} \\
 & + \begin{bmatrix} K_1 & 0 & 0 \\ 0 & 0 & 0 \\ 0 & 0 & K \end{bmatrix} \begin{Bmatrix} x_1 \\ x_2 \\ x_3 \end{Bmatrix} + \frac{3EI}{L^3} \begin{bmatrix} k_2 & -1 & k_2 \\ -1 & 2 & -1 \\ k_2 & -1 & k_2 \end{bmatrix} \begin{Bmatrix} w_1 \\ w_2 \\ w_3 \end{Bmatrix} \\
 & = \begin{Bmatrix} F_1(t) \\ F_2(t) \\ F_3(t) \end{Bmatrix} \tag{B.1}
 \end{aligned}$$

where

$$w = x - x_d$$

$x$  = total displacement of shaft

$x_d$  = mechanical bow of shaft

Or equation (C.1) can be written as

$$M\dot{x}' + C\dot{x} + K_D x + K_W x = K_W x_d + F(t) \tag{B.2}$$

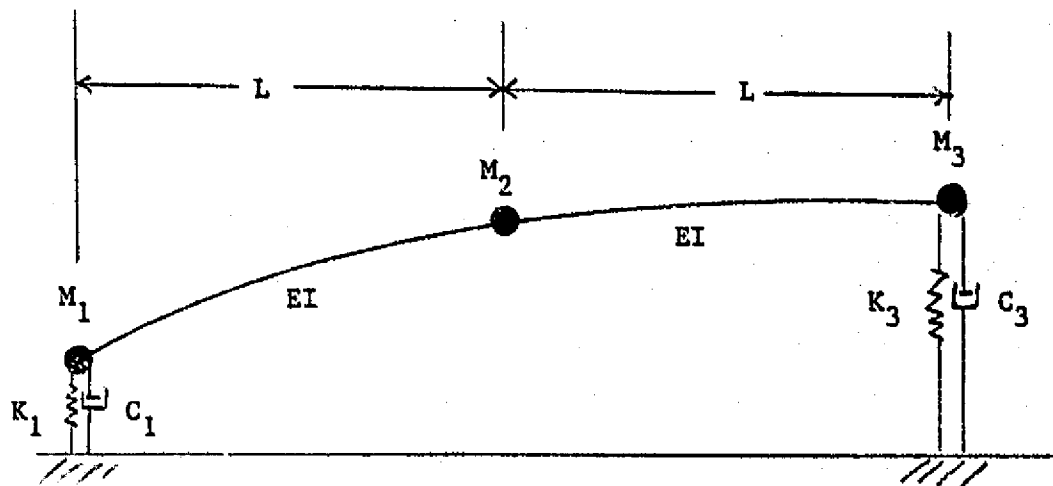


Figure B.1 Simple Three-Mass Uniform Rotor Model

ORIGINAL PAGE IS  
OF POOR QUALITY

where  $K_w x_d$  is the shaft bow effect of the system. This effect can be put into the right-hand side of the equation and considered as part of the driving force of the system.

For using the modal analysis, the undamped modes  $\{\phi_j\}$  are calculated by solving the homogeneous matrix equation of

$$M\ddot{x} + \{K_b + K_w\} x = 0 \quad (B.3)$$

Let

$$\{x\} = \sum_{j=1}^n A_j \{\phi_j\} \quad (B.4)$$

then

$$\begin{aligned} [M] \sum_{j=1}^n \ddot{A}_j \{\phi_j\} + [C] \sum_{j=1}^n \dot{A}_j \{\phi_j\} + [K] \sum_{j=1}^n A_j \{\phi_j\} \\ = [K_w] \{x_d\} + \{F(t)\} \end{aligned} \quad (B.5)$$

Premultiply equation (B.5) by  $\{\phi_i\}^T$  and using the orthogonality conditions derived in Chapter 3, the following equation results

$$M_i \ddot{A}_i + \sum_{j=1}^n C_{ij} \dot{A}_j + \omega_i^2 A_i = \{\phi_i\}^T \left\{ [K_w] \{x_d\} + \{F(t)\} \right\} \quad (B.6)$$

APPENDIX C INTEGRATION PROCEDURES

Initial conditions provide  $\dot{y}_n, y_n$ . From equations of motion calculate  $\ddot{y}_n$

## 1. Starting conditions (using Modified Euler)

$$\dot{y}_{n+1}^{(1)} = \dot{y}_n + \Delta t \ddot{y}_n$$

$$y_{n+1}^{(1)} = y_n + \frac{\Delta t}{2} (\dot{y}_{n+1}^{(1)} + \dot{y}_n)$$

Calculate  $\ddot{y}_{n+1}$  from equations of motion

$$\ddot{y}_{n+1}^{(1)} = F(t) - [C] \dot{y}_{n+1}^{(1)} - [k] y_{n+1}^{(1)}$$

## 2. Iterative procedure (Newmark Beta method)

$$\dot{y}_{n+1}^{(p+1)} = \dot{y}_n + \frac{\Delta t}{2} (\dot{y}_{n+1}^{(p)} + \dot{y}_n)$$

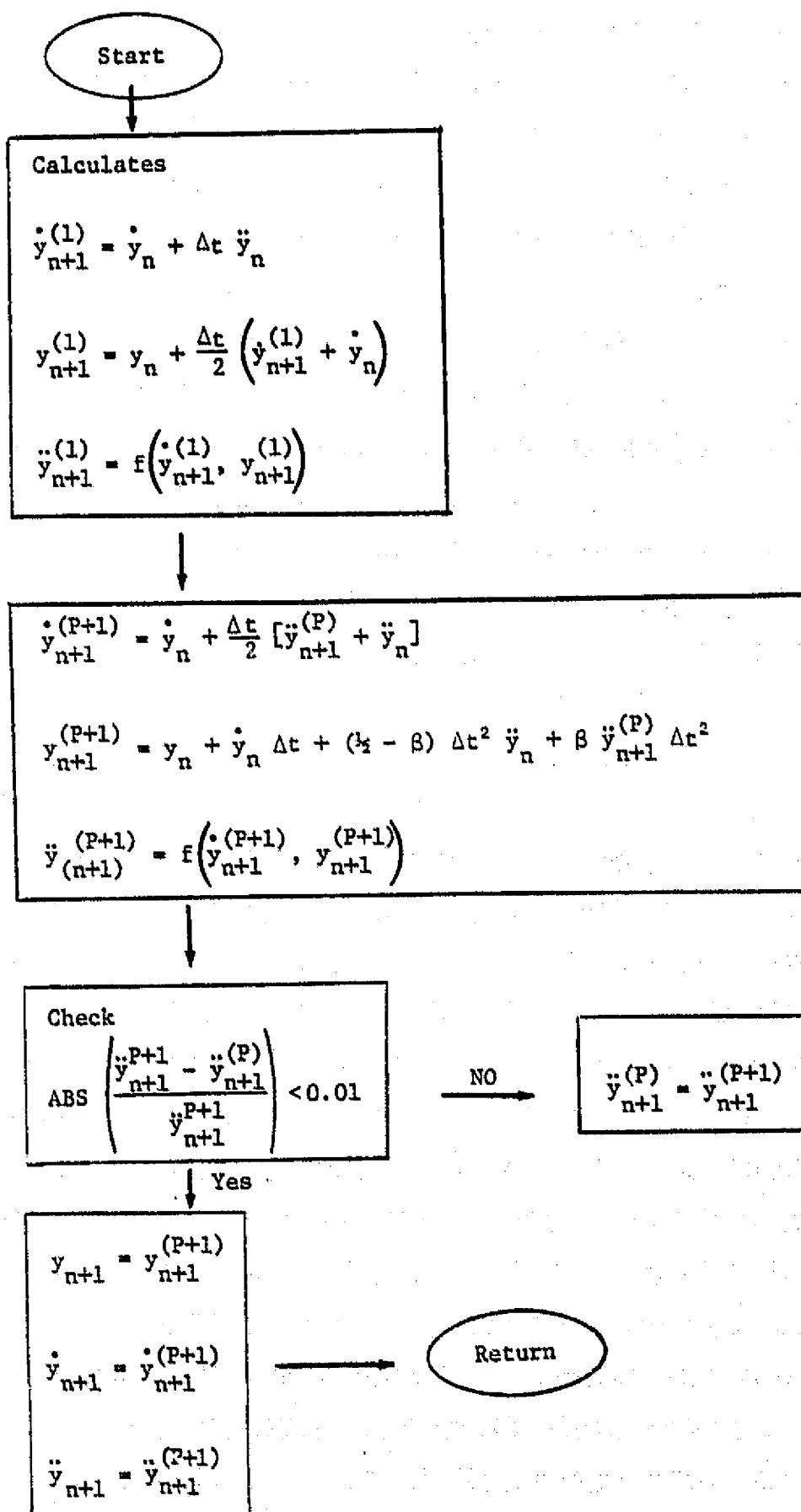
$$y_{n+1}^{(p+1)} = y_n + \dot{y}_n \Delta t + (\frac{1}{2} - \beta) (\Delta t)^2 [\ddot{y}_n] + \beta \ddot{y}_{n+1}^{(p)} \Delta t^2$$

Then

$$\ddot{y}_{n+1}^{(p+1)} = F(t) - [C] \dot{y}_{n+1}^{(p+1)} - [k] y_{n+1}^{(p+1)}$$

ORIGINAL PAGE IS  
OF POOR QUALITY

# FLOWCHART FOR NUMERICAL INTEGRATION



**APPENDIX D****INPUT INSTRUCTIONS AND LISTING  
OF COMPUTER PROGRAM MODAL 1**



The special features of computer program Modal 1 can be listed as follows:

1. Calculation of undamped critical speeds of rotor-bearing systems using matrix transfer method
  - 1.1 with linear spring stiffness
  - 1.2 maximum of 100 mass stations and 10 bearings
  - 1.3 with or without the effects of transverse moment of inertia
  - 1.4 calculates normalized and orthonormal rotational and translational mode shapes
2. Stability and damped natural frequency analysis using the undamped modes
  - 2.1 damped critical speed calculations with two dimensional bearings (8 bearing coefficients)
  - 2.2 includes effects of moment resisting bearings (32 bearing coefficients)
  - 2.3 amplification factors and peak response speed from single mass theory
  - 2.4 damped three-dimensional mode shapes of the system
3. Steady state unbalance response of the system
  - 3.1 effects of mass unbalance
  - 3.2 effects of shaft bow
  - 3.3 effects of disc skew
  - 3.4 effects of external force
  - 3.5 gyroscopic effects

3.6 results are tabulated in response vs speed and also in terms of elliptical orbits

4. Transient response analysis of the system

4.1 effects of unbalance

4.2 effects of disc skew

4.3 effects of shaft bow

4.4 effects of nonlinear bearing forces (using hydrodynamic bearing theory)

4.5 effects of rotor acceleration

4.6 plots of transient orbits and transient vs time plots

4.7 choice of initial conditions (zero or steady state with small perturbation)

## INPUT INSTRUCTIONS FOR PROGRAM MODAL 1

1. Read 3 comment cards (1 to 80 columns)
2. N, NB,>NNLIN, NMB, NF, NU, NS, NBOW, ISTAB, IMODE, ISKU, NUFPT  
(12I5)

N = No. of mass stations (max. 100)

NB = No. of regular linear bearings (max. 10)

NNLIN = No. of nonlinear bearings (max. 5)

NMB = No. of coment resisting bearings (32 coeff.) (e.g.  
balance piston) (max. 3)

NF = No. of external force (max. 10)

NU = No. of unbalance (max. 10)

NS = No. of skewed disc (max. 10)

NBOW = 1 bow shaft (Input shaft bow data)  
= 0 no shaft bow

ISTAB = 0 calculates stability  
= 1 no calculation

IMODE = No. of damped mode shapes desired (if = 0) no mode  
shape calculation

ISKU = 0 calculates unbalance response  
= 1 no calculation

NUFPT = No. of station need to printout for unbalance  
response analysis (max. 10)

3. ISKIP, NSTEP, NCYCLE, NITP, NINT, NPLOT, NORBIT, NTIME, NSPEED,  
NINC, NOPT, NT (12I5)

ISKIP = 0 calculates transient orbit

= 1 no calculation

NSTEP = No. of steps of integration per cycle

NCYCLE = No. of cycles (NSTEP\*NCYCLE < 4000)

NITP = No. of steps per printout

NINT = 1 Newark -  $\beta$  intergration (with iteration)

= 2 Euler integration

NPLOT = 0 plots of transient desired

= 1 no plots

NORBIT = No. of transient orbit stations desired to be  
plotted (=NT)

NTIME = No. of stations to be plotted in response vs time  
curve (=NT)

NSPEED = 0

NINC = 0 input initial condition

= 1 initial conditions from steady state orbit with small  
perturbation

NOPT = 0

NT = no. of station for transient printout (max. 10)

4. LLBD (J), J = 1, NB (10I5) Skip (4) and (5) if NB = 0 Bearing  
location station numbers.

5.  $K_{xx}(J)$ ,  $K_{xy}(J)$ ,  $K_{yx}(J)$ ,  $K_{yy}(J)$ ,  $C_{xx}(J)$ ,  $C_{xy}(J)$ ,  $C_{yx}(J)$   
 $C_{yy}(J)$  (8G10.3) NB Cards  
(Bearing Coefficient) (skip if NB = 0)

6. LLNB(J), NLB(J), VIS(J), ANR(J), ANL(J), ANC(J), J = 1,>NNLIN  
(skip if>NNLIN = 0) (2I5, 4G10.2)

LLNB(J) = station no. of Jth nonlinear bearings

NLB(J) = bearing no. of Jth nonlinear bearings

VIS(J) = viscosity of lubricant (lb/in<sup>2</sup>)

ANR(J) = radius of Jth bearing (in)

ANL(J) = length of Jth bearing (in)

ANC(J) = clearance of Jth bearing (in)

\*A linear bearing station must be assigned to a nonlinear bearing even with zero linear stiffness and damping.

7. LLNB(J), J = 1, NMB (3I5) (skip 7 and 8 if NMB = 0)

LLNB(J) = Station no. of the Jth moment resisting bearing

8. NMB sets of card, each set 4 cards (8G10.3)

$Bk_{xx}, Bk_{x\theta}, Bk_{xy}, Bk_{x\psi}, Bc_{xx}, Bc_{x\theta}, Bc_{xy}, Bc_{x\psi}$

$Bk_{\theta x}, Bk_{\theta\theta}, Bk_{\theta y}, Bk_{\theta\psi}, Bc_{\theta x}, Bc_{\theta\theta}, Bc_{\theta y}, Bc_{\theta\psi}$

$Bk_{yx}, Bk_{y\theta}, Bk_{yy}, Bk_{y\psi}, Bc_{yx}, Bc_{y\theta}, Bc_{yy}, Bc_{y\psi}$

$Bk_{\psi x}, Bk_{\psi\theta}, Bk_{\psi y}, Bk_{\psi\psi}, Bc_{\psi x}, Bc_{\psi\theta}, Bc_{\psi y}, Bc_{\psi\psi}$

These are the 32 bearing stiffness and damping coefficients for a moment resisting bearing. The first subscript represents the direction of force, and the second subscript represents displacement.

x = x-direction displacement

$\theta$  = rotation at positive y-axis (right-hand rule)

y = y-direction displacement

$\psi$  = rotation at negative x-axis (right-hand rule)

9. NGYR, E, SPEED1, SPEED ANGACL, FSPEED, BETA (I5, 5x, 5G10.3)

NGYR = 1 calculation shaft gyroscopics

= 0 no shaft gyroscopics

E = Section Young's Modulus  $\times 10^{-6}$  (E = 30. for steel)

SPEED1 = Rotor operating speed (RPM) (use for gyroscopic calculation in damped modes)

SPEED2 = use as initial speed for transient

ANGACL = rad/sec<sup>2</sup> (use in transient cal.)

TSPEED = 0

BETA = Beta parameter used for Newmark beta integration  
(usually = 1/6)

10. EXTW(J), DX(J), DEXT(J), DINT(J), RP(J), RT(J), ZM6(J), RO(J),

J = 1, N

(N cards) (8(F10.3))

EXTW(J) = external weights at J-mass station (lb)

DX(J) = length of Jth element (in)

DEXT(J) = external diameter of Jth element (in)

DINT(J) = internal diameter of Jth element (in)

RP(J) = polar moment of inertia at Jth station (lb-in<sup>2</sup>)

RT(J) = transverse moment of inertia at Jth station (lb-in<sup>2</sup>)

EM6(J) = Young's modulus of Jth element  $\times 10^{-6}$  (=E lb/in<sup>2</sup>)

if set to zero)

RO(J) = density of Jth element (= 0.283 lb/in<sup>3</sup> if set to zero)

11. LLFF(J), FX(J), FY(J), J = 1, NF (I5, 5x, 2G10.3) NF cards,

skip if NF = 0

LLFF(J) = station no. of Jth external force

FX(J) = forces in x-direction (lb)

FY(J) = forces in y-direction (lb)

12. LLUF(J), UX(J), UY(J), J = 1, NU

(15, 5x, 2G10.3) NU cards, skip if NU = 0

LLUF(J) = station no. of Jth unbalance

UX(J) = unbalance at x-direction (oz-in)

UY(J) = unbalance at y-direction (oz-in)

13. LLSK(J), FSK(J), PSK(J), J = 1, NS

(15, 5x, 2G10.3) NS cards, skip if NS = 0

LLSK(J) = station no. of Jth skewed disc

FSK(J) = maximum skew of the disc (rad) (positive skew is  
opposite to positive  $\theta_x$ )

PSK(J) = angle between maximum skew to the x-axis (rad)

14. LLUT(J), J = 1, NUFPT (10I5), skip if NUFPT = 0

LLUT(J) = station no. of printout stations for unbalance  
response

15. LLNT(J), J = 1, NT (10I5), skip if NT = 0

LLNT(J) = station no. of printout stations for transient  
analysis

16. BOW(J), PBOW(J), XIC(J), YIC(J), VXIC(J), VYIC(J), J = 1, N

(6G10.3)

BOW(J) = Jth station initial bow (mils) (= 0 if no bow)

PBOW(J) = angle of bow to the positive x-axis (rad)

(= 0 if no bow)

XIC(J) = Jth station initial displacement (mils)

YIC(J) = Jth station initial displacement at y-direction (mils)

VXIC(J) = Jth station initial velocity at x-direction (mils/sec)

VYIC(J) = Jth station initial velocity at y-direction (mils/sec)

17. SPI, SPL, DSP (3G10.3)

SPI = initial speed (RPM)

SPL = final speed (RPM) (for critical speed analysis)

DSP = speed increment (RPM)

18. SPS, SPF, SPN (3G10.3)

SPS = initial speed (RPM)

SPF = final speed (RPM) (for unbalance response calculations)

SPN = speed increment (RPM)

19. TITLE1, TITLE2, TITLE3

3 TITLE cards for label in plots (1 to 80 columns)



C	PROGRAM MODES(INPUT,OUTPUT,TAPE1=INPUT,TAPE3=OUTPUT,TAPE7,TAPE10)	A	1
C	*****	A	2
C	THIS PROGRAM CALCULATE THE UNDAMPED CRITICAL SPEEDS AND THEIR	A	3
C	CORRESPONDING MODE SHAPES,DAMPED NATURAL FREQUENCIES AND THEIR	A	4
C	CORRESPONDING MODE SHAPES,ROTOR UNBALANCE RESPONSE, AND TRANSIENT	A	5
C	RESPONSE OF MULTIMASS ROTOR BEARING SYSTEMS.	A	6
C	SPECIAL FEATURES INCLUDED ASSYMMETRIC BEARING, BEARING ROTATIONAL	A	7
C	DAMPING AND STIFFNESS EFFECTS,SHAFT RESIDUAL BOW AND DISC SKEW	A	8
C	EFFECTS.	A	9
C	NONLINEAR BEARING FORCES CAN ALSO BE CALCULATED FOR EACH TIME	A	10
C	STEP DURING TRANSIENT ANALYSIS WITH BEARING CHARACTERISTICS	A	11
C	THE PROGRAM CAN ALSO GENERATE PLOTS OF TRANSIENT ORBITS AND	A	12
C	TIME VS TRANSIENT RESPONSE PLOTS.	A	13
C	BY K. C. CHOY	A	14
C	DEPARTMENT OF MECHANICAL ENGINEERING, UNIVERSITY OF VIRGINIA	A	15
C	MARCH 4, 1977	A	16
C	*****	A	17
	COMPLEX BB(20,21),CC(20)	A	18
	REAL KXX(10),KXY(10),KYY(10),MFX(10),MFY(10),MUU(10),MUX(1	A	19
	10),KMX(10,10),KMY(10,10),MBX(10),MBY(10)	A	20
	DIMENSION CGMENT1(8), CGMENT2(8), CGMENT3(8)	A	21
	DIMENSION EM6(100), CRT(10), LLBD(10), LLNB(5), LLNMB(9), LLSK(10)	A	22
	1, LLNT(10), LLUF(10), LLFF(10), LLUT(10)	A	23
	DIMENSION DX(100), W(100), ENER(100), EY1(100), EY2(100), DPC(100)	A	24
	DIMENSION DEFL(100), LB(100), SK(100), WA(50), DEXT(100), DINT(100	A	25
	1)	A	26
	DIMENSION EXTW(100), SW1(100), RD(100), RT(100), RP(100), EI(100)	A	27
	DIMENSION WMOD(50), AKK(10)	A	28
	DIMENSION EAN1(100), EAN2(100), EYTH(100), EYTH(10,100), DDPC(10,	A	29
	1100)	A	30
	DIMENSION TMX(10,10)	A	31
	DIMENSION A1(2,10), A2(2,10), A3(2,10), B1(2,10), B2(2,10), B3(2,1	A	32
	10)	A	33
	DIMENSION CMX(10,10), CMY(10,10), DMX(10,10), DMY(10,10), EMX(10,1	A	34
	10), EMY(10,10)	A	35
	DIMENSION DOX(10,10), DOY(10,10), EDX(10,10), EDY(10,10)	A	36
	DIMENSION AAA(42), BBB(42), CCC(42), HHH(42), UUU(42), VVV(42)	A	37
	DIMENSION CXX(10), CXY(10), CYX(10), CYY(10), UX(10), UY(10)	A	38

DIMENSION FX(10), FY(10)	A	39
DIMENSION SLNMB(9,4,4), CLNMB(9,4,4)	A	40
DIMENSION SNLB(5,8,3), FSK(10), PSK(10), BOW(100), PBDW(100)	A	41
DIMENSION BXA(100), BYA(100), XIDC(100), YIDC(100), VXIDC(100), VY	A	42
1IDC(100)	A	43
DIMENSION ADUMMY(8002)	A	44
DIMENSION ALABEL1(8), ALABEL2(8), ALABEL3(8)	A	45
DIMENSION WMY(10), VIS(5), ANR(5), ANL(5), ANC(5), NLB(5)	A	46
COMMON /BLK1/ N,NB,NNLIN,NMB,NF,NU,NS,NBOW,ISTAB,IMGDE,ISKU,NCT,NU	A	47
1FPT	A	48
COMMON /BLK2/ ISKIP,NSTEP,NCYCLE,NITP,NINT,NPLOT,NORBIT,NTIME,NSPE	A	49
1ED,NINC,NOPT,NT	A	50
COMMON /BLK3/ CRT,LLBD,LLNB,LLNMB,LLSK,LLNT,LLUF,LLFF,LLUT	A	51
COMMON /BLK4/ KXX,KXY,KYX,KYY,CXX,CXY,CYX,CYY,SLNMB,CLNMB	A	52
COMMON /BLK5/ UX,UY,FX,FY,FSK,PSK	A	53
COMMON /BLK6/ BOW,PBOW,XIDC,YIDC,VXIDC,VYIDC,BXA,BYA	A	54
COMMON /BLK7/ CMX,KMX,EMX,CMY,KMY,EMY	A	55
COMMON /BLK8/ MFX,MFY,MUX,MUY,MBX,MBY	A	56
COMMON /BLK9/ DDPC,EEYTH	A	57
COMMON /BLK10/ SPS,SPF,SPN,SPEED1	A	58
COMMON /BLK11/ DDY,DEY,EDX,EDY	A	59
COMMON /BLK14/ AAA,UUU,VVV,HHH,BBB,CCC	A	60
COMMON /BLK15/ RP,RT	A	61
COMMON /BLK16/ SPEED2,ANGSP,ANGACL,FSPEED	A	62
COMMON /BLK18/ AKK	A	63
COMMON /BLK19/ DX	A	64
COMMON /BLK20/ A1,A2,A3,B1,B2,B3	A	65
COMMON /BLK21/ DMX,DMY	A	66
COMMON /BLK22/ W	A	67
COMMON /BLK24/ BB,CC	A	68
COMMON /BLK25/ BETA	A	69
COMMON /BLK28/ ALABEL1,ALABEL2,ALABEL3	A	70
COMMON /BLK29/ PASP	A	71
COMMON /BLK35/ WMY,VIS,ANR,ANL,ANC,NLB	A	72
COMMON ADUMMY	A	73
NNPLT=0	A	74
READ (1,690) COMMENT1	A	75
READ (1,690) COMMENT2	A	76

ORIGINAL PAGE IS  
OF POOR QUALITY

	READ (1,690) COMENT3	A 77
	WRITE (3,1080)	A 78
	WRITE (3,700) CGMENT1,COMENT2,COMENT3	A 79
	WRITE (3,710)	A 80
	READ (1,720) N,NB,NNLIN,NMB,NF,NU,NS,NBOW,ISTAB,IMODE,ISKU,NUFPT	A 81
	READ (1,730) ISKIP,NSTEP,NCYCLE,NITP,NINT,NPLOT,NORBIT,NTIME,NSPEE	A 82
	ID,NINC,NOPT,NT	A 83
	IF (NB.EQ.0) GO TO 20	A 84
	READ (1,740) (LLBD(J),J=1,NB)	A 85
	READ (1,750) (KXX(J),KXY(J),KYY(J),CXX(J),CXY(J),CYX(J),CYY	A 86
	1(J),J=1,NB)	A 87
20	CONTINUE	A 88
	IF (NNLIN.EQ.0) GO TO 30	A 89
	READ (1,760) (LLNB(J),NLB(J),VIS(J),ANR(J),ANL(J),ANC(J),J=1,NNLIN	A 90
	1)	A 91
30	CONTINUE	A 92
	IF (NMB.EQ.0) GO TO 40	A 93
	READ (1,770) (LLNMB(J),J=1,NMB)	A 94
	READ (1,780) (((SLNMB(I,J,K),K=1,4),(CLNMB(I,J,K),K=1,4)),J=1,4),	A 95
	1I=1,NMB)	A 96
40	CONTINUE	A 97
	READ (1,790) NGR,E,SPEED1,SPEED2,ANGACL,FSPEED,BETA	A 98
	READ (1,800) (EXTW(J),DX(J),DEXT(J),DINT(J),RP(J),RT(J),EM6(J),RDI	A 99
	1J),J=1,N)	A 100
	IF (NF.EQ.0) GO TO 50	A 101
	READ (1,810) (LLFF(J),FX(J),FY(J),J=1,NF)	A 102
50	CONTINUE	A 103
	IF (NU.EQ.0) GO TO 60	A 104
	READ (1,810) (LLUF(J),UX(J),UY(J),J=1,NU)	A 105
60	CONTINUE	A 106
	IF (NS.EQ.0) GO TO 70	A 107
	PEAD (1,810) (LLSK(J),FSK(J),PSK(J),J=1,NS)	A 108
70	CONTINUE	A 109
	IF (NUFPT.EQ.0) GO TO 80	A 110
	READ (1,820) (LLUT(J),J=1,NUFPT)	A 111
80	CONTINUE	A 112
	IF (NT.EQ.0) GO TO 90	A 113
	READ (1,820) (LLNT(J),J=1,NT)	A 114

90	CONTINUE	A 115
	READ (1,830) (BGW(J),PBGW(J),XIDC(J),YIDC(J),VXIDC(J),VYIDC(J),J=1	A 116
	1,N)	A 117
	READ (1,840) SPI,SPL,DSP	A 118
	IF (ISKU.EQ.1) GO TO 100	A 119
	READ (1,850) SPS,SPF,SPN	A 120
100	CONTINUE	A 121
	READ (1,690) ALABEL1	A 122
	READ (1,690) ALABEL2	A 123
	READ (1,690) ALABEL3	A 124
	WRITE (3,860) NCYCLE,NSTEP,NINT,NINC,NOPT,SPEED2,ANGACL,BETA	A 125
	WRITE (3,870)	A 126
	DO 110 I=1,N	A 127
	IF (RO(I).EQ.0.0) RO(I)=0.283	A 128
	ENER(I)=3.14159*(DEXT(I)**4.-DINT(I)**4.)/64.	A 129
	IF (EM6(I).EQ.0.0) EM6(I)=E	A 130
	EI(I)=EM6(I)*ENER(I)	A 131
	DL=ABS(DX(I))	A 132
110	SW1(I)=3.14159*(DEXT(I)**2.-DINT(I)**2.)*DL*RO(I)/4.0	A 133
	W(1)=SW1(1)/2.+EXTW(1)	A 134
	WT=W(1)	A 135
	ZLT=DX(1)	A 136
	DO 120 I=2,N	A 137
	W(I)=SW1(I-1)/2.0+SW1(I)/2.0+EXTW(I)	A 138
C	W(I)=TOTAL EFFECTIVE SHAFT WEIGHT	A 139
	WT=WT+W(I)	A 140
120	ZLT=ZLT+DX(I)	A 141
	IF (NGYR) 130,150,130	A 142
130	RP(1)=RP(1)+ENER(1)*RO(1)*DX(1)	A 143
	RT(1)=RT(1)+SW1(1)*((DEXT(1)**2.0+DINT(1)**2.0)/16.0+((DX(1)/2.0)*	A 144
	1*2.0)/3.0)/2.0	A 145
	DO 140 I=2,N	A 146
	RP(I)=RP(I)+RO(I)*ENER(I)*DX(I)+ENER(I-1)*DX(I-1)*RO(I-1)	A 147
	RT(I)=RT(I)+SW1(I)*((DEXT(I)**2.0+DINT(I)**2.0)/16.0+((DX(I)/2.0)*	A 148
	1*2.0)/3.0)/2.0+SW1(I-1)*((DEXT(I-1)**2.0+DINT(I-1)**2.0)/16.0+((DX	A 149
	2(I-1)/2.0)**2.0)/3.0)/2.0	A 150
140	CONTINUE	A 151
150	SRP=0.0	A 152

ORIGINAL PAGE IS  
OF POOR QUALITY

	DD 160 I=1,N	A 153
160	SRP=SRP+RP(1)	A 154
	DD 180 I=1,N	A 155
	WRITE (3,880) (I,W(I),DX(I),DEXT(I),DINT(I),ENER(I),RP(I),RT(I),EM	A 156
	16(I),EI(I))	A 157
	IF (I-50) 180,170,180	A 158
170	WRITE (3,1080)	A 159
180	CONTINUE	A 160
	WRITE (3,890) WT,ZLT	A 161
	WRITE (3,900)	A 162
	WRITE (3,910)	A 163
	WRITE (3,920) (J,LLBD(J),KXX(J),KXY(J),KYX(J),KYY(J),J=1,NB)	A 164
	WRITE (3,930)	A 165
	WRITE (3,940)	A 166
	WRITE (3,920) (J,LLBD(J),CXX(J),CXY(J),CYX(J),CYY(J),J=1,NB)	A 167
	IF (NMB.EQ.0) GO TO 200	A 168
	DD 190 I=1,NMB	A 169
	WRITE (3,950) I,LLNMB(I)	A 170
	WRITE (3,960) ((SLNMB(I,J,K),K=1,4),J=1,4),((CLNMB(I,J,K),K=1,4),J	A 171
	1=1,4)	A 172
190	CONTINUE	A 173
200	IF (NNLIN.EQ.0) GO TO 220	A 174
	WRITE (3,1170)	A 175
	DD 210 J=1,NNLIN	A 176
	WRITE (3,1180) J,LLNB(J),NLB(J),VIS(J),ANR(J),ANL(J),ANC(J)	A 177
210	CONTINUE	A 178
220	IF (NF.EQ.0) GO TO 230	A 179
	WRITE (3,970)	A 180
	WRITE (3,980) (LLFF(J),FX(J),FY(J),J=1,NF)	A 181
230	IF (NS.EQ.0) GO TO 240	A 182
	WRITE (3,990)	A 183
	WRITE (3,1000) (LLSK(J),FSK(J),PSK(J),J=1,NS)	A 184
240	IF (NU.EQ.0) GO TO 260	A 185
	WRITE (3,1010)	A 186
	WRITE (3,1020)	A 187
	WRITE (3,1030) (LLUF(J),UX(J),UY(J),J=1,NU)	A 188
	DD 250 J=1,NU	A 189
	UX(J)=UX(J)/(16.*386.4)	A 190

250	UY(J)=UY(J)/(16.*386.4)	A 191
260	CONTINUE	A 192
	WRITE (3,1040)	A 193
	DO 270 J=1,N	A 194
	WRITE (3,1050) J,BGW(J),PBGW(J),XIDC(J),YIDC(J),VXIDC(J),VYIDC(J)	A 195
270	CONTINUE	A 196
	WRITE (3,1060)	A 197
	DO 280 I=1,NB	A 198
	AVK=(KXX(I)+KYY(I))/2.	A 199
	WRITE (3,1070) I,AVK	A 200
280	CONTINUE	A 201
	NC=1	A 202
C	NC=LOCAL CRITICAL SPEED NO.	A 203
C	WRITE (3,700)	A 204
	WRITE (3,1080)	A 205
	LN=3	A 206
C	SPI=INITIAL SPEED,SPL=FINAL SPEED,DSP=SPEED INCREMENT-RPM	A 207
	SPD=SPI	A 208
	DETP=0.	A 209
	MA=0	A 210
	MB=0	A 211
C	IF(LN-50)54,54,53	A 212
	WRITE (3,1080)	A 213
	WRITE (3,1090) SPI,SPL,DSP	A 214
	LN=1	A 215
	WRITE (3,1100)	A 216
	LN=LN+3	A 217
	DIN=DSP	A 218
290	I=1	A 219
	J=1	A 220
	SPSQ=SPD*SPD	A 221
C	COMPUTE ANG. VELOCITY	A 222
	ANSP=SPD*0.10471976	A 223
	ANSP2=ANSP*ANSP	A 224
	VP=0.	A 225
	ZMP=0.	A 226
	EYP=0.	A 227
	ETHP=1.0	A 228

ORIGINAL PAGE IS  
OF POOR QUALITY

	M=1	A 229
300	I=I+1	A 230
	II=I-1	A 231
	IF (II-LLBD(J)) 330,310,330	A 232
310	AK=(KXX(J)+KYY(J))/2.	A 233
	AKK(J)=AK	A 234
	IF (J-NB) 320,340,340	A 235
320	J=J+1	A 236
	GO TO 340	A 237
330	AK=0.	A 238
340	VP=VP+(W(I-1)*ANSP2/386.4-AK)*EYP	A 239
	ZMP=ZMP-ANSP2*(RT(I-1))*ETHP/386.4	A 240
	EY=EYP+DX(I-1)*ETHP+DX(I-1)**2*ZMP/(2.E6*EI(I-1))+DX(I-1)**3*VP/(6	A 241
	1.E6*EI(I-1))	A 242
	ETH=ETHP+DX(I-1)*ZMP/(1.E6*EI(I-1))+DX(I-1)**2*VP/(2.E6*EI(I-1))	A 243
	ZM=ZMP+DX(I-1)*VP	A 244
	V=VP	A 245
	IF (M.EQ.2) GO TO 350	A 246
	EY1(I)=EY	A 247
	EAN1(I)=ETH	A 248
	IF (I.GT.N) GO TO 360	A 249
	ZMP=ZM	A 250
	VP=V	A 251
	EYP=EY	A 252
	ETHP=ETH	A 253
	GO TO 300	A 254
350	EY2(I)=EY	A 255
	EAN2(I)=ETH	A 256
	ZMP=ZM	A 257
	VP=V	A 258
	EYP=EY	A 259
	ETHP=ETH	A 260
	IF (I.GT.N) GO TO 370	A 261
	GO TO 300	A 262
360	M=2	A 263
	ZM1=ZM	A 264
	VR1=V	A 265
	J=1	A 266

```

I=1
EYP=1.
ZMP=0.
ETHP=0.
VP=0.
GO TO 300
370 DET=VR1*ZM-V*ZM1
    IF (DETP.EQ.0.) GO TO 420
    IF (MA.EQ.1) GO TO 400
    IF (ABS(DET).LT.1.) GO TO 450
    IF (DETP*DET) 380,420,420
380 DOLD=DETP
390 MA=1
    IF (ABS(DET).LT.1.) GO TO 450
    IF (DIN.LT.1.E-6) GO TO 450
    DIN=DIN/2.
    DETPP=DETP
    DETP=DET
    SPD=SPD-DIN
    GO TO 290
400 IF (ABS(DET).LT.1.) GO TO 450
    IF (DOLD*DET) 390,420,410
410 CONTINUE
    IF (ABS(DET).LT.1.) GO TO 450
    IF (DIN.LT.1.E-6) GO TO 450
    DIN=DIN/2.
    SPD=SPD+DIN
    DETPP=DETP
    DETP=DET
    GO TO 290
420 IF (LN-54) 440,440,430
430 WRITE (3,1080)
    LN=1
440 WRITE (3,1110) SPD,DET
    LN=LN+1
    SPD=SPD+DSP
    DIN=DSP
    IF (SPD.GT.SPL) GO TO 620

```

```

A 267
A 268
A 269
A 270
A 271
A 272
A 273
A 274
A 275
A 276
A 277
A 278
A 279
A 280
A 281
A 282
A 283
A 284
A 285
A 286
A 287
A 288
A 289
A 290
A 291
A 292
A 293
A 294
A 295
A 296
A 297
A 298
A 299
A 300
A 301
A 302
A 303
A 304

```



```

      DETPP=DETP
      DETP=DET
      SSPD=SPD
      GO TO 290
450   MA=0
      WRITE (3,1110) SPD,DET
      LN=LN+1
      IF (LN-50) 470,470,460
460   WRITE (3,1080)
      LN=1
470   WRITE (3,1120) NC
      WRITE (3,1130)
      WRITE (3,1110) SPD,DET
      CRT(NC)=SPD
      NC=NC+1
      LN=LN+3
      EY1(1)=0.
      EY2(1)=1.
      DTX=0.
      I=1
      IF (LN-50) 490,490,480
480   WRITE (3,1080)
      LN=1
490   WRITE (3,1140)
      LN=LN+2
500   DEFL(I)=V*EY1(I)-VR1*EY2(I)
      IF (I.NE.1) GO TO 510
      EYTH(I)=V
      GO TO 520
510   EYTH(I)=EAN1(I)*V-EAN2(I)*VR1
520   DEFA=ABS(DEFL(I))
      DMXA=ABS(DTX)
      I=I+1
      IF (DEFA-DMXA) 540,540,530
530   DTX=DEFL(I-1)
540   IF (I-N) 550,550,560
550   GO TO 500
560   DO 570 I=1,N

```

```

A 305
A 306
A 307
A 308
A 309
A 310
A 311
A 312
A 313
A 314
A 315
A 316
A 317
A 318
A 319
A 320
A 321
A 322
A 323
A 324
A 325
A 326
A 327
A 328
A 329
A 330
A 331
A 332
A 333
A 334
A 335
A 336
A 337
A 338
A 339
A 340
A 341
A 342

```

	DPC(I)=DEFL(I)/DTX	A 343
	EYTH(I)=EYTH(I)/DTX	A 344
	EEYTH(NC-1,I)=EYTH(I)	A 345
570	DDPC(NC-1,I)=DPC(I)	A 346
	DO 600 I=1,N	A 347
	LN=LN+1	A 348
	IF (LN-54) 590,590,580	A 349
580	WRITE (3,1080)	A 350
	LN=1	A 351
590	WRITE (3,1150) I,DPC(I),EYTH(I)	A 352
	LN=LN+1	A 353
600	CONTINUE	A 354
	SPD=SSPD+DSP	A 355
	DETP=0.	A 356
	GO TO 290	A 357
610	CONTINUE	A 358
	DO 620 IK=1,NB	A 359
	KXX(IK)=KXX(IK)-AKK(IK)	A 360
620	KYY(IK)=KYY(IK)-AKK(IK)	A 361
	NCS=NC-1	A 362
	DO 650 II=1,NCS	A 363
	WMOD(II)=0.	A 364
	DO 630 JJ=1,N	A 365
630	WMOD(II)=WMOD(II)+RT(JJ)*EEYTH(II,JJ)**2+W(JJ)*DDPC(II,JJ)**2	A 366
	WMOD(II)=WMOD(II)/386.4	A 367
	DO 640 KI=1,N	A 368
	EEYTH(II,KI)=EEYTH(II,KI)/(WMOD(II)**0.5)	A 369
640	DDPC(II,KI)=DDPC(II,KI)/(WMOD(II)**0.5)	A 370
650	CONTINUE	A 371
	DO 660 II=1,NCS	A 372
	WRITE (3,1190) II,CRT(II),WMOD(II)	A 373
	DO 660 JJ=1,N	A 374
	WRITE (3,1200) JJ,DDPC(II,JJ),EEYTH(II,JJ)	A 375
660	CONTINUE	A 376
	WRITE (3,1210)	A 377
	DO 680 II=1,NCS	A 378
	DO 670 JJ=1,NCS	A 379
	TMX(II,JJ)=0.	A 380

ORIGINAL PAGE IS  
OF POOR QUALITY

	DD 670 KI=1,N	A 381
	TMX(II,JJ)=TMX(II,JJ)+W(KI)*DDPC(JJ,KI)*DDPC(II,KI)/386.4+RT(KI)*E	A 382
	1EYTH(II,KI)+EEYTH(JJ,KI)/386.4	A 383
670	CONTINUE	A 384
	WRITE (3,1160) (TMX(II,JJ),JJ=1,NCS)	A 385
680	CONTINUE	A 386
	NCT=NCS	A 387
	CALL TMM	A 388
C		A 389
C		A 390
690	FORMAT (8A10)	A 391
700	FORMAT (1X,3(8A10/1X))	A 392
710	FORMAT (/,20X, #MODAL ANALYSIS VERSION 3, APRIL 6, 1977#)	A 393
720	FORMAT (12I5)	A 394
730	FORMAT (12I5)	A 395
740	FORMAT (10I5)	A 396
750	FORMAT (8G10.3)	A 397
760	FORMAT (2I5,4G10.2)	A 398
770	FORMAT (9I5)	A 399
780	FORMAT (8G10.3)	A 400
790	FORMAT (I5,5X,6G10.3)	A 401
800	FORMAT (8G10.3)	A 402
810	FORMAT (I5,5X,2G10.3)	A 403
820	FORMAT (10I5)	A 404
830	FORMAT (6G10.3)	A 405
840	FORMAT (3G10.3)	A 406
850	FORMAT (3G10.3)	A 407
860	FORMAT (//,10X, #NCYCLE= #, I3,5X, #NSTEP= #, I3,5X, #NINT= #, I3,5X, #NINC=	A 408
	1 #, I3,5X, #NOPT= #, I3,/,10X, #SPEED2= #, F10.2,5X, #ANGACL(1/SEC)= #, F10.3	A 409
	2,5X, #BETA= #, F10.5, //)	A 410
870	FORMAT (120H STATION NO.      WEIGHT      LENGTH      SHAFT DIA.      SHAFT D	A 411
	1IA.      I      IF-POLAR MOM.      IT-TRANS. MOM.      EX10-6      EI	A 412
	2, /120H      (LP)      (IN.)      OUTSIDE      INSIDE      (	A 413
	3IN**4)      (LP-IN**2)      (LB-IN**2)      ,//)	A 414
880	FORMAT (I7,F16.3,F12.3,F10.3,F10.3,F11.2,F12.3,F16.3,F11.2,G10.3)	A 415
890	FORMAT (16X,7H-----,5X,7H-----/7X,F16.3,F12.3//)	A 416
900	FORMAT (/,34X, #      LINEAR SUPPORT BEARING STIFFNESS CHARACTERISTICS#//)	A 417
910	FORMAT (5X,16HBEARING      BEARING,12X,3HKXX,16X,3HKXY,16X,3HKYX,16X,3	A 418

	1HKYY, /5X, 6HNUMBER, 3X, 6HLOCATION, 8X, 7H(LB/IN), 11X, 7H(LB/IN), 11X, 7H(	A 419
	2LB/IN), 11X, 7H(LB/IN))	A 420
920	FORMAT (5X, I3, 8X, I3, 9X, F11.1, 5X, F11.1, 8X, F11.1, 8X, F11.1)	A 421
930	FORMAT (/ , 35X, # LINEAR SUPPORT BEARING DAMPING CHARACTERISTICS# /	A 422
	1)	A 423
940	FORMAT (5X, 16HDAMPING DAMPING, 12X, 3HCXX, 16X, 3HCXY, 16X, 3HCYX, 16X, 3	A 424
	1HCYY, / , 5X, 6HNUMBER, 3X, 8HLOCATION, 6X, 11H(LB-SEC/IN), 10X, 11H(LB-SEC/	A 425
	2IN), 10X, 11H(LB-SEC/IN), 10X, 11H(LB-SEC/IN))	A 426
950	FORMAT (//, 10X, #FULL BEARING NO. #, I2, 3X, #AT STATION#, I3, /)	A 427
960	FORMAT (10X, #BEARING STIFFNESS LB/IN#, //, 4(4(5X, G15.3), /), //, 10X, #	A 428
	1BEARING DAMPING LB-SEC/IN#, //, 4(4(5X, G15.3), /))	A 429
970	FORMAT (//, 20X, #EXTERNAL FORCES#, /, 5X, #STATION NO. #, 10X, #X#, 15X, #Y	A 430
	1#, /)	A 431
980	FORMAT (10X, I3, 2(5X, G15.5))	A 432
990	FORMAT (//, 20X, #SKEWED DISC#, /, 5X, #STATION NO. #, 10X, #SKEW(RAD) #, 5X	A 433
	1, #PHASE ANGLE DEG. #, /)	A 434
1000	FORMAT (10X, I3, 2(5X, G15.5))	A 435
1010	FORMAT (///, 25X, #ROTOR UNBALANCE IN OZ-IN. #, /)	A 436
1020	FORMAT (5X, #STATION#, 10X, #X-UNBALANCE#, 10X, #Y-UNBALANCE#, /)	A 437
1030	FORMAT (8X, I2, 12X, F10.3, 11X, F10.3)	A 438
1040	FORMAT (//, 20X, #SHAFT INITIAL CONDITIONS#, //, 5X, #STATION NO. #, 5X, #	A 439
	1BOW-MILS#, 5X, #PHASE ANGLE#, 5X, #X-DISP#, 10X, #Y-DISP#, 10X, #X-VEL#, 10X	A 440
	2, #Y-VEL#, /, 34X, #(DEGREES) #, 6X, #(MILS) #, 10X, #(MILS) #, 10X, #MIL/IN#, 1	A 441
	30X, #MIL/IN#, /)	A 442
1050	FORMAT (5X, I3, 6(5X, F10.2))	A 443
1060	FORMAT (//, 10X, #AVERAGE BEARING STIFFNESS USED FOR CRITICAL SPEED	A 444
	1CALCULATIONS#)	A 445
1070	FORMAT (10X, #BEARING NO. #, I2, 5X, #STIFFNESS(LB/IN) #, F12.2)	A 446
1080	FORMAT (1H1, /)	A 447
1090	FORMAT (//, 5X, # INITIAL SPEED=#, F10.2, 5X, #FINAL SPEED=#, F10.2, 5X, #	A 448
	1SPEED INCREMENT=#, F10.2, # RPM#, /)	A 449
1100	FORMAT (/13X, 3HRPM, 20X, 5HDELTA, 12X, 2HK1, 13X, 2HK2/)	A 450
1110	FORMAT (10X, F8.1, 9X, E17.9)	A 451
1120	FORMAT (//, 10X, #CRITICAL SPEED NO. #, I2)	A 452
1130	FORMAT (/ , 10X, 14HCRITICAL SPEED, 11X, 5HDELTA, /)	A 453
1140	FORMAT (/ , 12X, 6HSTA NO, 10X, 14HNET DEFLECTION, 10X, 5HANGLE)	A 454
1150	FORMAT (12X, I5, 13X, F9.5, 13X, F9.5)	A 455
1160	FORMAT (5X, 10(F8.2, 2X))	A 456

1170	FORMAT (//,10X,#NONLINEAR BEARING FORCES#,//,5X,#BEARING NO.#,4X,#	A 457
	1STATION NO.#,4X,#CAVITATION#,5X,#VISCOSITY#,6X,#RADIUS#,9X,#LENGTH	A 458
	2#,9X,#CLEARANCE#,/,35X,#CONDITION#,6X,#LB/IN**2#,7X,#(IN.)#,10X,#(	A 459
	3IN.)#,10X,#(IN.)#,/)	A 460
1180	FORMAT (10X,I5,10X,I5,10X,I5,5X,E10.4,5X,E10.4,5X,E10.4,5X,E10.4)	A 461
1190	FORMAT (1H1,//,10X,#CRITICAL SPEED NO.#,I5,15X,F10.1,#RPM#,/,10X,#	A 462
	1MODAL MASS=#,F10.3,2X,#LE-SEC**2/IN#,//,10X,#THE ORTHONORMAL MODE	A 463
	2SHAPES#,//,5X,#STATION#,8X,#TRANSLATIONAL#,7X,#ROTATIONAL#)	A 464
1200	FORMAT (9X,I3,10X,F10.5,10X,F10.5)	A 465
1210	FORMAT (///,10X,#THE ORTHOGONAL CONDITIONS OF MODES#,/)	A 466
	END	A 467-

	SUBROUTINE TMM	B	1
C	*****	B	2
C	THIS SUBROUTINE CONTROLS THE MODAL ANALYSIS OPERATION AFTER THE	B	3
C	PLANAR CRITICAL SPEEDS AND MODE SHAPES HAVE BEEN CALCULATED.	B	4
C	*****	B	5
	COMPLEX B,C	B	6
	REAL KXX,KXY,KYX,KYY,MFX,MFY,MUX,MUY,KMX,KMY	B	7
	COMMON /BLK1/ N,NB,NLIN,NMB,NF,NU,NS,NBOW,ISTAB,IMODE,ISKU,NNCT,N	B	8
	1UFPT	B	9
	COMMON /BLK2/ ISKIP,NSTEP,NCYCLE,NITP,NINT,NPLOT,NORBIT,NTIME,NSPE	B	10
	IED,NINC,NOPT,NT	B	11
	COMMON /BLK3/ CRT(10),LLBD(10),LLNB(5),LLNMB(9),LLSK(10),LLNT(10),	B	12
	1LLUF(10),LLFF(10),LLUT(10)	B	13
	COMMON /BLK4/ KXX(10),KXY(10),KYX(10),KYY(10),CXX(10),CXY(10),CYX(	B	14
	110),CYY(10),SLNMB(9,4,4),CLNMB(9,4,4)	B	15
	COMMON /BLK5/ UX(10),UY(10),FX(10),FY(10),FSK(10),PSK(10)	B	16
	COMMON /BLK6/ BOW(100),PBOW(100),XIDC(100),YIDC(100),VXIDC(100),VY	B	17
	1IDC(100),BXA(100),BYA(100)	B	18
	COMMON /BLK7/ CMX(10,10),KMX(10,10),EMX(10,10),CMY(10,10),KMY(10,1	B	19
	10),EMY(10,10)	B	20
	COMMON /BLK8/ MFX(10),MFY(10),MUX(10),MUY(10),MBX(10),MBY(10)	B	21
	COMMON /BLK9/ DDPC(10,100),EEYTH(10,100)	B	22
	COMMON /BLK10/ SPS,SPF,SPN,SPEED1	B	23
	COMMON /BLK11/ DDY(10,10),DDX(10,10),EDY(10,10),EDX(10,10)	B	24
	COMMON /BLK15/ RP(100),RT(100)	B	25
	COMMON /BLK16/ SPEED2,ANGSP,ANGACL,FSPEED	B	26
	COMMON /BLK18/ AKK(10)	B	27
	COMMON /BLK20/ A1(2,10),A2(2,10),A3(2,10),B1(2,10),B2(2,10),B3(2,1	B	28
	10)	B	29
	COMMON /BLK24/ B(20,21),C(20)	B	30
	COMMON /BLK25/ BETA	B	31
	COMMON /BLK29/ PASP	B	32
	IF (NBOW.EQ.0) GO TO 10	B	33
	CALL SFTBOW	B	34
10	CONTINUE	B	35
	CALL TMODE1	B	36
	IF (ISTAB.EQ.1) GO TO 20	B	37
	CALL STAB	B	38

ORIGINAL PAGE IS  
OF POOR QUALITY

```

20  CONTINUE
    IF (ISKU.EQ.1) GO TO 30
    CALL UBST (0,SPEED2)
30  CONTINUE
    IF (ISKIP.EQ.1) GO TO 120
    SPEED=SPEED2
    NSTEP1=NSTEP+1
    STEP=NSTEP
    TCYCLE=60./SPEED
    TIME=0.
    IINT=1
    IF (NINC.EQ.0) GO TO 50
    CALL UBST (1,SPEED)
    DO 40 I=1,NNCT
    II=I+NNCT
    A3(1,I)=REAL(C(I))*0.9
    B3(1,I)=REAL(C(II))*0.9
    A2(1,I)=-AIMAG(C(I))*SPEED*0.10471975*0.9
40  B2(1,I)=-AIMAG(C(II))*SPEED*0.10471975*0.9
    GO TO 60
50  CALL TINC
    IF (NBOW.EQ.0) GO TO 60
    CALL SFTBOW
60  CONTINUE
    REWIND 7
    CALL TSTORE (NNCT,1,0.0)
    ICOUNT=1
    NK=0
    NPLUS=0
    IF (ANGACL.NE.0.) NPLUS=99999
    NJ=NPLUS+1
    PASP=0.
    DO 110 I=IINT,NCYCLE
    TEEM=TIME
    DO 100 J=1,NSTEP
    DELTAT=TCYCLE/STEP
    IF (J.GT.NJ) NK=1
    CALL TMODE2 (TIME,DELTAT,SPEED,NK)

```

```

8  39
8  40
8  41
8  42
8  43
8  44
8  45
8  46
8  47
8  48
8  49
8  50
8  51
8  52
8  53
8  54
8  55
8  56
8  57
8  58
8  59
8  60
8  61
8  62
8  63
8  64
8  65
8  66
8  67
8  68
8  69
8  70
8  71
8  72
8  73
8  74
8  75
8  76

```

```

      CALL TACCEL
      TIME=TIME+DELTAT
      GO TO (70,80), NINT
70    CALL TBETA (NNCT,DELTAT,BETA)
      GO TO 90
80    CALL TINTG (NNCT,DELTAT)
90    CONTINUE
      ICOUNT=ICOUNT+1
      CALL TSTORE (NNCT,ICOUNT,TIME)
      PASP=PASP+DELTAT*SPEED*0.104719
      TCYCLE=60./SPEED
100   CONTINUE
110   CONTINUE
      CALL TDISPL (TIME)
120   CONTINUE
      RETURN
      END

```

```

B 77
B 78
B 79
B 80
B 81
B 82
B 83
B 84
B 85
B 86
B 87
B 88
B 89
B 90
B 91
B 92
B 93-

```

ORIGINAL PAGE IS  
OF POOR QUALITY



	SUBROUTINE TMODEL	C	1
C	*****	C	2
C	THIS SUBROUTINE CALCULATES THE MODAL COEFFICIENTS WHICH ARE INDEPE	C	3
C	OF SPEED AND ACCELERATION. THEY CAN BE USED IN OTHER SUBROUTINES.	C	4
C	*****	C	5
	REAL KXX,KXY,KYX,KYY,MFX,MFY,MUX,MUY,KMX,KMY	C	6
	COMMON /BLK1/ N,NB,NNLIN,NMB,NF,NU,NS,NBOW,ISTAB,IMODE,ISKU,NNCT,N	C	7
	1UFPT	C	8
	COMMON /BLK3/ CRT(10),LLBD(10),LLNB(5),LLNMB(9),LLSK(10),LLNT(10),	C	9
	1LLUF(10),LLFF(10),LLUT(10)	C	10
	COMMON /BLK4/ KXX(10),KXY(10),KYX(10),KYY(10),CXX(10),CXY(10),CYX(	C	11
	110),CYY(10),SLNMB(9,4,4),CLNMB(9,4,4)	C	12
	COMMON /BLK7/ CMX(10,10),KMX(10,10),EMX(10,10),CMY(10,10),KMY(10,1	C	13
	10),EMY(10,10)	C	14
	COMMON /BLK8/ MFX(10),MFY(10),MUX(10),MUY(10),MBX(10),MBY(10)	C	15
	COMMON /BLK9/ DDPC(10,100),EEYTH(10,100)	C	16
	COMMON /BLK11/ DOX(10,10),DOY(10,10),EOX(10,10),EOY(10,10)	C	17
	COMMON /BLK22/ W(100)	C	18
	COMMON /BLK35/ WMY(10),VIS(5),ANR(5),ANL(5),ANC(5),NLB(5)	C	19
	DO 10 I=1,NNCT	C	20
	DO 10 J=1,NNCT	C	21
	CMX(I,J)=0.	C	22
	CMY(I,J)=0.	C	23
	KMX(I,J)=0.	C	24
	KMY(I,J)=0.	C	25
	DOX(I,J)=0.	C	26
	DOY(I,J)=0.	C	27
	EOX(I,J)=0.	C	28
	EOY(I,J)=0.	C	29
10	CONTINUE	C	30
	DO 30 I=1,NB	C	31
	J=LLBD(I)	C	32
	DO 20 K=1,NNCT	C	33
	DO 20 L=1,NNCT	C	34
	CMX(K,L)=CMX(K,L)+CXX(I)*DDPC(K,J)*DDPC(L,J)	C	35
	CMY(K,L)=CMY(K,L)+CYY(I)*DDPC(K,J)*DDPC(L,J)	C	36
	KMX(K,L)=KMX(K,L)+KXX(I)*DDPC(K,J)*DDPC(L,J)	C	37
	KMY(K,L)=KMY(K,L)+KYY(I)*DDPC(K,J)*DDPC(L,J)	C	38

	L X(K,L)=DOX(K,L)+CXY(I)*DDPC(K,J)*DDPC(L,J)	C	39
	DOY(K,L)=DOY(K,L)+CYX(I)*DDPC(K,J)*DDPC(L,J)	C	40
	EOX(K,L)=EOX(K,L)+KXY(I)*DDPC(K,J)*DDPC(L,J)	C	41
20	EOY(K,L)=EOY(K,L)+KYX(I)*DDPC(K,J)*DDPC(L,J)	C	42
30	CONTINUE	C	43
	IF (NMB.EQ.0) GO TO 50	C	44
	DO 40 I=1,NMB	C	45
	L=LLNMB(I)	C	46
	DO 40 J=1,NNCT	C	47
	DO 40 K=1,NNCT	C	48
	CMX(J,K)=CMX(J,K)+CLNMB(I,1,1)*DDPC(J,L)*DDPC(K,L)+CLNMB(I,1,2)*DDPC(J,L)*EEYTH(K,L)+CLNMB(I,2,1)*EEYTH(J,L)*DDPC(K,L)+CLNMB(I,2,2)*EEYTH(J,L)*EEYTH(K,L)	C	49
	CMY(J,K)=CMY(J,K)+CLNMB(I,3,3)*DDPC(J,L)*DDPC(K,L)+CLNMB(I,3,4)*DDPC(J,L)*EEYTH(K,L)+CLNMB(I,4,3)*EEYTH(J,L)*DDPC(K,L)+CLNMB(I,4,4)*EEYTH(J,L)*EEYTH(K,L)	C	50
	KMX(J,K)=KMX(J,K)+SLNMB(I,1,1)*DDPC(J,L)*DDPC(K,L)+SLNMB(I,1,2)*DDPC(J,L)*EEYTH(K,L)+SLNMB(I,2,1)*EEYTH(J,L)*DDPC(K,L)+SLNMB(I,2,2)*EEYTH(J,L)*EEYTH(K,L)	C	51
	KMY(J,K)=KMY(J,K)+SLNMB(I,3,3)*DDPC(J,L)*DDPC(K,L)+SLNMB(I,3,4)*DDPC(J,L)*EEYTH(K,L)+SLNMB(I,4,3)*EEYTH(J,L)*DDPC(K,L)+SLNMB(I,4,4)*EEYTH(J,L)*EEYTH(K,L)	C	52
	DOX(J,K)=DOX(J,K)+CLNMB(I,1,3)*DDPC(J,L)*DDPC(K,L)+CLNMB(I,1,4)*DDPC(J,L)*EEYTH(K,L)+CLNMB(I,2,3)*EEYTH(J,L)*DDPC(K,L)+CLNMB(I,2,4)*EEYTH(J,L)*EEYTH(K,L)	C	53
	DOY(J,K)=DOY(J,K)+CLNMB(I,3,1)*DDPC(J,L)*DDPC(K,L)+CLNMB(I,3,2)*DDPC(J,L)*EEYTH(K,L)+CLNMB(I,4,1)*EEYTH(J,L)*DDPC(K,L)+CLNMB(I,4,2)*EEYTH(J,L)*EEYTH(K,L)	C	54
	EOX(J,K)=EOX(J,K)+SLNMB(I,1,3)*DDPC(J,L)*DDPC(K,L)+SLNMB(I,1,4)*DDPC(J,L)*EEYTH(K,L)+SLNMB(I,2,3)*EEYTH(J,L)*DDPC(K,L)+SLNMB(I,2,4)*EEYTH(J,L)*EEYTH(K,L)	C	55
	EOY(J,K)=EOY(J,K)+SLNMB(I,3,1)*DDPC(J,L)*DDPC(K,L)+SLNMB(I,3,2)*DDPC(J,L)*EEYTH(K,L)+SLNMB(I,4,1)*EEYTH(J,L)*DDPC(K,L)+SLNMB(I,4,2)*EEYTH(J,L)*EEYTH(K,L)	C	56
40	CONTINUE	C	57
	DO 60 I=1,NNCT	C	58
	MFY(I)=0.	C	59
60	MFY(I)=0.	C	60
		C	61
		C	62
		C	63
		C	64
		C	65
		C	66
		C	67
		C	68
		C	69
		C	70
		C	71
		C	72
		C	73
		C	74
		C	75
		C	76

```

      IF (NNLIN.EQ.0) GO TO 90
      DO 80 I=1,NNCT
      DO 70 J=1,N
70    MFY(I)=MFY(I)+DDPC(I,J)*W(J)
      WMY(I)=MFY(I)
80    CONTINUE
90    CONTINUE
      RETURN
      END

```

```

C 77
C 78
C 79
C 80
C 81
C 82
C 83
C 84
C 85-

```

	SUBROUTINE STAB	D	1
C	*****	D	2
C	THIS SUBROUTINE CALCULATES THE DAMPED NATURAL FREQUENCIES	D	3
C	AND THE STABILITY OF THE ROTOR BEARING SYSTEM USING LEVERRIERS	D	4
C	ALGORITHM.	D	5
C	*****	D	6
	REAL KXX,KXY,KYX,KYY,MFX,MFY,MUX,MUY,KMX,KMY	D	7
	REAL LOD	D	8
	COMMON /BLK1/ N,NB,NNLIN,NMB,NF,NU,NS,NBDW,ISTAB,IMODE,ISKU,NNCT,N	D	9
	1UFPT	D	10
	COMMON /BLK3/ CRT(10),LLBD(10),LLNB(5),LLNMB(9),LLSK(10),LLNT(10),	D	11
	1LLUF(10),LLFF(10),LLUT(10)	D	12
	COMMON /BLK7/ CMX(10,10),KMX(10,10),EMX(10,10),CMY(10,10),KMY(10,1	D	13
	10),EMY(10,10)	D	14
	COMMON /BLK8/ MFX(10),MFY(10),MUX(10),MUY(10),MBX(10),MBY(10)	D	15
	COMMON /BLK9/ DDPC(10,100),EEYTH(10,100)	D	16
	COMMON /BLK10/ SPS,SPF,SPN,SPEED1	D	17
	COMMON /BLK11/ DOX(10,10),DOY(10,10),EOX(10,10),EOY(10,10)	D	18
	COMMON /BLK15/ RP(100),RT(100)	D	19
	COMMON /BLK14/ A(42),U(42),V(42),H(42),B(42),C(42)	D	20
	COMMON AM(40,40),BM(40,40),CM(40,40),DM(40,40),EM(40,40),FM(2)	D	21
	N3=NNCT*4	D	22
	DO 10 I=1,N3	D	23
	DO 10 J=1,N3	D	24
10	AM(I,J)=0.	D	25
	DO 30 I=1,NNCT	D	26
	DO 20 J=1,NNCT	D	27
	I1=I+NNCT	D	28
	J1=J+NNCT	D	29
	I2=I+NNCT*2	D	30
	J2=J+NNCT*2	D	31
	I3=I+NNCT*3	D	32
	J3=J+NNCT*3	D	33
	AM(I,J)=-CMX(I,J)	D	34
	AM(I,J1)=-DOX(I,J)	D	35
	AM(I,J2)=-KMX(I,J)	D	36
	AM(I,J3)=-EOX(I,J)	D	37
	AM(I1,J)=-DOY(I,J)	D	38

ORIGINAL PAGE IS  
OF POOR QUALITY

	AM(I1,J1)=-CMY(I,J)	D	39
	AM(I1,J2)=-EOY(I,J)	D	40
20	AM(I1,J3)=-KMY(I,J)	D	41
	AM(I2,I)=1.	D	42
	AM(I3,I1)=1.	D	43
	AM(I,I2)=AM(I,I2)-(CRT(I)*3.14159/30.)*2	D	44
30	AM(I1,I3)=AM(I1,I3)-(CRT(I)*3.14159/30.)*2	D	45
	RSPEED=SPEED1*3.14159/30.	D	46
	DO 40 I=1,NNCT	D	47
	DO 40 J=1,NNCT	D	48
	I1=I+NNCT	D	49
	J1=J+NNCT	D	50
	J2=J+NNCT*2	D	51
	DO 40 K=1,N	D	52
	AM(I,J1)=AM(I,J1)-RSPEED*RP(K)*EEYTH(I,K)*EEYTH(J,K)/386.4	D	53
40	AM(I1,J)=AM(I1,J)+RSPEED*RP(K)*EEYTH(I,K)*EEYTH(J,K)/386.4	D	54
	N4=NNCT*4	D	55
	TRACE=0.	D	56
	A(N4+1)=1.	D	57
	DO 50 I=1,N4	D	58
50	TRACE=TRACE-AM(I,I)	D	59
	A(N4)=TRACE	D	60
	DO 70 I=1,N4	D	61
	DO 60 J=1,N4	D	62
60	BM(I,J)=AM(I,J)	D	63
70	BM(I,I)=BM(I,I)+TRACE	D	64
	DO 80 I=1,N4	D	65
	OM(I,1)=BM(I,1)	D	66
80	CONTINUE	D	67
	DO 140 K=2,N4	D	68
	K1=N4+1-K	D	69
	TRACE=0.	D	70
	DO 90 I=1,N4	D	71
	DO 90 J=1,N4	D	72
	CM(I,J)=0.	D	73
	DO 90 L=1,N4	D	74
90	CM(I,J)=CM(I,J)+AM(I,L)*BM(L,J)	D	75
	DO 100 I=1,N4	D	76

100	TRACE=TRACE-CM(I,I)	D	77
	TK=K	D	78
	A(K1)=TRACE/TK	D	79
	DO 120 I=1,N4	D	80
	DO 110 J=1,N4	D	81
110	BM(I,J)=CM(I,J)	D	82
120	BM(I,I)=BM(I,I)+A(K1)	D	83
	DO 130 I=1,N4	D	84
	BM(I,K)=BM(I,1)	D	85
130	CONTINUE	D	86
140	CONTINUE	D	87
	NPLUS2=N4+2	D	88
	CALL PROOT (N4,CONV,NPLUS2)	D	89
	WRITE (3,180)	D	90
	WRITE (3,210) SPEED1	D	91
	WRITE (3,190)	D	92
	DO 160 I=1,N4,2	D	93
	K=N4-I+1	D	94
	J=(I+1)/2	D	95
	UNDF=CRT(J)	D	96
	DMF=0.	D	97
	AMF=0.	D	98
	LDD=0.	D	99
	UNF=0.	D	100
	IF (V(K).EQ.0.) GO TO 150	D	101
	IF (U(K).EQ.0.) GO TO 150	D	102
	DMF=V(K)*9.549296	D	103
	AMF=(U(K)*U(K)+V(K)*V(K))/(-2.*U(K)*V(K))	D	104
	LDD=-2.*3.14159*U(K)/V(K)	D	105
	IF (ABS(U(K)).GT.ABS(V(K))) GO TO 150	D	106
	UNF=(U(K)*U(K)+V(K)*V(K))*9.549296/((V(K)*V(K)-U(K)*U(K))**.5)	D	107
150	CONTINUE	D	108
	WRITE (3,200) J,UNDF,U(K),DMF,UNF,AMF,LDD	D	109
160	CONTINUE	D	110
	IF (IMODE.EQ.0) GO TO 170	D	111
	CALL DMODE	D	112
170	CONTINUE	D	113
	RETURN	D	114

ORIGINAL PAGE IS  
OF POOR QUALITY

180	FORMAT (IH1, //)	D 115
190	FORMAT (5X, #MODE#, 4X, #UNDAMPED#, 7X, #DAMPING#, 8X, #DAMPED#, 9X, #UNBAL	D 116
	1ANCE#, 6X, #AMP.#, 11X, #LOG#, /, 5X, #NO.#, 5X, #FREQUENCY#, 6X, #EXPONENT#,	D 117
	27X, #FREQUENCY#, 6X, #FREQUENCY#, 6X, #FACTOR#, 9X, #DECREMENT#, /, 13X, #(R	D 118
	3PM)#, 9X, #(1/SEC)#, 8X, #(RPM)#, 10X, #(RPM)#, 10X, #(DIM)#, 10X, #(DIM)#, /	D 119
	4, 13X, #(AVE. K)#, //)	D 120
200	FORMAT (6X, I2, 5(5X, F10.2), 5X, E10.4)	D 121
210	FORMAT (# SPEED IN RPM = #, F15.2)	D 122
	END	D 123
		D 124-

```

SUBROUTINE PROOT (N,CONV,NPLUS2)
COMMON /BLK14/ A(42),U(42),V(42),H(42),B(42),C(42)
C
C   THIS IS A SUBROUTINE SOLVING FOR THE ROOTS OF A POLYNOMIAL
C
CONV=1.E-35
NC=N+1
C   SEND COEFFICIENTS TO REDUCED COEFFICIENT STORAGE
DO 10 I=1,NC
10  H(I)=A(I)
C   INITIALIZE GUESSES AND SET REVERSAL INDICATOR NORMAL
P=0.
Q=0.
R=0.
IREV=1
C   SCALING TO BE DONE AT THIS POINT
C   REMOVE ALL ZERO ROOTS
20  IF (H(1)) 50,30,50
30  NC=NC-1
V(NC)=0.
U(NC)=0.
DO 40 I=1,NC
40  H(I)=H(I+1)
GO TO 20
C   TEST FOR VARIOUS DEGREES
50  IF (NC-1) 60,460,60
60  IF (NC-2) 80,70,80
70  R=-H(1)/H(2)
GO TO 330
80  IF (NC-3) 100,90,100
90  P=H(2)/H(3)
Q=H(1)/H(3)
GO TO 380
C   TEST TO REVERSE COEFFICIENTS AND DO SO IF TEST SUCCEEDS
100 IF (ABS(H(NC-1)/H(NC))-ABS(H(2)/H(1))) 110,170,170
110 IREV=-IREV
M=NC/2
DO 120 I=1,M

```

```

E 1
E 2
E 3
E 4
E 5
E 6
E 7
E 8
E 9
E 10
E 11
E 12
E 13
E 14
E 15
E 16
E 17
E 18
E 19
E 20
E 21
E 22
E 23
E 24
E 25
E 26
E 27
E 28
E 29
E 30
E 31
E 32
E 33
E 34
E 35
E 36
E 37
E 38

```



```

      NL=NC+1-I
      F=H(NL)
      H(NL)=H(I)
120   H(I)=F
      IF (Q) 140,130,140
130   P=0.
      GO TO 150
140   P=P/Q
      Q=1./Q
150   IF (R) 160,170,160
160   R=1./R
C     NEWTON, CALCULATE F(R) AND TEST FOR ROOT
170   E=5.E-20
      B(NC)=H(NC)
      C(NC)=H(NC)
      B(NC+1)=0.
      C(NC+1)=0.
      NP=NC-1
180   DO 310 J=1,1000
      DO 190 I1=1,NP
      I=NC-I1
      B(I)=H(I)+R*B(I+1)
190   C(I)=B(I)+R*C(I+1)
      IF (ABS(B(1)/H(1))-E) 330,330,200
200   IF (C(2)) 220,210,220
210   R=R+1.
      GO TO 230
220   R=R-B(1)/C(2)
C     MAKE A BAIRSTOW REDUCTION AND CORRECT
230   DO 240 I1=1,NP
      I=NC-I1
      B(I)=H(I)-P*B(I+1)-Q*B(I+2)
240   C(I)=B(I)-P*C(I+1)-Q*C(I+2)
C     TEST FOR CONVERGENCE OF BAIRSTOW PROCESS.
      IF (H(2)) 260,250,260
250   IF (ABS(B(2)/H(1))-E) 270,270,280
260   IF (ABS(B(2)/H(2))-E) 270,270,280
270   IF (ABS(B(1)/H(1))-E) 380,380,280

```

```

E 39
E 40
E 41
E 42
E 43
E 44
E 45
E 46
E 47
E 48
E 49
E 50
E 51
E 52
E 53
E 54
E 55
E 56
E 57
E 58
E 59
E 60
E 61
E 62
E 63
E 64
E 65
E 66
E 67
E 68
E 69
E 70
E 71
E 72
E 73
E 74
E 75
E 76

```

280	CBAR=C(2)-B(2)	E	77
	D=C(3)**2-CBAR*C(4)	E	78
	IF (D) 300,290,300	E	79
290	P=P-2.	E	80
	Q=Q*(Q+1.)	E	81
	GO TO 310	E	82
300	P=P+(B(2)*C(3)-B(1)*C(4))/D	E	83
	Q=Q+(-B(2)*CBAR+B(1)*C(3))/D	E	84
310	CONTINUE	E	85
	E=E*10.	E	86
	IF (E-CONV) 180,180,320	E	87
320	CONV=E	E	88
	GO TO 180	E	89
C	LINEAR. COMPUTE AND STORE LINEAR ROOTS	E	90
330	NC=NC-1	E	91
	V(NC)=0.	E	92
	IF (IREV) 340,350,350	E	93
340	U(NC)=1./R	E	94
	GO TO 360	E	95
350	U(NC)=R	E	96
360	DO 370 I=1,NC	E	97
370	H(I)=B(I+1)	E	98
	GO TO 50	E	99
C	QUADRATIC. SOLVE QUADRATIC AND STORE ROOTS	E	100
380	NC=NC-2	E	101
	IF (IREV) 390,400,400	E	102
390	QP=1./Q	E	103
	PP=P/(Q*2.0)	E	104
	GO TO 410	E	105
400	QP=Q	E	106
	PP=P/2.0	E	107
410	F=(PP)**2-QP	E	108
	IF (F) 420,430,430	E	109
C	CASE OF IMAGINARY ROOTS.	E	110
420	U(NC+1)=-PP	E	111
	U(NC)=-PP	E	112
	V(NC+1)=SQRT(-F)	E	113
	V(NC)=-V(NC+1)	E	114

```

      GO TO 440
C     CASE OF REAL ROOTS.
430   U(NC+1)=-SIGN(ABS(PP)+SORT(F),PP)
      V(NC+1)=0.
      U(NC)=QP/U(NC+1)
      V(NC)=0.
C     FORM NEW REDUCED COEFFICIENTS
440   DO 450 I=1,NC
450   H(I)=B(I+2)
      GO TO 50
460   RETURN
      END

```

```

E 115
E 116
E 117
E 118
E 119
E 120
E 121
E 122
E 123
E 124
E 125
E 126-

```

	SUBROUTINE DMODE	F	1
C	*****	F	2
C	THIS SUBROUTINE CALCULATES THE DAMPED MODE SHAPES OF THE SYSTEM	F	3
C	USING THE LEVERRIERS ALGORITHM.	F	4
C	*****	F	5
	COMPLEX SMODE(2,100), SHAPE(40), C1, C2, C3	F	6
	COMPLEX CD(40)	F	7
	DIMENSION Z(100), P(100)	F	8
	COMMON /BLK1/ N, NB,>NNLIN, NMB, NF, NU, NS, NBDW, ISTAB, IMODE, ISKU, NNCT, N	F	9
	1UFPT	F	10
	COMMON /BLK9/ DCPC(10,100), EEYTH(10,100)	F	11
	COMMON /BLK14/ AA(42), U(42), V(42), H(42), BB(42), CC(42)	F	12
	COMMON A(40,40), B(40,40), C(40,40), D(40,40), E(40,40), FM(2)	F	13
	N4=NNCT*4	F	14
	DO 110 I=1, IMODE	F	15
	KK=N4-2*I+2	F	16
	IF (ABS(V(KK)).LT.1.) GO TO 110	F	17
	C1=CMPLX(U(KK), V(KK))	F	18
	C2=1./C1	F	19
	N3=N4-1	F	20
	DO 10 J=1, N4	F	21
10	SHAPE(J)=CMPLX(0., 0.)	F	22
	SHAPE(1)=CMPLX(1., 0.)	F	23
	DO 50 J=1, N3	F	24
	DO 20 K=1, N4	F	25
20	CD(K)=CMPLX(D(K, J), 0.)	F	26
	DO 30 L=1, N4	F	27
	DO 30 K=1, J	F	28
	CD(L)=CD(L)*C2	F	29
30	CONTINUE	F	30
	DO 40 K=1, N4	F	31
40	SHAPE(K)=SHAPE(K)+CD(K)	F	32
50	CONTINUE	F	33
	DO 60 J=1, N	F	34
	SMODE(1, J)=CMPLX(0., 0.)	F	35
60	SMODE(2, J)=CMPLX(0., 0.)	F	36
	N2=N4/2	F	37
	N1=N2/2	F	38

ORIGINAL PAGE IS  
OF POOR QUALITY

	DO 80 J=1,N1	F	39
	JL=J+N2	F	40
	JM=J+N2+N1	F	41
	DO 70 K=1,N	F	42
	SMDDE(1,K)=SMDDE(1,K)+SHAPE(JL)*DDPC(J,K)	F	43
70	SMDDE(2,K)=SMDDE(2,K)+SHAPE(JM)*DDPC(J,K)	F	44
60	CONTINUE	F	45
	ZMAX=0.	F	46
	DO 90 J=1,N	F	47
	D1=REAL(SMDDE(1,J))	F	48
	D2=REAL(SMDDE(2,J))	F	49
	Z(J)=SQRT(D1*D1+D2*D2)	F	50
	P(J)=57.295779*ATAN2(-D2,D1)	F	51
	IF (ZMAX.GT.Z(J)) GO TO 90	F	52
	ZMAX=Z(J)	F	53
90	CONTINUE	F	54
	VI=9.549296*V(KK)	F	55
	WRITE (3,120) U(KK),V(KK),VI	F	56
	WRITE (3,130)	F	57
	DO 100 J=1,N	F	58
	X1=REAL(SMDDE(1,J))/ZMAX	F	59
	X2=AIMAG(SMDDE(1,J))/ZMAX	F	60
	X3=REAL(SMDDE(2,J))/ZMAX	F	61
	X4=AIMAG(SMDDE(2,J))/ZMAX	F	62
	TMAJ=(.5*(X1*X1+X2*X2+X3*X3+X4*X4)+(.25*(X1*X1+X2*X2-X3*X3-X4*X4)*	F	63
	1*2+(X1*X3+X2*X4)**2)**.5)**.5	F	64
	TMIN=(X2*X3-X1*X4)/TMAJ	F	65
	CON1=2.*(X1*X3+X2*X4)	F	66
	CON2=(X1*X1+X2*X2-X3*X3-X4*X4)	F	67
	PHASE=.5*57.29578*ATAN2(CON1,CON2)	F	68
	IF (PHASE.LT.0) PHASE=PHASE+360.	F	69
	ZDIM=Z(J)/ZMAX	F	70
	WRITE (3,140) J,TMAJ,TMIN,PHASE,P(J),ZDIM	F	71
100	CONTINUE	F	72
110	CONTINUE	F	73
	RETURN	F	74
C		F	75
120	FORMAT (1H1,///,10X,#EIGENVECTOR FOR EIGENVALUE=#,F10.2,#+#,F10.2,	F	76

	1#I	DAMPED FREQUENCY=#,F12.2,#RPM#)	F	77
130	FORMAT (/ ,5X,#STATION#,3X,#MAJOR AXIS#,5X,#MINOR AXIS#,5X,#ELLIPSE		F	76
	1# ,8X,#PHASE#,10X,#ROTOR#,/,5X,#NO.#,37X,#ANGLE#,10X,#ANGLE#,10X,#A		F	79
	2#PLITUDE#,,//)		F	80
140	FORMAT (5X,I3,7X,5(F10.3,5X))		F	81
	END		F	82-

ORIGINAL PAGE IS  
OF POOR QUALITY

	SUBROUTINE UBST (IND,SD)	G	1
C	*****	G	2
C	THIS SUBROUTINE CALCULATES THE UNBALANCE RESPONSE OF ROTOR SYSTEM	G	3
C	USING THE PLARAK MODES. WHICH CAN LATER BE TRANSFORMED INTO REAL	G	4
C	DISPLACEMENTS.	G	5
C	*****	G	6
	REAL MBX,MBY	G	7
	DIMENSION SPED(50)	G	8
	COMPLEX B,C,DUM	G	9
	COMPLEX EUM	G	10
	REAL KXX,KXY,KYX,KYY,MFX,MFY,MUX,MUY,KMX,KMY	G	11
	COMMON /BLK1/ N,NB,NNLIN,NMB,NF,NU,NS,NBOW,ISTAB,IMODE,ISKU,NNCT,N	G	12
	10FPT	G	13
	COMMON /BLK3/ CRT(10),LLBD(10),LLNB(5),LLNMB(9),LLSK(10),LLNT(10),	G	14
	1LLUF(10),LLFF(10),LLUT(10)	G	15
	COMMON /BLK5/ UX(10),UY(10),FX(10),FY(10),FSK(10),PSK(10)	G	16
	COMMON /BLK7/ CMX(10,10),KMX(10,10),EMX(10,10),CMY(10,10),KMY(10,1	G	17
	10),EMY(10,10)	G	18
	COMMON /BLK8/ MFX(10),MFY(10),MUX(10),MUY(10),MBX(10),MBY(10)	G	19
	COMMON /BLK9/ DDPC(10,100),EEYTH(10,100)	G	20
	COMMON /BLK10/ SPS,SPF,SPH,SPEED1	G	21
	COMMON /BLK11/ DDY(10,10),DDY(10,10),EDX(10,10),EDY(10,10)	G	22
	COMMON /BLK15/ RP(100),RT(100)	G	23
	COMMON /BLK12/ AKK(10)	G	24
	COMMON /BLK21/ EMX(10,10),DMY(10,10)	G	25
	COMMON /BLK24/ B(20,21),C(20)	G	26
	COMMON UDISPYR(10,50),UDISPYT(10,50),UDISPYF(10,50),UDISPYI(10,50)	G	27
	1,XMAJ(10,50),XMIN(10,50),PMAJ(10,50),PMIN(10,50),ADUMMY(4002)	G	28
	SPI=SPN	G	29
	IJ=1	G	30
	DO 170 JSP=1,50	G	31
	IF (IND.EQ.1) GO TO 10	G	32
	SP=SPS+(JSP-1)*SPI	G	33
	IF (SP.GT.SPF) GO TO 180	G	34
	ANGSP=SP*3.14159/30.	G	35
	SPED(IJ)=SP	G	36
	GO TO 20	G	37
10	ANGSP=SD*3.14159/30.	G	38

20	CONTINUE	G	39
	NN=NNCT*2	G	40
	MM=NNCT*2+1	G	41
	DUM=CMPLX(0.,1.)	G	42
	EUM=CMPLX(1.,0.)	G	43
	DO 30 I=1,NNCT	G	44
	MUX(I)=0.	G	45
	MUY(I)=0.	G	46
30	CONTINUE	G	47
	IF (NU.EQ.0) GO TO 60	G	48
	DO 50 I=1,NU	G	49
	J=LLUF(I)	G	50
	DO 40 K=1,NNCT	G	51
	MUX(K)=MUX(K)+ANGSP*ANGSP*UX(I)*DDPC(K,J)	G	52
	MUY(K)=MUY(K)+ANGSP*ANGSP*UY(I)*DDPC(K,J)	G	53
40	CONTINUE	G	54
50	CONTINUE	G	55
60	IF (NS.EQ.0) GO TO 90	G	56
	DO 80 I=1,NS	G	57
	J=LLSK(I)	G	58
	PAS=FSK(I)/57.29576	G	59
	PCOS=COS(PAS)	G	60
	PSIN=SIN(PAS)	G	61
	DO 70 K=1,NNCT	G	62
	MUX(K)=MUX(K)+ANGSP*ANGSP*FSK(I)*PCOS*(RP(J)-RT(J))*EEYTH(K,J)/386	G	63
	1.4	G	64
70	MUY(K)=MUY(K)+ANGSP*ANGSP*FSK(I)*PSIN*(RP(J)-RT(J))*EEYTH(K,J)/386	G	65
	1.4	G	66
80	CONTINUE	G	67
90	CONTINUE	G	68
	IF (NBOX.EQ.0) GO TO 110	G	69
	DO 100 I=1,NNCT	G	70
	MUX(I)=MUX(I)+MBX(I)	G	71
100	MUY(I)=MUY(I)+MBY(I)	G	72
110	CONTINUE	G	73
	DO 120 K=1,NNCT	G	74
	DO 120 L=1,NNCT	G	75
	EMX(K,L)=EOM(K,L)	G	76



	EMY(K,L)=E0Y(K,L)	G 77
	DMX(K,L)=D0X(K,L)	G 78
	DMY(K,L)=D0Y(K,L)	G 79
	DO 120 J=1,N	G 80
	DMX(K,L)=DMX(K,L)+ANGSP*RP(J)*EEYTH(K,J)*EEYTH(L,J)/386.4	G 81
	DMY(K,L)=DMY(K,L)-ANGSP*RP(J)*EEYTH(K,J)*EEYTH(L,J)/386.4	G 82
120	CONTINUE	G 83
	DO 140 I=1,10	G 84
	DO 130 J=1,11	G 85
130	B(I,J)=CMPLX(0.,0.)	G 86
140	C(I)=CMPLX(0.,0.)	G 87
	DO 160 I=1,NNCT	G 88
	II=I+NNCT	G 89
	DO 150 J=1,NNCT	G 90
	JJ=J+NNCT	G 91
	B(I,J)=B(I,J)+KMx(I,J)*EUM+CMX(I,J)*DUM*ANGSP	G 92
	B(II,J)=B(II,J)+EMY(I,J)*EUM+DMY(I,J)*DUM*ANGSP	G 93
	B(I,JJ)=B(I,JJ)+EMX(I,J)*EUM+DMX(I,J)*DUM*ANGSP	G 94
150	B(II,JJ)=B(II,JJ)+KMY(I,J)*EUM+CMY(I,J)*DUM*ANGSP	G 95
	B(I,I)=B(I,I)+((CRT(I)*3.14159/30.)**2-ANGSP**2)*EUM	G 96
	B(II,II)=B(II,II)+((CRT(I)*3.14159/30.)**2-ANGSP**2)*EUM	G 97
	NEX=NNCT*2+1	G 98
	B(I,NEX)=-CMPLX(MUX(I),MUY(I))	G 99
160	B(II,NEX)=-CMPLX(MUY(I),-MUX(I))	G 100
	CALL SOLVE (NN,MM)	G 101
	IF (IND.EQ.1) RETURN	G 102
	CALL ELLIP (NN,IJ)	G 103
	IJ=IJ+1	G 104
170	CONTINUE	G 105
180	CONTINUE	G 106
	NPP=IJ-1	G 107
	CALL UPRINT (NPP,SPED)	G 108
	RETURN	G 109
	END	G 110-

```

SUBROUTINE SOLVE (NN,MM)
COMPLEX B,C,DUMMY,CONJG
COMMON /BLK24/ B(20,21),C(20)
DO 80 I=1,NN
K=1
10 IF (CABS(B(K,I)).GT.0.000001) GO TO 20
K=K+1
IF (K=NN) 10,10,90
20 IF (I=K) 30,50,90
30 DO 40 M=1,MM
DUMMY=B(I,M)
B(I,M)=B(K,M)
40 B(K,M)=DUMMY
50 II=I+1
IF (II.GT.NN) GO TO 80
DO 70 N=II,NN
IF (CABS(B(N,I)).LT.0.000001) GO TO 70
SQ=(CABS(B(I,I)))**2
DUMMY=B(N,I)*CONJG(B(I,I))/SQ
DO 60 M=1,MM
60 B(N,M)=B(N,M)-B(I,M)*DUMMY
70 CONTINUE
80 CONTINUE
GO TO 100
90 IF (I.EQ.NN) WRITE (3,150)
IF (I.LT.NN) WRITE (3,160)
STOP
C
START BACK SUBSTITUTIONS
100 I=NN
110 DUMMY=(C.0,C.0)
IF (I.EQ.NN) GO TO 130
JJJ=I+1
DO 120 J=JJJ,NN
120 DUMMY=DUMMY+B(I,J)*C(J)
130 SQ=(CABS(B(I,I)))**2
C(I)=- (DUMMY+B(I,MM))*CONJG(B(I,I))/SQ
I=I-1
IF (I) 140,140,110

```

H	1
H	2
H	3
H	4
H	5
H	6
H	7
H	8
H	9
H	10
H	11
H	12
H	13
H	14
H	15
H	16
H	17
H	18
H	19
H	20
H	21
H	22
H	23
H	24
H	25
H	26
H	27
H	28
H	29
H	30
H	31
H	32
H	33
H	34
H	35
H	36
H	37
H	38

ORIGINAL PAGE IS  
OF POOR QUALITY

140 RETURN  
C  
150 FJRMAT (4X,19HMATRIX HAS ZERO ROW)  
160 FJRMAT (4X,22HMATRIX HAS ZERO COLUMN)  
END

H 39  
H 40  
H 41  
H 42  
H 43-

	SUBROUTINE ELLIP (NN,IJ)	I	1
C	*****	I	2
C	THIS CALCULATES THE REAL DISPLACEMENTS FROM MEDAL COORDINATES	I	3
C	AND THE INTO ELLIPTICAL ORBITS. ALSO CALCULATES THE PHASE ANGLES	I	4
C	WITH PROBES AT X-DIR AND Y-DIR.	I	5
C	*****	I	6
	COMPLEX B,C	I	7
	COMMON /BLK1/ N,NB,NNLIN,NMB,NF,NU,NS,NBDW,ISTAB,IMEDE,ISKU,NNCT,N	I	8
	1UFPT	I	9
	COMMON /BLK3/ CRT(10),LLBD(10),LLNB(5),LLNMB(9),LLSK(10),LLNT(10),	I	10
	1LLUF(10),LLFF(10),LLUT(10)	I	11
	COMMON /BLK9/ DDPC(10,100),EEYTH(10,100)	I	12
	COMMON /BLK24/ B(20,21),C(20)	I	13
	COMMON UDISPXR(10,50),UDISPXI(10,50),UDISPYR(10,50),UDISPYI(10,50)	I	14
	1,XMAJ(10,50),XMIN(10,50),PMAJ(10,50),PMIN(10,50),ADUMMY(4002)	I	15
	DO 10 I=1,10	I	16
	XMAJ(I,IJ)=0.	I	17
	XMIN(I,IJ)=0.	I	18
	PMAJ(I,IJ)=0.	I	19
10	PMIN(I,IJ)=0.	I	20
	DO 50 I=1,NUFPT	I	21
	II=LLUT(I)	I	22
	X1=0.	I	23
	X2=0.	I	24
	X3=0.	I	25
	X4=0.	I	26
	NNCT=NN/2	I	27
	DO 20 J=1,NNCT	I	28
	JJ=J+NNCT	I	29
	C1=REAL(C(JJ))	I	30
	C2=AIMAG(C(JJ))	I	31
	C3=REAL(C(JJ))	I	32
	C4=AIMAG(C(JJ))	I	33
	X1=X1+C1*DDPC(J,II)*1000.	I	34
	X2=X2+C2*DDPC(J,II)*1000.	I	35
	X3=X3+C3*DDPC(J,II)*1000.	I	36
20	X4=X4+C4*DDPC(J,II)*1000.	I	37
	UDISPXR(I,IJ)=X1	I	38

	UDISPXI(I,IJ)=X2	I	39
	UDISPYK(I,IJ)=X3	I	40
	UDISPYI(I,IJ)=X4	I	41
	XMAJ(I,IJ)=(.5*(X1*X1+X2*X2+X3*X3+X4*X4)+(.25*(X1*X1+X2*X2-X3*X3-X	I	42
	14*X4)**2+(X1*X3+X2*X4)**2)**5)**5	I	43
	XMIN(I,IJ)=(X2*X3-X1*X4)/XMAJ(I,IJ)	I	44
	CON1=2.*(X1*X3+X2*X4)	I	45
	CON2=(X1*X1+X2*X2-X3*X3-X4*X4)	I	46
	IF (CON2.EQ.0.) GO TO 30	I	47
	PMAJ(I,IJ)=.5*57.29578*ATAN2(CON1,CON2)	I	48
	GO TO 40	I	49
30	PMAJ(I,IJ)=0.	I	50
40	CONTINUE	I	51
	IF (PMAJ(I,IJ).LT.0.) PMAJ(I,IJ)=PMAJ(I,IJ)+360.	I	52
50	CONTINUE	I	53
	RETURN	I	54
	END	I	55-

	SUBROUTINE UPRINT (NPP,SPED)	J	1
C	*****	J	2
C	THIS SUBROUTINE PRINT OUT THE UNBALANCE RESPONSE OF THE ROTOR AND	J	3
C	ITS CORRESPONDING ELLIPTICAL ORBITS.	J	4
C	*****	J	5
	DIMENSION SPED(50)	J	6
	COMMON /BLK1/ N,NB,NNLIN,NMB,NF,NU,NS,NBOW,ISTAB,IMODE,ISKU,NNCT,N	J	7
	1UFPT	J	8
	COMMON /BLK3/ CRT(10),LLBD(10),LLNB(5),LLNMB(9),LLSK(10),LLNT(10),	J	9
	1LLUF(10),LLFF(10),LLUT(10)	J	10
	COMMON UDISPXR(10,50),UDISPXI(10,50),UDISPYR(10,50),UDISPYI(10,50)	J	11
	1,XMAJ(10,50),XMIN(10,50),PMAJ(10,50),PMIN(10,50),ADUMMY(4002)	J	12
	DO 20 II=1,NUFPT	J	13
	NTB=LLUT(II)	J	14
	WRITE (3,80) NTB	J	15
	WRITE (3,50)	J	16
	DO 10 JJ=1,NPP	J	17
	P=PANG(UDISPYI(II,JJ),UDISPYR(II,JJ))	J	18
	PA=CGS(P*3.14159/180.)	J	19
	R=UDISPYI(II,JJ)/PA	J	20
	WRITE (3,60) SPED(JJ),UDISPXR(II,JJ),UDISPXI(II,JJ),UDISPYR(II,JJ)	J	21
	1,UDISPYI(II,JJ)	J	22
10	CONTINUE	J	23
20	CONTINUE	J	24
	DO 40 II=1,NUFPT	J	25
	NTB=LLUT(II)	J	26
	WRITE (3,80) NTB	J	27
	WRITE (3,70)	J	28
	DO 30 JJ=1,NPP	J	29
	PX=57.29578*ATAN2(-UDISPXI(II,JJ),UDISPXR(II,JJ))	J	30
	PY=57.29578*ATAN2(-UDISPYR(II,JJ),-UDISPYI(II,JJ))	J	31
30	WRITE (3,90) SPED(JJ),XMAJ(II,JJ),XMIN(II,JJ),PMAJ(II,JJ),PX,PY	J	32
40	CONTINUE	J	33
	RETURN	J	34
C		J	35
50	FORMAT (//,9X,*,SPEED*,10X,*,X-REAL*,10X,*,X-IMAG*,10X,*,Y-REAL*,10X,*,	J	36
	1Y-IMAG*)	J	37
60	FORMAT (5X,F10.0,4(5X,F10.5))	J	38

70	FORMAT (//,9X,#SPEED#,8X,#MAJOR AXIS#,8X,#MINOR AXIS#,2X,#	MAJOR	J	39
	1 AXIS ANGLE#,5X,#PROBE AT X#,5X,#PROBE AT Y#,/,9X,#(RPM)#,12X,#(MI		J	40
	2LS)#,10X,#(MILS)#,10X,#DEGREES#,10X,#PHASE DEG#,8X,#PHASE DEG#,/)		J	41
80	FORMAT (1H1,//,#	UNBALANCE RESPONSE OF STATION NO.#,I5,/)	J	42
90	FORMAT (5X,F10.0,6(4X,F13.5))		J	43
	END		J	44-

	FUNCTION PANG (AFCS,AFSN)	K	1
C		K	2
C	* THIS IS A FUNCTION USED TO CALCULATE THE ANGLE	K	3
C	* WHOSE ARCTAN VALUE IS GIVEN *****	K	4
C		K	5
	ACS=AFCS	K	6
	ASN=AFSN	K	7
	IF (ASN) 40,10,40	K	8
10	IF (ACS) 20,30,30	K	9
20	ANG=180.0	K	10
	GO TO 120	K	11
30	ANG=0.0	K	12
	GO TO 120	K	13
40	IF (ACS) 90,50,80	K	14
50	IF (ASN) 60,30,70	K	15
60	ANG=270.	K	16
	GO TO 120	K	17
70	ANG=90.	K	18
	GO TO 120	K	19
80	ANG=0.	K	20
	GO TO 100	X	21
90	ANG=-180.	K	22
100	ASN=ASN/ACS	K	23
	ACS=ABS(ASN)	K	24
	ACS=ATAN(ACS)	K	25
	ANG=ANG+ACS*57.295780	K	26
	IF (ASN) 110,120,120	K	27
110	ANG=-ANG	K	28
120	IF (ANG) 130,140,140	K	29
130	ANG=ANG+360.	K	30
140	PANG=ANG	K	31
	RETURN	K	32
	END	K	33-



	SUBROUTINE SFTBOW	L	1
C	*****	L	2
C	THIS SUBROUTINE CALCULATES THE SHAFT BOW EFFECTS INTO MODAL	L	3
C	COORDINATES. (FOR INITIAL CONDITIONS AND UNBALANCE EFFEC	L	4
C	*****	L	5
	DIMENSION BX(100), BY(100)	L	6
	DIMENSION X(10), Y(10), Z(10,10)	L	7
	REAL MBX,MBY	L	8
	COMMON /BLK1/ N,NB,NNLIN,NMB,NF,NU,NS,NBOW,ISTAB,IMODE,ISKU,NNCT,N	L	9
	1UFPT	L	10
	COMMON /BLK3/ CRT(10),LLBD(10),LLNB(5),LLNMB(9),LLSK(10),LLNT(10),	L	11
	1LLUF(10),LLFF(10),LLUT(10)	L	12
	COMMON /BLK6/ BOW(100),PBOW(100),XIDC(100),YIDC(100),VXIDC(100),VY	L	13
	1IDC(100),BXA(100),BYA(100)	L	14
	COMMON /BLK8/ MFX(10),MEY(10),MUX(10),MUY(10),MBX(10),MBY(10)	L	15
	COMMON /BLK9/ DDPC(10,100),EEYTH(10,100)	L	16
	COMMON /BLK15/ RP(100),RT(100)	L	17
	COMMON /BLK18/ AKK(10)	L	18
	COMMON /BLK19/ DX(100)	L	19
	COMMON /BLK22/ W(100)	L	20
	DO 10 I=1,N	L	21
	CT=PBOW(I)*3.14159/180.	L	22
	BX(I)=BOW(I)*COS(CT)/1000.	L	23
10	BY(I)=BOW(I)*SIN(CT)/1000.	L	24
	TC=(BX(2)-BX(1))/DX(1)	L	25
	TD=(BY(2)-BY(1))/DX(1)	L	26
	BXA(1)=ATAN(TC)	L	27
	BYA(1)=ATAN(TD)	L	28
	TC=(BX(N)-BX(N-1))/DX(N-1)	L	29
	TD=(BY(N)-BY(N-1))/DX(N-1)	L	30
	BXA(N)=ATAN(TC)	L	31
	BYA(N)=ATAN(TD)	L	32
	N1=N-1	L	33
	DO 20 I=2,N1	L	34
	TC=(BX(I+1)-BX(I-1))/(DX(I-1)+DX(I))	L	35
	TD=(BY(I+1)-BY(I-1))/(DX(I-1)+DX(I))	L	36
	BXA(I)=ATAN(TC)	L	37
	BYA(I)=ATAN(TD)	L	38

20	CONTINUE	L	39
	DO 60 I=1,NNCT	L	40
	X(I)=0.	L	41
	Y(I)=0.	L	42
	DO 40 J=1,NNCT	L	43
	Z(I,J)=0.	L	44
	DO 30 K=1,NB	L	45
	L=LLBD(K)	L	46
30	Z(I,J)=Z(I,J)-DDPC(I,L)*AKK(K)*DDPC(J,L)	L	47
40	CONTINUE	L	48
	DO 50 K=1,N	L	49
	X(I)=X(I)+(DDPC(I,K)*W(K)*BX(K)+EEYTH(I,K)*RT(K)*BXA(K))/386.4	L	50
50	Y(I)=Y(I)+(DDPC(I,K)*W(K)*BY(K)+EEYTH(I,K)*RT(K)*BYA(K))/386.4	L	51
60	Z(I,I)=Z(I,I)+(CRT(I)*0.1047197)**2	L	52
	DO 70 I=1,NNCT	L	53
	MBX(I)=0.	L	54
	MBY(I)=0.	L	55
	DO 70 J=1,NNCT	L	56
	MBX(I)=MBX(I)+Z(I,J)*X(J)	L	57
70	MBY(I)=MBY(I)+Z(I,J)*Y(J)	L	58
	RETURN	L	59
	END	L	60-

ORIGINAL PAGE IS  
OF POOR QUALITY

C-4

	SUBROUTINE TMODE2 (T, DELTAT, SPEED, NK)	M	1
C	*****	M	2
C	THIS SUBROUTINE CALCULATES THE MODAL COEFFICIENTS FOR TRANSIENT	M	3
C	RESPONSE ANALYSIS	M	4
C	*****	M	5
	REAL MBX, MBY	M	6
	REAL KXX, KXY, KYX, KYY, MFX, MFY, MUX, MUY, KMX, KMY	M	7
	COMMON /BLK1/ N, NB, NNLIN, NMB, NF, NU, NS, NBDW, ISTAB, IMODE, ISKU, NNCT, N	M	8
	1UFPT	M	9
	COMMON /BLK2/ ISKIP, NSTEP, NCYCLE, NITP, NINT, NPLT, NORBIT, NTIME, NSPE	M	10
	IED, NINC, NOPT, NT	M	11
	COMMON /BLK3/ CRT(10), LLBD(10), LLNB(5), LLNMB(9), LLSK(10), LLNT(10),	M	12
	1LLUF(10), LLFF(10), LLUT(10)	M	13
	COMMON /BLK5/ UX(10), UY(10), FX(10), FY(10), FSK(10), PSK(10)	M	14
	COMMON /BLK6/ BDW(100), PBDW(100), XIDC(100), YIDC(100), VXIDC(100), VY	M	15
	1IDC(100), BXA(100), BYA(100)	M	16
	COMMON /BLK7/ CMX(10,10), KMX(10,10), EMX(10,10), CMY(10,10), KMY(10,1	M	17
	10), EMY(10,10)	M	18
	COMMON /BLK8/ MFX(10), MFY(10), MUX(10), MUY(10), MBX(10), MBY(10)	M	19
	COMMON /BLK9/ DDPC(10,100), EETH(10,100)	M	20
	COMMON /BLK11/ DOX(10,10), DDOY(10,10), EDOX(10,10), EDOY(10,10)	M	21
	COMMON /BLK15/ RP(100), RT(100)	M	22
	COMMON /BLK16/ SPEED2, ANGSP, ANGACL, FSPEED	M	23
	COMMON /BLK18/ AKK(10)	M	24
	COMMON /BLK21/ DMX(10,10), DMY(10,10)	M	25
	COMMON /BLK29/ PASP	M	26
	PI=3.14159	M	27
	ANGSP=SPEED*PI/30.	M	28
	DO 10 I=1, NNCT	M	29
	MUX(I)=0.	M	30
	MUY(I)=0.	M	31
	MFX(I)=0.	M	32
10	MFY(I)=0.	M	33
	IF (NU.EQ.0) GO TO 40	M	34
	DO 30 I=1, NU	M	35
	J=LLUF(I)	M	36
	PHI=ATAN2(UY(I), UX(I))	M	37
	DMT=ANGSP*T+PHI	M	38

	IF (NK.EQ.0) DMT=PASP+PHI	M	39
	TME=(UX(I)*UX(I)+UY(I)*UY(I))*0.5	M	40
	DO 20 K=1,NNCT	M	41
	MUX(K)=MUX(K)+(ANGACL*SIN(DMT)+ANGSP*ANGSP*COS(DMT))*TME*DDPC(K,J)	M	42
20	MUY(K)=MUY(K)+(ANGSP*ANGSP*SIN(DMT)-ANGACL*COS(DMT))*TME*DDPC(K,J)	M	43
30	CONTINUE	M	44
40	IF (NS.EQ.0) GO TO 60	M	45
	TIME=T	M	46
	DO 50 I=1,NS	M	47
	KK=LLSK(I)	M	48
	CAN=ANGSP*TIME+PSK(I)/57.29578	M	49
	IF (NK.EQ.0) CAN=PASP+PSK(I)/57.29578	M	50
	DO 50 J=1,NNCT	M	51
	MUX(J)=MUX(J)+(ANGSP*ANGSP*COS(CAN)+ANGACL*SIN(CAN))*FSK(I)*(RP(KK	M	52
	1)-RT(KK))*EEYTH(J,KK)/386.4	M	53
50	MUY(J)=MUY(J)+(ANGSP*ANGSP*SIN(CAN)-ANGACL*COS(CAN))*FSK(I)*(RP(KK	M	54
	1)-RT(KK))*EEYTH(J,KK)/386.4	M	55
60	IF (NBOW.EQ.0) GO TO 80	M	56
	DO 70 I=1,NNCT	M	57
	TMAG=(MBY(I)**2+MBX(I)**2)**0.5	M	58
	ANG=ATAN2(MBY(I),MBX(I))	M	59
	TANG=ANG+T*ANGSP	M	60
	IF (NK.EQ.0) TANG=PASP+ANG	M	61
	MUX(I)=MUX(I)+TMAG*COS(TANG)	M	62
70	MUY(I)=MUY(I)+TMAG*SIN(TANG)	M	63
80	CONTINUE	M	64
	IF (NK.EQ.1) GO TO 100	M	65
	DO 90 K=1,NNCT	M	66
	DO 90 L=1,NNCT	M	67
	EMX(K,L)=EGX(K,L)	M	68
	EMY(K,L)=EOY(K,L)	M	69
	DMX(K,L)=DOX(K,L)	M	70
	DMY(K,L)=DOY(K,L)	M	71
	DO 90 J=1,N	M	72
	EMX(K,L)=EMX(K,L)+0.5*ANGACL*RP(J)*EEYTH(K,J)*EEYTH(L,J)/386.4	M	73
	EMY(K,L)=EMY(K,L)-0.5*ANGACL*RP(J)*EEYTH(K,J)*EEYTH(L,J)/386.4	M	74
	DMX(K,L)=DMX(K,L)+ANGSP*RP(J)*EEYTH(K,J)*EEYTH(L,J)/386.4	M	75
90	DMY(K,L)=DMY(K,L)-ANGSP*RP(J)*EEYTH(K,J)*EEYTH(L,J)/386.4	M	76

100

SPEED=SPEED+30.\*ANGACL\*DELTAT/PI  
CONTINUE  
RETURN  
END

M 77  
M 78  
M 79  
M 80-

	SUBROUTINE TACCEL	N	1
C	*****	N	2
C	THIS SUBROUTINE CALCULATES THE MODAL ACCELERATION BY SOLVING	N	3
C	THE MODAL EQUATIONS OF MOTION	N	4
C	*****	N	5
	REAL KXX,KXY,KYX,KYY,MFX,MFY,MUX,MUY,KMX,KMY	N	6
	COMMON /BLK1/ N,NB,NNLIN,NMB,NF,NU,NS,NBOW,ISTAB,IMODE,ISKU,NNCT,N	N	7
	1UFPT	N	8
	COMMON /BLK3/ CRT(10),LLBD(10),LLNB(5),LLNMB(9),LLSK(10),LLNT(10),	N	9
	1LLUF(10),LLFF(10),LLUT(10)	N	10
	COMMON /BLK7/ CMX(10,10),KMX(10,10),EMX(10,10),CMY(10,10),KMY(10,1	N	11
	10),EMY(10,10)	N	12
	COMMON /BLK8/ MFX(10),MFY(10),MUX(10),MUY(10),MBX(10),MBY(10)	N	13
	COMMON /BLK9/ DDPC(10,100),EYTH(10,100)	N	14
	COMMON /BLK20/ A1(2,10),A2(2,10),A3(2,10),B1(2,10),B2(2,10),B3(2,1	N	15
	10)	N	16
	COMMON /BLK21/ DMX(10,10),DMY(10,10)	N	17
	IF (NNLIN.EQ.0) GO TO 10	N	18
	CALL BNF	N	19
10	CONTINUE	N	20
	DO 30 I=1,NNCT	N	21
	A1(1,I)=MFX(I)+MUX(I)-(CRT(I)*0.10471975)**2*A3(1,I)	N	22
	B1(1,I)=MFY(I)+MUY(I)-(CRT(I)*0.10471975)**2*B3(1,I)	N	23
	DO 20 J=1,NNCT	N	24
	A1(1,I)=A1(1,I)-CMX(I,J)*A2(1,J)-KMX(I,J)*A3(1,J)-DMX(I,J)*B2(1,J)	N	25
	1-EMX(I,J)*B3(1,J)	N	26
20	B1(1,I)=B1(1,I)-CMY(I,J)*B2(1,J)-KMY(I,J)*B3(1,J)-DMY(I,J)*A2(1,J)	N	27
	1-EMY(I,J)*A3(1,J)	N	28
30	CONTINUE	N	29
	RETURN	N	30
	END	N	31-

```

SUBROUTINE TINTG (NNCT,DELTAT)
*****
C THIS SUBROUTINE INTEGRATES THE MODAL ACCELERATION INTO VELOCITY
C AND DISPLACEMENT BY MODIFIED EULER METHOD
C *****
COMMON /BLK2/ ISKIP,NSTEP,NCYCLE,NITP,NINT,NPLOT,NORBIT,NTIME,NSPE
1ED,NINC,NOPT,NT
COMMON /BLK20/ A1(2,10),A2(2,10),A3(2,10),B1(2,10),B2(2,10),B3(2,1
10)
DO 10 I=1,NNCT
  A2(2,I)=A2(1,I)+DELTAT*A1(1,I)
  B2(2,I)=B2(1,I)+DELTAT*B1(1,I)
  A3(2,I)=A3(1,I)+DELTAT*0.50*(A2(1,I)+A2(2,I))
10  B3(2,I)=B3(1,I)+DELTAT*0.50*(B2(1,I)+B2(2,I))
DO 20 I=1,NNCT
  A1(1,I)=A1(2,I)
  A2(1,I)=A2(2,I)
  A3(1,I)=A3(2,I)
  B1(1,I)=B1(2,I)
  B2(1,I)=B2(2,I)
20  B3(1,I)=B3(2,I)
RETURN
END

```

```

0 1
0 2
0 3
0 4
0 5
0 6
0 7
0 8
0 9
0 10
0 11
0 12
0 13
0 14
0 15
0 16
0 17
0 18
0 19
0 20
0 21
0 22
0 23-

```

	SUBROUTINE TBETA (NNCT,DELTAT,BETA)	P	1
	*****	P	2
C	THIS SUBROUTINE INTEGRATES THE MODAL ACCELERATIONS INTO MODAL	P	3
C	VELOCITY AND DISPLACEMENT BY NEWMARK BETA METHOD	P	4
C	*****	P	5
	DIMENSION STORE(6,10)	P	6
	COMMON /BLK20/ A1(2,10),A2(2,10),A3(2,10),B1(2,10),B2(2,10),B3(2,1	P	7
	10)	P	8
	DO 10 I=1,NNCT	P	9
	STORE(1,I)=A1(1,I)	P	10
	STORE(2,I)=B1(1,I)	P	11
	STORE(3,I)=A2(1,I)	P	12
	STORE(4,I)=B2(1,I)	P	13
	STORE(5,I)=A3(1,I)	P	14
10	STORE(6,I)=B3(1,I)	P	15
	DO 20 I=1,NNCT	P	16
	A2(1,I)=STORE(3,I)+DELTAT*STORE(1,I)	P	17
	B2(1,I)=STORE(4,I)+DELTAT*STORE(2,I)	P	18
	A3(1,I)=STORE(5,I)+.5*DELTAT*(STORE(3,I)+A2(1,I))	P	19
20	B3(1,I)=STORE(6,I)+.5*DELTAT*(STORE(4,I)+B2(1,I))	P	20
	CALL TACCEL	P	21
	DO 30 I=1,NNCT	P	22
	A2(1,I)=STORE(3,I)+.5*DELTAT*(A1(1,I)+STORE(1,I))	P	23
	B2(1,I)=STORE(4,I)+.5*DELTAT*(B1(1,I)+STORE(2,I))	P	24
	A3(1,I)=STORE(5,I)+DELTAT*STORE(3,I)+(.5-BETA)*STORE(1,I)*DELTAT*D	P	25
	1ELTAT+BETA*DELTAT*DELTAT*A1(1,I)	P	26
	B3(1,I)=STORE(6,I)+DELTAT*STORE(4,I)+(.5-BETA)*STORE(2,I)*DELTAT*D	P	27
	1ELTAT+BETA*DELTAT*DELTAT*B1(1,I)	P	28
	A3(2,I)=A3(1,I)	P	29
30	B3(2,I)=B3(1,I)	P	30
	RETURN	P	31
	END	P	32-



	SUBROUTINE TINC	Q	1
	*****	Q	2
C	THIS SUBROUTINE TRANSFORMS THE ROTOR INITIAL CONDITIONS INTO	Q	3
C	MODAL INITIAL CONDITIONS OF VELOCITIES AND DISPLACEMENTS	Q	4
C	*****	Q	5
	DIMENSION XTH(100), YTH(100), VXTH(100), VYTH(100)	Q	6
	COMMON /BLK1/ N,NB,NNLIN,NMB,NF,NU,NS,NBOW,ISTAB,IMODE,ISKU,NNCT,N	Q	7
	1UFPT	Q	8
	COMMON /BLK6/ BDW(100),PBDW(100),XIDC(100),YIDC(100),VXIDC(100),VY	Q	9
	1IDC(100),BXA(100),BYA(100)	Q	10
	COMMON /BLK9/ DDPC(10,100),EEYTH(10,100)	Q	11
	COMMON /BLK15/ RP(100),RT(100)	Q	12
	COMMON /BLK19/ DX(100)	Q	13
	COMMON /BLK20/ A1(2,10),A2(2,10),A3(2,10),B1(2,10),B2(2,10),B3(2,1	Q	14
	10)	Q	15
	COMMON /BLK22/ W(100)	Q	16
	DO 10 I=1,100	Q	17
	XIDC(I)=XIDC(I)/1000.	Q	18
	YIDC(I)=YIDC(I)/1000.	Q	19
	VXIDC(I)=VXIDC(I)/1000.	Q	20
10	VYIDC(I)=VYIDC(I)/1000.	Q	21
	TC=(XIDC(2)-XIDC(1))/DX(1)	Q	22
	TD=(YIDC(2)-YIDC(1))/DX(1)	Q	23
	TE=(VXIDC(2)-VXIDC(1))/DX(1)	Q	24
	TF=(VYIDC(2)-VYIDC(1))/DX(1)	Q	25
	XTH(1)=ATAN(TC)	Q	26
	YTH(1)=ATAN(TD)	Q	27
	VXTH(1)=ATAN(TE)	Q	28
	VYTH(1)=ATAN(TF)	Q	29
	TC=(XIDC(N)-XIDC(N-1))/DX(N-1)	Q	30
	TD=(YIDC(N)-YIDC(N-1))/DX(N-1)	Q	31
	TE=(VXIDC(N)-VXIDC(N-1))/DX(N-1)	Q	32
	TF=(VYIDC(N)-VYIDC(N-1))/DX(N-1)	Q	33
	YTH(N)=ATAN(TD)	Q	34
	XTH(N)=ATAN(TC)	Q	35
	VXTH(N)=ATAN(TE)	Q	36
	VYTH(N)=ATAN(TF)	Q	37
	N1=N-1	Q	38

	DO 20 I=2,N1	Q	39
	TC=(XIDC(I+1)-XIDC(I-1))/(DX(I-1)+DX(I))	Q	40
	TD=(YIDC(I+1)-YIDC(I-1))/(DX(I-1)+DX(I))	Q	41
	TE=(VXIDC(I+1)-VXIDC(I-1))/(DX(I-1)+DX(I))	Q	42
	TF=(VYIDC(I+1)-VYIDC(I-1))/(DX(I-1)+DX(I))	Q	43
	XTH(I)=ATAN(TC)	Q	44
	YTH(I)=ATAN(TD)	Q	45
	VXTH(I)=ATAN(TE)	Q	46
	VYTH(I)=ATAN(TF)	Q	47
20	CONTINUE	Q	48
	DO 30 I=1,NNCT	Q	49
	A3(1,I)=0.	Q	50
	B3(1,I)=0.	Q	51
	A2(1,I)=0.	Q	52
	B2(1,I)=0.	Q	53
	DO 30 J=1,N	Q	54
	A3(1,I)=A3(1,I)+(DDPC(I,J)*W(J)*XIDC(J)+EEYTH(I,J)*RT(J)*XTH(J))/3	Q	55
	186.4	Q	56
	B3(1,I)=B3(1,I)+(DDPC(I,J)*W(J)*YIDC(J)+EEYTH(I,J)*RT(J)*YTH(J))/3	Q	57
	186.4	Q	58
	A2(1,I)=A2(1,I)+(DDPC(I,J)*W(J)*VXIDC(J)+EEYTH(I,J)*RT(J)*VXTH(J))	Q	59
	1/386.4	Q	60
30	B2(1,I)=B2(1,I)+(DDPC(I,J)*W(J)*VYIDC(J)+EEYTH(I,J)*RT(J)*VYTH(J))	Q	61
	1/386.4	Q	62
	RETURN	Q	63
	END	Q	64-

ORIGINAL PAGE IS  
OF POOR QUALITY

	SUBROUTINE TSTORE (NNCT,ICOUNT,TIME)	R	1
C	*****	R	2
C	THIS SUBROUTINE STORES THE MODAL DISPLACEMENTS FOR EACH TIME	R	3
C	STEP INTO TAPE 7	R	4
C	*****	R	5
	COMMON /BLK20/ A1(2,10),A2(2,10),A3(2,10),B1(2,10),B2(2,10),B3(2,1	R	6
	10)	R	7
	DO 10 I=1,NNCT	R	8
	WRITE (7) A3(1,I),B3(1,I)	R	9
10	CONTINUE	R	10
	RETURN	R	11
	END	R	12-

	SUBROUTINE TDISPL (FTIME)	S	1
C	*****	S	2
C	THIS SUBROUTINE CALCULATES THE TRANSIENT RESPONSE FROM THE MODAL	S	3
C	DISPLACEMENTS STORED IN TAPE 7 AND OUTPUT IT IN TABULAR FORM OR	S	4
C	IN CALCLMP PLOTS	S	5
C	*****	S	6
	COMMON /BLK1/ N,NB,NNLIN,NMB,NF,NU,NS,NBOW,ISTAB,IMODE,ISKU,NNCT,N	S	7
	1UFPT	S	8
	COMMON /BLK2/ ISKIP,NSTEP,NCYCLE,NITP,NINT,NPLOT,NORBIT,NTIME,NSPE	S	9
	IED,NINC,NOPT,NT	S	10
	COMMON /BLK3/ CRT(10),LLBD(10),LLNB(5),LLNMB(9),LLSK(10),LLNT(10),	S	11
	1LLUF(10),LLFF(10),LLUT(10)	S	12
	COMMON /BLK9/ DDPC(10,100),EEYTH(10,100)	S	13
	COMMON /BLK16/ SPEED2,ANGSP,ANGACL,FSPEED	S	14
	COMMON SX(4001),SY(4001)	S	15
	IF (NPLOT.NE.0) GO TO 10	S	16
	CALL CALCOMP (10)	S	17
10	CONTINUE	S	18
	NLPT=NSTEP*NCYCLE+1	S	19
	DO 100 I=1,NT	S	20
	REWIND 7	S	21
	ID=LLNT(1)	S	22
	SPEED=SPEED2	S	23
	STEP=NSTEP	S	24
	NCC=1	S	25
	NPF=NCC*NSTEP	S	26
	DELTAT=60./(SPEED*STEP)	S	27
	TIME=0.	S	28
	WRITE (3,120) ID	S	29
	XMAX=0.	S	30
	YMAX=0.	S	31
	IJK=0	S	32
	NCLM=1	S	33
	DO 60 J=1,NLPT	S	34
	X=0.	S	35
	Y=0.	S	36
	DO 20 K=1,NNCT	S	37
	READ (7) AX,BY	S	38

	X=X+AX*DDPC(K,ID)*1000.	S	39
20	Y=Y+BY*DDPC(K,ID)*1000.	S	40
	IF (ABS(X).LE.XMAX) GO TO 30	S	41
	XMAX=ABS(X)	S	42
30	IF (ABS(Y).LE.YMAX) GO TO 40	S	43
	YMAX=ABS(Y)	S	44
40	IF (J.NE.NCCM) GO TO 50	S	45
	IJK=IJK+1	S	46
	AB=SQRT(X*X+Y*Y)	S	47
	P=PANG(X,Y)	S	48
	WRITE (3,130) J,TIME,X,Y,AB,P,SPEED	S	49
	NCCM=IJK*NITP+1	S	50
50	SX(J)=X	S	51
	SY(J)=Y	S	52
	TIME=TIME+DELTAT	S	53
	SPEED=SPEED+DELTAT*ANGACL*9.54929	S	54
	IF (K.NE.NPP) GO TO 60	S	55
	NCC=NCC+1	S	56
	NPP=NCC*NSTEP	S	57
	DELTAT=60./((SPEED*STEP)	S	58
60	CONTINUE	S	59
	IF (NORBIT.EQ.0) GO TO 70	S	60
	CALL GBPLT (XMAX,YMAX,NLPT,ID,NSTEP)	S	61
70	IF (NTIME.EQ.0) GO TO 80	S	62
	CALL TMPLT (XMAX,YMAX,NLPT,ID,FTIME,NSTEP)	S	63
80	IF (NSPEED.EQ.0) GO TO 90	S	64
	CALL SOPLT	S	65
90	CONTINUE	S	66
100	CONTINUE	S	67
	IF (NPLT.NE.0) GO TO 110	S	68
	CALL ENOPLT	S	69
110	CONTINUE	S	70
	RETURN	S	71
C		S	72
120	FORMAT (1H1,10X,#MOGAL TRANSIENT ANALYSIS AT STATION NO.#,I3,/,10	S	73
	1X,#STEP NO.#,5X,#TIME(SECONDS)#,5X,#X-MILS#,10X,#Y-MILS#,8X,#ABS-D	S	74
	2ISPL#,6X,#PHASE ANGLE#,6X,#SPEED(RPM)#,/,)	S	75
130	FORMAT (12X,I4,5X,F10.5,5X,F10.5,6X,F10.5,6X,F10.5,6X,F10.2,6X,F10	S	76

S 77  
S 78-

1.2)  
END

	SUBROUTINE CBPLGT (XMAX,YMAX,NLPT,ID,NSTEP)	T	1
C	*****	T	2
C	THIS SUBROUTINE PLOTS THE TRANSIENT ORBITS IN X AND Y DIRECTIONS	T	3
C	*****	T	4
	COMMON /BLK28/ AL1(8),AL2(8),AL3(8)	T	5
	COMMON SX(4001),SY(4001)	T	6
	CALL PLOT (15.,5.,-3)	T	7
	CALL SYMBOL (-3.0,-4.00,.105,AL1,0.0,80)	T	8
	CALL SYMBOL (-3.0,-4.25,.105,AL2,0.0,80)	T	9
	CALL SYMBOL (-3.0,-4.50,.105,AL3,0.0,80)	T	10
	C=AMAX1(XMAX,YMAX)	T	11
	G=1.	T	12
	IF (C.LT.1.) G=10.	T	13
	B=C*G/3.+1.	T	14
	O=AINT(B)/C	T	15
	E=-3.*D	T	16
	CALL AXIS (-3.0,-3.0,11HY-DIR(MILS),11,6.0,90.0,E,D)	T	17
	CALL AXIS (-3.0,-3.0,11HX-DIR(MILS),-11,6.0,0.0,E,D)	T	18
	CALL PLOT (3.,-3.,3)	T	19
	CALL PLOT (3.,3.,2)	T	20
	CALL PLGT (-3.,3.,2)	T	21
	CALL SYMBOL (1.0,3.25,.14,11HSTATION NO.,0.0,11)	T	22
	CALL NUMBER (2.2,3.25,.14,ID,0.0,2HI3)	T	23
	KK=1	T	24
	JJ=0	T	25
	DO 30 J=1,NLPT	T	26
	X=SX(J)	T	27
	Y=SY(J)	T	28
	X=X/D	T	29
	Y=Y/D	T	30
	IF (J.NE.1) GO TO 10	T	31
	CALL PLOT (X,Y,3)	T	32
10	CALL PLGT (X,Y,2)	T	33
	IF (J.EQ.KK) GO TO 20	T	34
	GO TO 30	T	35
20	CALL SYMBOL (X,Y,.0675,11,0.,-1)	T	36
	CALL PLGT (X,Y,3)	T	37
	JJ=JJ+1	T	38

30

KK=JJ+NSTEP+1  
CONTINUE  
CALL NEWBLOK  
RETURN  
END

T 39  
T 40  
T 41  
T 42  
T 43-

ORIGINAL PAGE IS  
OF POOR QUALITY



	SUBROUTINE TRPLCT (XMAX,YMAX,NLPT,ID,FTIME,NSTEP)	U	1
	*****	U	2
C	THIS SUBROUTINE PLOTS TRANSIENT RESPONSE AMPLITUDES VS REAL TIME	U	3
C	*****	U	4
	COMMON /BLK16/ SPEED2,ANGSP,ANGACL,FSPEED	U	5
	COMMON /BLK28/ AL1(8),AL2(8),AL3(8)	U	6
	COMMON SX(4001),SY(4001)	U	7
	C=AMAX1(XMAX,YMAX)	U	8
	G=1.	U	9
	IF (C.LT.1.) G=10.	U	10
	B=C*G/2.+1.	U	11
	D=AIN(TB)/G	U	12
	CC=-2.*D	U	13
	CALL PLGT (5.,2.,-3)	U	14
	E=FTIME*1000./B.+1.	U	15
	F=AIN(TE)/1000.	U	16
	CALL AXIS (C.C,0.0,15HTIME IN SECONDS,-15,8.0,0.0,0.0,F)	U	17
	CALL AXIS (C.C,0.0,23HROTOR DISPLACEMENT-MILS,23,4.,90.,CC,D)	U	18
	CALL PLGT (0.,2.0,3)	U	19
	CALL PLGT (8.0,2.0,2)	U	20
	CALL SYMBOL (0.0,-1.1,.105,AL1,0.0,80)	U	21
	CALL SYMBOL (0.0,-1.3,.105,AL2,0.0,80)	U	22
	CALL SYMBOL (0.0,-1.5,.105,AL3,0.0,80)	U	23
	CALL SYMBOL (3.5,4.0,.14,11HSTATION NO.,0.,11)	U	24
	CALL NUMBER (4.7,4.0,.14,10,0.0,2HI3)	U	25
	CALL SYMBOL (6.0,3.8,C.105,12HX=,Y=,0.,12)	U	26
	CALL SYMBOL (6.4,3.9,C.105,11,0.,-1)	U	27
	CALL SYMBOL (7.3,3.9,C.105,2,0.,-1)	U	28
	P=C	U	29
10	CONTINUE	U	30
	JJ=0	U	31
	KK=1	U	32
	TIME=0.	U	33
	SPEED=SPEED2	U	34
	STEP=NSTEP	U	35
	DELTAT=0.	U	36
	DO 50 I=1,NLPT	U	37
	TIME=TIME+DELTAT	U	38

```

T=TIME
SPEED=SPEED+DELTAT*ANGACL*9.54929
X=SX(I)
T=T/F
Z=X/D+2.
N=11
IF (N.EQ.0) GO TO 20
Y=SY(I)
Z=Y/D+2.
N=2
20  CONTINUE
    IF (I.NE.1) GO TO 30
    CALL PLOT (T,Z,3)
30  CALL PLOT (T,Z,2)
    IF (I.EQ.KK) GO TO 40
    GO TO 50
40  CALL SYMBOL (T,Z,.07,N,0.,-1)
    DELTAT=60./((SPEED*STEP)
    JJ=JJ+1
    KK=JJ*NSTEP+1
50  CONTINUE
    IF (M.EQ.1) GO TO 60
    M=1
    GO TO 10
60  CONTINUE
    CALL NEWBLOK
    RETURN
    END

```

```

U 39
U 40
U 41
U 42
U 43
U 44
U 45
U 46
U 47
U 48
U 49
U 50
U 51
U 52
U 53
U 54
U 55
U 56
U 57
U 58
U 59
U 60
U 61
U 62
U 63
U 64
U 65
U 66-

```

	SUBROUTINE SDPLOT	V	1
C	*****	V	2
C	TO RESERVE FOR FUTURE DISPLACEMENT-SPEED PLOTS	V	3
C	*****	V	4
	RETURN	V	5
	END	V	6-

	SUBROUTINE ENF	W	1
C	*****	W	2
C	THIS SUBROUTINE CALCULATES THE NONLINEAR BEARING FORCES FOR EACH	W	3
C	TIME STEP . THE BEARING USED ARE ASSUMED TO BE SHORT JOURNAL	W	4
C	BEARING 180 DEG. CAVITATED FILM OR WITH 360. DEG FLUID FILM.	W	5
C	THIS CAN ALSO BE USED TO APPROXIMATE STRAIGHT SEAL FORCES.	W	6
C	*****	W	7
	REAL LEN	W	8
	REAL MFX,MFY	W	9
	REAL KXX,KYY	W	10
	COMMON /BLK1/ N,NB,NNLIN,NMB,NF,NU,NS,NBOW,ISTAB,IMODE,ISKU,NNCT,N	W	11
	IUFPT	W	12
	COMMON /BLK3/ CRT(10),LLBD(10),LLNB(5),LLNMB(9),LLSK(10),LLNT(10),	W	13
	ILLUF(10),LLFF(10),LLUT(10)	W	14
	COMMON /BLK4/ KXX(10),KXY(10),KYX(10),KYY(10),CXX(10),CXY(10),CYX(	W	15
	110),CYY(10),SLNMB(9,4,4),CLNMB(9,4,4)	W	16
	COMMON /BLK6/ MFX(10),MFY(10),MUX(10),MUY(10),MBX(10),MBY(10)	W	17
	COMMON /BLK9/ DDPC(10,100),EEYTH(10,100)	W	18
	COMMON /BLK16/ SPEED2,ANGSP,ANGACL,FSPEED	W	19
	COMMON /BLK18/ AKK(10)	W	20
	COMMON /BLK20/ A1(2,10),A2(2,10),A3(2,10),B1(2,10),B2(2,10),B3(2,1	W	21
	10)	W	22
	COMMON /BLK35/ WMY(10),VIS(5),R(5),LEN(5),C(5),NLB(5)	W	23
	DO 10 I=1,NNCT	W	24
	MFX(I)=0.	W	25
10	MFY(I)=0.	W	26
	DO 60 I=1,NNLIN	W	27
	L=LLNB(I)	W	28
	X=0.	W	29
	Y=0.	W	30
	VX=0.	W	31
	VY=0.	W	32
	DO 20 J=1,NNCT	W	33
	X=X+A3(1,J)*DDPC(J,L)	W	34
	Y=Y+B3(1,J)*DDPC(J,L)	W	35
	VX=VX+A2(1,J)*DDPC(J,L)	W	36
	VY=VY+B2(1,J)*DDPC(J,L)	W	37
20	CONTINUE	W	38

ORIGINAL PAGE IS  
OF POOR QUALITY

D=X*X+Y*Y	W	39
SD=0.	W	40
DEU=G.	W	41
SD=SQRT(D)	W	42
U=X*VX+Y*VY	W	43
DU=C(I)*SD*ANGSP	W	44
DEU=U/DU	W	45
EU=SD/C(I)	W	46
IF (EU.GT.1.) EU=.99	W	47
PHIDOT=(X*VY-Y*VX)/(ANGSP*D)	W	48
PI=3.14159	W	49
TEST=(1.-2.*PHIDOT)	W	50
SIGN=1.	W	51
SIGN1=1.	W	52
IF (TEST.LT.0.) SIGN=-1.	W	53
IF (DEU.LT.0.) SIGN1=-1.	W	54
CS=EU*ABS(TEST)/SQRT(EU*EU*TEST**2+4.*DEU*DEU)	W	55
AS=(1.+EU)/(1.-EU)	W	56
IF (CS.EQ.0.) GO TO 30	W	57
U=SQRT((1.-CS)/(1.+CS))	W	58
GO TO 40	W	59
30 U=0.	W	60
40 CONTINUE	W	61
TI1=SIGN*4.*EU*CS**3/((1.-EU*EU*CS*CS)**2)	W	62
C1=(1.-EU*EU)	W	63
C2=(3.-5.*AS*AS)	W	64
C3=(5.-3.*AS*AS)	W	65
TA=ATAN(U*(AS*AS-1.)/(AS*(1.+U*U)))	W	66
C4=(1.+2.*EU*EU)	W	67
CON=PI*C4/(C1**2.5)	W	68
CON2=(C2*U*U+C3*AS*AS)/(U*U+AS*AS)**2+(C2+C3*AS*AS*U*U)/(1.+AS*AS*U*U)**2	W	69
TI2=CON+SIGN1*(2.*C4*TA/(C1**2.5)-U*CON2/(C1**2))	W	70
CON=2./C1**1.5	W	71
TI3=CON*(PI/2.+SIGN1*(TA-AS*U*(U*U-AS*AS)/(U*U+AS*AS)**2-AS*U*(1.-AS*AS*U*U)/(1.+AS*AS*U*U)**2))	W	72
SOM=VIS(I)*ANGSP*2.*R(I)*LEN(I)**3/(8.*C(I)*C(I))	W	73
F1=SOM*(EU*TEST*TI1+2.*DEU*TI2)	W	74
	W	75
	W	76

```

F2=SLH*(EU+TEST*TI3+2.*DEU*TI1)
FX=-(F1*X+F2*Y)/SD
FY=(F2*X-F1*Y)/SD
WRITE (3,70) F1,F2,FX,FY,X,Y
ID=NLB(1)
FY=FX+KXX(ID)*X+AKK(ID)*X
FY=FY+KYY(ID)*Y+AKK(ID)*Y
DO 50 K=1,NNC1
  MFX(K)=MFX(K)+FX*DDPC(K,L)
  MFY(K)=MFY(K)+FY*DDPC(K,L)
50 CONTINUE
RETURN
C
70 FORMAT (5X,E615.5)
END

```

```

W 77
W 78
W 79
W 80
W 81
W 82
W 83
W 84
W 85
W 86
W 87
W 88
W 89
W 90
W 91-

```

## APPENDIX E

INPUT INSTRUCTIONS AND LISTING  
OF COMPUTER PROGRAM MODAL 2

## INPUT INSTRUCTIONS FOR PROGRAM MODAL 2

1. Read 3 comment cards (1 to 80 columns)
2. N, NB,>NNLIN, NMB, NF, NU, NS, NBOW, ISTAB, IMODE, ISKU, NUFPT  
(12I5)

N = No. of mass stations (max. 100)

NB = No. of regular linear bearings (max. 10)

NNLIN = No. of nonlinear bearings (max. 5)

NMB = No. of coment resisting bearings (32 coeff.)(e.g.)  
balance piston) (max. 3)

NF = No. of external force (max. 10)

NU = No. of unbalance (max. 10)

NS = No. of skewed disc (max. 10)

NBOW = 1 bow shaft (Input shaft bow data)

= 0 no shaft bow

ISTAB = 1

= 0

IMODE = 0

= 1

ISKU = 0

= 1

NUFPT = 1

3. ISKIP, NSTEP, NCYCLE, NITP, NINT, NPLOT, NORBIT, NTIME, NSPEED,  
NINC, NOPT, NT (12I5)



ISKIP = 0

NSTEP = 100

NCYCLE = 20

NITP = No. of steps per printout

NINT = 1 Newark -  $\beta$  intergration (with iteration)

= 2 Euler Integration

NPLOT = 0 plots of transient desired

= 1 no plots

NORBIT = 1

NTIME = 1

NSPEED = 0

NINC = 0 input initial condition

= 1 initial conditions from steady state orbit with small perturbation

NOPT = 0

NT = 1

4. LLBD (J), J = 1, NB (1015) Skip (4) and (5) if NB = 0 Bearing location station numbers.

5. NSPD (I5)

NSPD = number of speed cases of transient analysis

6. SSPEED (I), I = 1, NSPD (8G10.3) (max. 8)

SSPEED (I) = Speed for the  $I^{th}$  transient case

7. ((KKxx (I, J), KKxy (I, J), KKyx (I, J), KKyy (I, J), KKxx (I, J),

KCxy (I, J), KCyx (I, J), KCyy (I, J), J = 1, NB) I = 1, NSPD)

8 bearing stiffness and damping coefficients in NSPD sets of NB cards.

8. ((LLNB (I, J), INLB (I, J), BVIS (I, J), BANR (I, J), BANL (I, J),  
BAN (I, J), J = 1,>NNLIN) I = 1, NSPD)  
(2I10, 4G10.3)

(Skip if>NNLIN = 0)

LLNB (I, J) = station no. of Jth nonlinear bearings

INLB (I, J) = bearing no. of Jth nonlinear bearings

BVIS (I, J) = viscosity of lubricant (lb/in<sup>2</sup>)

BANR (I, J) = radius of Jth bearing (in)

BANL (I, J) = length of Jth bearing (in)

BANC (I, J) = clearance of Jth bearing (in)

\*A linear bearing station must be assigned to a nonlinear bearing even with zero linear stiffness and damping.

9. LLNMB (J), J = 1, NMB (3I5) (skip 7 and 8 if NMB = 0)

LLNMB (J) = station no. of the Jth moment resisting bearing

\*Only one set for all speed cases.

10. NMB sets of card, each set 4 cards (8G10.3)

$Bk_{xx}, Bk_{x\theta}, Bk_{xy}, Bk_{x\psi}, Bc_{xx}, Bc_{x\theta}, Bc_{xy}, Bc_{x\psi}$

$Bk_{\theta x}, Bk_{\theta\theta}, Bk_{\theta y}, Bk_{\theta\psi}, Bc_{\theta x}, Bc_{\theta\theta}, Bc_{\theta y}, Bc_{\theta\psi}$

$Bk_{yx}, Bk_{y\theta}, Bk_{yy}, Bk_{y\psi}, Bc_{yx}, Bc_{y\theta}, Bc_{yy}, Bc_{y\psi}$

$Bk_{\psi x}, Bk_{\psi\theta}, Bk_{\psi y}, Bk_{\psi\psi}, Bc_{\psi x}, Bc_{\psi\theta}, Bc_{\psi y}, Bc_{\psi\psi}$

These are the 32 bearing stiffness and damping coefficients for a moment resisting bearing. The first subscript represents the direction of force, and the second subscript represents displacement.

$x$  = x-direction displacement  
 $\theta$  = rotation at positive y-axis (right-hand rule)  
 $y$  = y-direction displacement  
 $\psi$  = rotation at negative x-axis (right-hand rule)

11. NGYR, E, SPEED1, SPEED ANGACL, FSPEED, BETA (15, 5x, 5GL0.3)

NGYR = 1 calculation shaft gyroscopics

= 0 no. shaft gyroscopics

E = Section Young's Modulus  $\times 10^{-6}$  (E = 30. for steel)

SPEED1 = Rotor operating speed (RPM) (use for gyroscopic  
calculation in damped modes)

SPEED2 = use as initial speed for transient

ANGACL = rad/sec<sup>2</sup> (use in transient cal.)

TSPEED = 0

BETA = Beta parameter used for Newmark beta integration  
(usually = 1/6)

12. EXTW(J), DX(J), DEXT(J), DINT(J), RP(J), RT(J), ZM6(J), RO(J),

J = 1, N

(N cards) (8(F10.3))

EXTW(J) = external weights at J-mass station (lb)

DX(J) = length of Jth element (in)

DEXT(J) = external diameter of Jth element (in)

DINT(J) = internal diameter of Jth element (in)

RP(J) = polar moment of inertia at Jth station (lb-in<sup>2</sup>)

RT(J) = transverse moment of inertia at Jth station (lb-in<sup>2</sup>)

EM6(J) = Young's modules of Jth element  $\times 10^{-6}$  (=E lb/in<sup>2</sup>  
if set to zero)

RO(J) = density of Jth element (= 0.283 lb/in<sup>3</sup> if set to zero)

13. LLFF(J), FX(J), FY(J), J = 1, NF (I5, 5x, 2G10.3) NF cards,  
skip if NF = 0

LLFF(J) = station no. of Jth external force

FX(J) = forces in x-direction (lb)

FY(J) = forces in y-direction (lb)

14. LLUF(J), UX(J), UY(J), J = 1, NU  
(I5, 5x, 2G10.3) NU cards, skip if NU = 0

LLUF(J) = station no. of Jth unbalance

UX(J) = unbalance at x-direction (oz-in)

UY(J) = unbalance at y-direction (oz-in)

15. LLSK(J), FSK(J), PSK(J), J = 1, NS  
(I5, 5x, 2G10.3) NS cards, skip if NS = 0

LLSK(J) = station no. of Jth skewed disc

FSK(J) = maximum skew of the disc (rad) (positive skew is  
opposite to positive  $\theta_x$ )

PSK(J) = angle between maximum skew to the x-axis (rad)

16. LLNT(J), J = 1, NT (I0I5), (NT = 1)

LLNT(J) = station which the transient results are used in  
frequency spectrum analysis

17. BOW(J), PBOW(J), XIC(J), YIC(J), VXIC(J), VYIC(J), J = 1, N  
(6G10.3)

BOW(J) = Jth station initial bow (mils) (= 0 if no bow)

PBOW(J) = angle of bow to the positive x-axis (rad)

(= 0 if no bow)

XIC(J) = Jth station initial displacement (mils)

YIC(J) = Jth station initial displacement at y-direction (mils)

VXIC(J) = Jth station initial velocity at x-direction (mils/sec)

VYIC(J) = Jth station initial velocity at y-direction (mils/sec)

18. SPI, SPL, DSP (3G10.3)

SPI - initial speed (RPM)

SPL = final speed (RPM) (for critical speed analysis)

DSP = speed increment (RPM)

19. TITLE1, TITLE2, TITLE3

3 TITLE cards for label in plots (1 to 80 columns)

C	PROGRAM MODES(INPUT,OUTPUT,TAPE1=INPUT,TAPE3=OUTPUT,TAPE7,TAPE10)	A	1
C	*****	A	2
C	THIS PROGRAM CALCULATES THE UNDAMPED CRITICAL SPEEDS AND THEIR	A	3
C	CORRESPONDING MODE SHAPES.	A	4
C	A MAXIMUM NUMBER OF EIGHT SPEED CASES OF TRANSIENT ANALYSIS	A	5
C	CAN BE OBTAINED IN ONE SINGLE ANALYSIS.	A	6
C	TRANSIENT MOTION ORBITS AND AMPLITUDE VS TIME PLOT AT ONE	A	7
C	PARTICULAR STATION WILL BE GENERATED FOR EVERY SPEED CASE	A	8
C	FAST FOURIER TRANSFORMATION IS APPLIED TO PRODUCE FREQUENCY	A	9
C	SPECTRUM ANALYSIS FOR EVERY SPEED CASE	A	10
C	CAMPBELL PLOTS OF THE SYSTEM ARE ALSO GENERATED	A	11
C	BY K. C. CHOY	A	12
C	DEPARTMENT OF MECHANICAL ENGINEERING, UNIVERSITY OF VIRGINIA	A	13
C	MARCH 4, 1977	A	14
C	*****	A	15
	COMPLEX BB(20,21),CC(20)	A	16
	REAL KXX(10),KXY(10),KYX(10),KYY(10),MFX(10),MFY(10),MUY(10),MUX(1	A	17
	10),KMX(10,10),KNY(10,10),MBX(10),MBY(10)	A	18
	REAL KKXX(10,10),KKXY(10,10),KKYX(10,10),KKYY(10,10),KCXX(10,10),K	A	19
	1CXY(10,10),KCYX(10,10),KCYY(10,10)	A	20
	DIMENSION SSPEED(10)	A	21
	DIMENSION COMENT1(8), COMENT2(8), COMENT3(8)	A	22
	DIMENSION EM6(100), CRT(10), LLBD(10), LLNB(5), LLNMB(9), LLSK(10)	A	23
	1, LLNT(10), LLUF(10), LLFF(10), LLUT(10)	A	24
	DIMENSION DX(100), W(100), ENER(100), EY1(100), EY2(100), DPC(100)	A	25
	DIMENSION DEFL(100), LB(100), SK(100), WA(50), DEXT(100), DINT(100	A	26
	1)	A	27
	DIMENSION EXTW(100), SW1(100), RD(100), RT(100), RP(100), EI(100)	A	28
	DIMENSION WMOD(50), AKK(10)	A	29
	DIMENSION EAN1(100), EAN2(100), EYTH(100), EYTH(10,100), DDPC(10,	A	30
	1100)	A	31
	DIMENSION TMX(10,10)	A	32
	DIMENSION A1(2,10), A2(2,10), A3(2,10), B1(2,10), B2(2,10), B3(2,1	A	33
	10)	A	34
	DIMENSION CMX(10,10), CMY(10,10), DMX(10,10), DMY(10,10), EMX(10,1	A	35
	10), EMY(10,10)	A	36
	DIMENSION DOX(10,10), DOY(10,10), EOX(10,10), EOX(10,10)	A	37
	DIMENSION AAA(42), BBB(42), CCC(42), HHH(42), UUU(42), VVV(42)	A	38

ORIGINAL PAGE IS  
OF POOR QUALITY

DIMENSION CXX(10), CXY(10), CYX(10), CYY(10), UX(10), UY(10)	A	39
DIMENSION FX(10), FY(10)	A	40
DIMENSION SLNMB(9,4,4), CLNMB(9,4,4)	A	41
DIMENSION SNLB(5,8,3), FSK(10), PSK(10), BOW(100), PBOW(100)	A	42
DIMENSION BXA(100), BYA(100), XIDC(100), YIDC(100), VXIDC(100), VY	A	43
1IDC(100)	A	44
DIMENSION ADUMMY(8002)	A	45
DIMENSION ALABEL1(8), ALABEL2(8), ALABEL3(8)	A	46
DIMENSION WMY(10), VIS(5), ANR(5), ANL(5), ANC(5), NLB(5)	A	47
DIMENSION FC(512), SFC(8,512)	A	48
DIMENSION BVIS(8,5), BANR(8,5), BANL(8,5), BANC(8,5), INLB(8,5)	A	49
COMMON /BLK1/ N,NB,NNLIN,NMB,NF,NU,NS,NBOW,ISTAB,IMODE,ISKU,NCT,NU	A	50
1FPT	A	51
COMMON /BLK2/ ISKIP,NSTEP,NCYCLE,NITP,NINT,NPLOT,NORBIT,NTIME,NSPE	A	52
1ED,NINC,NGPT,NT	A	53
COMMON /BLK3/ CRT,LLBD,LLNB,LLNMB,LLSK,LLNT,LLUF,LLFF,LLUT	A	54
COMMON /BLK4/ KXX,KXY,KYX,KYY,CXX,CXY,CYX,CYY,SLNMB,CLNMB	A	55
COMMON /BLK5/ UX,UY,FX,FY,FSK,PSK	A	56
COMMON /BLK6/ BLW,PBW,XIDC,YIDC,VXIDC,VYIDC,BXA,BYA	A	57
COMMON /BLK7/ CMX,KMX,EMX,CMY,KMY,EMY	A	58
COMMON /BLK8/ MFX,MFY,MUX,MUY,MBX,MBY	A	59
COMMON /BLK9/ DDPC,EEYTH	A	60
COMMON /BLK10/ SPS,SPF,SPN,SPEED1	A	61
COMMON /BLK11/ DOX,DGY,EOX,EQY	A	62
COMMON /BLK14/ AAA,UUU,VVV,HHH,BBB,CCC	A	63
COMMON /BLK15/ RP,RT	A	64
COMMON /BLK16/ SPEED2,ANGSP,ANGACL,FSPEED	A	65
COMMON /BLK18/ AKK	A	66
COMMON /BLK19/ DX	A	67
COMMON /BLK20/ A1,A2,A3,B1,B2,B3	A	68
COMMON /BLK21/ DMX,DHY	A	69
COMMON /BLK22/ W	A	70
COMMON /BLK24/ BB,CC	A	71
COMMON /BLK25/ BETA	A	72
COMMON /BLK28/ ALABEL1,ALABEL2,ALABEL3	A	73
COMMON /BLK29/ PASP	A	74
COMMON /BLK35/ WMY,VIS,ANR,ANL,ANC,NLB	A	75
COMMON /BLK39/ NSPD,SSPEED	A	76

	COMMON /BLK40/ FC,SFC	A 77
	COMMON /BLK41/ KKXX,KKXY,KKYX,KKYY,KCXX,KCXY,KCYX,KCYY	A 78
	COMMON /BLK42/ LVIS,BANR,BANL,BANC,INLB	A 79
	COMMON ADUMMY	A 80
	NPLOT=0	A 81
	READ (1,730) COMMENT1	A 82
	READ (1,730) COMMENT2	A 83
	READ (1,730) COMMENT3	A 84
	WRITE (3,1110)	A 85
	WRITE (3,740) COMMENT1,COMMENT2,COMMENT3	A 86
	WRITE (3,750)	A 87
	READ (1,760) N,NB,NNLIN,NMB,NF,NU,NS,NBW,ISTAB,IMODE,ISKU,NUFPT	A 88
	READ (1,770) ISKIP,NSTEP,NCYCLE,NITP,NINT,NPLOT,NORBIT,NTIME,NSPEE	A 89
	10,NINC,NOPT,NT	A 90
	READ (1,780) (LLBD(J),J=1,NB)	A 91
	READ (1,700) NSPD	A 92
	READ (1,710) (SSPEED(J),J=1,NSPD)	A 93
	IF (NB.EQ.0) GO TO 30	A 94
	DO 20 I=1,NSPD	A 95
	READ (1,790) (KKXX(I,J),KKXY(I,J),KKYX(I,J),KKYY(I,J),KCXX(I,J),KC	A 96
	1XY(I,J),KCYX(I,J),KCYX(I,J),KCYX(I,J),J=1,NB)	A 97
20	CONTINUE	A 98
30	CONTINUE	A 99
	IF (NNLIN.EQ.0) GO TO 50	A 100
	DO 40 I=1,NSPD	A 101
	READ (1,800) (LLNB(J),INLB(I,J),BVIS(I,J),BANR(I,J),BANL(I,J),BANC	A 102
	1(I,J),J=1,NNLIN)	A 103
40	CONTINUE	A 104
50	CONTINUE	A 105
	IF (NMB.EQ.0) GO TO 60	A 106
	READ (1,810) (LLNMB(J),J=1,NMB)	A 107
	READ (1,820) (((SLNMB(I,J,K),K=1,4),(CLNMB(I,J,K),K=1,4)),J=1,4),	A 108
	11=1,NMB)	A 109
60	CONTINUE	A 110
	READ (1,830) NGYR,F,SPEED1,SPEED2,ANGACL,FSPEED,BETA	A 111
	READ (1,840) (EXTW(J),DX(J),DEXT(J),DINT(J),RP(J),RT(J),EM6(J),RD(	A 112
	1J),J=1,N)	A 113
	IF (NF.EQ.0) GO TO 70	A 114



	READ (1,850) (LLFF(J),FX(J),FY(J),J=1,NF)	A 115
70	CONTINUE	A 116
	IF (NU.EQ.0) GO TO 80	A 117
	READ (1,850) (LLUF(J),UX(J),UY(J),J=1,NU)	A 118
80	CONTINUE	A 119
	IF (NS.EQ.0) GO TO 90	A 120
	READ (1,850) (LLSK(J),FSK(J),PSK(J),J=1,NS)	A 121
90	CONTINUE	A 122
	IF (NT.EQ.0) GO TO 100	A 123
	READ (1,860) (LLNT(J),J=1,NT)	A 124
100	CONTINUE	A 125
	READ (1,870) (BOW(J),PBOW(J),XIDC(J),YIDC(J),VXIDC(J),VYIDC(J),J=1,N)	A 126
	READ (1,880) SPI,SPL,DSP	A 127
	READ (1,730) ALABEL1	A 128
	READ (1,730) ALABEL2	A 129
	READ (1,730) ALABEL3	A 130
	WRITE (3,890) NCYCLE,NSTEP,NINT,NINC,NOPT,SPEED2,ANGACL,BETA	A 131
	WRITE (3,900)	A 132
	DO 110 I=1,N	A 133
	IF (RD(I).EQ.0.0) RD(I)=0.283	A 134
	ENER(I)=3.14159*(DEXT(I)**4.-DINT(I)**4.)/64.	A 135
	IF (EM6(I).EQ.0.0) EM6(I)=E	A 136
	EI(I)=EM6(I)*ENLR(I)	A 137
	DL=ABS(DX(I))	A 138
110	SW1(I)=3.14159*(DEXT(I)**2.-DINT(I)**2.)*DL*RD(I)/4.0	A 139
	W(1)=SW1(1)/2.+EXTW(1)	A 140
	WT=W(1)	A 141
	ZLT=DX(1)	A 142
	DO 120 I=2,N	A 143
	W(I)=SW1(I-1)/2.0+SW1(I)/2.0+EXTW(I)	A 144
C	W(1)=TOTAL EFFECTIVE SHAFT WEIGHT	A 145
	WT=WT+W(1)	A 146
120	ZLT=ZLT+DX(I)	A 147
	IF (NGYR) 130,150,150	A 148
130	RP(1)=RP(1)+ENER(1)*RD(1)*DX(1)	A 149
	RT(1)=RT(1)+SW1(1)*((DEXT(1)**2.0+DINT(1)**2.0)/16.0+((DX(1)/2.0)*	A 150
	1*2.0)/3.0)/2.0	A 151
		A 152

	DO 140 I=2,N	A 153
	RP(I)=RP(I)+RG(I)*ENER(I)*DX(I)+ENER(I-1)*DX(I-1)*RO(I-1)	A 154
	RT(I)=RT(I)+SW1(I)*((DEXT(I)**2.0+DINT(I)**2.0)/16.0+((DX(I)/2.0)*	A 155
	1*2.0)/3.0)/2.0+SW1(I-1)*((DEXT(I-1)**2.0+DINT(I-1)**2.0)/16.0+((DX	A 156
	2(I-1)/2.0)**2.0)/3.0)/2.0	A 157
140	CONTINUE	A 158
150	SRP=C.0	A 159
	DO 160 I=1,N	A 160
160	SRP=SRP+RP(I)	A 161
	DO 160 I=1,N	A 162
	WRITE (3,910) (I,W(I),DX(I),DEXT(I),DINT(I),ENER(I),RP(I),RT(I),EM	A 163
	16(I),E1(I))	A 164
	IF (I-50) 180,170,180	A 165
170	WRITE (3,1110)	A 166
180	CONTINUE	A 167
	WRITE (3,920) WT,ZLT	A 168
	DO 190 I=1,NSPD	A 169
	WRITE (3,720) I,SSPEED(I)	A 170
	WRITE (3,930)	A 171
	WRITE (3,940)	A 172
	WRITE (3,950) (J,LLBD(J),KKXX(I,J),KKXY(I,J),KKYX(I,J),KKYY(I,J),J	A 173
	I=1,NB)	A 174
	WRITE (3,960)	A 175
	WRITE (3,970)	A 176
	WRITE (3,950) (J,LLBD(J),KCXX(I,J),KCXY(I,J),KCYX(I,J),KCYI(I,J),J	A 177
	I=1,NB)	A 178
190	CONTINUE	A 179
	IF (NMB.EQ.0) GO TO 210	A 180
	DO 200 I=1,NMB	A 181
	WRITE (3,980) I,LLNMB(I)	A 182
	WRITE (3,990) ((SLNMB(I,J,K),K=1,4),J=1,4),((CLNMB(I,J,K),K=1,4),J	A 183
	I=1,4)	A 184
200	CONTINUE	A 185
210	IF (NNLIN.EQ.0) GO TO 240	A 186
	DO 230 I=1,NSPD	A 187
	WRITE (3,720) I,SSPEED(I)	A 188
	WRITE (3,1200)	A 189
	DO 220 J=1,NNLIN	A 190

ORIGINAL PAGE IS  
OF POOR QUALITY

	WRITE (3,1210) J,LLNB(J),INLB(I,J),BVIS(I,J),BANR(I,J),BANL(I,J),B	A 191
	1ANC(I,J)	A 192
220	CONTINUE	A 193
230	CONTINUE	A 194
240	IF (NF.EQ.0) GO TO 250	A 195
	WRITE (3,1000)	A 196
	WRITE (3,1010) (LLFF(J),FX(J),FY(J),J=1,NF)	A 197
250	IF (NS.EQ.0) GO TO 260	A 198
	WRITE (3,1020)	A 199
	WRITE (3,1030) (LLSK(J),FSK(J),PSK(J),J=1,NS)	A 200
260	IF (NU.EQ.0) GO TO 280	A 201
	WRITE (3,1040)	A 202
	WRITE (3,1050)	A 203
	WRITE (3,1060) (LLUF(J),UX(J),UY(J),J=1,NU)	A 204
	DO 270 J=1,NU	A 205
	UX(J)=UX(J)/(16.*386.4)	A 206
270	UY(J)=UY(J)/(16.*386.4)	A 207
280	CONTINUE	A 208
	WRITE (3,1070)	A 209
	DO 290 J=1,N	A 210
	WRITE (3,1080) J,BOW(J),PBOW(J),XIDC(J),YIDC(J),VXIDC(J),VYIDC(J)	A 211
290	CONTINUE	A 212
	DO 300 I=1,100	A 213
	XIDC(I)=XIDC(I)/1000.	A 214
	YIDC(I)=YIDC(I)/1000.	A 215
	VXIDC(I)=VXIDC(I)/1000.	A 216
300	VYIDC(I)=VYIDC(I)/1000.	A 217
	WRITE (3,1090)	A 218
	DO 310 I=1,N8	A 219
	AVK=(KKXX(1,I)+KKYY(1,I))/2.	A 220
	WRITE (3,1100) I,AVK	A 221
310	CONTINUE	A 222
	NC=1	A 223
C	NC=LGICAL CRITICAL SPEED NO.	A 224
C	WRITE (3,700)	A 225
	WRITE (3,1110)	A 226
	LN=3	A 227
C	SPI=INITIAL SPEED,SPL=FINAL SPEED,DSP=SPEED INCREMENT-RPM	A 228

	SPD=SPI	A 229
	DETP=0.	A 230
	MA=0	A 231
	MB=0	A 232
C	IF(LN-50)54,54,53	A 233
	WRITE (3,1110)	A 234
	WRITE (3,1120) SPI,SPL,DSP	A 235
	LN=1	A 236
	WRITE (3,1130)	A 237
	LN=LN+3	A 238
	DIN=DSP	A 239
320	I=1	A 240
	J=1	A 241
	SPSQ=SPD*SPD	A 242
C	COMPUTE ANG. VELOCITY	A 243
	ANSP=SPD*0.10471976	A 244
	ANSP2=ANSP*ANSP	A 245
	VP=0.	A 246
	ZMP=0.	A 247
	EYP=0.	A 248
	ETHP=1.0	A 249
	M=1	A 250
330	I=I+1	A 251
	II=I-1	A 252
	IF (II-LLBD(J)) 360,340,360	A 253
340	AK=(KKXX(1,J)+KKYY(1,J))/2.	A 254
	AKK(J)=AK	A 255
	IF (J-NB) 350,370,370	A 256
350	J=J+1	A 257
	GO TO 370	A 258
360	AK=0.	A 259
370	VP=VP+(W(I-1)*ANSP2/386.4-AK)*EYP	A 260
	ZMP=ZMP-ANSP2*(RT(I-1))*ETHP/386.4	A 261
	EY=EYP+DX(I-1)*ETHP+DX(I-1)**2*ZMP/(2.E6*EI(I-1))+DX(I-1)**3*VP/(6	A 262
	1.E6*EI(I-1))	A 263
	ETH=ETHP+DX(I-1)*ZMP/(1.E6*EI(I-1))+DX(I-1)**2*VP/(2.E6*EI(I-1))	A 264
	ZM=ZMP+DX(I-1)*VP	A 265
	V=VP	A 266

	IF (M.EQ.2) GO TO 380	A 267
	EY1(I)=EY	A 268
	EAN1(I)=ETH	A 269
	IF (I.GT.N) GO TO 390	A 270
	ZMP=ZM	A 271
	VP=V	A 272
	EYP=EY	A 273
	ETHP=ETH	A 274
	GO TO 330	A 275
380	EY2(I)=EY	A 276
	EAN2(I)=ETH	A 277
	ZMP=ZM	A 278
	VP=V	A 279
	EYP=EY	A 280
	ETHP=ETH	A 281
	IF (I.GT.N) GO TO 400	A 282
	GO TO 330	A 283
390	M=2	A 284
	ZM1=ZM	A 285
	VR1=V	A 286
	J=1	A 287
	I=1	A 288
	EYP=1.	A 289
	ZMP=0.	A 290
	ETHP=0.	A 291
	VP=0.	A 292
	GO TO 330	A 293
400	DET=VR1*ZM-V*ZM1	A 294
	IF (DETP.EQ.0.) GO TO 450	A 295
	IF (MA.EQ.1) GO TO 430	A 296
	IF (ABS(DET).LT.1.) GO TO 480	A 297
	IF (DETP*DET) 410,450,450	A 298
410	DOLO=DETP	A 299
420	MA=1	A 300
	IF (ABS(DET).LT.1.) GO TO 480	A 301
	IF (DIN.LT.1.E-6) GO TO 480	A 302
	DIN=DIN/2.	A 303
	DETPP=DETP	A 304

```

      DETP=DET
      SPD=SPD-DIN
      GO TO 320
430   IF (ABS(DET).LT.1.) GO TO 480
      IF (DOLD*DET) 420,450,440
440   CONTINUE
      IF (ABS(DET).LT.1.) GO TO 480
      IF (DIN.LT.1.E-6) GO TO 480
      DIN=DIN/2.
      SPD=SPD+DIN
      DETPP=DETP
      DETP=DET
      GO TO 320
450   IF (LN-54) 470,470,460
460   WRITE (3,1110)
      LN=1
470   WRITE (3,1140) SPD,DET
      LN=LN+1
      SPD=SPD+DSP
      DIN=DSP
      IF (SPD.GT.SPL) GO TO 640
      DETPP=DETP
      DETP=DET
      SSPD=SPD
      GO TO 320
480   MA=0
      WRITE (3,1140) SPD,DET
      LN=LN+1
      IF (LN-50) 500,500,490
490   WRITE (3,1110)
      LN=1
500   WRITE (3,1150) NC
      WRITE (3,1160)
      WRITE (3,1140) SPD,DET
      CRT(NC)=SPD
      NC=NC+1
      LN=LN+3
      EY1(1)=0.

```

```

A 305
A 306
A 307
A 308
A 309
A 310
A 311
A 312
A 313
A 314
A 315
A 316
A 317
A 318
A 319
A 320
A 321
A 322
A 323
A 324
A 325
A 326
A 327
A 328
A 329
A 330
A 331
A 332
A 333
A 334
A 335
A 336
A 337
A 338
A 339
A 340
A 341
A 342

```

ORIGINAL PAGE IS  
OF POOR QUALITY

```

      EY2(1)=1.
      DTX=0.
      I=1
      IF (LN-50) 520,520,510
510   WRITE (3,1110)
      LN=1
520   WRITE (3,1170)
      LN=LN+2
530   DEFL(I)=V*EY1(I)-VR1*EY2(I)
      IF (I.NE.1) GO TO 540
      EYTH(I)=V
      GO TO 550
540   EYTH(I)=EAN1(I)*V-EAN2(I)*VR1
550   DEFA=ABS(DEFL(I))
      DMXA=ABS(DTX)
      I=I+1
      IF (DEFA-DMXA) 570,570,560
560   DTX=DEFL(I-1)
570   IF (I-N) 580,580,590
580   GO TO 530
590   DO 600 I=1,N
      DPC(I)=DEFL(I)/DTX
      EYTH(I)=EYTH(I)/DTX
      EEYTH(NC-1,I)=EYTH(I)
600   DDPC(NC-1,I)=DPC(I)
      DO 630 I=1,N
      LN=LN+1
      IF (LN-54) 620,620,610
610   WRITE (3,1110)
      LN=1
620   WRITE (3,1180) I,DPC(I),EYTH(I)
      LN=LN+1
630   CONTINUE
      SPD=SSPD+DSP
      DETP=0.
      GO TO 320
640   CONTINUE
      NCS=NC-1

```

```

A 343
A 344
A 345
A 346
A 347
A 348
A 349
A 350
A 351
A 352
A 353
A 354
A 355
A 356
A 357
A 358
A 359
A 360
A 361
A 362
A 363
A 364
A 365
A 366
A 367
A 368
A 369
A 370
A 371
A 372
A 373
A 374
A 375
A 376
A 377
A 378
A 379
A 380

```

	DO 670 II=1,NCS	A 381
	WMOD(II)=0.	A 382
	DO 650 JJ=1,N	A 383
650	WMOD(II)=WMOD(II)+RT(JJ)*EEYTH(II,JJ)**2+W(JJ)*DDPC(II,JJ)**2	A 384
	WMOD(II)=WMOD(II)/386.4	A 385
	DO 660 KI=1,N	A 386
	EEYTH(II,KI)=EEYTH(II,KI)/(WMOD(II)**0.5)	A 387
660	DDPC(II,KI)=DDPC(II,KI)/(WMOD(II)**0.5)	A 388
670	CONTINUE	A 389
	DO 690 II=1,NCS	A 390
	DO 680 JJ=1,NCS	A 391
	TMX(II,JJ)=0.	A 392
	DO 680 KI=1,N	A 393
	TMX(II,JJ)=TMX(II,JJ)+W(KI)*DDPC(JJ,KI)*DDPC(II,KI)/386.4+RT(KI)*E	A 394
	IEYTH(II,KI)*EEYTH(JJ,KI)/386.4	A 395
680	CONTINUE	A 396
	WRITE (3,1190) (TMX(II,JJ),JJ=1,NCS)	A 397
690	CONTINUE	A 398
	NCT=NCS	A 399
	CALL TMM	A 400
C		A 401
C		A 402
700	FORMAT (I5)	A 403
710	FORMAT (8G10.3)	A 404
720	FORMAT (//,5X, #SPEED CASE NO. #, I5, 5X, F15.0, #RPM #)	A 405
730	FORMAT (8A10)	A 406
740	FORMAT (1X, 3(8A10/1X))	A 407
750	FORMAT (//, 20X, #MODAL ANALYSIS VERSION 3, APRIL 6, 1977 #)	A 408
760	FORMAT (12I5)	A 409
770	FORMAT (12I5)	A 410
780	FORMAT (10I5)	A 411
790	FORMAT (8G10.3)	A 412
800	FORMAT (2I5, 4G10.2)	A 413
810	FORMAT (9I5)	A 414
820	FORMAT (8G10.3)	A 415
830	FORMAT (I5, 5X, 6G10.3)	A 416
840	FORMAT (8G10.3)	A 417
850	FORMAT (I5, 5X, 2G10.3)	A 418

ORIGINAL PAGE IS  
OF POOR QUALITY



860	FORMAT (10I5)	A 419
870	FORMAT (6G10.3)	A 420
880	FORMAT (3G10.3)	A 421
890	FORMAT (//,10X,#NCYCLE=#,I3,5X,#NSTEP=#,I3,5X,#NINT=#,I3,5X,#NINC=	A 422
	1#,I3,5X,#NOPT=#,I3,/,10X,#SPEED2=#,F10.2,5X,#ANGACL(1/SEC)=#,F10.3	A 423
	2,5X,#BETA=#,F10.5,/) )	A 424
900	FORMAT (120H STATION NO. WEIGHT LENGTH SHAFT DIA. SHAFT D	A 425
	1IA. I IP-POLAR MOM. IT-TRANS. MOM. EX10-6 EI	A 426
	2,/,120H (LP) (IN.) OUTSIDE INSIDE (	A 427
	3IN**4) (LP-IN**2) (LB-IN**2) ,/)	A 428
910	FORMAT (I7,F16.3,F12.3,F10.3,F10.3,F11.2,F12.3,F16.3,F11.2,G10.3)	A 429
920	FORMAT (16X,7H-----,5X,7H-----/7X,F16.3,F12.3/)	A 430
930	FORMAT (/,34X,# LINEAR SUPPORT BEARING STIFFNESS CHARACTERICS#/) )	A 431
940	FORMAT (5X,16HBEARING BEARING,12X,3HKXX,16X,3HKXY,16X,3HKYX,16X,3	A 432
	1HKYY,/,5X,6HNUMBER,3X,8HLOCATION,8X,7H(LB/IN),11X,7H(LB/IN),11X,7H(	A 433
	2LB/IN),11X,7H(LB/IN))	A 434
950	FORMAT (5X,I3,8X,I3,9X,F11.1,5X,F11.1,8X,F11.1,8X,F11.1)	A 435
960	FORMAT (/,35X,# LINEAR SUPPORT BEARING DAMPING CHARACTERISTICS#/	A 436
	1)	A 437
970	FORMAT (5X,16HDAMPING DAMPING,12X,3HCXX,16X,3HCXY,16X,3HCYX,16X,3	A 438
	1HCYY,/,5X,6HNUMBER,3X,8HLOCATION,6X,11H(LB-SEC/IN),10X,11H(LB-SEC/	A 439
	2IN),10X,11H(LB-SEC/IN),10X,11H(LB-SEC/IN))	A 440
980	FORMAT (//,10X,#FULL BEARING NO.#,I2,3X,#AT STATION#,I3,/) )	A 441
990	FORMAT (10X,#BEARING STIFFNESS LB/IN#,,/,4(4(5X,G15.3),/),/,10X,#	A 442
	1BEARING DAMPING LB-SEC/IN#,,/,4(4(5X,G15.3),/))	A 443
1000	FORMAT (//,20X,#EXTERNAL FORCES#,,/,5X,#STATION NO.#,10X,#X#,15X,#Y	A 444
	1#,,/)	A 445
1010	FORMAT (10X,I3,2(5X,G15.5))	A 446
1020	FORMAT (//,20X,#SKEWED DISC#,,/,5X,#STATION NO.#,10X,#SKEW(RAD)#,5X	A 447
	1,#PHASE ANGLE DEG.#,,/)	A 448
1030	FORMAT (10X,I3,2(5X,G15.5))	A 449
1040	FORMAT (///,25X,#ROTOR UNBALANCE IN OZ-IN.#,/) )	A 450
1050	FORMAT (5X,#STATION#,10X,#X-UNBALANCE#,10X,#Y-UNBALANCE#,/) )	A 451
1060	FORMAT (8X,I2,12X,F10.3,11X,F10.3)	A 452
1070	FORMAT (//,20X,#SHAFT INITIAL CONDITIONS#,,/,5X,#STATION NO.#,5X,#	A 453
	1BDW-MILS#,5X,#PHASE ANGLE#,5X,#X-DISP#,10X,#Y-DISP#,10X,#X-VEL#,10X	A 454
	2,#Y-VEL#,/,34X,#(DEGREES)#,6X,#(MILS)#,10X,#(MILS)#,10X,#MIL/IN#,1	A 455
	30X,#MIL/IN#,/)	A 456

1080	FORMAT (5X,I3,6(5X,F10.2))	A 457
1090	FORMAT (//,10X,#AVERAGE BEARING STIFFNESS USED FOR CRITICAL SPEED 1CALCULATIONS#)	A 458 A 459
1100	FORMAT (10X,#BEARING NO.#,I2,5X,#STIFFNESS(LB/IN)#,F12.2)	A 460
1110	FORMAT (1H1,/) )	A 461
1120	FORMAT (//,5X,# INITIAL SPEED=#,F10.2,5X,#FINAL SPEED=#,F10.2,5X,# 1SPEED INCREMENT=#,F10.2,# RPM#,//)	A 462 A 463
1130	FORMAT (/13X,3HRPM,20X,5HDELTA,12X,2HK1,13X,2HK2/)	A 464
1140	FORMAT (10X,F8.1,9X,E17.9)	A 465
1150	FORMAT (//,10X,#CRITICAL SPEED NO.#,I2)	A 466
1160	FORMAT (/1,10X,14HCRITICAL SPEED,11X,5HDELTA,/) )	A 467
1170	FORMAT (/1,12X,6HSTA NG,10X,14HNET DEFLECTION,10X,5HANGLE)	A 468
1180	FORMAT (12X,I5,13X,F9.5,13X,F9.5)	A 469
1190	FORMAT (5X,10(F8.2,2X))	A 470
1200	FORMAT (//,10X,#NONLINEAR BEARING DATA#,//,5X,#NONLINEAR#,6X,#STAT 1ION NO.#,4X,#BEARING NO.#,4X,#VISCOSITY#,6X,#RADIUS#,9X,#LENGTH#,9 2X,#CLEARANCE#,/,5X,#BEARING #,38X,#LB/IN**2#,7X,#(IN.)#,10X,#(IN. 3)#,10X,#(IN.)#,/)	A 471 A 472 A 473 A 474
1210	FORMAT (5X,I5,10X,I5,10X,I5,10X,E10.4,5X,E10.4,5X,E10.4,5X,E10.4) END	A 475 A 476-

ORIGINAL PAGE IS  
OF POOR QUALITY

	SUBROUTINE TMM	B	1
C	*****	B	2
C	THIS SUBROUTINE CONTROLS THE MODAL ANALYSIS OPERATION AFTER THE	B	3
C	PLANAR CRITICAL SPEEDS AND MODE SHAPES HAVE BEEN CALCULATED.	B	4
C	*****	B	5
	COMPLEX B,C	B	6
	REAL KXX,KXY,KYX,KYY,MFX,MFY,MUX,MUY,KMX,KMY	B	7
	REAL KKXX,KKXY,KKYX,KKYY,KCXX,KCXY,KCYX,KCYY	B	8
	COMMON /BLK1/ N,NB,NNLIN,NMB,NF,NU,NS,NBW,ISTAB,IMODE,ISKU,NNCT,N	B	9
	1UFPT	B	10
	COMMON /BLK2/ ISKIP,NSTEP,NCYCLE,NITP,NINT,NPLOT,NORBIT,NTIME,NSPE	B	11
	LED,NINC,NOPT,NT	B	12
	COMMON /BLK3/ CRT(10),LLBD(10),LLNB(5),LLNMB(9),LLSK(10),LLNT(10),	B	13
	1LLUF(10),LLFF(10),LLUT(10)	B	14
	COMMON /BLK4/ KXX(10),KXY(10),KYX(10),KYY(10),CXX(10),CXY(10),CYX(	B	15
	110),CYY(10),SLNMB(9,4,4),CLNMB(9,4,4)	B	16
	COMMON /BLK5/ UX(10),UY(10),FX(10),FY(10),FSK(10),PSK(10)	B	17
	COMMON /BLK6/ BW(100),PBW(100),XIDC(100),YIDC(100),VXIDC(100),VY	B	18
	1IDC(100),BXA(100),BYA(100)	B	19
	COMMON /BLK7/ CMX(10,10),KMX(10,10),EMX(10,10),CMY(10,10),KMY(10,1	B	20
	10),EMY(10,10)	B	21
	COMMON /BLK8/ MFX(10),MFY(10),MUX(10),MUY(10),MBX(10),MBY(10)	B	22
	COMMON /BLK9/ DDPC(10,100),EEYTH(10,100)	B	23
	COMMON /BLK10/ SPS,SPF,SPN,SPEED1	B	24
	COMMON /BLK11/ DDY(10,10),DDY(10,10),EDX(10,10),EDY(10,10)	B	25
	COMMON /BLK15/ RP(100),RT(100)	B	26
	COMMON /BLK16/ SPEED2,ANGSP,ANGACL,FSPEED	B	27
	COMMON /BLK18/ AKK(10)	B	28
	COMMON /BLK20/ A1(2,10),A2(2,10),A3(2,10),B1(2,10),B2(2,10),B3(2,1	B	29
	10)	B	30
	COMMON /BLK24/ B(20,21),C(20)	B	31
	COMMON /BLK25/ BETA	B	32
	COMMON /BLK29/ PASP	B	33
	COMMON /BLK35/ WMY(10),VIS(5),ANR(5),ANL(5),ANC(5),NLB(5)	B	34
	COMMON /BLK39/ NSPD,SSPEED(10)	B	35
	COMMON /BLK40/ FC(512),SFC(8,512)	B	36
	COMMON /BLK41/ KKXX(10,10),KKXY(10,10),KKYX(10,10),KKYY(10,10),KCX	B	37
	1X(10,10),KCXY(10,10),KCYX(10,10),KCYY(10,10)	B	38

	COMMON /BLK42/ BVIS(8,5),BANR(8,5),BANL(8,5),BANC(8,5),INLB(8,5)	B	39
	COMMON S1(4001),S2(4001)	B	40
	IF (NBOW.EQ.0) GO TO 10	B	41
	CALL SFTBDW	B	42
10	CONTINUE	B	43
	STEP=NSTEP	B	44
	FMAX=0.	B	45
	NUM=NCYCLE*NSTEP	B	46
	CALL CALCOMP (10)	B	47
	DO 140 K=1,NSPD	B	48
	XMAX=0.	B	49
	YMAX=0.	B	50
	SPEED2=SSPEED(K)	B	51
	DELTAT=60./((SSPEED(K)+STEP)	B	52
	DO 20 J=1,NB	B	53
	KXX(J)=KKXX(K,J)-AKK(J)	B	54
	KXY(J)=KKXY(K,J)	B	55
	KYX(J)=KKYX(K,J)	B	56
	KYY(J)=KKYY(K,J)-AKK(J)	B	57
	CXX(J)=KCXX(K,J)	B	58
	CXY(J)=KCXY(K,J)	B	59
	CYX(J)=KCYX(K,J)	B	60
	CYY(J)=KCYX(K,J)	B	61
20	CONTINUE	B	62
	IF (NNLIN.EQ.0) GO TO 40	B	63
	DO 30 J=1,NNLIN	B	64
	VIS(J)=BVIS(K,J)	B	65
	ANR(J)=BANR(K,J)	B	66
	ANL(J)=BANL(K,J)	B	67
	ANC(J)=BANC(K,J)	B	68
	NLB(J)=INLB(K,J)	B	69
30	CONTINUE	B	70
40	CONTINUE	B	71
	SPEED=SPEED2	B	72
	CALL TMODEL	B	73
	NSTEP1=NSTEP+1	B	74
	TIME=0.	B	75
	IINT=1	B	76

ORIGINAL PAGE IS  
OF POOR QUALITY

```

IF (NINC.EQ.0) GO TO 60
CALL UBST (1,SPEED)
DO 50 I=1,NNCT
II=I+NNCT
A3(1,I)=REAL(C(I))*0.9
B3(1,I)=REAL(C(II))*0.9
A2(1,I)=-AIMAG(C(I))*SPEED*0.10471975*.9
50 B2(1,I)=-AIMAG(C(II))*SPEED*0.10471975*.9
GO TO 70
60 CALL TINC
IF (NBOW.EQ.0) GO TO 70
CALL SFTBOW
70 CONTINUE
ICOUNT=1
CALL TSTORE (NNCT,1,XMAX,YMAX)
NK=0
NPLUS=0
IF (ANGACL.NE.0.) NPLUS=99999
NJ=NPLUS+1
PASP=0.
DO 110 I=1,NUM
TIME=TIME+DELTAT
IF (I.GT.NJ) NK=1
CALL TMODE2 (TIME,DELTAT,SPEED,NK)
CALL TACCEL
GO TO (80,90), NINT
80 CALL TBETA (NNCT,DELTAT,BETA)
GO TO 100
90 CALL TINTG (NNCT,DELTAT)
100 CONTINUE
ICOUNT=ICOUNT+1
CALL TSTORE (NNCT,ICOUNT,XMAX,YMAX)
PASP=PASP+DELTAT*SPEED
110 CONTINUE
CALL TFFT (FC,NSTEP)
DO 120 J=1,512
CFC=FC(J)*SSPEED(1)/SSPEED(K)
IF (CFC.LT.FMAX) GO TO 120

```

```

B 77
B 78
B 79
B 80
B 81
B 82
B 83
B 84
B 85
B 86
B 87
B 88
B 89
B 90
B 91
B 92
B 93
B 94
B 95
B 96
B 97
B 98
B 99
B 100
B 101
B 102
B 103
B 104
B 105
B 106
B 107
B 108
B 109
B 110
B 111
B 112
B 113
B 114

```

	FMAX=CFC	B 115
120	CONTINUE	B 116
130	SFC(K,J)=CFC	B 117
	FTIME=TIME	B 118
	NPLT=20*NSTEP+1	B 119
	IF (NPLT.EQ.1) GO TO 140	B 120
	CALL OBPLT (XMAX,YMAX,NPLT,LLNT(1),NSTEP,K)	B 121
	CALL THPLOT (XMAX,YMAX,NPLT,LLNT(1),FTIME,NSTEP)	B 122
140	CONTINUE	B 123
	CALL SPLOT (FMAX)	B 124
	RETURN	B 125
	END	B 126-

ORIGINAL PAGE IS  
OF POOR QUALITY

	SUBROUTINE TMODEL	C	1
C	*****	C	2
C	THIS SUBROUTINE CALCULATES THE MODAL COEFFICIENTS WHICH ARE INDEPE	C	3
C	OF SPEED AND ACCELERATION. THEY CAN BE USED IN OTHER SUBROUTINES.	C	4
C	*****	C	5
	REAL KXX,KXY,KYX,KYY,MFX,MFY,MUX,MUY,KMX,KMY	C	6
	COMMON /BLK1/ N,NB,NNLIN,NMB,NF,NU,NS,NBOW,ISTAB,IMODE,ISKU,NNCT,N	C	7
	1UFPT	C	8
	COMMON /BLK3/ CRT(10),LLBD(10),LLNB(5),LLNMB(9),LLSK(10),LLNT(10),	C	9
	1LLUF(10),LLFF(10),LLUT(10)	C	10
	COMMON /BLK4/ KXX(10),KXY(10),KYX(10),KYY(10),CXX(10),CXY(10),CYX(	C	11
	110),CYY(10),SLNKB(9,4,4),CLNMB(9,4,4)	C	12
	COMMON /BLK7/ CMX(10,10),KMX(10,10),EMX(10,10),CHY(10,10),KMY(10,1	C	13
	10),ENY(10,10)	C	14
	COMMON /BLK8/ MFX(10),MFY(10),MUX(10),MUY(10),MBX(10),MBY(10)	C	15
	COMMON /BLK9/ DDPC(10,100),EYTH(10,100)	C	16
	COMMON /BLK11/ DOX(10,10),DOY(10,10),EOX(10,10),EOY(10,10)	C	17
	COMMON /BLK22/ W(100)	C	18
	COMMON /BLK35/ WMY(10),VIS(5),ANR(5),ANL(5),ANC(5),NLB(5)	C	19
	DO 10 I=1,NNCT	C	20
	DO 10 J=1,NNCT	C	21
	CMX(I,J)=0.	C	22
	CMY(I,J)=0.	C	23
	KMX(I,J)=0.	C	24
	KMY(I,J)=0.	C	25
	DOX(I,J)=0.	C	26
	DOY(I,J)=0.	C	27
	EOX(I,J)=0.	C	28
	EOY(I,J)=0.	C	29
10	CONTINUE	C	30
	DO 30 I=1,NB	C	31
	J=LLBD(I)	C	32
	DO 20 K=1,NNCT	C	33
	DO 20 L=1,NNCT	C	34
	CMX(K,L)=CMX(K,L)+CXX(I)*DDPC(K,J)*DDPC(L,J)	C	35
	CMY(K,L)=CMY(K,L)+CYY(I)*DDPC(K,J)*DDPC(L,J)	C	36
	KMX(K,L)=KMX(K,L)+KXX(I)*DDPC(K,J)*DDPC(L,J)	C	37
	KMY(K,L)=KMY(K,L)+KYY(I)*DDPC(K,J)*DDPC(L,J)	C	38

	DDX(K,L)=DDX(K,L)+CXY(I)*DDPC(K,J)*DDPC(L,J)	C	39
	DDY(K,L)=DDY(K,L)+CYX(I)*DDPC(K,J)*DDPC(L,J)	C	40
	EDX(K,L)=EDX(K,L)+KXY(I)*DDPC(K,J)*DDPC(L,J)	C	41
20	EDY(K,L)=EDY(K,L)+KYX(I)*DDPC(K,J)*DDPC(L,J)	C	42
30	CONTINUE	C	43
	IF (NMB.EQ.0) GO TO 50	C	44
	DO 40 I=1,NMB	C	45
	L=LLNMB(I)	C	46
	DO 40 J=1,NNCT	C	47
	DO 40 K=1,NNCT	C	48
	CHX(J,K)=CHX(J,K)+CLNMB(I,1,1)*DDPC(J,L)*DDPC(K,L)+CLNMB(I,1,2)*DD	C	49
	1PC(J,L)*EEYTH(K,L)+CLNMB(I,2,1)*EEYTH(J,L)*DDPC(K,L)+CLNMB(I,2,2)*	C	50
	2*EEYTH(J,L)*EEYTH(K,L)	C	51
	CHY(J,K)=CHY(J,K)+CLNMB(I,3,3)*DDPC(J,L)*DDPC(K,L)+CLNMB(I,3,4)*DD	C	52
	1PC(J,L)*EEYTH(K,L)+CLNMB(I,4,3)*EEYTH(J,L)*DDPC(K,L)+CLNMB(I,4,4)*	C	53
	2*EEYTH(J,L)*EEYTH(K,L)	C	54
	KHX(J,K)=KHX(J,K)+SLNMB(I,1,1)*DDPC(J,L)*DDPC(K,L)+SLNMB(I,1,2)*DD	C	55
	1PC(J,L)*EEYTH(K,L)+SLNMB(I,2,1)*EEYTH(J,L)*DDPC(K,L)+SLNMB(I,2,2)*	C	56
	2*EEYTH(J,L)*EEYTH(K,L)	C	57
	KHY(J,K)=KHY(J,K)+SLNMB(I,3,3)*DDPC(J,L)*DDPC(K,L)+SLNMB(I,3,4)*DD	C	58
	1PC(J,L)*EEYTH(K,L)+SLNMB(I,4,3)*EEYTH(J,L)*DDPC(K,L)+SLNMB(I,4,4)*	C	59
	2*EEYTH(J,L)*EEYTH(K,L)	C	60
	DDX(J,K)=DDX(J,K)+CLNMB(I,1,3)*DDPC(J,L)*DDPC(K,L)+CLNMB(I,1,4)*DD	C	61
	1PC(J,L)*EEYTH(K,L)+CLNMB(I,2,3)*EEYTH(J,L)*DDPC(K,L)+CLNMB(I,2,4)*	C	62
	2*EEYTH(J,L)*EEYTH(K,L)	C	63
	DDY(J,K)=DDY(J,K)+CLNMB(I,3,1)*DDPC(J,L)*DDPC(K,L)+CLNMB(I,3,2)*DD	C	64
	1PC(J,L)*EEYTH(K,L)+CLNMB(I,4,1)*EEYTH(J,L)*DDPC(K,L)+CLNMB(I,4,2)*	C	65
	2*EEYTH(J,L)*EEYTH(K,L)	C	66
	EDX(J,K)=EDX(J,K)+SLNMB(I,1,3)*DDPC(J,L)*DDPC(K,L)+SLNMB(I,1,4)*DD	C	67
	1PC(J,L)*EEYTH(K,L)+SLNMB(I,2,3)*EEYTH(J,L)*DDPC(K,L)+SLNMB(I,2,4)*	C	68
	2*EEYTH(J,L)*EEYTH(K,L)	C	69
40	EDY(J,K)=EDY(J,K)+SLNMB(I,3,1)*DDPC(J,L)*DDPC(K,L)+SLNMB(I,3,2)*DD	C	70
	1PC(J,L)*EEYTH(K,L)+SLNMB(I,4,1)*EEYTH(J,L)*DDPC(K,L)+SLNMB(I,4,2)*	C	71
	2*EEYTH(J,L)*EEYTH(K,L)	C	72
50	CONTINUE	C	73
	DO 60 I=1,NNCT	C	74
	MFX(I)=0.	C	75
60	MFY(I)=0.	C	76



```
      IF (NNLIN.EQ.0) GO TO 90
      DO 80 I=1,NNCT
      DO 70 J=1,N
70      MFY(I)=MFY(I)+DDPC(I,J)*W(J)
      WMY(I)=MFY(I)
80      CONTINUE
90      CONTINUE
      RETURN
      END
```

```
C 77
C 78
C 79
C 80
C 81
C 82
C 83
C 84
C 85-
```

	SUBROUTINE UBST (IND,SD)	D	1
C	*****	D	2
C	THIS SUBROUTINE CALCULATES THE UNBALANCE RESPONSE OF ROTOR SYSTEM	D	3
C	USING THE PLAKAK MODES. WHICH CAN LATER BE TRANSFORMED INTO REAL	D	4
C	DISPLACEMENTS.	D	5
C	*****	D	6
	REAL MBX,MBY	D	7
	DIMENSION SPED(50)	D	8
	COMPLEX B,C,DUM	D	9
	COMPLEX EUM	D	10
	REAL KXX,KXY,KYX,KYY,MFX,MFY,MUX,MUY,KMX,KMY	D	11
	COMMON /BLK1/ N,NB,NNLIN,NMB,NF,NU,NS,NBOW,ISTAB,IMODE,ISKU,NNCT,N	D	12
	1UFPT	D	13
	COMMON /BLK3/ CRT(10),LLBD(10),LLNB(5),LLNMB(9),LLSK(10),LLNT(10),	D	14
	1LLUF(10),LLFF(10),LLUT(10)	D	15
	COMMON /BLK5/ UX(10),UY(10),FX(10),FY(10),FSK(10),PSK(10)	D	16
	COMMON /BLK7/ CMX(10,10),KMX(10,10),EMX(10,10),CMY(10,10),KMY(10,1	D	17
	10),EMY(10,10)	D	18
	COMMON /BLK8/ MFX(10),MFY(10),MUX(10),MUY(10),MBX(10),MBY(10)	D	19
	COMMON /BLK9/ DDPC(10,100),EEYTH(10,100)	D	20
	COMMON /BLK10/ SPS,SPF,SPN,SPEED1	D	21
	COMMON /BLK11/ DDY(10,10),DDY(10,10),EDX(10,10),EDY(10,10)	D	22
	COMMON /BLK15/ RP(100),RT(100)	D	23
	COMMON /BLK18/ AKK(10)	D	24
	COMMON /BLK21/ DMX(10,10),DMY(10,10)	D	25
	COMMON /BLK24/ B(20,21),C(20)	D	26
	COMMON UDISPXR(10,50),UDISPXI(10,50),UDISPYR(10,50),UDISPYI(10,50)	D	27
	1,XKAJ(10,50),XKIN(10,50),PMAJ(10,50),PKIN(10,50),ADUMMY(4002)	D	28
	SP1=SPN	D	29
	IJ=1	D	30
	ANGSP=SD*3.14159/30.	D	31
	NN=NNCT*2	D	32
	MM=NNCT*2+1	D	33
	DUM=CMPLX(0.,1.)	D	34
	EUM=CMPLX(1.,0.)	D	35
	DO 10 I=1,NNCT	D	36
	MUX(I)=0.	D	37
	MUY(I)=0.	D	38

ORIGINAL PAGE IS  
OF POOR QUALITY

10	CONTINUE	D	39
	IF (NU.EQ.0) GO TO 40	D	40
	DO 30 I=1,NU	D	41
	J=LLUF(I)	D	42
	DO 20 K=1,NNCT	D	43
	MUX(K)=MUX(K)+ANGSP*ANGSP*UX(I)*DDPC(K,J)	D	44
	MUY(K)=MUY(K)+ANGSP*ANGSP*UY(I)*DDPC(K,J)	D	45
20	CONTINUE	D	46
30	CONTINUE	D	47
40	IF (NS.EQ.0) GO TO 70	D	48
	DO 60 I=1,NS	D	49
	J=LLSK(I)	D	50
	PAS=PSK(I)/57.29578	D	51
	PCOS=COS(PAS)	D	52
	PSIN=SIN(PAS)	D	53
	DO 50 K=1,NNCT	D	54
	MUX(K)=MUX(K)+ANGSP*ANGSP*FSK(I)*PCOS*(RP(J)-RT(J))*EEYTH(K,J)/386	D	55
	1.4	D	56
50	MUY(K)=MUY(K)+ANGSP*ANGSP*FSK(I)*PSIN*(RP(J)-RT(J))*EEYTH(K,J)/386	D	57
	1.4	D	58
60	CONTINUE	D	59
70	CONTINUE	D	60
	IF (NBOW.EQ.0) GO TO 90	D	61
	DO 80 I=1,NNCT	D	62
	MUX(I)=MUX(I)+MBX(I)	D	63
80	MUY(I)=MUY(I)+MBY(I)	D	64
90	CONTINUE	D	65
	DO 100 K=1,NNCT	D	66
	DO 100 L=1,NNCT	D	67
	EMX(K,L)=EGX(K,L)	D	68
	EMY(K,L)=EY(K,L)	D	69
	DMX(K,L)=DOX(K,L)	D	70
	DMY(K,L)=DOY(K,L)	D	71
	DO 100 J=1,N	D	72
	DMX(K,L)=DMX(K,L)+ANGSP*RP(J)*EEYTH(K,J)*EEYTH(L,J)/386.4	D	73
	DMY(K,L)=DMY(K,L)-ANGSP*RP(J)*EEYTH(K,J)*EEYTH(L,J)/386.4	D	74
100	CONTINUE	D	75
	DO 120 I=1,10	D	76

	DO 110 J=1,11	D	77
110	B(I,J)=CMPLX(0.,0.)	D	78
120	C(I)=CMPLX(0.,0.)	D	79
	IF (NNLIN.EQ.0) GO TO 140	D	80
	DO 130 I=1,NNCT	D	81
130	MUY(I)=MUY(I)-MFY(I)	D	82
140	CONTINUE	D	83
	DO 160 I=1,NNCT	D	84
	II=I+NNCT	D	85
	DO 150 J=1,NNCT	D	86
	JJ=J+NNCT	D	87
	B(I,J)=B(I,J)+KMX(I,J)*EUM+CMX(I,J)*DUM*ANGSP	D	88
	B(II,J)=B(II,J)+EMY(I,J)*EUM+DMY(I,J)*DUM*ANGSP	D	89
	B(I,JJ)=B(I,JJ)+EMX(I,J)*EUM+DMX(I,J)*DUM*ANGSP	D	90
150	B(II,JJ)=B(II,JJ)+KMY(I,J)*EUM+CHY(I,J)*DUM*ANGSP	D	91
	B(I,I)=B(I,I)+((CRT(I)*3.14159/30.)**2-ANGSP**2)*EUM	D	92
	B(II,II)=B(II,II)+((CRT(I)*3.14159/30.)**2-ANGSP**2)*EUM	D	93
	NEX=NNCT*2+1	D	94
	B(I,NEX)=-CMPLX(MUX(I),MUY(I))	D	95
160	B(II,NEX)=-CMPLX(MUY(I),-MUX(I))	D	96
	CALL SOLVE (NN,MM)	D	97
	RETURN	D	98
	END	D	99-

```

SUBROUTINE SOLVE (NN,MM)
COMPLEX B,C,DUMMY,CONJG
COMMON /BLK24/ B(20,21),C(20)
DO 80 I=1,NN
K=I
10 IF (CABS(B(K,1)).GT.0.000001) GO TO 20
K=K+1
IF (K-NN) 10,10,90
20 IF (I-K) 30,50,90
30 DO 40 M=1,MM
DUMMY=B(I,M)
B(I,M)=B(K,M)
40 B(K,M)=DUMMY
50 II=I+1
IF (II.GT.NN) GO TO 80
DO 70 N=II,NN
IF (CABS(B(N,I)).LT.0.000001) GO TO 70
SQ=(CABS(B(I,I)))**2
DUMMY=B(N,I)*CONJG(B(I,I))/SQ
GO 60 M=I,MM
60 B(N,M)=B(N,M)-B(I,M)*DUMMY
70 CONTINUE
80 CONTINUE
GO TO 100
90 IF (I.EQ.NN) WRITE (3,150)
IF (I.LT.NN) WRITE (3,160)
STOP
C
START BACK SUBSTITUTIONS
100 I=NN
110 DUMMY=(0.0,0.0)
IF (I.EQ.NN) GO TO 130
JJJ=I+1
DO 120 J=JJJ,NN
120 DUMMY=DUMMY+B(I,J)*C(J)
130 SQ=(CABS(B(I,I)))**2
C(I)=-((DUMMY+B(I,MM))*CONJG(B(I,I))/SQ)
I=I-1
IF (I) 140,140,110

```

```

E 1
E 2
E 3
E 4
E 5
E 6
E 7
E 8
E 9
E 10
E 11
E 12
E 13
E 14
E 15
E 16
E 17
E 18
E 19
E 20
E 21
E 22
E 23
E 24
E 25
E 26
E 27
E 28
E 29
E 30
E 31
E 32
E 33
E 34
E 35
E 36
E 37
E 38

```

140 RETURN  
C  
150 FORMAT (4X,19HMATRIX HAS ZERO ROW)  
160 FORMAT (4X,22HMATRIX HAS ZERO COLUMN)  
END

E 39  
E 40  
E 41  
E 42  
E 43-

ORIGINAL PAGE IS  
OF POOR QUALITY

	FUNCTION PANG (AFCS,AFSN)	F	1
C		F	2
C	* THIS IS A FUNCTION USED TO CALCULATE THE ANGLE ****	F	3
C	* WHOSE ARCTAN VALUE IS GIVEN *****	F	4
C		F	5
	ACS=AFCS	F	6
	ASN=AFSN	F	7
	IF (ASN) 40,10,40	F	8
10	IF (ACS) 20,30,30	F	9
20	ANG=180.0	F	10
	GO TO 120	F	11
30	ANG=0.0	F	12
	GO TO 120	F	13
40	IF (ACS) 90,50,80	F	14
50	IF (ASN) 60,30,70	F	15
60	ANG=270.	F	16
	GO TO 120	F	17
70	ANG=90.	F	18
	GO TO 120	F	19
80	ANG=0.	F	20
	GO TO 100	F	21
90	ANG=-180.	F	22
100	ASN=ASN/ACS	F	23
	ACS=ABS(ASN)	F	24
	ACS=ATAN(ACS)	F	25
	ANG=ANG+ACS*57.295780	F	26
	IF (ASN) 110,120,120	F	27
110	ANG=-ANG	F	28
120	IF (ANG) 130,140,140	F	29
130	ANG=ANG+360.	F	30
140	PANG=ANG	F	31
	RETURN	F	32
	END	F	33-

	SUBROUTINE SFTBOW	G	1
C	*****	G	2
C	THIS SUBROUTINE CALCULATES THE SHAFT BOW EFFECTS INTO MODAL	G	3
C	COORDINATES. (FOR INITIAL CONDITIONS AND UNBALANCE EFFEC	G	4
C	*****	G	5
	DIMENSION BX(100), BY(100)	G	6
	DIMENSION X(10), Y(10), Z(10,10)	G	7
	REAL MBX,MBY	G	8
	COMMON /BLK1/ N,NB,NNLIN,NMB,NF,NU,NS,NBOW,ISTAB,IMODE,ISKU,NNCT,N	G	9
	1UFPT	G	10
	COMMON /BLK3/ CRT(10),LLBD(10),LLNB(5),LLNMB(9),LLSK(10),LLNT(10),	G	11
	1LLUF(10),LLFF(10),LLUT(10)	G	12
	COMMON /BLK6/ BOW(100),PBOW(100),XIDC(100),YIDC(100),VXIDC(100),VY	G	13
	1IDC(100),BXA(100),BYA(100)	G	14
	COMMON /BLK8/ MFX(10),MFY(10),MUX(10),MUY(10),MBX(10),MBY(10)	G	15
	COMMON /BLK9/ DDPC(10,100),EEYTH(10,100)	G	16
	COMMON /BLK15/ RP(100),RT(100)	G	17
	COMMON /BLK18/ AKK(10)	G	18
	COMMON /BLK19/ DX(100)	G	19
	COMMON /BLK22/ W(100)	G	20
	DO 10 I=1,N	G	21
	CT=PBOW(I)*3.14159/180.	G	22
	BX(I)=BOW(I)*COS(CT)/1000.	G	23
10	BY(I)=BOW(I)*SIN(CT)/1000.	G	24
	TC=(BX(2)-BX(1))/DX(1)	G	25
	TD=(BY(2)-BY(1))/DX(1)	G	26
	BXA(1)=ATAN(TC)	G	27
	BYA(1)=ATAN(TD)	G	28
	TC=(BX(N)-BX(N-1))/DX(N-1)	G	29
	TD=(BY(N)-BY(N-1))/DX(N-1)	G	30
	BXA(N)=ATAN(TC)	G	31
	BYA(N)=ATAN(TD)	G	32
	N1=N-1	G	33
	DO 20 I=2,N1	G	34
	TC=(BX(I+1)-BX(I-1))/(DX(I-1)+DX(I))	G	35
	TD=(BY(I+1)-BY(I-1))/(DX(I-1)+DX(I))	G	36
	BXA(I)=ATAN(TC)	G	37
	BYA(I)=ATAN(TD)	G	38



20	CONTINUE	G	39
	DO 60 I=1,NNCT	G	40
	X(I)=0.	G	41
	Y(I)=0.	G	42
	DO 40 J=1,NNCT	G	43
	Z(I,J)=0.	G	44
	DO 30 K=1,NB	G	45
	L=LLBD(K)	G	46
30	Z(I,J)=Z(I,J)-DDPC(I,L)*AKK(K)*DDPC(J,L)	G	47
40	CONTINUE	G	48
	DO 50 K=1,N	G	49
	X(I)=X(I)+(DDPC(I,K)*W(K)*BX(K)+EEYTH(I,K)*RT(K)*BXA(K))/386.4	G	50
50	Y(I)=Y(I)+(DDPC(I,K)*W(K)*BY(K)+EEYTH(I,K)*RT(K)*BYA(K))/386.4	G	51
60	Z(I,I)=Z(I,I)+(CRT(I)*0.1047197)**2	G	52
	DO 70 I=1,NNCT	G	53
	MBX(I)=0.	G	54
	MBY(I)=0.	G	55
	DO 70 J=1,NNCT	G	56
	MBX(I)=MBX(I)+Z(I,J)*X(J)	G	57
70	MBY(I)=MBY(I)+Z(I,J)*Y(J)	G	58
	RETURN	G	59
	END	G	60-

ORIGINAL PAGE IS  
OF POOR QUALITY

	SUBROUTINE TMODE2 (T,DELTAT,SPEED,NK)	H	1
C	*****	H	2
C	THIS SUBROUTINE CALCULATES THE MODAL COEFFICIENTS FOR TRANSIENT	H	3
C	RESPONSE ANALYSIS	H	4
C	*****	H	5
	REAL MBX,MBY	H	6
	REAL KXX,KXY,KYX,KYY,MFX,MFY,MUX,MUY,KMX,KMY	H	7
	COMMON /BLK1/ N,NB,NNLIN,NMB,NF,NU,NS,NBOW,ISTAB,IMODE,ISKU,NNCT,N	H	8
	1UFPT	H	9
	COMMON /BLK2/ ISKIP,NSTEP,NCYCLE,NITP,NINT,NPLOT,NORBIT,NTIME,NSPE	H	10
	1ED,NINC,NOPT,NT	H	11
	COMMON /BLK3/ CRT(10),LLBD(10),LLNB(5),LLNMB(9),LLSK(10),LLNT(10),	H	12
	1LLUF(10),LLFF(10),LLUT(10)	H	13
	COMMON /BLK5/ UX(10),UY(10),FX(10),FY(10),FSK(10),PSK(10)	H	14
	COMMON /BLK6/ BOW(100),PBOW(100),XIDC(100),YIDC(100),VXIDC(100),VY	H	15
	1IDC(100),BXA(100),BYA(100)	H	16
	COMMON /BLK7/ CMX(10,10),KMX(10,10),EMX(10,10),CMY(10,10),KMY(10,1	H	17
	10),EMY(10,10)	H	18
	COMMON /BLK8/ MFX(10),MFY(10),MUX(10),MUY(10),MBX(10),MBY(10)	H	19
	COMMON /BLK9/ DDPC(10,100),EEYTH(10,100)	H	20
	COMMON /BLK11/ DOX(10,10),DOY(10,10),EOX(10,10),EODY(10,10)	H	21
	COMMON /BLK15/ RP(100),RT(100)	H	22
	COMMON /BLK16/ SPEED2,ANGSP,ANGACL,FSPEED	H	23
	COMMON /BLK18/ AKK(10)	H	24
	COMMON /BLK21/ DMX(10,10),DMY(10,10)	H	25
	COMMON /BLK29/ PASP	H	26
	PI=3.14159	H	27
	ANGSP=SPEED*PI/30.	H	28
	DO 10 I=1,NNCT	H	29
	MUX(I)=0.	H	30
	MUY(I)=0.	H	31
	MFX(I)=0.	H	32
10	MFY(I)=0.	H	33
	IF (NU.EQ.0) GO TO 40	H	34
	DO 30 I=1,NU	H	35
	J=LLUF(I)	H	36
	PHI=ATAN2(UY(I),UX(I))	H	37
	DMT=ANGSP*T+PHI	H	38

ORIGINAL PAGE IS  
OF POOR QUALITY

	IF (NK.EQ.0) GMT=PASP+PHI	H	39
	TME=(UX(I)*UX(I)+UY(I)*UY(I))*0.5	H	40
	IF (NK.EQ.0) GMT=PASP+PHI	H	39
	TME=(UX(I)*UX(I)+UY(I)*UY(I))*0.5	H	40
	DO 20 K=1,NNCT	H	41
	MUX(K)=MUX(K)+(ANGACL*SIN(GMT)+ANGSP*ANGSP*COS(GMT))*TME*DDPC(K,J)	H	42
20	MUY(K)=MUY(K)+(ANGSP*ANGSP*SIN(GMT)-ANGACL*COS(GMT))*TME*DDPC(K,J)	H	43
30	CONTINUE	H	44
40	IF (NS.EQ.0) GO TO 60	H	45
	TIME=T	H	46
	DO 50 I=1,NS	H	47
	KK=LLSK(I)	H	48
	CAN=ANGSP*TIME+PSK(I)/57.29578	H	49
	IF (NK.EQ.0) CAN=PASP+PSK(I)/57.29578	H	50
	DO 50 J=1,NNCT	H	51
	MUX(J)=MUX(J)+(ANGSP*ANGSP*COS(CAN)+ANGACL*SIN(CAN))*FSK(I)*(RP(KK	H	52
	1)-RT(KK))*EETH(J,KK)/386.4	H	53
50	MUY(J)=MUY(J)+(ANGSP*ANGSP*SIN(CAN)-ANGACL*COS(CAN))*FSK(I)*(RP(KK	H	54
	1)-RT(KK))*EETH(J,KK)/386.4	H	55
60	IF (NBOW.EQ.0) GO TO 80	H	56
	DO 70 I=1,NNCT	H	57
	TMAG=(MBY(I)**2+MBX(I)**2)**0.5	H	58
	ANG=ATAN2(MBY(I),MBX(I))	H	59
	TANG=ANG+T*ANGSP	H	60
	IF (NK.EQ.0) TANG=PASP+ANG	H	61
	MUX(I)=MUX(I)+TMAG*COS(TANG)	H	62
70	MUY(I)=MUY(I)+TMAG*SIN(TANG)	H	63
80	CONTINUE	H	64
	IF (NK.EQ.1) GO TO 100	H	65
	DO 90 K=1,NNCT	H	66
	DO 90 L=1,NNCT	H	67
	EMX(K,L)=EOX(K,L)	H	68
	EMY(K,L)=EY(K,L)	H	69
	DMX(K,L)=DOX(K,L)	H	70
	DMY(K,L)=DOY(K,L)	H	71
	DO 90 J=1,N	H	72
	EMX(K,L)=EMX(K,L)+0.5*ANGACL*RP(J)*EETH(K,J)*EETH(L,J)/386.4	H	73
	EMY(K,L)=EMY(K,L)-0.5*ANGACL*RP(J)*EETH(K,J)*EETH(L,J)/386.4	H	74

90 DMX(K,L)=DMX(K,L)+ANGSP\*RP(J)\*EEYTH(K,J)\*EEYTH(L,J)/386.4  
 DMY(K,L)=DMY(K,L)-ANGSP\*RP(J)\*EEYTH(K,J)\*EEYTH(L,J)/386.4  
 100 SPEED=SPEED+30.\*ANGACL\*DELTAT/PI  
 CONTINUE  
 RETURN  
 END

H 75  
 H 76  
 H 77  
 H 78  
 H 79  
 H 80-

ORIGINAL PAGE IN  
 OF FOUR QUARTER

	SUBROUTINE TACCEL	I	1
C	*****	I	2
C	THIS SUBROUTINE CALCULATES THE MODAL ACCELERATION BY SOLVING	I	3
C	THE MODAL EQUATIONS OF MOTION	I	4
C	*****	I	5
	REAL KXX,KXY,KYX,KYY,MFX,MFY,MUX,MUY,KMX,KMY	I	6
	COMMON /BLK1/ N,NB,NNLIN,NMB,NF,NU,NS,NBOW,ISTAB,IMODE,ISKU,NNCT,N	I	7
	1UFPT	I	8
	COMMON /BLK3/ CRT(10),LLBD(10),LLNB(5),LLNMB(9),LLSK(10),LLNT(10),	I	9
	1LLUF(10),LLFF(10),LLUT(10)	I	10
	COMMON /BLK7/ CMX(10,10),KMX(10,10),EMX(10,10),CHY(10,10),KMY(10,1	I	11
	10),EMY(10,10)	I	12
	COMMON /BLK8/ MFX(10),MFY(10),MUX(10),MUY(10),MBX(10),MBY(10)	I	13
	COMMON /BLK9/ DDPC(10,100),EEYTH(10,100)	I	14
	COMMON /BLK20/ A1(2,10),A2(2,10),A3(2,10),B1(2,10),B2(2,10),B3(2,1	I	15
	10)	I	16
	COMMON /BLK21/ DMX(10,10),DMY(10,10)	I	17
	IF (NNLIN.EQ.0) GO TO 10	I	18
	CALL BNF	I	19
10	CONTINUE	I	20
	DO 30 I=1,NNCT	I	21
	A1(1,I)=MFX(I)+MUX(I)-(CRT(I)*0.10471975)**2*A3(1,I)	I	22
	B1(1,I)=MFY(I)+MUY(I)-(CRT(I)*0.10471975)**2*B3(1,I)	I	23
	DO 20 J=1,NMB	I	24
	A1(1,I)=A1(1,I)-CMX(I,J)*A2(1,J)-KMX(I,J)*A3(1,J)-DMX(I,J)*B2(1,J)	I	25
	1-EMX(I,J)*B3(1,J)	I	26
20	B1(1,I)=B1(1,I)-CHY(I,J)*B2(1,J)-KMY(I,J)*B3(1,J)-DMY(I,J)*A2(1,J)	I	27
	1-EMY(I,J)*A3(1,J)	I	28
30	CONTINUE	I	29
	RETURN	I	30
	END	I	31-

	SUBROUTINE TINTG (NNCT,DELTAT)	J	1
C	*****	J	2
C	THIS SUBROUTINE INTEGRATES THE MODAL ACCELERATION INTO VELOCITY	J	3
C	AND DISPLACEMENT BY MODIFIED EULER METHOD	J	4
C	*****	J	5
	COMMON /BLK2/ ISKIP,NSTEP,NCYCLE,NITP,NINT,NPLOT,NORBIT,NTIME,NSPE	J	6
	1ED,NINC,NOP1,NT	J	7
	COMMON /BLK20/ A1(2,10),A2(2,10),A3(2,10),B1(2,10),B2(2,10),B3(2,1	J	8
	10)	J	9
	DO 10 I=1,NNCT	J	10
	A2(2,I)=A2(1,I)+DELTAT*A1(1,I)	J	11
	B2(2,I)=B2(1,I)+DELTAT*B1(1,I)	J	12
	A3(2,I)=A3(1,I)+DELTAT*0.50*(A2(1,I)+A2(2,I))	J	13
10	B3(2,I)=B3(1,I)+DELTAT*0.50*(B2(1,I)+B2(2,I))	J	14
	DO 20 I=1,NNCT	J	15
	A1(1,I)=A1(2,I)	J	16
	A2(1,I)=A2(2,I)	J	17
	A3(1,I)=A3(2,I)	J	18
	B1(1,I)=B1(2,I)	J	19
	B2(1,I)=B2(2,I)	J	20
20	B3(1,I)=B3(2,I)	J	21
	RETURN	J	22
	END	J	23-

ORIGINAL PAGE IS  
OF POOR QUALITY

	SUBROUTINE TBETA (NNCT,DELTAT,BETA)	K	1
C	*****	K	2
C	THIS SUBROUTINE INTEGRATES THE MODAL ACCELERATIONS INTO MODAL	K	3
C	VELOCITY AND DISPLACEMENT BY NEWMARK BETA METHOD	K	4
C	*****	K	5
	DIMENSION STORE(6,10)	K	6
	COMMON /BLK20/ A1(2,10),A2(2,10),A3(2,10),B1(2,10),B2(2,10),B3(2,1	K	7
	10)	K	8
	DO 10 I=1,NNCT	K	9
	STORE(1,I)=A1(1,I)	K	10
	STORE(2,I)=B1(1,I)	K	11
	STORE(3,I)=A2(1,I)	K	12
	STORE(4,I)=B2(1,I)	K	13
	STORE(5,I)=A3(1,I)	K	14
10	STORE(6,I)=B3(1,I)	K	15
	DO 20 I=1,NNCT	K	16
	A2(1,I)=STORE(3,I)+DELTAT*STORE(1,I)	K	17
	B2(1,I)=STORE(4,I)+DELTAT*STORE(2,I)	K	18
	A3(1,I)=STORE(5,I)+.5*DELTAT*(STORE(3,I)+A2(1,I))	K	19
20	B3(1,I)=STORE(6,I)+.5*DELTAT*(STORE(4,I)+B2(1,I))	K	20
	CALL TACCEL	K	21
	DO 30 I=1,NNCT	K	22
	A2(1,I)=STORE(3,I)+.5*DELTAT*(A1(1,I)+STORE(1,I))	K	23
	B2(1,I)=STORE(4,I)+.5*DELTAT*(B1(1,I)+STORE(2,I))	K	24
	A3(1,I)=STORE(5,I)+DELTAT*STORE(3,I)+(.5-BETA)*STORE(1,I)*DELTAT*D	K	25
	1ELTAT+BETA*DELTAT*DELTAT*A1(1,I)	K	26
	B3(1,I)=STORE(6,I)+DELTAT*STORE(4,I)+(.5-BETA)*STORE(2,I)*DELTAT*D	K	27
	1ELTAT+BETA*DELTAT*DELTAT*B1(1,I)	K	28
	A3(2,I)=A3(1,I)	K	29
30	B3(2,I)=B3(1,I)	K	30
	RETURN	K	31
	END	K	32-

	SUBROUTINE TINC	L	1
C	*****	L	2
C	THIS SUBROUTINE TRANSFORMS THE ROTOR INITIAL CONDITIONS INTO	L	3
C	MODAL INITIAL CONDITIONS OF VELOCITIES AND DISPLACEMENTS	L	4
C	*****	L	5
	DIMENSION XTH(100), YTH(100), VXTH(100), VYTH(100)	L	6
	COMMON /BLK1/ N,NB,NNLIN,NMB,NF,NU,NS,NBOW,ISTAB,IMODE,ISKU,NNCT,N	L	7
	1UFPT	L	8
	COMMON /BLK6/ BDW(100),PBDW(100),XIDC(100),YIDC(100),VXIDC(100),VY	L	9
	1IDC(100),BXA(100),BYA(100)	L	10
	COMMON /BLK9/ DDPC(10,100),EEYTH(10,100)	L	11
	COMMON /BLK15/ RP(100),RT(100)	L	12
	COMMON /BLK19/ DX(100)	L	13
	COMMON /BLK20/ A1(2,10),A2(2,10),A3(2,10),B1(2,10),B2(2,10),B3(2,1	L	14
	10)	L	15
	COMMON /BLK22/ W(100)	L	16
	TC=(XIDC(2)-XIDC(1))/DX(1)	L	17
	TD=(YIDC(2)-YIDC(1))/DX(1)	L	18
	TE=(VXIDC(2)-VXIDC(1))/DX(1)	L	19
	TF=(VYIDC(2)-VYIDC(1))/DX(1)	L	20
	XTH(1)=ATAN(TC)	L	21
	YTH(1)=ATAN(TD)	L	22
	VXTH(1)=ATAN(TE)	L	23
	VYTH(1)=ATAN(TF)	L	24
	TC=(XIDC(N)-XIDC(N-1))/DX(N-1)	L	25
	TD=(YIDC(N)-YIDC(N-1))/DX(N-1)	L	26
	TE=(VXIDC(N)-VXIDC(N-1))/DX(N-1)	L	27
	TF=(VYIDC(N)-VYIDC(N-1))/DX(N-1)	L	28
	YTH(N)=ATAN(TD)	L	29
	XTH(N)=ATAN(TC)	L	30
	VXTH(N)=ATAN(TE)	L	31
	VYTH(N)=ATAN(TF)	L	32
	N1=N-1	L	33
	DO 10 I=2,N1	L	34
	TC=(XIDC(I+1)-XIDC(I-1))/(DX(I-1)+DX(I))	L	35
	TD=(YIDC(I+1)-YIDC(I-1))/(DX(I-1)+DX(I))	L	36
	TE=(VXIDC(I+1)-VXIDC(I-1))/(DX(I-1)+DX(I))	L	37
	TF=(VYIDC(I+1)-VYIDC(I-1))/(DX(I-1)+DX(I))	L	38



	XTH(I)=ATAN(TC)	L	39
	YTH(I)=ATAN(TD)	L	40
	VXTH(I)=ATAN(TE)	L	41
	VYTH(I)=ATAN(TF)	L	42
10	CONTINUE	L	43
	DO 20 I=1,NNCT	L	44
	A3(I,I)=0.	L	45
	B3(I,I)=0.	L	46
	A2(I,I)=0.	L	47
	B2(I,I)=0.	L	48
	DO 20 J=1,N	L	49
	A3(I,I)=A3(I,I)+(DDPC(I,J)*W(J)*XIDC(J)+EEYTH(I,J)*RT(J)*XTH(J))/3	L	50
	186.4	L	51
	B3(I,I)=B3(I,I)+(DDPC(I,J)*W(J)*YIDC(J)+EEYTH(I,J)*RT(J)*YTH(J))/3	L	52
	186.4	L	53
	A2(I,I)=A2(I,I)+(DDPC(I,J)*W(J)*VXIDC(J)+EEYTH(I,J)*RT(J)*VXTH(J))	L	54
	1/386.4	L	55
20	B2(I,I)=B2(I,I)+(DDPC(I,J)*W(J)*VYIDC(J)+EEYTH(I,J)*RT(J)*VYTH(J))	L	56
	1/386.4	L	57
	RETURN	L	58
	END	L	59-

	SUBROUTINE TSTORE (NNCT,ICOUNT,XMAX,YMAX)	M	1
C	*****	M	2
C	THIS SUBROUTINE STORES THE MODAL DISPLACEMENTS FOR EACH TIME	M	3
C	STEP INTO THE STORAGE BLOCK	M	4
C	*****	M	5
	COMMON /BLK3/ CRT(10),LLBD(10),LLNB(5),LLNMB(9),LLSK(10),LLNT(10),	M	6
	1LLUF(10),LLFF(10),LLUT(10)	M	7
	COMMON /BLK9/ DDPC(10,100),EEYTH(10,100)	M	8
	COMMON /BLK20/ A1(2,10),A2(2,10),A3(2,10),B1(2,10),B2(2,10),B3(2,1	M	9
	10)	M	10
	COMMON S1(4001),S2(4001)	M	11
	S1(ICOUNT)=0.	M	12
	S2(ICOUNT)=0.	M	13
	J=LLNT(1)	M	14
	DO 10 I=1,NNCT	M	15
	S1(ICOUNT)=S1(ICOUNT)+DDPC(I,J)*A3(1,I)*1000.	M	16
10	S2(ICOUNT)=S2(ICOUNT)+DDPC(I,J)*B3(1,I)*1000.	M	17
	X=ABS(S1(ICOUNT))	M	18
	Y=ABS(S2(ICOUNT))	M	19
	IF (X.GT.XMAX) XMAX=X	M	20
	IF (Y.GT.YMAX) YMAX=Y	M	21
	RETURN	M	22
	END	M	23-

ORIGINAL PAGE IS  
OF POOR QUALITY

	SUBROUTINE BNF	N	1
C	*****	N	2
C	THIS SUBROUTINE CALCULATES THE NONLINEAR BEARING FORCES FOR EACH	N	3
C	TIME STEP . THE BEARING USED ARE ASSUMED TO BE SHORT JOURNAL	N	4
C	BEARING 180 DEG. CAVITATED FILM OR WITH 360. DEG FLUID FILM.	N	5
C	THIS CAN ALSO BE USED TO APPROXIMATE STRAIGHT SEAL FORCES.	N	6
C	*****	N	7
	REAL LEN	N	8
	REAL MFX,MFY	N	9
	REAL KXX,KYY	N	10
	COMMON /BLK1/ N,NB,NNLIN,NMB,NF,NU,NS,NBOW,ISTAB,IMODE,ISKU,NNCT,N	N	11
	1UFPT	N	12
	COMMON /BLK3/ CRT(10),LLBD(10),LLNB(5),LLNMB(9),LLSK(10),LLNT(10),	N	13
	1LLUF(10),LLFF(10),LLUT(10)	N	14
	COMMON /BLK4/ KXX(10),KXY(10),KYX(10),KYY(10),CXX(10),CXY(10),CYX(	N	15
	110),CYY(10),SLNMB(9,4,4),CLNMB(9,4,4)	N	16
	COMMON /BLK8/ MFX(10),MFY(10),MUX(10),MUY(10),MBX(10),MBY(10)	N	17
	COMMON /BLK9/ DDPC(10,100),EEYTH(10,100)	N	18
	COMMON /BLK16/ SPEED2,ANGSP,ANGACL,FSPEED	N	19
	COMMON /BLK18/ AKK(10)	N	20
	COMMON /BLK20/ A1(2,10),A2(2,10),A3(2,10),B1(2,10),B2(2,10),B3(2,1	N	21
	10)	N	22
	COMMON /BLK35/ WMY(10),VIS(5),R(5),LEN(5),C(5),NLB(5)	N	23
	DO 10 I=1,NNCT	N	24
	MFX(I)=0.	N	25
10	MFY(I)=0.	N	26
	DO 70 I=1,NNLIN	N	27
	FX=0.	N	28
	FY=0.	N	29
	L=LLNB(I)	N	30
	X=0.	N	31
	Y=0.	N	32
	VX=0.	N	33
	VY=0.	N	34
	DO 20 J=1,NNCT	N	35
	X=X+A3(1,J)*DDPC(J,L)	N	36
	Y=Y+B3(1,J)*DDPC(J,L)	N	37
	VX=VX+A2(1,J)*DDPC(J,L)	N	38

	VY=VY+B2(1,J)*DDPC(J,L)	N	39
20	CONTINUE	N	40
	D=X*X+Y*Y	N	41
	IF (D.LT.1.E-12) GO TO 50	N	42
	SD=0.	N	43
	DEU=0.	N	44
	SD=SQRT(D)	N	45
	U=X*VX+Y*VY	N	46
	DU=C(I)*SD*ANGSP	N	47
	DEU=U/DU	N	48
	EU=SD/C(I)	N	49
	IF (EU.GT.1.) EU=.99	N	50
	PHIDOT=(X*VY-Y*VX)/(ANGSP*D)	N	51
	PI=3.14159	N	52
	TEST=(1.-2.*PHIDOT)	N	53
	SIGN=1.	N	54
	SIGN1=1.	N	55
	IF (TEST.LT.0.) SIGN=-1.	N	56
	IF (DEU.LT.0.) SIGN1=-1.	N	57
	CS=EU*ABS(TEST)/SQRT(EU*EU*TEST**2+4.*DEU*DEU)	N	58
	AS=(1.+EU)/(1.-EU)	N	59
	IF (CS.EQ.0.) GO TO 30	N	60
	U=SQRT((1.-CS)/(1.+CS))	N	61
	GO TO 40	N	62
30	U=0.	N	63
40	CONTINUE	N	64
	T11=SIGN*4.*EU*CS**3/((1.-EU*EU*CS*CS)**2)	N	65
	C1=(1.-EU*EU)	N	66
	C2=(3.-5.*AS*AS)	N	67
	C3=(5.-3.*AS*AS)	N	68
	TA=ATAN(U*(AS*AS-1.)/(AS*(1.+U*U)))	N	69
	C4=(1.+2.*EU*EU)	N	70
	CON=PI*C4/(C1**2.5)	N	71
	CON2=(C2*U*U+C3*AS*AS)/(U*U+AS*AS)**2+(C2+C3*AS*AS*U*U)/(1.+AS*AS*	N	72
	U*U)**2	N	73
	T12=CON+SIGN1*(2.*C4*TA/(C1**2.5)-U*CON2/(C1**2))	N	74
	CON=2./C1**1.5	N	75
	T13=CON*(PI/2.+SIGN1*(TA-AS*U*(U*U-AS*AS)/(U*U+AS*AS)**2-AS*U*(1.-	N	76

ORIGINAL PAGE IS  
OF POOR QUALITY

```

1AS*AS*U*U)/(1.+AS*AS*U*U)**2))
SDM=VIS(I)*ANGSP*2.*R(I)*LEN(I)**3/(8.*C(I)*C(I))
F1=SDM*(EU*TEST*TI1+2.*DEU*TI2)
F2=SDM*(EU*TEST*TI3+2.*DEU*TI1)
FX=-(F1*X+F2*Y)/SD
FY=(F2*X-F1*Y)/SD
50 CONTINUE
ID=NLB(I)
FX=FX+KXX(ID)*X+AKK(ID)*X
FY=FY+KYY(ID)*Y+AKK(ID)*Y
DO 60 K=1,NNCT
60 MFX(K)=MFX(K)+FX*DDPC(K,L)
70 MFY(K)=MFY(K)+FY*DDPC(K,L)
CONTINUE
RETURN
END

```

```

N 77
N 78
N 79
N 80
N 81
N 82
N 83
N 84
N 85
N 86
N 87
N 88
N 89
N 90
N 91
N 92-

```

	SUBROUTINE OBPLOT (XMAX,YMAX,NLPT,IO,NSTEP,IJ)	0	1
C	*****	0	2
C	THIS SUBROUTINE PLOTS THE TRANSIENT ORBITS IN X AND Y DIRECTIONS	0	3
C	*****	0	4
	COMMON /BLK28/ AL1(8),AL2(8),AL3(8)	0	5
	COMMON /BLK39/ NSPD,SSPEED(10)	0	6
	COMMON SX(4001),SY(4001)	0	7
	CALL PLOT (15.,5.,-3)	0	8
	CALL SYMBOL (-3.0,-4.00,.105,AL1,0.0,80)	0	9
	CALL SYMBOL (-3.0,-4.25,.105,AL2,0.0,80)	0	10
	CALL SYMBOL (-3.0,-4.50,.105,AL3,0.0,80)	0	11
	CALL SYMBOL (-3.,-4.75,.105,25HROTOR SPEED= RPM,0.,25)	0	12
	CALL NUMBER (-1.9,-4.75,.105,SSPEED(IJ),0.,4HF6.0)	0	13
	C=AMAX1(XMAX,YMAX)	0	14
	G=1.	0	15
	IF (C.LT.1.) G=10.	0	16
	B=C*G/3.+1.	0	17
	D=AIN(TB)/G	0	18
	E=-3.*D	0	19
	CALL AXIS (-3.0,-3.0,11HY-DIR(MILS),11,6.0,90.0,E,D)	0	20
	CALL AXIS (-3.0,-3.0,11HX-DIR(MILS),-11,6.0,0.0,E,D)	0	21
	CALL PLOT (3.,-3.,3)	0	22
	CALL PLOT (3.,3.,2)	0	23
	CALL PLOT (-3.,3.,2)	0	24
	CALL SYMBOL (1.0,3.25,.14,11HSTATION NO.,0.0,11)	0	25
	CALL NUMBER (2.2,3.25,.14,10,0.0,2HI3)	0	26
	KK=1	0	27
	JJ=0	0	28
	DO 30 J=1,NLPT	0	29
	X=SX(J)	0	30
	Y=SY(J)	0	31
	X=X/D	0	32
	Y=Y/D	0	33
	IF (J.NE.1) GO TO 10	0	34
	CALL PLOT (Y,Y,3)	0	35
10	CALL PLOT (X,Y,2)	0	36
	IF (J.EQ.KK) GO TO 20	0	37
	GO TO 30	0	38

ORIGINAL PAGE IS  
OF POOR QUALITY

20 CALL SYMBOL (X,Y,.0875,11,0.,-1)  
CALL PLOT (X,Y,3)  
JJ=JJ+1  
KK=JJ\*NSTEP+1  
30 CONTINUE  
CALL NEWBLOK  
RETURN  
END

0 39  
0 40  
0 41  
0 42  
0 43  
0 44  
0 45  
0 46-

	SUBROUTINE TMPLOT (XMAX,YMAX,NLPT,ID,FTIME,NSTEP)	P	1
C	*****	P	2
C	THIS SUBROUTINE PLOTS TRANSIENT RESPONSE AMPLITUDES VS REAL TIME	P	3
C	*****	P	4
	COMMON /BLK16/ SPEED2,ANGSP,ANGACL,FSPEED	P	5
	COMMON /BLK28/ AL1(8),AL2(8),AL3(8)	P	6
	COMMON SX(4001),SY(4001)	P	7
	C=AMAX1(XMAX,YMAX)	P	8
	G=1.	P	9
	IF (C.LT.1.) G=10.	P	10
	B=C*G/2.+1.	P	11
	D=AINTE(B)/G	P	12
	CC=-2.*D	P	13
	CALL PLOT (5.,2.,-3)	P	14
	E=FTIME*1000./8.+1.	P	15
	F=AINTE(E)/1000.	P	16
	CALL AXIS (0.0,0.0,15HTIME IN SECONDS,-15,8.0,0.0,0.0,F)	P	17
	CALL AXIS (0.0,0.0,23HROTOR DISPLACEMENT-MILS,23,4.,90.,CC,D)	P	18
	CALL PLOT (0.,2.0,3)	P	19
	CALL PLOT (8.0,2.0,2)	P	20
	CALL SYMBOL (0.0,-1.1,.105,AL1,0.0,80)	P	21
	CALL SYMBOL (0.0,-1.3,.105,AL2,0.0,80)	P	22
	CALL SYMBOL (0.0,-1.5,.105,AL3,0.0,80)	P	23
	CALL SYMBOL (3.5,4.0,.14,11HSTATION NO.,0.,11)	P	24
	CALL NUMBER (4.7,4.0,.14,ID,0.0,2HI3)	P	25
	CALL SYMBOL (6.0,3.8,0.105,12HX=,Y=,0.,12)	P	26
	CALL SYMBOL (6.4,3.9,0.105,11,0.,-1)	P	27
	CALL SYMBOL (7.3,3.9,0.105,2,0.,-1)	P	28
	M=0	P	29
10	CONTINUE	P	30
	JJ=0	P	31
	KK=1	P	32
	TIME=0.	P	33
	SPEED=SPEED2	P	34
	STEP=NSTEP	P	35
	DELTAT=0.	P	36
	DO 50 I=1,NLPT	P	37
	TIME=TIME+DELTAT	P	38

ORIGINAL PAGE IS  
OF POOR QUALITY



```

T=TIME
SPEED=SPEED+DELTAT*ANGACL*9.54929
X=SX(I)
T=T/F
Z=X/D+2.
N=11
IF (M.EQ.0) GO TO 20
Y=SY(I)
Z=Y/D+2.
N=2
20  CONTINUE
    IF (I.NE.1) GO TO 30
    CALL PLOT (T,Z,3)
30  CALL PLOT (T,Z,2)
    IF (I.EQ.KK) GO TO 40
    GO TO 50
40  CALL SYMBOL (T,Z,.07,N,0.,-1)
    DELTAT=60./(SPEED*STEP)
    JJ=JJ+1
    KK=JJ*NSTEP+1
50  CONTINUE
    IF (M.EQ.1) GO TO 60
    M=1
    GO TO 10
60  CONTINUE
    CALL NEWBLOK
    RETURN
    END

```

```

P 39
P 40
P 41
P 42
P 43
P 44
P 45
P 46
P 47
P 48
P 49
P 50
P 51
P 52
P 53
P 54
P 55
P 56
P 57
P 58
P 59
P 60
P 61
P 62
P 63
P 64
P 65
P 66-

```

	SUBROUTINE TFFT (CC,NSTEP)	Q	1
C	*****	Q	2
C	THIS SUBROUTINE SAMPLES DATA FOR THE FAST FOURIER TRANSFORMATION	Q	3
C	*****	Q	4
	DIMENSION A(1024), B(1024), CC(512)	Q	5
	COMMON S1(4001),S2(4001)	Q	6
	DO 10 I=1,1024	Q	7
	A(I)=0.	Q	8
10	B(I)=0.	Q	9
	N=NSTEP/10	Q	10
	M=NSTEP*4+1	Q	11
	DO 20 I=1,160	Q	12
	J=(I-1)*N+M	Q	13
20	A(I)=S1(J)	Q	14
	CALL DFT (10,1024,3,A,B)	Q	15
	DO 30 I=1,512	Q	16
	C=SQRT(A(I)*A(I)+B(I)*B(I))	Q	17
	CC(I)=C	Q	18
30	WRITE (3,40) I,C	Q	19
	RETURN	Q	20
C		Q	21
40	FORMAT (5X,I5,5X,F15.5)	Q	22
	END	Q	23-

ORIGINAL PAGE IS  
OF POOR QUALITY

	SUBROUTINE DFT (NPWR2,N,NTYPE,XRE,XIM)	R	1
	DIMENSION XRE(N), XIM(N)	R	2
C	*****	R	3
C	CALCULATES FOURIER SERIES FOR DR FROM THE VECTOR X, WHOSE LENGTH	R	4
C	IS N WHERE N = 2**NPWR2	R	5
C		R	6
C	DURING FOURIER ANALYSIS, THE INPUT VECTOR (XRE,XIM) REPRESENTS	R	7
C	CONSECUTIVE SAMPLES OF THE TIME FUNCTION X(N*DELTAT)	R	8
C	THE SUBROUTINE RETURNS THE COEFFICIENTS OF THE COMPLEX FOURIER	R	9
C	SERIES REPRESENTATION OF THE TIME FUNCTION	R	10
C		R	11
C	DURING FOURIER SYNTHESIS, THE INPUT VECTOR (XRE,XIM) CONSISTS	R	12
C	OF THE ABOVE MENTIONED FOURIER COEFFICIENTS.	R	13
C	THE SUBROUTINE RETURNS THE ORIGINAL TIME FUNCTION, SAMPLED AT	R	14
C	EVENLY SPACED INCREMENTS	R	15
C		R	16
C	THIS SUBROUTINE ALLOWS A FORTY PERCENT TIME SAVING IF THE	R	17
C	TIME FUNCTION IS REAL OR IF THE FOURIER COEFFICIENTS ARE THE	R	18
C	COEFFICIENTS OF A REAL FUNCTION	R	19
C		R	20
C	FOR FOURIER ANALYSIS OF A REAL FUNCTION IT IS UNNECESSARY TO	R	21
C	INSERT ZEROS IN THE XIM LOCATIONS BEFORE CALLING THIS SUBROUTINE	R	22
C		R	23
C	FOR FOURIER SYNTHESIS OF A REAL FUNCTION ONE NEED ENTER ONLY	R	24
C	THE REAL AND IMAGINARY PARTS OF THE FIRST (ONE HALF N + 1)	R	25
C	FOURIER COEFFICIENTS        THE SUBROUTINE AUTOMATICALLY ASSUMES	R	26
C	THAT THE REMAINING COEFFICIENTS ARE HERMITIAN SYMMETRIC	R	27
C		R	28
C	NTYPE = 1    COMPUTE FOURIER ANALYSIS OF COMPLEX VECTOR X	R	29
C	NTYPE = 2    COMPUTE FOURIER SYNTHESIS OF COMPLEX VECTOR X	R	30
C	NTYPE = 3    COMPUTE FOURIER ANALYSIS OF REAL VECTOR X	R	31
C	NTYPE = 4    COMPUTE FOURIER SYNTHESIS OF REAL VECTOR X	R	32
C		R	33
C	THIS SUBROUTINE SETS UP AND CALLS SUBROUTINE FFT	R	34
C	*****	R	35
C		R	36
C	DEFINE CONSTANTS	R	37

C		R	38
C	DEFINE CONSTANTS	R	37
C		R	38
	NPWM1=NPWR2-1	R	39
	N2=N/2	R	40
	N2P1=N2+1	R	41
	N2P2=N2+2	R	42
	N4=N/4	R	43
	N4P1=N4+1	R	44
	N4P2=N4+2	R	45
	Z=N	R	46
	C=6.2831853/Z	R	47
C		R	48
C	GO TO PROPER STATEMENT NUMBER ACCORDING TO NTYPE	R	49
C		R	50
	GO TO (10,20,30,90), NTYPE	R	51
C		R	52
C	STATEMENTS 1,2 FOR A COMPLEX VECTOR X	R	53
C		R	54
10	CALL FFT (1, NPWR2, N, XRE, XIM)	R	55
	RETURN	R	56
20	CALL FFT (0, NPWR2, N, XRE, XIM)	R	57
	RETURN	R	58
C		R	59
C	STATEMENT 3 FOR FOURIER ANALYSIS OF A REAL VECTOR X	R	60
C	SEE RANDOL READ#S MA THESIS, ELECTRICAL ENGG, RICE UNIV, 1968	R	61
C	INSERT EVEN ELEMENTS OF XRE INTO XIM	R	62
30	DO 40 I=2, N, 2	R	63
	I2=I/2	R	64
	IM1=I-1	R	65
	XIM(I2)=XRE(I)	R	66
40	XRE(I2)=XRE(IM1)	R	67
	CALL FFT (1, NPWM1, N2, XRE, XIM)	R	68
C		R	69
C	SEPARATE THE OUTPUT INTO ODD AND EVEN PARTS WITH ADDITIONAL	R	70
C	DIVISION BY 2	R	71

C	XRE(1)=XRE(1)/2.	R 72
	XRE(N2P1)=XIM(1)/2.	R 73
	XIM(1)=0.	R 74
	XIM(N2P1)=0.	R 75
	DO 50 I=2,N4P1	R 76
	J=N2+I	R 77
	K=N2+2-I	R 78
	XRE(J)=0.25*(XIM(I)+XIM(K))	R 79
	XIM(J)=0.25*(-XRE(I)+XRE(K))	R 80
	XRE(I)=0.25*(XRE(I)+XRE(K))	R 81
50	XIM(I)=0.25*(XIM(I)-XIM(K))	R 82
	DO 60 I=N4P2,N2	R 83
	J=N2+I	R 84
	K=N2+2-I	R 85
	L=N2+K	R 86
	XRE(I)=XRE(K)	R 87
	XRE(J)=XRE(L)	R 88
	XIM(I)=-XIM(K)	R 89
60	XIM(J)=-XIM(L)	R 90
C	COMBINE THE DFT'S OF ODD AND EVEN ELEMENTS	R 91
C		R 92
	SAVE=XRE(1)-XRE(N2P1)	R 93
	DO 70 I=1,N2	R 94
	J=N2+I	R 95
	Z=I-1	R 96
	ANGLE=Z*C	R 97
	WRE=COS(ANGLE)	R 98
	WIM=-SIN(ANGLE)	R 99
	XRE(I)=XRE(I)+WRE*XRE(J)-WIM*XIM(J)	R 100
70	XIM(I)=XIM(I)+WIM*XRE(J)+WRE*XIM(J)	R 101
	XRE(N2P1)=SAVE	R 102
	XIM(N2P1)=0.	R 103
	DO 80 I=N2P2,N	R 104
	J=N+2-I	R 105
	XRE(I)=XRE(J)	R 106
80	XIM(I)=-XIM(J)	R 107
	RETURN	R 108
		R 109

```

C
C STATEMENT 9 FOR FOURIER SYNTHESIS OF A REAL VECTOR X
C SEPARATE AND REARRANGE
90 DO 100 I=1,N2
    J=N2+I
    K=N2+2-I
    Z=I-1
    ANGLE=Z*C
    WRE=COS(ANGLE)
    WIM=SIN(ANGLE)
    SUM1=XIM(I)+XIM(K)
    SUM2=XRE(I)-XRE(K)
    XRE(J)=XRE(I)+XRE(K)-WRE*SUM1-WIM*SUM2
100 XIM(J)=XIM(I)-XIM(K)+WRE*SUM2-WIM*SUM1
    DO 110 I=1,N2
        J=N2+I
        XRE(I)=XRE(J)
        XIM(I)=XIM(J)
110 XIM(J)=0.
    CALL FFT (0,NPWN1,N2,XRE,XIM)
C
C REARRANGE RESULTS
C
    DO 120 I=1,N2
        J=N2P1-I
        K=2*J-1
120 XRE(K)=XRE(J)
    DO 130 I=1,N2
        J=2*I
        XRE(J)=XIM(I)
130 XIM(I)=0.
    RETURN
    END

```

```

R 110
R 111
R 112
R 113
R 114
R 115
R 116
R 117
R 118
R 119
R 120
R 121
R 122
R 123
R 124
R 125
R 126
R 127
R 128
R 129
R 130
R 131
R 132
R 133
R 134
R 135
R 136
R 137
R 138
R 139
R 140
R 141
R 142-

```

	SUBROUTINE FFT (IREV,NPWR2,N,XRE,XIM)	S	1
	DIMENSION XRE(N), XIM(N), WRE(1024), WIM(1024), INDEX(1024)	S	2
	EQUIVALENCE (WRE(1),INDEX(1))	S	3
C	*****	S	4
C	CALCULATES THE DISCRETE FOURIER TRANSFORM OF A SEQUENCE OF EQUALLY	S	5
C	SPACED SAMPLES OF THE COMPLEX FUNCTION X(I)	S	6
C		S	7
C	SEE GULD AND RADER, DIGITAL PROCESSING OF SIGNALS	S	8
C	CHAPTER 6 PAGE 176.	S	9
C		S	10
C	SET IREV = 0 TO OBTAIN THE DFT	S	11
C	DFT(J) = SUM ON K OF X(K)*EXP(+6.283*SQRT(-1)*JK/N)	S	12
C		S	13
C	SET IREV = 1 TO OBTAIN THE IDFT	S	14
C	IDFT(J) = X(J) = (I/N)*(SUM ON K OF DFT(K)*EXP(-6.283*SQRT(-1)*	S	15
C	JK/N))	S	16
C		S	17
C	NPWR2 THE BASE TWO LOGARITHM OF THE NUMBER OF ELEMENTS IN THE	S	18
C	SEQUENCE	S	19
C	N = 2**(NPWR2; = NUMBER OF ELEMENTS IN THE COMPLEX VECTOR X	S	20
C		S	21
C	XRE AND XIM CONTAIN THE SEQUENCE TO BE TRANSFORMED. THIS	S	22
C	SUBROUTINE REPLACES XRE AND XIM BY THE REAL AND IMAGINARY PARTS	S	23
C	OF THEIR TRANSFORM.	S	24
C		S	25
C	WRE AND WIM ARE VALUES OF THE COMPLEX EXPONENTIAL	S	26
C		S	27
C	INDEX IS A VECTOR CONTAINING ONES WHERE INDICES HAVE ALREADY BEEN	S	28
C	REVERSED.	S	29
C		S	30
C	WRITTEN BY JETHRO MECK (RICE UNIVERSITY, HOUSTON, TEXAS)	S	31
C	JUNE, 1970.	S	32
C	*****	S	33
C		S	34
C	DEFINE CONSTANTS AND PREPARE FOR COMPUTATION	S	35
C		S	36
10	DD 10 I=1,N	S	37
	INDEX(I)=0	S	38

	ZN=N	S	39
	RATIO=1./ZN	S	40
	C=RATIO*6.2831653	S	41
	IF (IREV) 30,20,30	S	42
20	S=1.	S	43
	GO TO 40	S	44
30	S=-1.	S	45
C		S	46
C	PUT THE INPUT SEQUENCE IN BIT REVERSED ORDER	S	47
C	INSERT X(IBFOR+1) IN LOCATION X(IAFTR+1), WHERE IAFTR IS THE	S	48
C	BASE TEN VERSION OF A NUMBER FORMED BY REVERSING THE BINARY	S	49
C	DIGITS OF THE BINARY TRANSLATION OF THE BASE TEN INDEX IBFOR.	S	50
C	FIRST AND LAST ELEMENTS OF VECTOR X ARE ALREADY IN THE PROPER	S	51
C	LOCATIONS.	S	52
C		S	53
40	DO 90 IDO=3,N	S	54
	IBFOR=IDO-2	S	55
	IF (INDEX(IBFOR)) 90,50,90	S	56
50	IAFTR=0	S	57
	NDNOM=N	S	58
	NNUM=IBFOR	S	59
	IADD=1	S	60
C	COMPUTE IAFTR	S	61
C		S	62
	DO 70 I=1,NPWR2	S	63
	NDNOM=NDNOM/2	S	64
	NQUOT=NNUM/NDNOM	S	65
	IF (NQUOT) 60,70,60	S	66
60	NNUM=NNUM-NDNOM	S	67
	IAFTR=IAFTR+IADD	S	68
	IF (NNUM) 70,80,70	S	69
70	IADD=2*IADD	S	70
80	IBFP1=IBFOR+1	S	71
	IAFP1=IAFTR+1	S	72
C		S	73
C	INSERT X(IBFOR+1) INTO X(IAFTR+1)	S	74
C		S	75
	SAVE=XRE(IAFP1)	S	76

ORIGINAL PAGE 1  
OF POOR QUALITY

ORIGINAL PAGE 1  
OF POOR QUALITY



	XRE(IAFP1)=XRE(IBFP1)	S	77
	XRE(IBFP1)=SAVE	S	78
	SAVE=XIM(IAFP1)	S	79
	XIM(IAFP1)=XIM(IBFP1)	S	80
	XIM(IBFP1)=SAVE	S	81
	INDEX(IAFTR)=1	S	82
90	CONTINUE	S	83
C		S	84
C	CALCULATE TWIDDLE FACTORS WRE AND WIM	S	85
C		S	86
	DO 100 I=1,N	S	87
	ZIM1=I-1	S	88
	T=ZIM1*C	S	89
	WRE(I)=COS(T)	S	90
100	WIM(I)=S*SIN(T)	S	91
C		S	92
C	COMPUTE DISCRETE FOURIER TRANSFORM	S	93
C	SEE SIGNAL FLOW GRAPH, PAGE 178, GOLD AND RADER	S	94
C	ISTEP INDEXES THE COLUMNS OF FIGURE 6.10	S	95
C	THE ROWS OF THE SIGNAL FLOW GRAPH ARE DIVIDED INTO GROUPS	S	96
C	NGRUP IS THE NUMBER OF GROUPS	S	97
C	IGRUP INDEXES THE GROUPS OF ROWS	S	98
C	EACH GROUP IS DIVIDED INTO PAIRS OF ROWS CORRESPONDING TO THE NODE	S	99
C	PAIRS.	S	100
C	NPAIR IS THE NUMBER OF NODE PAIRS IN EACH GROUP	S	101
C	IPAIR INDEXES THE NODE PAIRS WITHIN GROUPS	S	102
C	IX1 IS THE INDEX OF THE FIRST NODE OF A NODE PAIR	S	103
C	IX2 IS THE INDEX OF THE SECOND NODE OF A NODE PAIR	S	104
C	IW IS THE INDEX OF THE TWIDDLE FACTOR FOR A NODE PAIR	S	105
C		S	106
	NN=1	S	107
	DO 120 ISTEP=1,NPWR2	S	108
	NN=2*NN	S	109
	NGRUP=N/NN	S	110
	NPAIR=N/(2*NGRUP)	S	111
	IX1=1	S	112
	IX2=1+NPAIR	S	113
	DO 120 IGRUP=1,NGRUP	S	114

	IW=1	S 115
	DD 110 IPAIR=1,NPAIR	S 116
	PRODR=WRE(IW)*XRE(IX2)-WIM(IW)*XIM(IX2)	S 117
	PRODI=WIM(IW)*XRE(IX2)+WRE(IW)*XIM(IX2)	S 118
	SAVRE=XRE(IX1)	S 119
	SAVIM=XIM(IX1)	S 120
	XRE(IX1)=SAVRE+PRODR	S 121
	XIM(IX1)=SAVIM+PRODI	S 122
	XRE(IX2)=SAVRE-PRODR	S 123
	XIM(IX2)=SAVIM-PRODI	S 124
	IX1=IX1+1	S 125
	IX2=IX2+1	S 126
110	IW=IW+NGRUP	S 127
	IX1=IX1+NPAIR	S 128
120	IX2=IX2+NPAIR	S 129
C	IF IDFT IS DESIRED, MULTIPLY BY RATIO (1/N)	S 130
	IF (IREV) 130,150,130	S 131
130	DD 140 I=1,N	S 132
	XRE(I)=RATIO*XRE(I)	S 133
140	XIM(I)=RATIO*XIM(I)	S 134
150	RETURN	S 135
	END	S 136-

ORIGINAL PAGE IS  
OF POOR QUALITY

ORIGINAL PAGE IS  
OF POOR QUALITY

	SUBROUTINE SPLGT (YMAX)	T	1
C	*****	T	2
C	THIS SUBROUTINE GENERATES THE CAMPBELL PLOT OF THE SYSTEM	T	3
C	*****	T	4
	COMMON /BLK39/ NSPD,SSPEED(10)	T	5
	COMMON /BLK40/ FC(512),SFC(8,512)	T	6
	CALL PLOT (15.,1.,-3)	T	7
	CALL PLOT (0.,5.,2)	T	8
	CALL PLOT (0.,0.,3)	T	9
	BASE=.6	T	10
	SPMAX=5.*SSPEED(1)	T	11
	SDV=SPMAX/8.	T	12
	CALL AXIS (0.,0.,22H      FREQUENCY CPM      ,-22,8.,0.,0.,SDV)	T	13
	DO 30 I=1,NSPD	T	14
	CALL PLOT (0.,BASE,-3)	T	15
	YT=SFC(I,129)	T	16
	CALL NUMBER (-.8,0.,.14,SSPEED(I),0.,4HF6.0)	T	17
	CALL SYMBOL (-.6,-.17,.14,3HRPM,0.,3)	T	18
	CALL PLOT (0.,0.,3)	T	19
	CALL PLGT (0.2,0.,2)	T	20
	CALL PLOT (0.,0.,3)	T	21
	DIV=SSPEED(I)/(128.*SDV)	T	22
	X=0.	T	23
	DO 10 J=1,512	T	24
	Y=SFC(I,J)/YMAX	T	25
	IF (X.GT.8.) GO TO 20	T	26
	CALL PLOT (X,Y,2)	T	27
	X=X+DIV	T	28
10	CONTINUE	T	29
20	CONTINUE	T	30
	CALL PLOT (0.,0.,3)	T	31
30	CONTINUE	T	32
	CALL ENDPLT	T	33
	RETURN	T	34
	END	T	35-

## **UNIVERSITY OF VIRGINIA**

### **School of Engineering and Applied Science**

The University of Virginia's School of Engineering and Applied Science has an undergraduate enrollment of approximately 1,000 students with a graduate enrollment of 350. There are approximately 120 faculty members, a majority of whom conduct research in addition to teaching.

Research is an integral part of the educational program and interests parallel academic specialties. These range from the classical engineering departments of Chemical, Civil, Electrical, and Mechanical to departments of Biomedical Engineering, Engineering Science and Systems, Materials Science, Nuclear Engineering, and Applied Mathematics and Computer Science. In addition to these departments, there are interdepartmental groups in the areas of Automatic Controls and Applied Mechanics. All departments offer the doctorate; the Biomedical and Materials Science Departments grant only graduate degrees.

The School of Engineering and Applied Science is an integral part of the University (approximately 1,400 full-time faculty with a total enrollment of about 14,000 full-time students), which also has professional schools of Architecture, Law, Medicine, Commerce, and Business Administration. In addition, the College of Arts and Sciences houses departments of Mathematics, Physics, Chemistry and others relevant to the engineering research program. This University community provides opportunities for interdisciplinary work in pursuit of the basic goals of education, research, and public service.